IDENTIFICATION AND CHARACTERIZATION OF THE GENETIC DETERMINANTS FOR YELLOW FEVER VIRUS INFECTION AND DISSEMINATION IN *AEDES AEGYPTI*

by

YAN-JANG HUANG
B.Sc., National Taiwan University, 2007

AN ABSTRACT OF A DISSERTATION

submitted in partial fulfillment of the requirements for the degree

DOCTOR OF PHILOSOPHY

Department of Diagnostic Medicine/Pathobiology
College of Veterinary Medicine

KANSAS STATE UNIVERSITY
Manhattan, Kansas

2014

Abstract

The genetic composition of arboviruses is a critical determinant of viral infectivity and the capacity for virus dissemination in arthropod vectors. Due to concerns related to a hypothetical potential for loss of attenuation, the supression of vector infection and dissemination is a critical component for the rationale-based design of live-attenuated flavivirus vaccine candidates. The yellow fever virus (YFV) 17D vaccine virus is not only attenuated in vertebrates, but also has low infectivity for *Aedes agypti* mosquitoes and since it does not disseminate, it is not transmissible. Using a reverse genetics system, the mutations present in the envelope protein YFV 17D virus were characterized in Ae. aegypti to determine the role of mutations in limiting the viral infectivity and dissemination capacity. This knowledge would contribute to the rational design of live attenuated vaccines with the desirable phenotype of being non-transmissible by arthropod vectors.

The upper lateral portion of the YFV 17D envelope (E) protein domain III (EDIII) habors the T380R mutation in the FG loop. Experiments demonstrated that the T380R mutation was associated with the viral infectivity phenotype for mosquitoes, but did not influence dissemination into the secondary tissues. The G52R mutation in the molecular hinge region that is located between E protein domains I (EDI) and II, significantly reduced viral infectivity for mosquitoes. In contrast, when cloned into the Asibi wildtype virus genetic backbone, the T173I mutation in the loop structure between the G_0 and H_0 β-strands did not attenuate viral infection and dissemination. The double mutant virus containing both the G52R and T173I mutations in the E protein, showed a similar attenuated reduced infectivity to the single G52R mutant. The M299I mutation in the linker region between EDI and EDIII resulted in a significantly lower viral infectivity at the initial phase of viral infection at 7 days post-infection in *Ae. aegypti*.

In conclusion, the characterization on four mutations in the YFV 17D vaccine E protein have demonstrated three genetic loci, that can influence the process of YFV infection in *Ae. aegypti*. These results provide new knowledge and understanding which may have broad applications for the rationale design of safe flavivirus vaccines, via targeting genetic loci and introducing specific mutations that preclude infection of, and transmission by arthropod vectors.

IDENTIFICATION AND CHARACTERIZATION OF THE GENETIC DETERMINANTS FOR YELLOW FEVER VIRUS INFECTION AND DISSEMINATION IN *AEDES AEGYPTI*

by

YAN-JANG HUANG

B.Sc., National Taiwan University, 2007

A DISSERTATION

submitted in partial fulfillment of the requirements for the degree

DOCTOR OF PHILOSOPHY

Department of Diagnostic Medicine/Pathobiology
College of Veterinary Medicine

KANSAS STATE UNIVERSITY
Manhattan, Kansas

2014

Approved by:

Major Professor
Stephen Higgs

Copyright

Abstract

The genetic composition of arboviruses is a critical determinant of viral infectivity and the capacity for virus dissemination in arthropod vectors. Due to concerns related to a hypothetical potential for loss of attenuation, the supression of vector infection and dissemination is a critical component for the rationale-based design of live-attenuated flavivirus vaccine candidates. The yellow fever virus (YFV) 17D vaccine virus is not only attenuated in vertebrates, but also has low infectivity for *Aedes agypti* mosquitoes and since it does not disseminate, it is not transmissible. Using a reverse genetics system, the mutations present in the envelope protein YFV 17D virus were characterized in *Ae. aegypti* to determine the role of mutations in limiting the viral infectivity and dissemination capacity. This knowledge would contribute to the rational design of live attenuated vaccines with the desirable phenotype of being non-transmissible by arthropod vectors.

The upper lateral portion of the YFV 17D envelope (E) protein domain III (EDIII) habors the T380R mutation in the FG loop. Experiments demonstrated that the T380R mutation was associated with the viral infectivity phenotype for mosquitoes, but did not influence dissemination into the secondary tissues. The G52R mutation in the molecular hinge region that is located between E protein domains I (EDI) and II, significantly reduced viral infectivity for mosquitoes. In contrast, when cloned into the Asibi wildtype virus genetic backbone, the T173I mutation in the loop structure between the G_0 and H_0 β-strands did not attenuate viral infection and dissemination. The double mutant virus containing both the G52R and T173I mutations in the E protein, showed a similar attenuated reduced infectivity to the single G52R mutant. The M299I mutation in the linker region between EDI and EDIII resulted in a significantly lower viral infectivity at the initial phase of viral infection at 7 days post-infection in *Ae. aegypti*.

In conclusion, the characterization on four mutations in the YFV 17D vaccine E protein have demonstrated three genetic loci, that can influence the process of YFV infection in *Ae. aegypti*. These results provide new knowledge and understanding which may have broad applications for the rationale design of safe flavivirus vaccines, via targeting genetic loci and introducing specific mutations that preclude infection of, and transmission by arthropod vectors.

Table of Contents

List of Figures

List of Tables

Acknowledgements

There are a number of people who have been extremely supportive before and during my endeavors in graduate school. First of all, I would like to thank my family who have been teaching and supporting me before and during the process of my graduate education. Although the geographical locations substantially has been limiting the timing of living, laughing and crying together since 2000, my most profound gratitude goes toward my parents who taught me the importance of hard work and ethics and my sister who keeps my parents companied whilst I am going for what I want in life overseas. I could not have done this with my relatives, Ching, Anna, Doug, Cecilia, and Jennifer, who live in the United States and constantly provide the verbal encouragement and emotional support in person and via the phone.

I would like to express my deepest thanks to Dr. Stephen Higgs who provides not only the mentorship in conducting research but also words of encouragement and advice in life. And, to all the members on my supervisory committee, thank you for teaching me becoming a better scientist. Dr. Dana Vanlandingham has always acted as a role model in science with exceptional management skills. Dr. Alan Barrett has led me to the world of the structures of viral proteins. Dr. Kristin Michel has always been encouraging during the process of relocating and setting up the laboratory. Dr. Brian Geisbrecht has served at the critical position as my outside chairperson to oversee the process of final exam.

I am extremely grateful for the opportunities of working with numerous talented colleagues in the University of Texas Medical Branch and Kansas State University. Dr. John Nuckols has been a true friend who provided not only the relentless help in several key experiments but also the company whilst I am far away from home. Ms. Jing Huang shared her valueable experience in rearing and manipulating the mosquitoes. Andy, Allison and Sara offered the advice towards life and education prior and during the process of my relocation to Kansas. All the research support staff and colleagues at the Biosecurity Research Institute and the Agriculture Research Service have played the critical roles to make the set up of the laboratory possible.

Without all the help mentioned above and others, the science would not be done and the places would not be as wonderful as you make it. I am truly thankful to everyone.

Chapter 1 - Introduction to Arbovirology

1.1 Definition and biology of arboviruses

According to the World Health Organization (WHO), arthropod-borne viruses (arboviruses) are defined as "viruses which are maintained in nature principally, or to an important extent, through biological transmission between susceptible vertebrate hosts by hematophagous arthropods" (WHO 1967). The term being "arthropod-borne" with respect to pathogen transmission was first used for animal viruses that cause encephalitis in infected vertebrate hosts in 1942 and the term of "arbovirus" was officially recommended by the International Subcommittee on Viral Nomenclature in 1963 (WHO 1967, WHO 1985). Over 500 arboviruses have been recognized and more than 130 of them cause human diseases with a broad spectrum of clinical manifestations (CDC 1975). Among those with human and veterinary public health significance, the majority of them belong to different virus families including *Togaviridae, Flaviviridae, Bunyaviridae, Reoviridae and Rhabdoviridae*.

Arthropods are classified under the kingdom Animalia, phylum Arthropoda, class Arachnida and Insecta. The first demonstration of a pathogen being transmitted by an arthropod was the transmission of filarial nematodes by mosquitoes by Sir Patrick Manson in 1876. Subsequently, groups of arthropods that were found competent for the transmission of arboviruses include ticks (class Arachnida, order Ixodida, families *Ixodidae* and *Argasidae*); mosquitoes (class Insecta, order Diptera, family *Culicidae*); biting midges (class Insecta, order Diptera, family *Ceratopogonidae*); black flies (class Insecta, order Diptera, family *Simuliidae*); sand files (class Insecta, order Diptera, family *Psychodidae*) and tabanid flies (class Insecta, order Diptera, family *Tabanidae*) (Eldridge and Edman 2003, Marquardt and Kondratieff 2005). Although the early definitions of arboviruses required the virus to be maintained in nature through biological transmission, the modes of transmission can also be mechanical transmissions. In biological transmission, the propagation or the development of the pathogens take place in the vector prior to the transmission to another vertebrate host. Biological transmission also includes other variants such as transovarial transmission, which has been demonstrated primarily among the members of the family of *Bunyaviridae* (Watts, Pantuwatana et al. 1973, Borucki, Kempf et al. 2002). The contamination in the mouthpart of arthropod vectors by pathogens leads to the

mechanical transmission, where mosquitoes serve as “flying syringes” for arboviruses. However, both modes are not mutually exclusive or inclusive. The mechanical transmission by arthropods also has been reported in pathogens that are not known to be classified as arboviruses(Eldridge and Edman 2003).

Pathogen transmission between vertebrates typically involves arthropods that feed on blood i.e. are hematophagous. Although hematophagy occurs in many arthropod groups, not all blood-feeding arthropods are competent for the biological transmission of pathogens due to the requirement of permissive cells for the propagation of pathogens *in vivo*. To be classified as competent vectors for arboviruses, the permissive arthropod species in nature fulfill the epidemiological and ecological definitions of disease vectors, including: the isolation or detection of the pathogens in the absence of visible blood in the digestive system, the infection after the acquisition of viremic body fluid either from vertebrate hosts or artificial apparatus, the transmission of pathogens by inoculating the saliva through the bites, and having a proven role with respect to the epidemiological association with diseases and the ecological association with susceptible vertebrate hosts (WHO 1967, WHO 1985). The competence of pathogen vectors is subjected to the control over multiple factors that influence the efficiency of the transmission including the innate susceptibility to the pathogens, the longevity through adverse environmental and climate conditions prior to the transmission to vertebrate hosts, the abundance of the vector population and the susceptible vertebrate hosts and the likelihood of physically in contact with the vertebrate hosts. Mosquitoes are considered one of the most important vectors for various arboviruses with medical or public health importance. The members of both the subfamilies of Anophelinae and Culicinae are competent of transmitting specific arboviruses by feeding on vertebrate hosts. The propagation of arboviruses in the permissive tissues in the midgut cuboidal epithelial cells and the dissemination into secondary tissues occur before the transmission of arboviruses. The presence of infectious virus in the saliva due to the replication of virus in salivary gland acinar cells and the release into the salivary ducts leads to the transmission of the arboviruses as the vector feeds on the vertebrate. The time required for the propagation and the development of arboviruses, from initial feeding on an infected host to release of virus in the saliva, is defined as extrinsic incubation period. Throughout the virus transmission cycle, several barriers that may limit infection and dissemination in the vectors have been proposed. A midgut infection barrier determines the susceptibility of specific vector species to arboviruses and the

midgut escape barrier governs the successful dissemination into other tissues. The efficiency of infection amongst specific vectors is also determined by the viremic titers of the vertebrate hosts(Barnett 1956, Gubler and Rosen 1976, Tesh, Gubler et al. 1976). The details of the biology of mosquitoes and mosquito-virus interactions is further described in Section 1.2.

The complexity of the field of arbovirology is in part due to the nature of the arbovirus transmission cycle depending on alternation between the vertebrate hosts and arthropod vectors. Although the tools available for the studies in the laboratory and field have led to significant advancement in the knowledge on both the viruses and vectors, critical gaps in our knowledge still exists. It has long been known that only certain species of arthropod can transmit a given pathogen, and indeed even within a species, there is considerable variation in the susceptibility to infection with that pathogen and ability to transmit. Intuitively, it has been assumed that genetics of the arthropod control this variation in competence as a vector, but other factors including pathogen genetics and environmental factors also play a role. Despite publication of papers that suggested an understanding of vector competence, we still do not know the basis of species specificity for any mosquito-virus relationship. Vector competence for arboviruses is determined by several intrinsic and extrinsic factors including the environmental conditions, the genetics and the physiological conditions of the vectors (Tabachnick 1994). Using western equine encephalitis virus (WEEV) and *Culex tarsalis* as an experimental model, it was proven that the viral replication and dissemination in the infected mosquitoes can be impaired at relatively higher extrinsic incubation temperature of 32˚C(Kramer, Hardy et al. 1983). Additional factors that influence vector competence were also reported including the nutritional conditions at the larval stage and the variations in the viral population (Miller and Adkins 1988, Kay, Edman et al. 1989). The quasispecies nature of RNA viruses also led to observed variations in vector competence. The variants of YFV selected based on the plaque morphologies demonstrated the different capacity of dissemination in *Ae. aegypti* (Miller and Adkins 1988). There have been several lines of evidence suggesting that the same vector species obtained from different locations displays significant variation in vector competence for arboviruses including *Ae. aegypti* collected from various locations with the different ability of transmitting dengue viruses (DENV) and YFV (Gubler and Rosen 1976, Tabachnick, Wallis et al. 1985). The characterization of the underlying genetic basis in the laboratory that controls vector competence was initially performed by selecting susceptible and refractory strains of mosquitoes, and mating

between strains of different susceptibility (Hardy, Apperson et al. 1978, Wallis, Aitken et al. 1985, Bosio, Beaty et al. 1998). Although the mating experiments suggested that the susceptibility is genetically linked, the identification of single genetic loci that govern the vector competence has not been accomplished. Some progress has been made with the advancement of molecular techniques to manipulate viral genomes and more recent characterization of vector genetics. The revolutionary technique polymerase chain reaction has allowed the amplification of the genetic materials of mosquito vectors, which can be subsequently subjected to the genetic polymorphisms analysis. For *Ae. aegypti* and dengue virus serotype 2 (DENV-2), the quantitative trait loci analysis, which was based on the quantitative traits established by either the continuous distribution of the virus titers in infected tissues of mosquitoes or the percentage of viral infection and dissemination, has provided evidence that vector competence is determined by multiple genetic loci (Bosio, Beaty et al. 1998, Bosio, Fulton et al. 2000). Characterization of the genomic sequences in multiple mosquito species is expected to ultimately provide the critical knowledge on the preferential association of the members under the subfamily of Culicinae for the transmission of small enveloped RNA viruses in the families of *Flaviviridae* and *Togaviridae*. With respect to this goal, the genomic sequences of *Anopheles gambiae, Ae. aegypti* and *Cx. quinquefasciatus* have now been completely determined (Holt, Subramanian et al. 2002, Nene, Wortman et al. 2007, Arensburger, Megy et al. 2010). In contrast to the approach taken by analyzing the ampilicons of randomly probed or specific genes, the availability of genomic data has provided some critical details on the ecology of flaviviruses. For example, the largest number of olfactory-receptor-related genes encoded in the genome of *Cx. quinquefasciatus* may contribute to the opportunistic feeding behaviors on multiple vertebrate animals and explains the zoonotic nature of West Nile virus (Arensburger, Megy et al. 2010). Similarly, the wide host range of *Cx. quiquefasciatus* is also reflected by the presence of several unique proteins present in the saliva, which allows the acquisition of bloodmeals from humans, birds and other mammals (Ribeiro and Arca 2009). However, the currently available knowledge is still insufficient to define the specific genetic determinants required for the vector competence or refractoriness of arboviruses among the mosquitoes in nature. An impetus for such studies has been the idea that new control methods for vector-borne disease could be developed based on manipulation of the vector genome to effectively reduce competence. The approach can be taken by introducing genetic components that prevents the mosquitoes from completing the lifecycle

followed by the selection based on the selectable markers such as chemical compounds or fluorescent proteins at laboratory rearing facilities. With the remarkable success of the elimination of New World screwworm, a modified Sterile Insect Technique (SIT) has been devised for mosquitoes to produce laboratory-reared genetically altered male arthropods that compete with the wildtype male and produce no or fewer progeny. *Ae. aegypti* was transformed to contain the genetic lethality, which is suppressed by tetracycline under laboratory conditions, and the males were released to introduce the lethal gene to the populations in nature in order to suppress the vector population (Phuc, Andreasen et al. 2007). The other method utilizes the obligatory intracellular bacteria *Wolbachia.* The mating between an infected male *Ae. aegypti* and an uninfected female results in the embryonic lethality and the elimination of uninfected mosquitoes in the population. Additionally, the infection of *Wolbachia* led to the phenotypic changes of mosquitoes by not only shortening the life span but also by reducing the susceptibility to arboviruses (Walker, Johnson et al. 2011). Another approach that has been considered is to utilize the innate immunity components of mosquitoes targeting the viral genetic materials. The transformation of *Ae. aegypti* with the short sequences which are transcribed into the siRNA products targeting the DENV-2 prM gene. These have been shown to be effective to introduce resistance to DENV-2 (Franz, Sanchez-Vargas et al. 2006). However, the resistance was later reported to be transient within the limited generations after the transformation (Franz, Sanchez-Vargas et al. 2009). The development of novel tools for the potential control and prevention of arboviral diseases targeting both the viral and vector components have been actively and continuously conducted. It provides an alternative approach to block the transmission of arboviruses at the stage of mosquitoes in addition to the control of vector populations. In spite of all the efforts, the options for prophylaxis and antivirals remain limited. The public health measures for disease control and prevention still rely heavily on vaccines and the vector control.

The list of arboviruses has rapidly expanded with the advancement of tools developed for the molecular detection and identification of new viruses. It is unlikely to provide an up-to-date comprehensive list of arboviruses or mosquito-borne viruses. The following paragraphs and table **(Table 1.1)** provide a list of selected mosquito-borne viruses of human or veterinary public health importance.

Genus	Name	Major vector(s)	Geographic distribution

Flavivirus	Dengue viruses (DENV-1~4)	*Ae. aegypti* *Ae. albopictus*	Old world: Africa, Asia New world: America
	Japanese encephalitis virus	*Cx. tritaeniorhynchus*	Old world: eastern and southern Asia New world: northern Australia
	West Nile virus	*Cx.tarsalis* *Cx. pipiens quiquefasciatus*	Old world: western Asia and Europe New world: north America
	St. Louis encephalitis virus	*Cx. pipiens quiquefasciatus*	New world: America
	Yellow fever virus	*Ae. aegypti*	New world: America Old world: Africa
Alphavirus	Chikungunya virus	*Ae. aegypti* *Ae. albopictus*	Old world: Africa and Asia New world: America
	Eastern equine encephalitis virus	*Culiseta melanura*	New world: America
	O'nyong-nyong virus	*Anopheles* spp.	Old world: Africa
	Sindbis virus	*Ae. aegypti*	Old world: Asia. Africa, eastern Europe
	Venezuela equine encephalitis virus	*Culex melanoconion spp.*	New world: America
	Western equine encephalitis virus	*Cx. tarsalis* *Cx. pipiens quiquefasciatus*	New world: America
Orthobunyavirus	California serogroup viruses	*Aedes* spp. *Culiseta* spp.	New world: North America Old world: Europe

Phlebovirus	Rift Valley fever virus	*Aedes* spp.	Old world: Africa

Table 1.1 Selected mosquito-borne arboviruses with human or veterinary public health importance

A. Flaviviruses

Under the family of *Flaviviridae*, the genus of *flavivirus* consists of arthropod-borne viruses mainly transmitted by mosquitoes and ticks (Gould and Solomon 2008). Collectively, the flaviviruses are public health threats for over half of the global population, and become the category of arboviruses that have the highest human public health significance (Gubler 2002). The group of mosquito-borne flaviviruses, which display homology of their genome structures and virion morphologies, contains two major groups of viruses distinguished by their clinical presentations including; viral encephalitis caused by Japanese encephalitis virus (JEV) group and viral hemorrhagic fever caused by the DENV and YFV group. JEV, West Nile virus (WNV) and St. Louis encephalitis virus (SLEV), which all belong to the Japanese encephalitis group, are able to cause severe neurological diseases amongst infected individuals. The members of the JEV group infect multiple vertebrate species including equine species, avian species and human species through the bites of different vectors (Gould and Solomon 2008). DENV consists of four serotypes of dengue virus (DENV-1, 2, 3, 4), which are transmitted mainly by *Ae. aegypti* and *Ae. albopictus* and cause a wild spectrum of diseases from febrile illness to severe diseases such as dengue hemorrhagic fever (DHF) and dengue shock syndrome (DSS) without any currently available vaccines or antiviral therapies (WHO 2009). The members of the YFV and DENV are maintained by transmission between the susceptible primates and the vector species.

B. Alphaviruses

Alphaviruses are mosquito-borne viruses categorized under the genus of *Alphaviruses* in the family of *Togaviridae*. There have been seven complexes identified based on the antigenic characteristics of the alphaviruses. Pathogenic alphaviruses in the old world tend to cause rash and arthritis whereas the new world alphaviruses lead to the encephalitic symptoms amongst infected humans. The analyses on the nucleotide and amino acid sequences and the antigenic properties suggested the homology in the secondary structures amongst different alphaviruses

(Knipe and Howley 2013). Although the number of reported human infections by alphaviruses is substantially lower than for flaviviruses, the significance of alphaviruses in human and veterinary public health is established based on its characteristics in nature often as emerging and zoonotic pathogens. For example, the total number of reported chikungunya virus (CHIKV) cases in Oceania and Asia since 2005 has exceeded 1.9 million (WHO 2014). Sindbis virus which causes fever, rash and arthritis in humans has also been used as a genetic expression system through the genetic engineering of the subgenomic promoter in both vertebrate and invertebrate systems (Higgs, Powers et al. 1993). O'nyong-nyong virus (ONNV) is the only known alphavirus infecting the malaria vector *Anopheles gambiae* and causes large outbreaks (Williams, Woodall et al. 1965). Chikungunya virus recently has been spread rapidly and causing several epidemics in the Indian ocean and the southeast Asia due to the A226V mutation of the E1 protein, which has altered the vector specificity and epidemic potential (Tsetsarkin, Vanlandingham et al. 2007). Recently, CHIKV has also been detected as an emerging pathogen in the new world (Albuquerque, Marandino et al. 2012). Venezuela equine encephalitis virus (VEEV) causes high viremia in infected equine species and occasional human cases mainly reported in Latin America (Weaver and Barrett 2004). Western equine encephalitis virus was first isolated in California in 1930 and is transmitted primarily by *Cx. tarsalis* in its enzootic cycle and other bridging vectors, which feed on humans or equine species. Eastern equine encephalitis virus (EEEV) with its geographic distribution along both the Atlantic coast and the gulf coast and in the mid-west causing a higher mortality in horses than WEEV through the transmission by *Aedes*, *Coquilletidia* and *Culex* species which feed on humans and horses (Zacks and Paessler 2010).

Although alphaviruses are classified under *Togaviridae*, alphaviruses and flaviviruses share the similar receptor binding and membrane fusion mechanisms classified as type II fusion protein.(Harrison 2008) The research on alphaviruses in mosquitoes provided several examples with respect to how viral genetics can determine the choice of vector species among related viruses in the same complex and alter the vector competence among the different strains of a single virus. The monoclonal-antibody-1A3B-7-resistant VEEV variant was shown to lose its capacity in the infection and dissemination in *Ae. aegypti*.(Woodward, Miller et al. 1991) In the study described by Brault *et al*., the S218N mutation in the E2 glycoprotein was identified as a genetic substitution which increased the viral infectivity of VEEV in *Ochlerotatus*

taeniorhynchus.(Brault, Powers et al. 2004) Between the two closely related ONNV and CHIKV, which are vectored by *Anopheles gambiae* and *Ae. aegypti*, respectively, the genetic mapping between the genomes of ONNV and CHIKV demonstrated the choice of vector species is due to the distinct sequences in the structural genes. (Vanlandingham, Tsetsarkin et al. 2006) Such studies provided the mechanistic evidence that the different genetic composition of arboviruses are critical for the choice of vector species and the vector competence.

C. Bunyaviruses

Most bunyaviruses can be transmitted by arthropod vectors except for Hantaviruses, which are mainly transmitted by rodents. Members of the genera of Orthobunyavirus and Phlebovirus have been described to be transmitted by mosquitoes; whereas members of the genus of Nairovirus are exclusively transmitted by ticks in nature (Knipe and Howley 2013). In the genus of *Orthobunyavirus*, the California serogroup viruses contain a large number of viruses present in various geographic locations and are mostly vectored by *Aedes* mosquitoes. La Crosse virus (LAC) leading to encephalitic cases in infected children is maintained in rodents which can potentially develop high-titered viremia with limited symptoms and transmitted by *Ae. triseriatus* mosquitoes. Additionally, the infection of mosquito eggs is utilized as one of the strategies of overwintering. Horizontal transmissions also have been described from female mosquitoes to male mosquitoes (Watts, Pantuwatana et al. 1973). Members of the *Phlebovirus* genus are found worldwide except for Australia. Rift Valley fever virus (RVFV) infects both humans and livestock and utilizes *Aedes* mosquitoes as its vector in Africa. Large epizootic epidemics of RVFV cause serious economic loss due to the high abortion rates amongst infected ruminants (Weaver and Reisen 2010).

1.2 General biology of mosquitoes and mosquito-virus interactions

A. Taxonomy, morphology and evolution

In the family of *Culicidae* under the order of Diptera, mosquitoes are classified under the suborder of Nematocera. Mosquitoes are classified into three major groups known as the anophelines, the culicines and the aedines. The hematophagous feeding strategy renders mosquitoes the most important arthropod vectors with respect to human and veterinary public health. It is suggested the blood feeding behavior emerged independently during the course of

evolution and has become the significant approach utilized by pathogens to increase the mobility amongst various host species (Grimaldi and Engel 2005). All three groups of mosquitoes have a pair of wings, which is the major characteristic of the members in the order of Diptera. The morphology of the proboscis in female mosquitoes is distinct from that of the male mosquitoes. The long slender proboscis in female mosquitoes is required for the penetration of skin and the acquisition of blood from the host whilst the male mosquitoes are adapted to the acquisition of sugars from various sources.

There have been at least six independent emergences of hematophagy during the evolution. It is believed that the evolution of hematophagy has been closely associated with vertebrate hosts in the environment. The hematophagy of mobile aerial insects may emerge as an occasional event in the presence of vertebrates and later transform to obligatory hematophagy.

B. Classification

The subfamilies Anophelinae and Culicinae within the Culicidae are the two subfamilites of great public health significance. The Culicinae subfamily contains two tribes, which are Culicini (culicines) and Aedini (aedines). The third subfamily Toxorhynchitinae does not obtain blood from vertebrate hosts but has been used as a biological control agent based on its predaceous behavior at its larvae stage to other mosquito larvae.

Complete metamorphosis occurs amongst all mosquitoes with an egg stage, four larval stages, a single pupal stage and the adult. The eggs of Culicine mosquitoes are held together by a concave raft on the surface of the water compared to the individual floating eggs deposited by the Anophelines. The Aedine mosquitoes utilize moist substrates to deposit eggs which hatch during the later flooding conditions. (**Figure 1.1 (a)**) Both the larvae of culicine and aedine mosquitoes have an elongated air tube for air exchange. The larvae of anopheline mosquitoes obtain oxygen by lying right underneath the surface of water without the air tube. (**Figure 1.1 (b)**) The appearance of the pupae of most mosquito species is similar with very limited value for identification.

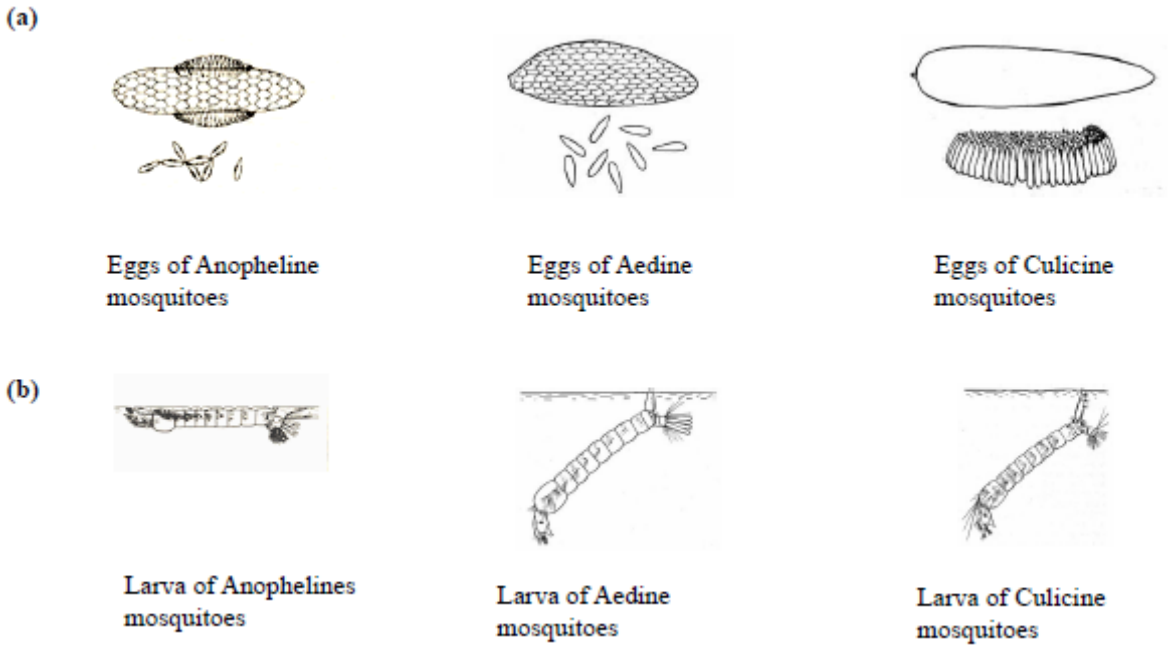

Figure 1.1 Eggs and larvae of mosquitoes

(a) The individual eggs of anophelines, adenine and culicine mosquitoes are listed in the upper section of figure 1.1(a). The multiple eggs of Anopheline and Aedine mosquitoes and the egg raft of culicine mosquitoes are listed in the bottom section of figure 1.1(a) (b) The larvae of Anopheline, Aedine, and Culicine mosquitoes. (adapted from (Littig 1966))

The relative importance of different vector species is based on the pathogens transmitted by the mosquitoes. The combinations of vectors and pathogens are also subjected to human behavior changes such as the increase of aviation transportation and deforestation. *Ae. aegypti* serves as the vector for viruses in both the family of *Flaviviridae* and *Togaviridae* including YFV, DENV and CHIKV amongst the tropical and subtropical regions worldwide (Rao 1964). There have been more than 40 species of *Anopheles* demonstrated to be able to transmit malaria parasites (Enayati and Hemingway 2010). *Culex quinquefasciatus* is responsible for the transmission of the lymphatic filariasis species and several other arboviruses (Simonsen and Mwakitalu 2013). St. Louis encephalitis virus and WNV in North America and Tahyna virus in Europe utilize the same vector within the *Cx. pipiens* complex. *Culex tarsalis* is responsible for the transmission of western equine encephalitis virus and SLEV in western North America (Weaver and Barrett 2004). In Asia, the transmission of JEV depends on *Cx. tritaeniorhynchus*

as its vector (van den Hurk, Ritchie et al. 2009). *Aedes (Neomelaniconion) macintoshi* is important for the transmission of RVFV in Africa (Weaver and Reisen 2010).

C. Life cycle

The time required for the development from larvae to adult varies from 10 days or less. It is subjected to the conditions of water including temperature, the abundance of nutrients and the larval densities. The larvae molt three times in order to progress to the fourth-stage larvae. The development to adult mosquitoes from pupae generally requires one or two days from the emergence of pupae.

The plant nectar is the primary source of carbohydrates, which are subsequently stored in the crop or ventral diverticulum of both male and female adults(Marquardt and Kondratieff 2005). Anautogenous mosquitoes require the blood meals for oviposition after the release from the arrest stage of oogenesis in the ovaries; whereas, the autogenous mosquitoes only require facultative bloodmeals (Spielman 1971). The behaviors of oviposition are subjected to multi-factorial controls including chemical, physical and environmental factors. The extrinsic light cues are important stimuli for the *Ae. aegypti*, which lay the eggs towards the later afternoon (Surtees 1967). The oviposition patterns vary among species. *Anopheles spp.* lay individual eggs on the surface of aqueous bodies. The *Culex spp.* mostly produce egg rafts floating on the surface of the water. The deposit of individual eggs of *Aedes spp.* takes place on the most surface of substrates or vegetation (Bentley and Day 1989). The embryogenesis takes place along with the hardening and darkening of the chorion after oviposition.

The process of blood-feeding, digestion and oviposition is referred to as the gonotrophic cycle, which is largely temperature dependent. The search of vertebrate hosts for blood feeding is a critical component for the transmission cycle of all vector-borne pathogens. The infected hosts serve as the source of pathogens, which render the vectors infectious and competent for the transmission to the next host. Therefore, the chance of transmitting the pathogens increases with the frequency of taking blood meals from the hosts. The acquisition of multiple bloodmeals during one single gonotrophic cycle has been reported in both malarial and arboviral mosquito vectors (Scott and Takken 2012).

D. Host-seeking behavior

The blood feeding behavior is not initiated until 1-2 days after eclosion (emergence of the adult from the pupa). Such period is defined as the previtellogenic period when the fat body matures and synthesizes the precursors of the yolk proteins (Deitsch, Chen et al. 1995, Sappington, Kokoza et al. 1996). The development of the blood feeding behavior amongst *Cx. pipiens* is controlled by the release of juvenile hormone (JH) (Spielman 1974). On the other hand, the development of host-seeking behavior of *Ae. aegypti* is JH-independent. The development of the midgut of the female *Ae. aegypti* is not complete until three days post eclosion making it less likely to consume blood (Bowen and Davis 1989, Marquardt and Kondratieff 2005).

Mosquitoes respond to various chemical, physical and environmental stimuli as clues for locating the vertebrate hosts (Eldridge and Edman 2003, Marquardt and Kondratieff 2005). Carbon dioxide (CO_2) has been considered the universal attractant for vectors. The change in the CO_2 concentration triggers the behavioral changes of the mosquitoes through the CO_2 receptors. The species-specific differential responses to CO_2 may be the determinant of the preference of the host species (Dekker and Takken 1998). Synergistic effects of other volatile compounds such as lactic acid, acetone, and octenol in the presence of CO_2 also assist the host-seeking behavior.

The host-seeking behavior relies heavily on olfaction. Numerous cuticular sensilla on the segmented antennae and the maxillary palps are responsible for receiving the external stimuli. In spite of the diversity in the morphologies and the structures, the scaffold underneath the cuticle structure is well-conserved. The bipolar neurons function as olfactory receptors with the dendrites extending into the sensillum shaft. Other supportive cellular structures such as trichogen and tormogen cells are responsible for both the integrity of the structure and the synthesis of components required in the aqueous lymph. The odorant molecules diffuse through the pores and initiate the signal transduction by its binding to the receptors. It's been postulated that the water-soluble odorant-binding proteins functions as the carriers to facilitate the movement and binding of odorant molecules. The intracellular signaling relies on the GTP-binding proteins, which govern the downstream enzymatic synthesis of secondary messengers cyclic AMP (cAMP) and inositol 1,4,5-triphosphate (IP_3) (Zwiebel and Takken 2004). The secondary messengers trigger the action of ion channels and lead to cellular depoloarization and the electropysiological signals to CNS. Negative regulation in the signaling pathway by reducing

the numbers of receptors on the cell surface and the decoupling of the active G-protein complexes can control the sensory response. Additionally, the degradation of odorant molecules by the biotransformation enzymes can thus control the olfactory process. Taken together, the host-seeking behavior of mosquitoes are regulated with multiple receptors and signaling pathways. The understanding at the molecular-, cellular- and systematic-level is still being developed.

E. Mechanisms of acquisition of blood meals

The mouthpart of the mosquitoes is used to pierce through the outer epidermis and the inner dermis. The mouthpart consists of the fascicle and the labium. The fascicle penetrates the skin during the acquisition of the blood whilst the labium is progressively bent during the process of probing (Marquardt and Kondratieff 2005). The blood vessels are later ruptured leading to the vasoconstriction, the formation of platelet plugs, activation of coagulation mechanisms, the host pain and inflammation. Therefore, the saliva of mosquitoes contains several macromolecules such as anti-coagulant, immunomodulator and vasodialator (Schneider and Higgs 2008). Additionally, the secretion of the saliva during blood feeding allows the transmission of pathogens to take place. *Ae. aegypti* utilizes a salivary gland-specific apyrase which belongs to the 5'-nucleotidase family to impair the aggregation of platelets (Cupp, Ribeiro et al. 1998). It has also been reported the genome of *An. albimanus* encodes the salivary peroxidase/ catechol oxidase which promotes the vasodilation (Ribeiro and Valenzuela 1999). By degrading adenosine to inosine and ammonia, the adenosine deaminase of *Ae. aegypti* therefore delays the initiation of pain and the inflammation (Ribeiro, Charlab et al. 2001). It has also been suggested the neurotransmission is also impaired by the anaesthetic components of the *Ae. aegypti* saliva. The secretion of various macromolecules leads to the depletion of the salivary glands and promotes the resynthesis of the components of saliva (Hudson, Bowman et al. 1960).

The cibarial and pharyngeal pump muscles facilitate the intake of the blood (Eldridge and Edman 2003, Marquardt and Kondratieff 2005). The ingestion of blood fills the hind most part of the midgut followed by the expansion of the anterior portion until the abdomen is filled. The determinants of the final location of the ingested meals have been suggested to be the components in the meals. Increase in the glucose concentration led to the dispatchment into the diverticulum (Day 1954). The blood-feeding action is driven by phagostimulants derived from

the cellular fractions of the host such as adenine nucleotides in the blood of the vertebrate hosts (Hosoi 1958, Friend and Smith 1977, Galun, Vardimon-Friedman et al. 1993). *Ae. agypti* responds to ATP during the gorging process. Removal of the phosphate groups reduced the gorging behavior. The binding of ATP induces the opening of the membrane channels to allow the influx of sodium. The acquisition of blood meal will continue up to the average intake of blood which weighs the same as the unfed body weight. The estimated volume of the blood meal can be over four microliter. The acquisition of blood leads to the mechanical stretch of receptors in the abdomen and the suppression of the blood-feeding drive. The stretch receptors in the abdominal also prevent the over-distention during blood meals (Gwadz 1969). The large-volume blood meals have been considered an effective strategy to reduce the opportunity of being swatted by the hosts. However, multiple blood meals can still occur due to the interruptions during blood feeding and other further nutritional needs. Due to the high water content in each blood meal, blood-sucking insects also utilize the epithelium that is adapted for the rapid excretion of water in the midgut.

F. Midgut of adult mosquitoes

The anatomy of the insect guts generally can be differentiated into three sections; the foregut, the midgut and the hindgut. The midguts of blood-sucking insects can be classified into two groups based on the structure of the alimentary canal for the storage of the blood meal. The structure of the midgut of Hemiptera (true bugs) and Siphonaptera (fleas) is characterized of a simple tube with no diverticulae. Members of the diptera have one or multiple diverticulae as an additional structure for fluid storage (Eldridge and Edman 2003, Marquardt and Kondratieff 2005). The midgut with the *cardia* as its opening can be further divided into two different regions, the anterior midgut and the posterior midgut. The cardia is located at the junction of the foregut and midgut and consists of the tissues from the intersuscepted foregut and the midgut. The midgut is composed of a layer of epithelium above the basolateral membrane. The anterior midgut (AMG) contains densely packed microvilli and basal labyrinth upon the continuous layer of basal lamina. It has been suggested that the AMG is the absorptive epithelium with microvilli for the sugar from the diverticulum (Billingsley 1990, Zieler, Garon et al. 2000). The posterior midgut (PMG) exhibits the properties of both secretory and absorptive tissues. The apical surface of the PMG epithelium contains organized microvilli structure whilst the basal surface lies above

the basal membrane with polarized distribution of mitochondria. The abundant intracellular membrane organelles such as rough endoplasmic reticulum (rER) and Golgi reveals its capacity of secreting macromolecules. The digestion and absorption of blood meals in mosquitoes take place in the posterior midgut, which harbors the alkaline digestive conditions (Billingsley 1990, Marquardt and Kondratieff 2005). Starvation or feeding on an exclusive sugar diet led to the degeneration of such structures. The degeneration caused by starvation was irreversible (Bauer, Rudin et al. 1977). Additionally, histological observations also demonstrated the storage function of the PMG with the presence of glycogen and lipid deposits (Billingsley 1990). The digestion was performed simultaneously over the entire surface of the food bolus described as the batch system.

The biological functions of midgut can also be defined by the presence of different cell types and their morphologies. The epithelial cells confer the digestive functions by secreting large quantities of digestive enzymes. The morphologies of the membrane organelles in the PMG epithelium suggested the secretory functions of the midguts with the presence of large quantities of rER, especially in response to blood meals (Hecker and Rudin 1981). The morphologies of epithelial cells appear to be columnar prior to the ingestion of the blood meal. The cells undergo a substantial morphological change and turn squamous with convex internal border while the mosquito is engorged (Gooding 1972). The integrity of the cellular and tissue structures is maintained by the continuous junctions (*zonula continua*) on the later surface of the epithelium (Reinhardt and Hecker 1973). The formation and reorganization of the intracellular whorl structures have been suggested to be important for the synthesis and secretion of digestive macromolecules and peritrophic matrix (Bertram and Bird 1961, Zhou, Isoe et al. 2011). Additionally, the microvillar structure maximizes the surface which can be utilized to absorb nutrients. However, both the secretory and absorptive cell types are unable to be distinguished based on the histological morphologies. Alternatively, the other two additional cell types also exist in the midgut including the endocrine and regenerative cells. In *Ae. aegypti*, there are more than 500 endocrine cells making the midgut the largest endocrine organ with unknown physiological functions. Despite the presence of the regenerative cells, there is no active cell division in the midgut. Interestingly, the distribution of the endocrine cells has been reported to be concentrated on the PMG and found adjacent to the regenerative cells (Brown, Raikhel et al. 1985, Brown, Crim et al. 1986, Glattli, Rudin et al. 1987). Immunoelectron microscopic staining

demonstrated the cells with electron-lucent cytoplasm produce the vertebrate pancriptic polypeptide in *Ae. aegypti* (Glattli, Rudin et al. 1987). The other peptide hormone identified was FMRF-amide, which can also be found in the nervous tissue (Brown, Crim et al. 1986).

There is considerable knowledge on the digestive mechanisms required for the process of blood meals. The lysis of the red blood cells is one of the most important parts in digestion in order to obtain the high protein content in the meal. *Ae. aegypti* lacks the cibarial armatures required for the mechanical disruption of the red blood cells and achieves haemolysis by chemical means (Geering and Freyvogel 1975, Eldridge and Edman 2003, Marquardt and Kondratieff 2005). Haemolysins can be produced in the midgut or alternatively secreted by the salivary glands. Due to the high protein concentration of the blood meals, proteases and peptidases are the predominant digestive molecules released in the midgut. Multiple trypsin genes have been identified in the genome of *Ae. aegypti* (Kalhok, Tabak et al. 1993). Other enzymes such as chymotrypsins also facilitate the digestion of the blood meal (Jiang, Hall et al. 1997). The production of digestive enzymes occurs in large quantities after the blood meals and is regulated by the concentrations of the proteins in the blood meal (Noriega, Edgar et al. 2001). After the degradation of the protein components, the amino acid transporters are responsible to transport the amino acids through the midgut epithelial cells for other physiological processes (Evans, Aimanova et al. 2009). In spite of the negligible concentration of lipids in the blood meals, the triacylglycerol lipases have been identified in *Ae. aegypti*. The lipid components of the eggs were found to derive from the conversion of the amino acids into lipids (Geering and Freyvogel 1975).

1.3 Flaviviruses

A. Epidemiology and ecology

There have been at least 53 species identified and classified under the genus of flavivirus. According to the type of hematophagous arthropod vectors, the members of the flavivirus genus can be classified as mosquito-borne, tick-borne or no-known-vector flaviviruses. Based on the clinical manifestations, flaviviruses can further be categorized into two major groups, the encephalitic flaviviruses and the viscerotropic/hemorrhagic flaviviruses. The tick-borne flaviviruses consist of one major complex- the tick borne encephalitis virus (TBEV) complex infecting mammals with other members infecting seabirds (Gould and Solomon 2008).

The encephalitic group of mosquito-borne flaviviruses are mainly transmitted by *Culex* mosquitoes. In addition to the mammalian hosts, which are considered incidental low-viremic dead-end hosts, the avian species infected by the encephalitic mosquito-borne flaviviruses serve as the amplification hosts, which develop high-titer viremia to sustain the transmission. The transmission cycle of the viruses is summarized in Figure 1.2.

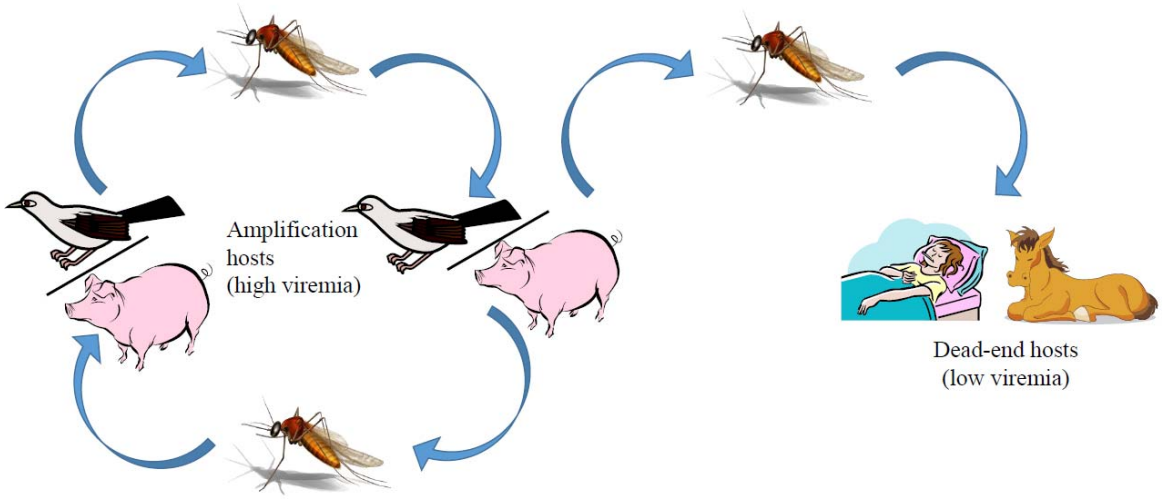

Figure 1.2 Transmission cycle of flaviviruses under the JEV-serocomplex

There are at least five mosquito-borne encephalitic flaviviruses associated with human diseases including JEV, WNV, SLEV, Kunjin virus (KUNV) and Murray Valley encephalitis virus (MVEV). JEV is estimated to cause 30,000-50,000 cases and 10,000 deaths per year.("WHO | Water-related diseases," n.d.) *Culex tritaeniorhynchys* serves as the primary vector in Asia. The unique ecology of JEV requires the swine species as the amplification host characterized by the high infection rate and the high viremia in the epidemic area and the maintenance host in the endemic area. Additionally, there have been more than 90 domestic and wild avian species that can be infected by JEV. There are three available vaccines- the live-attenuated 14-14-2 vaccine, the formalin-inactivated vaccine and the ChimeriVax-JE vaccine. (van den Hurk, Ritchie et al. 2009).

In North America, there have been several encephalitic arboviruses identified since 1930s. St. Louis encephalitis virus was once the most important mosquito-borne flavivirus throughout Canada and the United States (Weaver and Barrett 2004). Recently, SLEV has been reported to have a further expanded distribution to countries where to date, no known outbreaks were documented including Columbia and Argentina in Latin America (Mattar, Komar et al. 2011,

Valinotto, Barrero et al. 2012). *Culex* spp. mosquitoes have been shown to have varied susceptibility to SLEV. In western United States, it is believed that *Culex tarsalis* is the principle vector for SLEV; whereas *Culex pipiens quinquefasciatus* and *Culex nigripalpus* may be responsible for the transmissions in the east coast (Weaver and Barrett 2004). West Nile virus has become one of the most significant arboviruses for the human and veterinary public health in North America since its emergence in New York in 1999. There have been multiple species of *Culex* mosquitoes demonstrated to be competent for the transmission in North America. The transmission occurs most frequently in warmer months from July to October. The most common clinical presentation of WNV infection can be febrile illness. The incidence of its severe neurological diseases increases with age and the immunosuppression (Mackenzie 2002).

There are also two arboviruses, Murray Valley encephalitis virus (MVEV) and Kunjin virus (KUNV), in the JEV serocomplex isolated in Australia. Murray Valley encephalitis virus was described to be the potential etiological agent for the Australian X disease in the 1910s and 1920s. The maintenance of the virus relies on the enzootic cycle between the *Culex annulirostris* and the migratory waterbirds in the northern tip of west Australia. The spread of the virus is subjected to the flooded area due to the heavy rainfall and the routes of migratory birds. MVEV infection leads to febrile illness with the incidence of severe neurological diseases including fatal encephalitis between one in five hundred to one in one thousand cases (Knox, Cowan et al. 2012). The other etiological agent, KUNV, was first detected in northern Queensland in 1960 and is considered a subtype of WNV. However, asymptomatic infections and milder forms of diseases are more frequently seen in infected animals and humans. Severe fatal encephalitis is considered rare amongst the infected individuals. Kunjin virus also shares the vector *Culex annulirostris* with MVEV (Hall, Scherret et al. 2001).

The viscerotropic/hemorrhagic mosquito-borne flaviviruses cause significant mortality in the tropical and subtropical regions throughout the world. The two medically important viruses of such kind are DENV and YFV. Both viruses are transmitted by *Ae. aegypti* in its urban transmission cycle and have been reported to maintained in the sylvatic and jungle transmission cycles.**(Figure 1.3)** The jungle transmission cycle is maintained between the non-human primates as vertebrate hosts and jungle vectors that feed on non-human primates. The sylvatic transmission cycle is maintained by the vectors that feed on both non-human primates and humans, which come into contact with the vectors. The virus in the urban transmission cycles

alternates between humans and urban vectors. Although the sylvatic transmission is considered a critical component for the ecology of YFV, infections with DENV have largely been reported to be associated with urban transmission. Increased transmission, i.e. emergence and reemergence, have been attributed to rapid urbanization and other factors (Guzman, Halstead et al. 2010). The isolation of sylvatic DENV has only been described in specific locations in Brazil, Malaysia and West Africa, where the endemicity of DENV still lead to the higher number of cases in urban transmission (Diallo, Ba et al. 2003, Cardosa, Ooi et al. 2009, de Figueiredo, de et al. 2010).

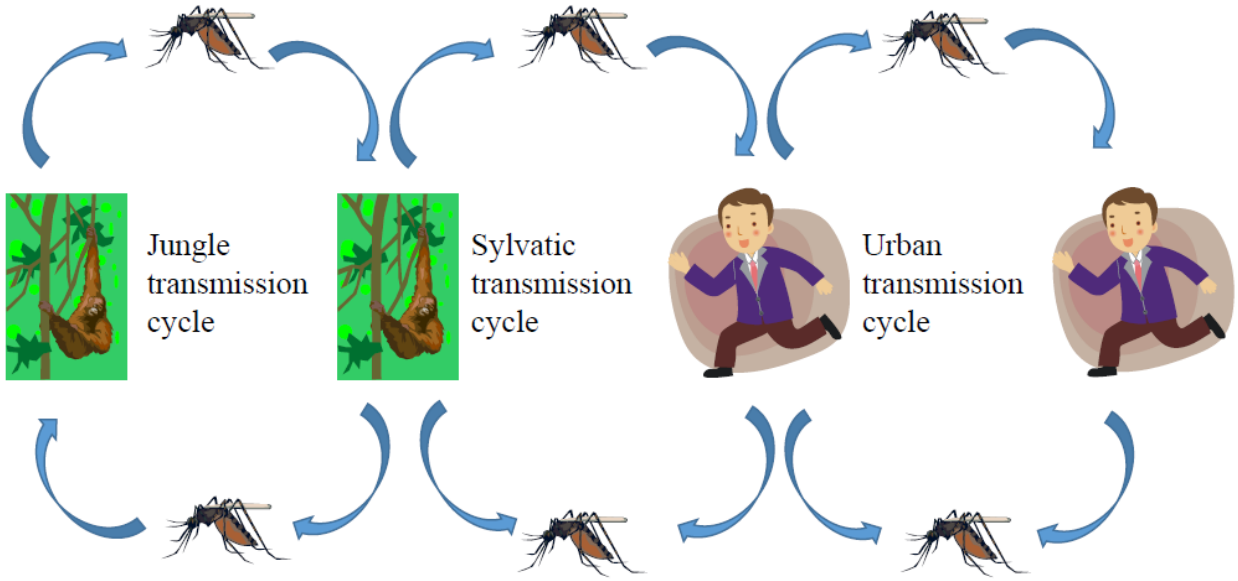

Figure 1.3 Transmission cycles of flaviviruses in YFV- serocomplexes

YFV is the first arbovirus transmitted by mosquitoes and considered to have public health significance. The virus can be transmitted in two ecologically distinct cycles, the urban cycle and the sylvatic cycle, both in Africa and central and south America. The mammalian hosts including nonhuman primates and humans are infected via the competent mosquito vectors which have previously fed on viremic hosts. In Africa, the sylvatic cycle can be maintained by sylvatic *Aedes* species such as *Ae. africanus*; whereas, the *Haemagogus* mosquitoes are the principle vectors for the sylvatic cycle in the central and south America (Monath 2001, Barrett and Higgs 2007).

The members of TBEV complex transmitted by ixodid ticks have been reported in both Europe and Asia. The biological transmission occurs through the secretion of contaminated saliva secreted by ticks. Six of the TBEV serocomplex members cause human diseases including the encephalitic Louping ill virus (LIV), tick-borne encephalitis virus (TBEV), the Langat virus (LGTV), Powassan virus (POWV) and the hemorrhagic Kyasanur Forest disease virus (KFDV)

and Omsk hemorrhagic fever virus (OHFV) (Gould and Solomon 2008). In addition to the infection through the blood meals from viremic hosts, the transmission of tick-borne viruses and pathogens can further be complicated by the prolonged period of feeding by ticks. Naïve ticks have also been reported to acquire the viruses through co-feeding on the same infected host (Labuda, Danielova et al. 1993, Hudson, Norman et al. 1995). Given the long lifespan of tick species, the infection can persist up to two years in infected ticks.

Since its first isolation in Russia leading to the name Russia spring and summer encephalitis virus (Levkovich 1945), there have been three subtypes of TBEV reported including the European TBEV-Eu transmitted by *Ixodes ricinus*, the Siberia (TBEV-Sib) transmitted by *Ix. persulcatus*, and Far Eastern (TBEV-FE) transmitted by *Ix. persulcatus*. TBEV causes the biphasic disease in humans. After the incubation period, the first viremic phase leads to the febrile symptoms, myalgia, general malaise and thrombocytopenia. The second phase is manifested by neurological symptoms from mild meningitis to severe encephalitis. Severe forms of the disease have been frequently reported in eastern Russia (Gould and Solomon 2008, Lindquist and Vapalahti 2008).

POWV is endemic in Canada and other parts of North America. The virus has been isolated from tick species in North America such as *Ixodes* spp. and *Dermacentor andersoni* (Hinten, Beckett et al. 2008). The virus can also be found in the Russian Far East although the actual mode of spread between two continents remains unclear (Deardorff, Nofchissey et al. 2013). LIV, the only tick-borne encephalitis virus in the British isles, is considered as a descendent of TBEV infecting sheep and red grouse through *Ix. ricinus* with limited numbers of human cases reported. However, the pathology of infected vertebrate hosts resembled that of human TBEV-infected cases (Davidson, Williams et al. 1991). Similar viruses have also been isolated in other parts of the European continent such as Spain and Greece (Gonzalez, Reid et al. 1987, Papa, Pavlidou et al. 2008). OHFV was first isolated in the Omsk region of Russia and can be isolated from *Dermacentor pictus* causing febrile illness, hemorrhage and leukopenia amongst infected individuals (Ruzek, Yakimenko et al. 2010). KFDV was first isolated from captured monkeys in India in 1957. It has been suggested the virus is maintained between the *haemaphysalis* spp. ticks and the forest animals (Gould and Solomon 2008, Holbrook 2012).

B. Intracellular lifecycle and molecular biology of flaviviruses

The transmission cycle of flaviviruses requires the viral particles to utilize cellular molecules and pathways that are expressed in arthropods, mammals and avians for virus entry and exocytosis. The successful establishment of infection by flaviviruses is initiated by the receptor binding through the viral envelope (E) protein followed by the viral and cellular membrane fusion in the acid endosomes (Chen, Maguire et al. 1997, Harrison 2008). The entry of flaviviruses has been demonstrated to predominantly depend on the clathrin-mediated endocytosis pathway (Krishnan, Sukumaran et al. 2007, Acosta, Castilla et al. 2008).

For single-stranded positive-sense RNA viruses, the viral genomes allow the translation of the host machinery in order to form the replication complex for the subsequent production of progeny virions. The 11-kilobase (kb) viral genome of flaviviruses encodes three structural genes, capsid (C), pre-membrane (prM), and E, and seven nonstructural (NS) genes, NS1, NS2A, NS2B, NS3, NS4A, NS4B and NS5. The 5' end of the viral genome is modified with the viral RNA cap structure but the 3' end of the viral genome lacks the polyA structure, which is common among the eukaryotic mRNA. The cap structure increases the stability of viral genome against the host nuclease digestion and functions as the immunomodulator antagonizing the host antiviral innate immunity (Daffis, Szretter et al. 2010). **(Figure 1.4(a))** The structure genes are the predominant components of the viral particles containing the viral genetic material. The nonstructural proteins function as enzymatic machineries for the propagation of the progeny viruses and antagonists for viral immunity. The translation of the genomic RNA leads to the production of a polyprotein, which is subjected to the cleavage of viral and host proteases (Chambers, Hahn et al. 1990).**(Figure 1.4(b))**

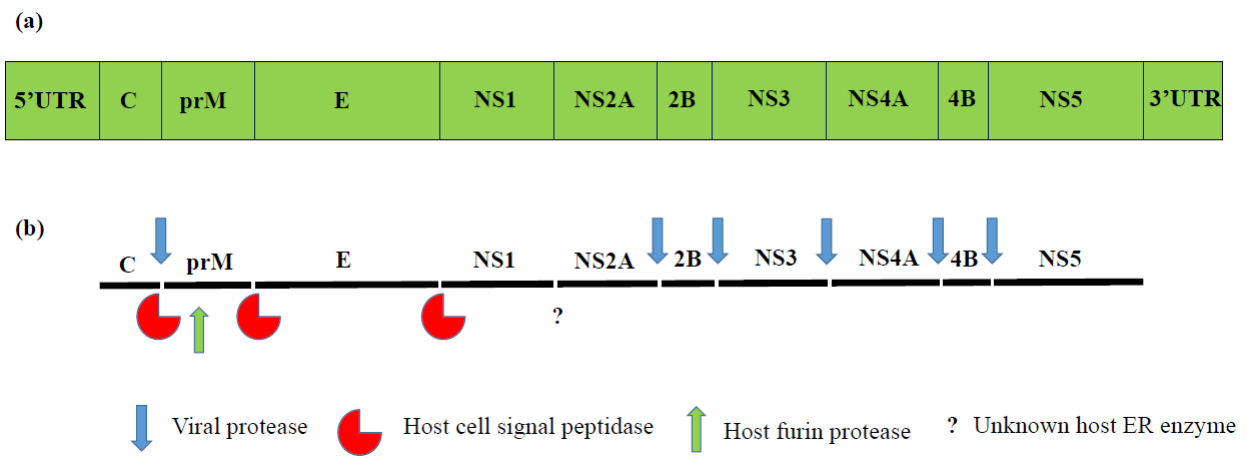

Figure 1.4 Genome organization and proteolytic processing of flaviviruses

The biochemical characterization has led to the discovery of several key enzymatic components for the viral replication complexes. The NS2B-NS3 complex forms the serine protease that is involved in the process of the viral polyprotein (Chambers, Weir et al. 1990, Chambers, Grakoui et al. 1991). The NS3 protein also has additional functions as RNA helicase and triphosphatase (Arias, Preugschat et al. 1993, Warrener, Tamura et al. 1993). The NS5 protein encodes the methylatransferase and the RNA-dependent RNA polymerase that catalyze the synthesis and modification of the viral genetic materials (Grun and Brinton 1986, Grun and Brinton 1987). The available evidence from immunostaining of the viral proteins and ultrastructure identified the replication complex of flaviviruses is likely to be located in the cytoplasm of infected cells, especially the perinuclear area and triggers the extensive formation of intracellular convoluted and vesicular membrane structures. However, several critical questions for functions of NS1, NS2A, NS4A and NS4B proteins remain unanswered. Although the large quantities of NS1 produced *in vitro* and *in vivo* and the antibody responses targeting the NS1 protein have been well documented in the available literature, its biological functions and contribution to disease pathogenesis remain unclear (Muller and Young 2013). NS2A, NS4A and NS4B proteins have been reported as immunomodulators that target the IFN-mediated antiviral signaling in the vertebrate hosts (Munoz-Jordan, Sanchez-Burgos et al. 2003). The membrane topology of NS2A protein has recently been reported and indicated its function is also critical for the viral particle assembly (Xie, Gayen et al. 2013). NS4B has been further demonstrated to block the transcription activation function of STAT1 protein in response to type-II IFN treatment (Munoz-Jordan, Sanchez-Burgos et al. 2003). Similarly, the degradation of STAT2 protein is mediated by the NS5 protein and the proteasomal degradation pathway (Ashour, Laurent-Rolle et al. 2009).

Virions are assembled in the endoplasmic reticulum (ER) and subsequently to the Golgi complex (Welsch, Miller et al. 2009). The gradient of pH between ER and the *trans*-Golgi network will allow the maturation of the viral particle and the cleavage of the pr peptide from the prM protein by furin will lead to the formation of the mature infectious viral particles ready for the release into the extracellular space (Zhang, Ge et al. 2013).

C. Envelope protein of flaviviruses

The flavivirus E proteins play significant roles in several steps of virus life cycle and have been extensively characterized. The protein consists of three discontinuous domains, domain I (EDI), domain II (EDII) and domain III (EDIII), based on the locations and functions (Rey, Heinz et al. 1995). The fusion property of flavivirus E proteins resembles other viral structural proteins under the category of class II fusion proteins (Harrison 2008). Although the crystal structure of YFV E protein has not yet been determined, the structures of several flaviviruses have been published. Although the overall structures of flavivirus E proteins resemble one another, minor and distinct variations in the structures exist. Functional characterization of the different domains of flavivirus E proteins provides the information critical for the understanding of the biology of the viruses as well as its application to develop preventive and therapeutic measures for the diseases. The pH-dependent conformational changes of E proteins in different cellular compartments are critical for the viral entry and the secretion of viral particles.

As the predominant component of the viron surface, 180 copies of E protein are arranged in the dimeric conformation in mature viral particles. In addition to the dimeric arrangement, the surface of viral particles contains 3-fold and 5-fold symmetrical units throughout the surface (Kuhn, Zhang et al. 2002). **(Figure 1.5)** The detailed 3D structure of flavivirus E protein is displayed and annotated in **Figure 1.6**. The EDI of flavivirus E proteins acts as a structurally central component, which has two β-sheets stabilized by the interior hydrophobic amino acids. The external β-sheet contains four β-strands $C_0D_0E_0F_0$ with a short A_0 β-strand that is parallel to the C_0 β-strand. The interior β-sheet faces the viral membrane and consists of four β-strands $G_0H_0I_0B_0$ (Kuhn, Zhang et al. 2002, Zhang, Zhang et al. 2004). EDII stabilizes two neighboring monomers through the dimerization domain and contains the fusion peptide that mediates the viral membrane fusion. The finger-like structure of EDII consists of the two large loop regions between β-strands D_0 and E_0 as well as H_0 and I_0. The base component of EDII contains five short β-strands GFEAH arranged in the antiparallel fashion and two α-helices αB and Aa; whereas, the elongated structure is stabilized by three disulfide bonds within the three-β-strands sheet BDC. Most importantly, the fusion loop is located in the cd loop at the tip of the domain and largely conserved among flaviviruses with its hydrophobicity (Rey, Heinz et al. 1995, Allison, Schalich et al. 2001). The binding of cellular receptors is mediated by EDIII (Chen, Maguire et al. 1997). The overall structure of EDIII shares an IgG-like fold and contains three β-

sheets. The NMR structure of YFV EDIII has been available and showed the gross similarity to other flaviviruses with minor differences. The first β-sheet is made of four β-strands ABDE and faces domain I and domain II. Two short β-strands Cx and Dx form the second β-sheet. And, β-strands CFG form the third β-sheet (Volk, Gandham et al. 2007, Volk, May et al. 2009).

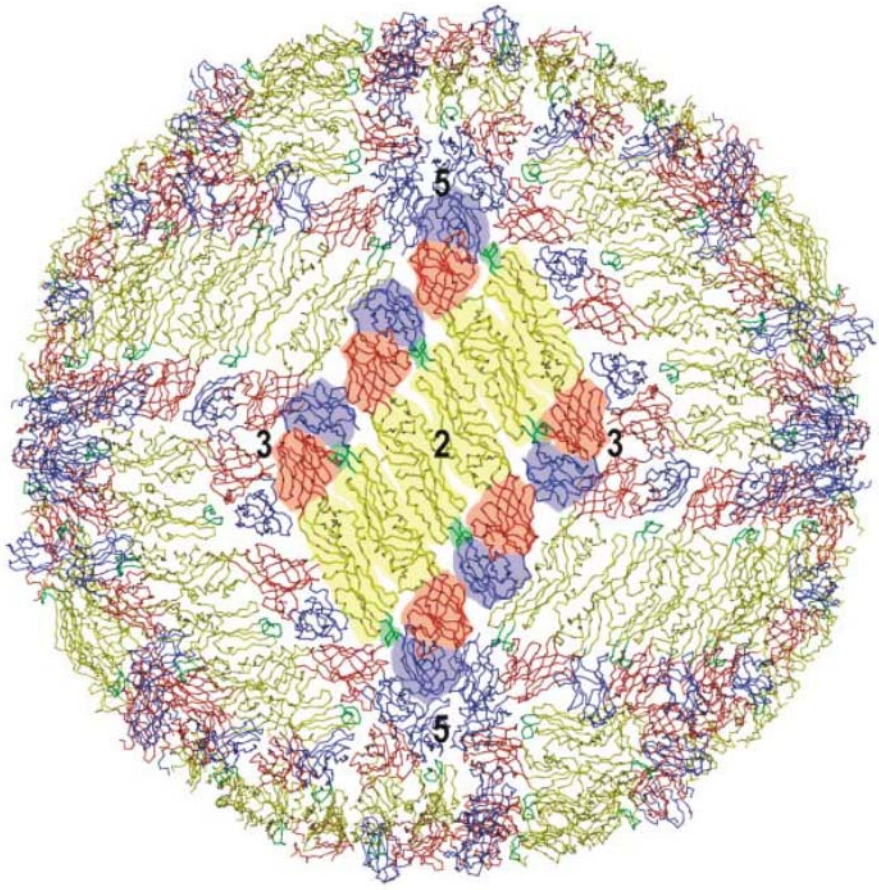

Figure 1.5 Structures of the flavivirus virion based on the Cryo-electron microscope (Cryo-EM) reconstructed images. (adapted from Zhang et al., 2004))
The surface of the virion is covered by 180 copies of flavivirus E protein monomers, which are dimerized to create 90 copies of dimers and the two-fold symmetric units. The three-fold and five-fold symmetric units can also be found by the neighboring monomers of flavivirus E protein. Three distinct domains displayed above are labeled with three different colors. EDI, the central domain, is labeled in red. EDII, the dimerization domain, is labeled in yellow with the fusion loop structure highlighted in green. EDIII, the receptor-binding domain is labeled in blue.

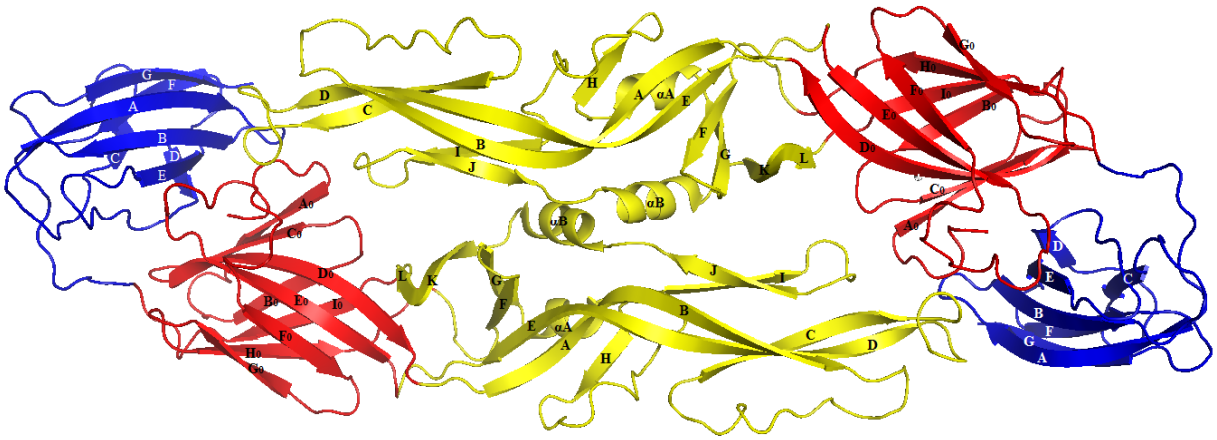

Figure 1.6 The crystal structure of flavivirus E protein (adapted from Modis *et al*., 2004) The crystal structure of flavivirus E protein is displayed as the dimerized structure. Three domains are labeled with distinct colors, EDI in red, EDII in yellow and EDIII in blue. The two β-sheets of EDI, $C_0D_0E_0F_0$ and $G_0H_0I_0B_0$, are annotated. EDII is composed of two β-sheet structures, GFEAH and BCD, and two α-helices, αA and αB. The two major β-sheets, ABED and CFG, of EDIII are labeled in blue.

The viral entry requires the transition from the dimeric conformation to the trimeric conformation in the endocytosis pathway. Such conformational change is triggered by the acidic environment of the endosomes and allows the insertion of the fusion peptide to protrude from the viron surface into the cellular membrane in order to bring both viral and cellular membranes into close proximity (Nawa 1997, Harrison 2008). The fused membranes allow the release of viral genome into the host cells.

The viral particles are assembled first in the immature form with the envelope proteins arranged in trimeric conformations. The fusion peptide is protected by the pr peptide of the prM protein. The prM protein functions as a chaperon protein for the E protein in the process of virion maturation. The maturation process is mainly triggered by the decrease of pH in the secretory pathways and critical for the production of infectious viral particles (Yu, Zhang et al. 2008). In

the acidic environment of trans-Golgi network, the viral particle is covered by the dimers of E protein on its smooth surface as oppose to the spiky virion surface in the immature virions (Zhang, Corver et al. 2003). Prior to the release into the extracellular space, the host furin protease removes the pr peptide producing the infectious viral particles.

Given its importance of viral infectivity and particle assembly in both mosquitoes and vertebrates *in vitro* and *in vivo*, the E proteins have been extensively tested for the vector competence. The genetic determinants of viral infection and dissemination have been found in flavivirus E proteins. The YFV E protein was demonstrated to contain the determinants for viral infection and dissemination in *Ae. aegypti*. Chimerization of the EDI and EDII region of YFV 17D strain to the backbone of Asibi strain reduced the viral infectivity; whereas, the EDIII of the Asibi strain was found critical for the viral dissemination in orally infected mosquitoes (McElroy, Tsetsarkin et al. 2006). For WNV, in addition to the potential alterations in amino acid sequences and secondary structures, the N154I mutation which abolished the N-linked glycosylation site, led to the reduced viral infection and dissemination in *Cx. quiquefasciatus* (Moudy, Payne et al. 2011). The T329A mutation in the EDIII of DENV-1 selected by the antibody escape was shown to increase the viral infectivity in *Ae. aegypti* (Shrestha, Austin et al. 2012). The EDI-EDII molecular hinge region and the FG-loop in EDIII were mapped to be the critical parts of the viral infectivity of DENV-2 in *Ae. aegypti* (Erb, Butrapet et al. 2010, Butrapet, Childers et al. 2011).

In addition to the importance in the cellular, molecular and structural biology of flaviviruses, the flavivirus E proteins have also been studied extensively as an immunogen for the humoral immunity response in vertebrate hosts. The study of B-cell epitopes on the flavivirus E proteins was first performed on yellow fever virus in order to distinguish the vaccine and wild-type viruses (Schlesinger, Brandriss et al. 1983). Flaviviruses E proteins, especially EDIIIs, later have been proved to elicit the protective antibody responses, which were further utilized to develop the therapeutic humanized monoclonal antibodies or subunit vaccine candidates (Oliphant, Engle et al. 2005, Clements, Coller et al. 2010, Shrestha, Brien et al. 2010, Sukupolvi-Petty, Austin et al. 2010). The studies were further expanded to other flaviviruses and the cross-reactive antibodies targeting the homologous sequences and structures of flavivirus E proteins (Gould, Buckley et al. 1985). The B-cell epitopes on YFV E protein have been found critical for the attenuation of YFV 17D strains. These vaccine epitopes are the determinants for the

virulence of various YFV strains *in vivo* (Sil, Dunster et al. 1992, Ryman, Xie et al. 1997). Interestingly, the immunogenicity of YFV 17D strains led to the repertoire of antibodies that target multiple neutralization epitopes, which retained the neutralizing capacities towards the neutralization escapes of 17D strains that contain several genetic substitutions (Daffis, Kontermann et al. 2005).

The extensive studies on flavivirus E proteins are expected to generate the information which is critical for vaccine development. The reverse genetic systems of flaviviruses based on the cDNA infectious clones and the infectious positive-sense viral RNA have also further fostered the functional characterization and mechanistic studies at the level of individual domains or amino acids. The currently available flavivirus vaccines and vaccine candidates are reviewed in the **section 1.3.D**. The reverse genetics system of flaviviruses is reviewed in the **section 1.3.E**.

D. Vaccines for flaviviruses

Currently, there are no specific antiviral therapies targeting mosquito-borne arboviruses. Therefore, vaccination and vector control still remain as the most effective public health measures for disease control and prevention. Several vaccines have been used to successfully control disease mortality and morbidity. The first success in generating live-attenuated flavivirus vaccines took place in 1937 through the serial passage of virulent YFV Asibi strain (Theiler and Smith 1937). Members of JEV serocomplex have been recognized as threats to both human and animal health and three human vaccines for JEV and several animal vaccines for WNV have been available. However, with the most significant amount of disease burden, mortality and economical loss, different DENV vaccine candidates are still in various stages of clinical trials. The currently available vaccines and vaccine candidates for flaviviruses are summarized in table 1.2.

Virus	Vaccine	Availability
YFV	Live-attenuated YFV17D strains produced from chicken embryos	Manufactured and available worldwide for human use
JEV	Live-attenuated SA_{14}-14-2 strain	Manufactured in China and available in Asia for human use
	Inactivated Ixiaro® vaccine based on SA_{14}-14-2 strain	Licensed in the United States and the European Union for human use
	Inactivated JEBIKV® vaccine and ENCEVAC® based on Beijing-1 strain	Manufactured and approved in Japan for human use
DENV	Live-attenuated chimeric vaccine based on ChimeriVax®	Phase III clinical trial in progress
	Live-attenuated tetravalent chimeric vaccine based on DENVax®	Phase II clinical trial in progress
	Live-attenuated tetravalent chimeric vaccine based on DENV-4-3'-Δ-30	Phase II clinical trial in progress
WNV	Formalin-inactivated WNV	Available in the United States for equine use
	Recombinant WNV based on the poxvirus vector	Available in the United States for equine use
TBEV	Formalin-inactivated TBEV purified from chicken embryos	Available in western Europe and Russian for human use

Table 1.2 The list of current available vaccines or vaccine candidates for flaviviruses

The YFV 17D vaccine was attenuated from its parental virulent Asibi strain through 176 passages in mouse brain and chicken tissues. The 17D vaccine strain has lost its viscerotropism in both non-human primates and vacinees (Smith and Theiler 1937, Theiler and Smith 1937, Theiler and Smith 1937). Additionally, the 17D vaccine strain has been repeatedly showed to be non-biologically transmissible by *Ae. aegypti*; whereas, the Asibi strain rapidly disseminates into

the salivary glands and is readily infectious to immunologically naïve non-human primates (Whitman 1937, Miller and Adkins 1988, McElroy, Tsetsarkin et al. 2005). The human immune responses to the 17D vaccine strain can potentially persist up to 35 years demonstrated by the presence of neutralizing antibodies (Poland, Calisher et al. 1981). There have been more than 540 million doses of the YFV 17D vaccine administered worldwide in human history. Although the vaccine-associated adverse effects have been report, the YFV 17D vaccine is still considered the one of the most successful live-attenuated vaccines in human history (Barrett and Teuwen 2009). The use of the YFV 17D vaccine has been further expanded to the field of viral vaccine candidates with molecular manipulations (Van Epps 2005). However, YFV 17D vaccine strain is not the only vaccine developed for YFV. Several other YFV vaccine viruses, including YFV 17DD and YFV FNV have also been developed and will be discussed in the **section 1.4.B**.

There have been two vaccines available for JEV, the mouse-brain-derived vaccine and the SA_{14}-14-2 live-attenuated vaccine. The mouse-brain-derived JEV vaccine requires three doses to achieve acceptable immunogenicity with several cases of vaccine-associated adverse effects (Darwish and Hammon 1966). The live-attenuated SA_{14}-14-2 vaccine has been given to more than 120 million children with negligible transient reactogenicity (0.2~6%) in China alone. In the United States, Australia and Europe, the IC51 vaccine obtained by passaged in primary dog kidney cells for eight times has been licensed and manufactured in the serum-free format. The SA_{14}-14-2 strain has also been used as the strain providing genetic materials for the development of the chimeric JEV vaccine candidate based on the backbone of the YFV 17D vaccine strain (Halstead and Thomas 2010). Since the introduction of WNV into the United States in 1999, there have been several veterinary vaccines approved for use in equine species including the formalin-inactivated whole-virus vaccine (WN-Innovator®; Fort Dodge Animal Health, KS, USA), the recombinant canarypox-vectored vaccine (Recombitek®equine Rwnv; Merial, GA, USA), the YFV-17D-based chimeric vaccine (PreveNile®; Invertec Inc., DE, USA) and the DNA vaccine expressing the prM and E proteins of WNV (West Nile-Innovator®DNA; Fort Dodge Animal Health, KS, USA). The human vaccines for WNV are currently undergoing different phases of trials including the YFV-17D-based chimeric vaccine (ChimeriVax®-WN02, Sanofi-Pasteur), the live-attenuated vaccine based on the DENV-4 backbone (WN/DENV-4-3'Δ30; National Institute of Allergy and Infectious Diseases(NIAID), MD, USA), the WNV prM-E

DNA vaccine (Vical Inc., PA, USA and NIAID), and the subunit truncated E protein vaccine (HBV-002; Hawaii Biotech, HI, USA) (Beasley 2011).

Due to the frequent epidemics, high number of cases and wide geographic distribution, vaccines development for DENV has been a priority but for various reasons has been problematic. Several candidate vaccines are still being tested at different phases in various locations worldwide. The vaccine candidates that are currently evaluated in different phases of clinical trials are summarized in **table 1.3**. The recombinant ChimeriVax dengue tetravalent vaccine (Sanofi Pasteur) based on the YFV 17D vaccine backbone has recently completed the phase 3 clinical trial but requires the extended dosing schedule in order to achieve the level of protection. However, the tetravalent vaccine only provides partial protection to three of the four serotypes of DENV (Guy, Barrere et al. 2011, Sabchareon, Wallace et al. 2012). Similarly, NIAID has also utilized the recombinant DNA technology to produce the chimeric tetravalent vaccine based on the DENV-4 virus with the deletion in its 3' untranslated region (UTR), which is currently undergoing the Phase 2 clinical trial with specific formulations (Durbin, Kirkpatrick et al. 2013). The other molecular-biology-based tetravalent vaccine based on the cDNA infectious clone of the attenuated DENV-2 16681-PDK53 strain as its backbone is tested at the stage of the Phase 1 clinical trial (Osorio, Huang et al. 2011). In addition to the reverse-genetics-based vaccine candidates, the subunit vaccine based on the N-terminal 80% region of the E protein of four serotypes of DENV (Hawaii Biotech, HI, USA) is going through Phase 1 clinical trial (Clements, Coller et al. 2010).

Vaccine candidates	Property	Platform	Progress in clinical trials
ChimeriVax® dengue tetravalent vaccine	Live-attenuated	ChimeriVax® technology based on YFV 17D strain	Phase III clinical trial
DENVax® dengue tetravalent vaccine	Live-attenuated	DENVax® technology based on DENV-2 PDK53 strain	Phase II clinical trial
TV003 dengue tetravalent vaccine	Live-attenuated	DENV-4-3'-Δ-30 attenuated strain based on the deletion of 3' UTR	Phase II clinical trial
80E dengue tetravalent vaccine	Subunit	Insect cell expression of N-terminal 80% of the E protein	Phase I clinical trial
D1ME100 dengue	DNA vaccine	Naked plasmid DNA containing DENV-1 prM and E genes	Phase I clinical triall

Table 1.3 The vaccine candidates currently undergo clinical trials

The complicated process of developing flavivirus vaccines has led to the important discoveries and advancement in knowledge and experience that are also applicable to the production of vaccines against other mosquito-borne viruses primarily under *Togaviridae* and *Bunyaviridae*. Such vaccines and vaccine candidates are briefly discussed in the following paragraphs.

Similar to the YFV 17D vaccine strain, the VEEV TC83 vaccine strain virus was also attenuated by 83 *in vitro* passages through the guinea pig heart cells. However, the limited numbers of mutations throughout the viral genome has led to the potential concern of reversion. Additionally, the TC83 vaccine strain virus has been reported to be isolated from the vectors in nature.(Pedersen, Robinson et al. 1972) Currently, the TC83 vaccine of VEEV is limited for

human use as investigational new drug (IND) in the United States (Berge, Gleiser et al. 1961). Chikungunya virus strain AF15561, originating from strain 15561was plaque-to-plaque purified in the MRC-5 cells in order to produce the attenuated strain CHIK 181/clone25 (Levitt, Ramsburg et al. 1986). The attenuated strain completed the Phase 1 and the Phase 2 of its clinical trial but led to arthralgia in 8% of the vaccinees despite of the fact that the vaccine showed the advantage of the limited potential of being transmitted by mosquitoes (McClain, Pittman et al. 1998, Edelman, Tacket et al. 2000).

The demand from both the perspectives of human and veterinary public health has led to several vaccine candidates for RVFV with different strategies. The formalin-inactivated TSI-GSD-200 vaccine has been given to veterinarians and laboratory personnel who are at the risk of exposure. However, the vaccine has not achieved the immunogenicity as the live-attenuated viral vaccines and requires a six-month schedule for initial vaccination followed by the annual boosters (Kark, Aynor et al. 1982, Kark, Aynor et al. 1985, Pittman, Liu et al. 1999). The MP-12 live-attenuated vaccine for RVFV was produced by the serial passage of the ZH548 virulent strain in the presence of 5-fluorouracil (Caplen, Peters et al. 1985, Morrill, Carpenter et al. 1991). The vaccine protected the animals from the subsequent challenges in experimental animals. Recently, the vaccine was evaluated in the Phase 2 clinical trial for potential human adverse effects. The Clone13 isolate carrying deletion in the NSs genomic fragment is currently being tested for the use as a veterinary vaccine. The clone13 reassortant R566 strain which contains the L and M genomic fragments of the MP12 vaccine has also been evaluated for its veterinary use (Dungu, Louw et al. 2010).

The unique transmission cycles of flaviviruses and other arboviruses complicates the issue of disease control, especially with the presence of natural reservoirs and disease vectors. Although several vaccines have been available in different formats, the two live-attenuated vaccines, YFV 17D vaccines and JEV SA_{14}-14-2 vaccine, are still the most efficacious tools and lead to long-term protective immunity. Therefore, the development of live-attenuated vaccine candidates for flaviviruses has become one of the most important fields of virology and vaccinology. As detailed below, the reverse genetics systems now available has further facilitated the advancement in the field with the newly developed approaches to chimerize and introduce immunogenic components on the backbones of several attenuated flaviviruses such as

ChimeriVax® and DENVax®.(Pugachev, Guirakhoo et al. 2005) The reverse genetics systems for flaviviruses are reviewed in the following section.

E. Reverse genetics systems for flaviviruses

The positive-sense genomic RNA of flaviviruses and other small RNA viruses allow the production of viral particles by the transfection of viral RNA derived from cDNA infectious clones. The production of viral RNA can often be achieved by the *in vitro* transcription of cDNA fragments that contains the viral genome with bacteriophage DNA-dependent RNA polymerases and the appropriate promoters. The bacterial plasmid or artificial chromosome systems allow the propagation of such cDNA materials and the manipulation of specific residues or fragments of the genetic materials. The cDNA infectious clone of poliovirus was the first reverse genetics system available for the molecular manipulation of genomes amongst human single-stranded positive-sense RNA viruses (Racaniello and Baltimore 1981). Several variants of the methodologies such as the multi-plasmid systems coupled with *in vitro* ligation of nucleic acids and the introduction of intron sequences have been developed to overcome technical obstacles including the toxicity of viral genetic materials to the bacterial system and the instability of the sequences propagated in bacteria (Sumiyoshi, Hoke et al. 1992, Yamshchikov, Mishin et al. 2001, Messer, Yount et al. 2012).

The current one-plasmid reverse genetics system for YFV was modified from the original two plasmid system (Rice, Grakoui et al. 1989). The two-plasmid system was adopted due to the toxicity of the viral genome to the bacterial host and the laborious procedures for the λ phage-based full-length YFV cDNA clones. The stable infectious clone was established based on the cDNA derived from the YFV 17D strain and the low-copy pANCR1180 plasmid (Bredenbeek, Kooi et al. 2003). Through the amplification of the cDNA of the Asibi virus, the infectious clone of the virulent Asibi strain was developed and characterized. The phenotype of the Asibi virus derived from the infectious clone resembled the phenotype of the original virus (McElroy, Tsetsarkin et al. 2005). In addition to its application in studying the pathogenesis and the biology of YFV, the reverse genetics system of YFV has also been used to develop the chimeric flavivirus vaccines for various flaviviruses (Monath, Soike et al. 1999).

Shortly after the infectious clone of YFV was available, the infectious clones of DENV were developed. The viral genome of DENV-4 strain 814669 was the first cloned into the

pBR332 plasmid for the development of its infectious clone (Lai, Zhao et al. 1991). The neuro-adapted DENV-2 New Guinea C strain was also recovered from the T7-promoter-based *in vitro* transcribed RNA (Kapoor, Zhang et al. 1995). The infectious clone of DENV-2 16681 strain and the attenuated PDK-53 strain were developed and utilized as the backbone for the chimeric live-attenuated vaccines for other serotypes of DENV (Kinney, Butrapet et al. 1997).

The construction of infectious clones for JEV-serocomplex members was initially performed on multi-plasmid systems and *in vitro* ligation. The first JEV cDNA infectious clone was developed by *in vitro* ligating two cDNA fragments followed by the transcription of the full-length cDNA. However, the genome of JEV was found highly unstable in *E. coli* and the infectious clones of JEV were further optimized by the introduction of intron and the use of very-low-copy-number plasmid (Yamshchikov, Mishin et al. 2001, Zhao, Date et al. 2005). Similarly, WNV infectious clones have also been developed with the low-copy-number plasmids (Yamshchikov, Wengler et al. 2001, Shi, Tilgner et al. 2002).

The reverse genetics systems of flaviviruses provide a convenient platform for the production of viruses that can be easily manipulated in the genomic sequences. It has been used in the production of vaccine candidates for different flaviviruses by chimerizing the structural genes of flaviviruses with the backbone of YFV 17D strain or DENV-2 PDK-53 strain (Monath, Soike et al. 1999, Osorio, Huang et al. 2011). Several mechanistic studies based on the cDNA infectious clones and mutagenesis techniques have also provided the critical knowledge in identifying the genetic determinants for the disease pathogenesis.

1.4 Yellow fever virus

A. Epidemiology

Historically, yellow fever (YF) has also been described in various terms such as “black vomit”, “yellow jack”, and “king of terrors”, which describe the severity of diseases and symptoms as well as the consequences of infection in humans (Calisher 2013). Whilst the 17D vaccines are readily available, its etiological agent YFV is still categorized under the risk group three and required to be handled in the biosafety level 3 laboratories by the National Institutes of Health and Centers for Disease Control and Prevention (Chosewood, Wilson et al. 2009). The estimated numbers of YFV infection and fatal cases are 200,000 and 30,000 worldwide by WHO.

Currently, 900 million people are living at the risk of contracting the disease in the endemic tropical regions of Africa and Latin America (WHO 2014).

YFV was first hypothesized to be transmitted through mosquito bites by Carlos Finlay and subsequently became the first arbovirus recognized to be medically important (Chamberlain 1982). In a series of experiments by the U.S. Army yellow fever commission led by Walter Reed and others, the transmission was proved to require two key factors, the feeding of disease vectors on viremic hosts and the extrinsic incubation period prior to the transmission to another immune-naïve host (Bauer and Hudson 1928). Multiple vertebrate and mosquito species are involved in the maintenance and transmission of YFV and the epidemiological studies of yellow fever virus demonstrated the virus is maintained in three cycles in Africa and two cycles in south America, respectively (Barrett and Monath 2003, Barrett and Higgs 2007). In the urban cycle, the major vector for its transmission is *Ae. aegypti* feeding on viremic humans. The laboratory transmission of YFV by *Ae. aegypti* led to the misconception that YF is exclusively an urban disease, however, this was prior to the discovery of the jungle and sylvatic intermediate cycles. Other *Aedes* and *Haemagogus* spp. feeding on non-human primates in the jungle are responsible for the transmission of the jungle cycle reported in Africa and South America (Anderson and Osorno-Mesa 1946, Smithburn and Haddow 1946, De Rodaniche, Galindo et al. 1957).

The primates in the jungle cycles of Africa and South America are responsible for the maintenance of the virus in nature but show distinct consequences of infection. In Africa where YFV originated, non-human primates normally do not succumb to the infection; whereas, in South American where YFV was introduced in the 1800, infection of the indigenous primate species is typically fatal. Serological surveys demonstrated the high prevalence of YFV antibodies in baboons (*Papio* spp.) and grivet monkeys (*Cercopithecus* spp.) in Africa (Taylor, Haseeb et al. 1955). *Colobus* monkeys in Africa have also been demonstrated to be susceptible to YFV infection (Woodall, Dykes et al. 1968). Although *Galago* species exist in high abundance, the low seropositive rates suggested the less involvement of transmission (Taylor, Haseeb et al. 1955). The repeated virus isolation and high antibody prevalence in South American howler monkeys showed their importance in supporting virus transmission in the jungles of South America (Laemmert and Kumm 1950, Downs, Anderson et al. 1955, Mendez, Parra et al. 2007). The jungle cycle is primarily sustained by the biting behaviors of canopy-dowelling mosquitoes and primates. The jungle cycle in Africa has been found to be maintained by the principal vector

Ae. africanus (Smithburn, Haddow et al. 1949, Henderson, Metselaar et al. 1970). In 1938, *H. leucocelaenus* and *H. capricorni* were first reported to be susceptible to YFV infection (Shannon, Whitman et al. 1938). *Sabethes chloropterus, H. janthinomys* and other *Haemagogus* mosquitoes were later found to be vectors for the jungles of South America (De Rodaniche, Galindo et al. 1957). Human infections can be incidental and sometimes considered an occupational disease amongst people with histories working in the forest.

In addition to the jungle cycle, transmissions in the intermediate cycles in Africa happen in the areas with the presence of both human and non-human primates characterized by the focal outbreaks spaced by the areas without the presence of humans. The intrusion of human activities into areas where the jungle cycles take place initiates the spillover of virus from primates to humans. *Ae. luteocephalus, Ae. furcifer, Ae. metallicus, Ae. vittatus, Ae. opok, Ae. taylori* and members of *Ae. simpsoni* complex have been discussed in the literatures for the potential as vectors in the intermediate cycle (Lee and Moore 1972, Germain, Francy et al. 1980, Barrett and Higgs 2007).

The mechanisms that are responsible for the absence of YF outbreaks in Asia remain unclear. Although *Ae. aegypti* has been known as the vector for both DENV and YFV and the *Ae. aegypti* in Asia has been found susceptible to YFV, other epidemiological and ecological conditions ought to be taken into account (Tabachnick, Wallis et al. 1985). Gould *et al.* has proposed several hypotheses including the lack of sylvatic YFV transmission and the differences in disease severities which may impede the long-distance transmission of YFV (Gould, de Lamballerie et al. 2003). The experimental evidence of the viscerotropic YFV hamster model suggested that cross protections can also provide a plausible explanation, especially with the high incidence of DENV and JEV in Asia (Xiao, Guzman et al. 2003). Other alternatives were also proposed based on the relative viral fitness between DENV and YFV *in vitro* (Amaku, Coutinho et al. 2011). However, other evidence also challenge the hypothesis, for example, the reports of sylvatic transmissions of DENV and other flaviviruses suggesting the presence of potentially susceptible vectors and non-human primates due to the genetic homology between DENV and YFV and the shared use of vector species. However, the vertebrate hosts and the proposed vectors for the sylvatic transmission of DENV have not been challenged with YFV and whether the vertebrate hosts are susceptible to YFV or the vectors are competent for transmission remains unclear.

B. History of YFV

Although it is now regarded as a rare and exotic disease for the United States, historically epidemics caused by YFV were documented as far north as Boston and other parts of New England throughout the history of United States. However, the geographic distributions of the diseases were mostly restricted to the southern United States, especially the major port cities (Patterson 1992). One of the earliest notable outbreaks of YFV took place in Philadelphia, which was the largest city in the United States, in 1793. However, prior to such epidemic, the city has at least three epidemics in 1699, 1741 and 1762 (Foster, Jenkins et al. 1998). In 1874, Memphis Tennessee experienced the largest YF outbreak in the history of United States leading to 20,000 cases distributed along the Mississipi River (Wright 2001). The most recent notable outbreak happened in New Orleans Louisiana in 1905.

Prior to the 1930s in the 20th century, the virus has been isolated and subsequently used for the tests for the vaccine development and human immunity. The etiological agent was further confirmed using the laboratory model of *Macacus sinicus* that succumbed following the inoculation of viremic blood and had no detectable *Leptospira icteroides* (Stokes, Bauer et al. 2001). Two of the most important strains for vaccine production, the Asibi strain from a West African survivor of YF infection and the French viscerotropic strain, were isolated in 1920s. The Asibi strain later became the starting material in the serial passage experiments by Max Theiler to produce the attenuated 17D strain (Smith and Theiler 1937).

In 1949, the first isolation of YFV in 43 years took place in Panama followed by the expansion towards the border between Guatemala and Mexico in 1957, leaving 315 identified cases (Elton 1955). Interestingly, this epidemic also led to the discovery that the *Haemagogus* vectors are competent for the transmission in the western hemisephere in the laboratory established by the Rockefeller foundation in Trinidad. During this period, YFV epidemics were absent due to the comprehensive immunization campaigns in the French West and Equatorial Africa (Peltier 1947). However, the immunological naïve population in the British colonies including Ghana and Nigeria suffered from the outbreaks between 1950 and 1952 leading to at least 12,000 cases and 500-600 deaths during the single outbreak in the Jos Plateau (WHO 2014). In this epidemic, the knowledge that *Ae. africanus* feeds at the ground level and can be isolated in the household was established. In the early 1960s, the southwestern Ethiopia of East Africa was swept by the virus causing about 30,000 fatal cases with the estimated infection rate

at 10% of the total population in two years and recognized as the largest outbreak in history (Tignor, Casals et al. 1993). In West Africa, the termination of the vaccination with the French neurotropic vaccine amongst the children at the age of 10 led to the decision of reformulation for the pediatric vaccines to the 17D vaccine due to the severe neurological adverse effects (Macnamara 1953, Frierson 2010). The decade was concluded with an extensive epidemic affecting parts of Mali, Burkina Faso, Togo, Ghana and Nigeria leaving an estimated number of 100,000 infections in the area. Throughout the 1960s, in addition to the *Ae aegypti* which constantly was responsible for the transmission, the vectoring by *Ae luteocephalus*, *Ae africanus* and *Ae vittatus* was also observed (Lee and Moore 1972, Germain, Francy et al. 1980). In Latin America, the traditional boundaries of YFV were challenged in the 1960s by the reported cases between Brazil and Argentina due to the epizootic outbreaks. The jungle cycle of YFV can only be partially controlled by the vaccination among residents in the rural areas; whereas, the control of the urban YF can be achieved by the eradication of *Ae. aegypti* in the cities (Monath 1999). The control measures based on eliminating the breeding sites of *Ae. aegypti* were initiated by the International Health Commission of the Rockefeller Foundation, proved highly successful for disease control in Ecuado in 1918 (Strode and Rockefeller Foundation. International Health Division. 1951). Since the 1930s, the initiation of *Ae. aegypti* eradication has originated from Brazil and further expanded to other countries in the Americas. The success of joint disease control efforts by the Brazilian federal government and the Rockefeller Foundation was compromised by the reinfestation of border territory by *Ae. aegypti*, which further led to the proposal for much wider collaborative effort of vector eradication in multiple countries in 1947. The multinational campaign was approved by the Pan America Health Organization and maintained due to the constant threat of jungle YF reported in five to eight countries each year (Soper 1963, Soper 1967). Such campaigns were not only helpful for the control of YF but also led to the control of other arboviral diseases, especially dengue fever (DF) (Schliessmann 1967).

In 1971, the virus reemerged in Angola after its long period of silence for the last 99 years leaving 65 cases with 42 deaths. However, the serological evidence suggested the underestimation by finding at least 13% of the urban population were seropositive (Pinto and Filipe 1971). In Gambia between 1978 and 1979, the Chinese contract physicians first reported the jaundice and fatal cases leading to the discovery of an epidemic causing at least 8,400 cases and 1,600 deaths. It was the first outbreak providing the epidemiological insight of the

asymptomatic and symptomatic infections of YFV, the vulnerability of the immunologically naïve Gambian population to the epizootic virus from eastern Senegal, and the spillover of the virus leading to the transition of the vector choice from the sylvatic *Ae. furcifer* to the urban *Ae. aegypti* in eastern Gambia (Germain, Francy et al. 1980). In the Americas, the reemergence of sylvatic YFV from the Brazilian jungle started in 1972-1973 extending its distribution south to Paraguay and Bolivia. Additionally, the reinfestation of areas by *Ae aegypti* also posted significant concern on the spread of the epizootic YFV to the west of the Panama Canal (WHO 1985, Barrett and Higgs 2007).

In 1983, the massive outbreak transmitted by the sylvatic vector *Ae. furcifer* in Burkina Faso and Ghana caused 15,000 infections, amongst which 10% of the cases developed jaundice and 4% of the cases died (Robert, Lhuillier et al. 1993). In 1986, an even larger epidemic spread by the rural vector *Ae. africanus* occurred in eastern Nigeria leading to 10,000 jaundice cases and 5,000 fatal cases (De Cock, Monath et al. 1988). In 1987, the city of Ogbomosho in western Nigeria was struck by another epidemic transmitted by *Ae. aegypti* leaving twenty percent of the population infected (Nasidi, Monath et al. 1989). Cases have been reported in Bolivia, Brazil, Columbia, Ecuador and Peru between 1985 and 1994. In 1995, the largest epidemic in Peru since 1950s was reported (Barnett 2007).

Currently, there have been five genotypes reported to circulate in different regions of Africa whilst two genotypes have been found in Latin America (Mutebi and Barrett 2002, Barrett and Higgs 2007). The changing epidemiology and the reemergence of YFV have posted significant public health threat since 1980s. In Africa, the transmissions in the sylvatic cycle allow the virus to circulate between non-human primates and mosquitoes in spite of the vaccination. The vaccination has become the emergency strategy in order to control the outbreak. The pause of the routine vaccination coincided with the report of YF cases in 93% of the countries in West Africa in early 2000 (Barrett and Higgs 2007). With the rapid urban development in Africa, the non-vaccinated individuals have substantially increased the number of the susceptible populations to YFV infection in the urban areas (Barrett and Higgs 2007, Ellis and Barrett 2008, Gardner and Ryman 2010). Although the eradication of *Ae. aegypti* in the Americas since 1930s and 1940s temporarily suppressed the outbreaks of YF, the lack of persistent control measures led to the more extensive reestablishment of such vector species. Such reinfestation not only led to the reemerging threats of YFV in the urban area but also has

been further complicated by the rapidly expanding geographic distribution of the other flavivirus, dengue virus, which also utilizes *Ae. aegypti* as its primary vector (Guzman, Halstead et al. 2010). With the increase frequency of aviation travels, the epidemics of YFV in Africa or South America can easily be spread to other parts of the world, where the susceptible hosts and competent vectors exist. The imported case of YFV in Texas from Amazonas, Brazil in 2002 was considered a good example that the import of arboviruses through unvaccinated travelers becomes a significant public health issue in the United States (Centers for Disease and Prevention 2002). Additional challenges have also emerged due to the shortage of the YFV vaccine. Since 2013, the shortage has been reported in both the United States and the United Kingdom due to the failures in manufacturing procedures. The shortage of the vaccine limits the coverage for travelers who plan on traveling to high-risk areas and the capacity of health authorities in response to disease epidemics (CDC 2014).

C. Clinical Diseases

As the prototype of viral hemorrhagic fever, YF can result in up to 50% case mortality if the patients are not properly treated. The progression of the disease can be divided into three stages, infection, remission and intoxication. The severe human pathology and diseases are primarily documented as the lesions in the liver and other viscerotorpic symptoms, especially jaundice (WHO 2014).

The development of the viremic phase generally requires three to six days from the start of the infection by the wild-type YFV strains. The typical symptoms in the viremic phase resemble other viral hemorrhagic fevers and viral diseases such as high fever up to 39℃, myalgia, malaise and vomiting (Nassar Eda, Chamelet et al. 1995, Lefeuvre, Marianneau et al. 2004). Virus isolation can often be performed from the biopsy or serum samples from infected individuals (Pinto and Filipe 1971, Carey, Kemp et al. 1972). The stage of remission is characterized by the clearance of infectious virions in the blood. The patients may recover without further clinical signs or symptoms in the case of abortive infections. However, 15-25% of cases are likely to develop profound bleeding symptoms including jaundice, major bleeding, coffee-ground haematemesis, melaena or metrorrhagia (Monath 2001).

Biochemical laboratory tests have been found particularly helpful for the diagnosis of YF. The elevated levels of serum alanine transaminase (ALT) and aspartate transaminase (AST) are

the most common characteristics for the liver damages caused by YF (Francis, Moore et al. 1972). Although the hematological characteristics vary among patients, thrombocytopenia, prolonged clotting times and platelet dysfunction have also been reported (Francis, Moore et al. 1972, Monath 2001). The mortality of patients with hepatorenal diseases can range from 20 to 50% and deaths in the recovery phase has also been described in the past. In addition, the neutropenia and renal damage may lead to the superimposed bacterial infections, pneumonia or require dialysis due to the necrosis in the renal tissues (Lefeuvre, Marianneau et al. 2004). The disease incidence and mortality can be 1000-fold greater than those caused by Ebola virus leading to the name of the most lethal virus infections known to human (Van Epps 2005).

Two forms of YF-related diseases have been observed associated with vaccine adverse effects (Barrett and Teuwen 2009). Although the recent reviews have discussed the incidence of the diseases related to the YFV 17D vaccines occurred as early as 1973, the concept of the vaccine-associated effects in the literature was not introduced until 2002 (Centers for Disease and Prevention 2002). The incidence rates of the viscerotropic form (YEL-AVD) and neurotropic form (YEL-AND) of vaccine adverse effects are estimated to occur at 0.013 and 0.016 per 100,000 doses when the vaccines are used in endemic areas (Breugelmans, Lewis et al. 2013). The vaccine-associated viscerotropic disease is rare and mostly occurs in elderly vaccinees (≥65 years old). The disease symptoms mostly resemble those infected by the wildtype YF with viremia, jaundice and elevated ALT and AST. Case fatalities have been reported in severe cases with multiple organ failure. The liver pathology is commonly manifested with necrosis, acidophilic degeration, Kupffer cell hyperplasia and microvesicular fat. Antigens of YFV can often be detected in multiple organs (Centers for Disease and Prevention 2002, Kitchener 2004, Monath 2010). Multiple forms of neurological symptoms have been reported in YEL-AND cases including encephalitis, acute disseminated encephalomyelitis (ADEM) and Guillain-Barre Syndrome (GBS) (Kitchener 2004, McMahon, Eidex et al. 2007).

D. Yellow fever vaccines

There have been several approaches to describe the approaches to attenuate YFV. In the 1930s, two vaccines, the 17D vaccine and the French neurotropic vaccine, were developed concurrently. However, the reactogenicity of French neurotropic vaccine has been repeatedly reported since 1950s and its production and use have been discontinued (Macnamara 1953).

Prior to the era of YFV vaccines, laboratory-acquired infections repeatedly caused death in laboratory workers. The earlier attempt of vaccination among the laboratory personnel was made with the French neurotropic virus mixed with human immune serum (Sawyer, Kitchen et al. 1932). Theiler *et al.* showed the cultivation of YFV by intracerebral inoculation into mice was able to reduce the virulence in monkeys (Laemmert and Kumm 1950). The development of the 17D vaccine by the cultivation of the virulent Asibi strain *in vitro* was first proved to lose the viscerotropism in primates and further found non-transmissible in mosquitoes (Theiler and Smith 1937, Miller and Adkins 1988). Additional experimental evidence demonstrated the passage through chicken embryos led to the more efficient attenuation than the passage in either mouse embryonic tissues or testicles. The prolonged culture of the Asibi virulent strain in mouse embryonic tissues followed the minced chicken embryos with minimal brain and spinal cord for a total of 176 passages led to the attenuated phenotype of 17D vaccine strain. Such serial passage approach was first found to cause reduced neurovirulence in mice compared to the viruses passed through mouse embryonic tissues. Inoculation of rhesus monkeys showed reduced viremia and led to the production of neutralizing antibodies. Further attempts to vaccinate humans demonstrated the safety and the immunogenicity desired for the live-attenuated vaccines (Smith and Theiler 1937, Theiler and Smith 1937).

Immunization of YFV 17D vaccine causes self-limited viremia and induces both innate and adaptive immune responses. The vaccine is able to elicit innate and adaptive responses through the activation of Toll-like receptor signaling followed by the production of proinflammatory cytokines (Querec, Bennouna et al. 2006). In addition to the humoral immunity which persisted over a decade, the vaccination also led to CD8(+) T-cell memory responses by the T cell epitopes on the nonstructural proteins (Poland, Calisher et al. 1981, Akondy, Monson et al. 2009). Currently, the YFV 17D vaccines are based on two substrains, 17D-204 and 17DD strains. The 17D-204 substrain was obtained based on the 204th passage and the 17DD substrain was further passaged in eggs in South America from the 195th passage (Barrett 1997).

The French neurotropic vaccine (FNV) strain was derived from the serial passage of the French viscerotropic virus (FVV) isolated from Syrian in 1927. The parental virus underwent 128 passages in mouse brain in order to achieve the attenuation and the scale of vaccine production (Wang, Ryman et al. 1995, Barrett 1997, Frierson 2010). FNV was given to 80 million residents of French-speaking regions of Africa along with the smallpox vaccine through

scarification (Peltier 1947). Although FNV was more immunogenic than 17D vaccines, the production of FNV has been discontinued in 1980 due to the unacceptable high incidence of vaccine-associated encephalitis with mortality rate up to 40%, especially amongst vaccinated children under the age of 14 (Wang, Ryman et al. 1995, Barrett 1997, Frierson 2010).

17D vaccines have also been reported to cause adverse effects amongst the vaccines (Barrett and Teuwen 2009). The vaccine-associated neurotropic disease (YEL-AND) has been described and led to less than 5% case fatality rate (McMahon, Eidex et al. 2007). The other form of the vaccine-associated adverse events, the vaccine-associated viscerotropic disease (YEL-AVD), has first been described in 2002 and could be further dated back to 1973 (Centers for Disease and Prevention 2002, Monath 2010). The epidemiological analysis has identified several risk factors for YEL-AND including age, males and the history of thymus disease with a thymectomy (Barrett and Teuwen 2009). Due to the limited samples of YEL-AVD cases, the mechanistic evidence has been very limited centering the hypothesis on the disconnection between innate and adaptive immune responses. Fatal cases shared similar hematological characteristics with viremia similar to YFV infected individuals. Multiorgan failure, the elevation of liver enzymes and the impairment of coagulation have also been observed (Breugelmans, Lewis et al. 2013).

The other attempt of attenuating virulent YFV has also been reported in the passages through HeLa cells. The attenuated viruses have been described for multiple times in different literatures (Hearn, Soper et al. 1965, Barrett, Monath et al. 1990). The attenuated Asibi-LP-CDC HeLa p6 virus lost its viscerotropism in primates and reduced its neurovirulence in mice with fewer mutations identified in the genomes (Dunster, Wang et al. 1999). Most interestingly, the Asibi LP-CDC HeLa p6 virus was also found non-transmissible in *Ae. aegypti* (Miller and Adkins 1988).

Whilst the phenotypes of attenuated FNV and 17D strains had distinct safety profiles, the amino acid sequences of FVV and the Asibi strain have two nearly identical genomes, differing at only 9 amino acids and 23 nucleotides (Wang, Ryman et al. 1995). However, the distinct passage histories between two vaccines led to only two consensus mutations, the Leu→Phe mutation at the residue 36 of the prM protein and the Ile→Met mutation at the residue 94 of the NS4B protein.

Between the Asibi and 17D strains, our research focuses on comparing the different genetic composition and delineating the mechanisms leading to the distinct phenotypes of two viruses in *Ae. aegypti*. The sequence analysis identified 67 nucleotide changes leading to 31 amino acid substitutions between the Asibi strain and the 17D-204 strain, the critical determinants for viral attenuation have not yet been identified. The overall divergence is 0.623% and 0.94% at the nucleotide level and amino acid level, respectively. The envelope (E) protein contains the most amino acid mutations amongst the viral genes; whereas, the mutation rates were found to be highest in NS2A and NS2B (Hahn, Dalrymple et al. 1987). The genetic differences between the wildtype Asibi strain and the 17D strains are listed in **table 1.4**. Although it has been proved that the 17D vaccines contain a heterogeneous population of viruses that lead to different plaque morphologies and phenotypes, the recent report from the deep sequencing of the wildtype Asibi strain and the 17D-204 strain demonstrated the relative diversity of quasispecies can be a critical characteristic for viral attenuation. The phenotypes of 17D vaccines were derived from the accumulation of attenuating mutations (Beck, Tesh et al. 2014).

Gene	Position (nt)	Asibi	17D-204	17DD	Position(aa)	Asibi	17D-204	17DD
C	304	G	A	A				
	370	U	C	U				
M	854	C	U	U	36	L	F	F
	883	A	G	A				
E	1127	G	A	A	52	G	R	R
	1140	C	U	C	56	A	V	A
	1482	C	U	U	170	A	V	V
	1491	C	U	U	173	T	I	I
	1572	A	C	C	200	K	T	T
	1750	C	U	U				
	1819	C	U	U				
	1870	G	A	A	299	M	I	I
	1887	C	U	U	305	S	F	F
	1946	C	U	C	325	P	S	P
	1965	A	G	G	331	K	R	R
	2112	C	G	G	380	T	R	R
	2219	G	A	G	416	T	A	T
	2356	C	U	U				

NS1	2687	C	U	U	79	L	F	F
	2704	A	G	G				
	3274	G	A	A				
	3371	A	G	G	307	I	V	V
	3613	G	A	A				
NS2A	3817	G,A	G	G				
	3860	A	G	G	61	M	V	V
	3915	U,A	U	U				
	4007	A	G	G	110	T	A	A
	4013	C	U	C	112	L	F	L
	4022	A	G	G	115	T	A	T
	4054	C	U	C				
	4056	C	U	U	126	S	F	F
NS2B	4289	A	C	C	37	I	L	L
	4387	A	G	G				
	4505	A	C	C	109	I	L	L
	4507	U	C	C				
NS3	4612	U	C	U				
	4864	A,G	G	G				
	4873	U	G	U				
	5131	U,G	G	G	187	I,M	M	M
	5153	A	G	A	195	I	V	I
	5194	U	C	C				
	5431	C	U	U				
	5473	C	U	U				
	5641	G	A	G				
	6013	C	U	U				
	6023	G	A	A	485	D	N	N
	6448	G	U	U				
	6529	U	C	C				
NS4A	6758	A	G	A	107	I	V	I
	6829	U	C	C				
	6876	U	C	C	146	V	A	A
NS4B	7171	A	G	G	95	I	M	M
	7571	C	A	C				
	7580	U	C	C	232	Y	H	H
NS5	9605	A	G	A	657	N	D	N

	10075	G,U	G	G	814	M,I	M	M
	10142	G	A	A	836	E	K	K
	10243	G	A	A				
	10285	U	C	C				
	10312	A	G	G				
	10316	U,C	U	U	894	S,P	S	S
	10338	C	U	U	900	P	L	L
3' NCR	10367	U	C	C				
	10418	U	C	C				
	10454	A	G	A				
	10550	U	C	U				
	10800	G	A	A				
	10847	A	C	C				

Table 1.4 Genetic mutations between the wildtype Asibi strain and 17D vaccine strains at nucleotide (nt) and amino acid (aa) level

Efforts on characterizing mutations in YFV 17D genomes have been performed in mice and mosquitoes in the laboratory. The attenuated phenotypes of YFV 17D strains will be described in **section 1.4.E and 1.5**. With the neurovirulent variant of 17D Porterfield strain, several point mutations were identified and can potentially alter the virulence of YFV *in vivo*. Mutations in EDIII including the Arg→Thr reversion at the residue 380 to the Asibi sequence led to the neuroinvasive phenotype (Nickells and Chambers 2003). Together with the report from Lee *et al.*, the positive charges on the lateral surface of YFV EDIII are the critical determinants of the heparin binding sensitivity *in vitro* and the neurovirulence of YFV in mice (Lee and Lobigs 2008). The other critical region which was reported to be critical for the viral spread was the Val→Ala mutation at the residue 260 of the molecular hinge region between EDI and EDII of neuroadapted YFV 17D strain. The mutation changed the cell penetration capacity by altering the efficiency of the fusion process (Vlaycheva, Nickells et al. 2004). Although such change did not occur in the attenuation process from the Asibi strain, the other strand on the four-strand structures of the molecular hinge contains the Gly→Arg mutation at the residue of 52. However, the individual determinants for viral infection and dissemination in *Ae. aegypti* remain to be identified.

E. YFV in Ae. aegypti

Although the proposed concept of the transmission of YFV through the arthropod vectors by Dr. Carlos Finlay preceded the experiments by Walter Reed, the critical factors such as the extrinsic incubation period and the presence of viruses in mosquitoes were not determined or demonstrated until later (Bauer and Hudson 1928, Whitman 1937). The report that the Asibi strain was able to replicate, disseminate and be transmitted by *Ae. aegypti* was first established by oral infection with the Asibi strain propagated in mouse brains and further repeated with the cloned Asibi strain generated by the reverse genetics system (Whitman 1937, Miller and Adkins 1988, McElroy, Tsetsarkin et al. 2006). The infection ultimately led to the dissemination of virus into the salivary glands, which is required for the inoculation of infectious virions into the next immunological naïve host (Miller and Adkins 1988, McElroy, Tsetsarkin et al. 2005). In contrast, the infection of 17D strains and other attenuated strains showed the non-disseminating patterns that were primarily restricted to the midguts (Miller and Adkins 1988, McElroy, Tsetsarkin et al. 2005, McElroy, Girard et al. 2008).

Similar to the vector competence for other arboviruses, the infection and dissemination of YFV in *Ae. aegypti* are subjected to interactions between the genetics and the physiological conditions of mosquitoes. The variations observed in the susceptibility among *Ae. aegypti* populations collected from different geographic locations were first shown through the infection experiments of French viscerotropic virus (Aitken, Downs et al. 1977). The susceptibility of *Ae. aegypti* was further attributed to the differences in the genetic backgrounds of different strains (Tabachnick, Wallis et al. 1985). The selection and crossing of the inbred *Ae. aegypti* colonies with different susceptibilities suggested the genetic loci in individual mosquitoes can potentially govern the vector competence for YFV and other viruses (Wallis, Aitken et al. 1985, Miller and Mitchell 1991). Additionally, the laboratory colonization has also been taken into account as the susceptibility of *Ae. aegypti* to YFV varies between different generations (Lorenz, Beaty et al. 1984).

Significant advancements in the knowledge in identifying the viral determinants of infection and dissemination were achieved with the laboratory *Ae. aegypti RexD* strain and infectious clones of YFV by McElroy *et al.* The observations from the chimerized YFV genomes between the Asibi and 17D-204 strains suggested multiple genetic loci are related to the non-

disseminating phenotype of 17D strains (McElroy, Tsetsarkin et al. 2005, McElroy, Tsetsarkin et al. 2006, McElroy, Tsetsarkin et al. 2006).

1.5 Justification of the research

A. Infection and dissemination of virulent and attenuated YFV strains in Ae. aegypti

Although the phenotype of YFV 17D strains in *Ae. aegypti* has been repeatedly demonstrated to be non-disseminating in the infected mosquitoes, the mechanisms responsible for the attenuation remain largely unknown (Miller and Adkins 1988, McElroy, Girard et al. 2008). The purpose of the studies described in this dissertation was to perform functional characterization using molecular viriological approaches to provide the critical knowledge for the viral attenuation of YFV. The central hypothesis of the study is: "the amino acid substitutions in the E protein of YFV result in the change in the biochemical properties of the functionally important residues and the attenuated phenotype of YFV 17D strains in *Ae. aegypti*." The genetic characterization has identified 68 nucleotide substitutions between the virulent Asibi strain and the attenuated 17D-204 strain, which was used as the model for the study of viral attenuation (Hahn, Dalrymple et al. 1987). Among the 68 nucleotide substitutions, 15 point mutations are located in the E gene, resulting in 12 amino acid changes. The specific amino acid mutations of other flavivirus E proteins that led to different phenotypes will be reviewed in the sections of individual specific aims. The 15 nucleotide substitutions led to a total 12 amino acid mutations in the E protein of 17D-204 strain as summarized in **table 1.4**. The attenuating amino acid mutations of the E proteins of 17D-204 strain and 17DD strain differ only at the Thr→Ala/Thr mutations located at the residue 416 in EDIII, which is not exposed at the surface of virion based on the available structure (Volk, May et al. 2009). The following paragraph and **table 1.5** provide the summary of results that are specifically related to YFV Asibi and 17D-204 strains in *Ae. aegypti* as the justification for the targets for mutagenesis (McElroy, Tsetsarkin et al. 2006).

Virus	Infection rates	Dissemination Rates
Asibi	42/58 (72.4%)	35/42 (83.3%)
Asibi+17D M-E	16/60 (26.6%)	5/16 (31.3%)
Asibi M L36F	16/49 (32.7%)	8/16 (50.0%)
Asibi+17D EDI-EDII	9/58 (15.5%)	6/9 (66.7%)

Asibi+17D EDIII	22/58 (37.9%)	7/22 (31.8%)
17D+Asibi EDIII	28/85 (32.9%)	4/28 (14.3%)
17D+Asibi M-E	16/76 (21.1%)	11/16 (68.8%)
17D	17/56 (30.4%)	0/17 (0.0%)

Table 1.5 The infection and dissemination reported in YFV chimeras at 14 d.p.i. modified from McElroy *et al*. (2006)

The Asibi strain infected a higher percentage of mosquitoes and disseminated in the infected mosquitoes; whereas the 17D strain was only able to infected a lower percentage of mosquitoes with no or limited dissemination observed (McElroy, Tsetsarkin et al. 2005, McElroy, Tsetsarkin et al. 2006, McElroy, Girard et al. 2008). The chimerization of the structural genes of the 17D strain with the Asibi nonstructural genes led to the low viral infectivity and limited the dissemination into the secondary tissues. Due to the conserved sequences of the capsid genes between the Asibi and 17D strains, the attenuation determinants are located in the prM and E genes. The L36F mutation in the M protein resulted in the significant reduction in the infection rate of *Ae. aegypti*. However, the dissemination was still observed in 50% of the infected mosquitoes. The substitution of the E protein in the Asibi strain with the corresponding region of the 17D strain reduced both the infection and dissemination rates of the Asibi strain. Chimerization of the different domains of the E protein led to different consequences of viral infection and dissemination suggesting that the attenuation determinants are encoded in both EDI and EDII. The Asibi strain substituted with EDI and EDII of 17D strain was only able to infect a lower percentage of mosquitoes but disseminated at a comparable level as the Asibi strain at 14 days post infection (d.p.i.). The substitution of EDIII of the Asibi strain with EDIII of 17D strain led to a lower infection and dissemination rates. In contrast to the attenuation caused by the chimerization of the genetic materials from the 17D strain, the substitution of the prM and E structural proteins in the 17D strain with the corresponding regions of the Asibi strain only reproduced the disseminating phenotype of the wildtype virus without significantly increased the infection rates. Substituting the region of EDIII in the 17D strain with that of the Asibi strain failed to increase the infection and dissemination rates to the equivalent level of the Asibi strain.

Together, the results demonstrated that a partially attenuated phenotype can be produced by introducing the mutations in the E protein. However, the presence of attenuating mutations in the

nonstructural regions can be confirmed as the reversions to the sequences of the Asibi strain in the E protein of 17D strain was unable to restore the viral infection and dissemination. The research described in the dissertation is based on two cDNA infectious clones- the Asibi strain and the 17D/Asibi M-E chimera. Mutations were introduced to both infectious clones for the assessment of attenuation. The mutations tested in the Asibi strain were devised to evaluate the consequence of mutations in the E protein; whereas, the mutants based on the 17D/Asibi M-E chimera were generated to evaluate the attenuation caused by the mutations coupled with other attenuating mutations in the nonstructural genes.

The research is expected to characterize the mechanisms that attenuate YFV in *Ae. aegypti*. Such knowledge is critical for the design and optimization of the live-attenuated flavivirus vaccines and vaccine candidates by increasing the safety through the reduction of transmissibility. The identification of attenuating mutations will lead to the better understanding in the viral determinants that are critical for the vector competence of arboviruses.

B. Specific aims of the research

Four amino acid residues were selected for testing based on the locations, biochemical properties and functions in three different sets of infectious clones.

Specific aim 1 focuses on the assessment of mutants leading to the change in the positive charges on the lateral surface in YFV EDIII in *Ae. aegypti*. The positive charges introduced by the T380R mutation on the lateral surface of YFV EDIII were demonstrated to be critical for the binding between the negatively charged heparin sulfate *in vitro* and the viral dissemination in mice (Lee and Lobigs 2008, Nickells, Cannella et al. 2008). The increase of the heparin binding capacity *in vitro* has frequently been identified in RNA viruses passaged in naturally nonsusceptible hosts. The increase in the binding with heparin sulfate led to the higher binding affinity with other negatively charged cellular glycosaminoglycan molecules and this caused the subsequent retention and readsorption of the progeny virions, which assisted the withdraw of virions from the blood circulation and thereby limit systematic infection and viral dissemination. As the ubiquitously expressed cellular molecules, the presence of glycosaminoglycans in the midgut of mosquitoes also suggests the possibility of the retention of the virus through similar electrostatic interactions. Therefore, the hypothesis that the biochemically non-conservative T380R mutation in the RGD motif is responsible for the binding of cellular negatively charged

molecules was tested to evaluate the contribution for the mutation in viral attenuation in mosquitoes.

Specific Aim #1: Determine the impact of amino substitution in the RGD motif of YFV envelope protein domain III (EDIII) in changing the efficiencies of viral infection and dissemination in *Ae. aegypti*.

Specific aim #1a: develop and characterize the YFV cDNA infectious clones containing T380R mutation.

Specific aim #1b: evaluate the infection and dissemination of recovered mutants containing T380R mutations in orally infected *Ae. aegypti*.

Specific aim 2 was devised to analyze two mutations in EDI and EDII, which are independent from the receptor binding process. By incorporating the G52R and T173I mutations simultaneously and separately, the mutants were assessed for the viral infection and dissemination. The significance of the G52R mutation is based on its location IN the EDI-EDII molecular hinge region. Similarly, the non-disseminating FNV also contains A54V mutation in the neighboring region (Wang, Ryman et al. 1995). The T173I mutation was found to be a neurovirulence determinant as a vaccine specific B-cell epitope (Ryman, Xie et al. 1997). Its impact in the phenotype in mosquitoes remains unclear.

Specific Aim #2: Determine the minimal requirement of mutants responsible for the reduced infection rates in *Ae. aegypti* caused by the mutations in the YFV envelope protein domain I (EDI) and domain II (EDII)

Specific aim #2a: develop and characterize YFV cDNA infectious clones containing G52R and T173I mutations.

Specific aim #2b: evaluate the infection and dissemination of recovered mutants containing G52R and T173I mutations simultaneously and respectively in orally infected *Ae. aegypti*.

In specific aim 3, three infectious clones were generated to evaluate the M299I mutation in the molecular linker region between EDI and EDIII. The linker region was recently proved to change the dissemination of DENV-2 *in vitro* (de Wispelaere and Yang 2012).

Specific Aim #3: Determine the minimal requirement of mutants responsible for the reduced infection rates in *Ae. aegypti* caused by the mutations in the YFV envelope protein domain I (EDI) and domain III (EDIII)

Specific aim #3a: develop and characterize YFV cDNA infectious clones containing M299I mutations;

Specific aim #3b: evaluate the infection and dissemination of recovered mutants containing M299I mutation in orally infected *Ae aegypti*.

Chapter 2 - Materials and Methods

The research described in the dissertation requires the manipulation of YFV genomes, the propagation of YFV mutants, the *per os* infection and dissection of *Ae. aegypti*, the detection and quantification of viral antigens in mosquito tissues *in vitro*. Section 2.1 contains the information of the eukaryptic cell lines used for the propagation and titration of YFV and the bacterial competent cells for the manipulation of cDNA derived from the viral genomes. Section 2.2 is devised to provide the information of the molecular cloning strategies and procedures to generate viral mutants. The details of the rearing, *per os* infection and dissection of *Ae. aegypti* are described in section 2.3 The procedures of the detection and titration of infectious viruses from the mosquito tissues are listed in section 2.4. The statistical methods for the analysis are described in section 2.5.

2.1 Cell lines and competent cells

A. Mammalian cells

The cell line BHK-21 was derived from baby hamster (*Mesocrecitus auratus*) kidney. (MACPHERSON & STOKER, 1962) For this research project, it was maintained in minimum essential media (MEM) α media (Life Technologies) supplemented with 10% heat-inactivated fetal bovine serum (FBS) (Life technologies), antibiotics (penicillin at 100 units/ml and streptomycin at 100 μg/ml) (Life Technologies), L-glutamine at 2 mM (Life technologies) and MEM vitamins (Life technologies). The cells were maintained at 37℃ with 5% CO_2 and used for the recovery of YFV by electroporation.

African green monkey (*Cercopithecus aethiops*) kidney Vero cells were maintained in Leibovitz-15 (L-15) media (Life Technologies) with 10% FBS, 10% tryptose phosphate broth (TPB) (Sigma Aldrich), penicillin, streptomycin and L-glutamine (Simizu 1988). The cells were maintained at 37℃ without CO_2 and used for the titration of viremic blood meals and the homogenized mosquito tissues. The media for the titration of mosquito tissues were modified by the addition of Fungizone® antimycotic (Life Technologies) containing amphotericin B at 1μg/ml and sodium deoxycholate at 0.82μg/ml.

B. Bacterial Competent Cells

E. coli strain MC1061 was obtained from Dr. Ilya Frolov's laboratory. The MC1061 strain of *E. coli* was the original competent cells used for the construction of the YFV 17D cDNA infectious clone (pANCR-FLYF17Dx) and allows the stable maintenance of the cDNA of the full-length YFV genome (Bredenbeek, Kooi et al. 2003). Stocks were made from 16-hour overnight culture and preserved in 10% glycerol at -80℃. Cells for chemical transformation at the log phase of propagation were made in 2X YT both (1.6% peptone, 1% yeast extract and 0.5% NaCl) at 37℃ and 300 r.p.m. Competent cells transformed with plasmids were propagated in terrific broth supplemented with ampicillin at appropriate conditions. Details of the transformation and cloning procedures are listed in the **section 2.2**.

2.2 Plasmids and molecular cloning procedures

A. Plasmids for cDNA infectious clones of YFV mutants

The cDNA infectious clones of YFV 17D-204 strain, Asibi strain, and 17D/Asibi M-E chimera were established in previously published studies by Bredenbeek *et al.* (2003) and our laboratory (Bredenbeek, Kooi et al. 2003, McElroy, Tsetsarkin et al. 2005). The plasmids of the Asibi E M299I mutant and the 17D E I299M mutant were provided by Dr. Alan Barrett (University of Texas Medical Branch (UTMB) , Galveston Texas). All plasmids were selected based on the ampicillin resistance. The subcloned plasmids based on the pGEM® T Easy system were propagated in 2X YT broth supplemented by ampicillin at 100 μg/ml. The full-length cDNA infectious clones based on the low-copy number pANCR system were propagated in terrific broth (1.2% peptone, 2.4% yeast extract, 72 mM K_2HPO_4, 17 mM KH_2PO_4 and 0.4% glycerol) supplemented by ampicillin at 40 μg/ml.

The comprehensive list of YFV mutants characterized in this study is shown in **Figure 2.1** based on the locations of the mutations in the E protein. The mutants were designed based on the previously published results by McElroy *et al*. and described in **section 1.5.B**.(McElroy et al., 2006b) In specific aim #1, the T380R mutation in YFV EDIII was characterized in the two mutants, the Asibi E T380R mutant and the 17D+Asibi M-E E T380R mutant. The characterization of the G52R mutation in the molecular hinge region between EDI and EDII and the T173I mutation in EDI were performed in **specific aim #2**. The G52R and T173I mutations

were evaluated by introducing single mutations in the Asibi strain and the 17D+Asibi M-E chimera in **specific aim #2a**. The assessment of the attenuation caused by the simultaneous presence of the G52R and T173I mutations was performed in **specific aim #2b** by the oral challenge with the Asibi E G52R-T173I double mutant and the 17D+Asibi M-E E G52R-T173I double mutant. The phenotypic change associated with the M299I mutation in the EDI-EDIII linker region was determined in **specific aim #3** by orally infecting *Ae. aegypti* with the Asibi E M299I mutant, the 17D+Asibi M-E E M299I mutant and the 17D E I299M revertant. The M299I mutation was introduced to the Asibi strain and the Asibi M-E chimera, respectively. The I299M reversion was inserted to the 17D strain in order to generate the 17D E I299M revertant.

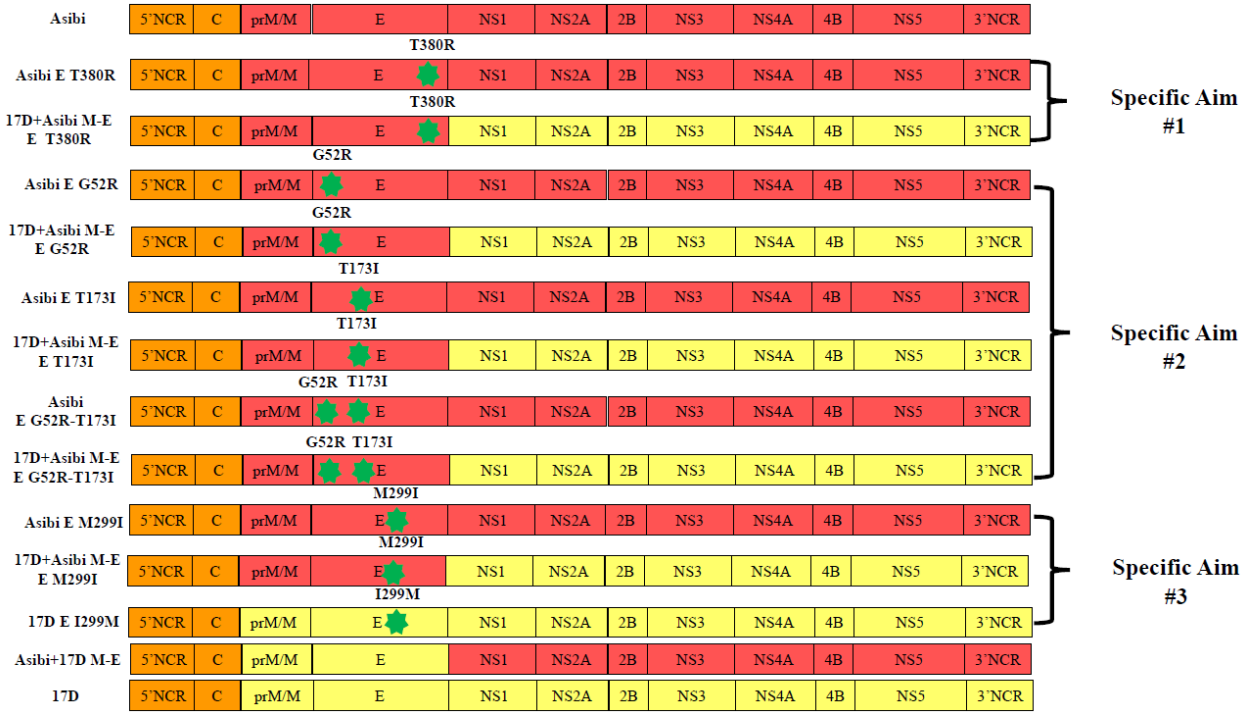

Figure 2.1 cDNA infectious clones of YFV characterized in this study

Four point mutations, T380R, G52R, T173I and M299I, in the E protein were characterized in three specific aims and are highlighted in green. The genes derived from the Asibi strain and the 17D strain are colored in red and yellow, respectively. The genetic materials in the 5' NCR region and the C gene contain the consensus amino acid sequences colored in orange.

The details of the molecular cloning strategies are listed in **figure 2.2**. The structural regions between the nucleotide position 474 and 2970 of the genome of Asibi strain were amplified by *Pfu* turbo polymerase (Stratagene) from the cDNA infectious clone of the Asibi

strain with the primer set, 17D-F2 and 17D-R3. The amplicons were generated by 25 cycles of denaturation at 95℃ for 30 seconds, annealing at 55℃ for 30 seconds and extension at 72℃ for 3 minutes, separated on 1% agarose gel and extracted with the Qiaquik PCR Purification kit (Qiagen) and modified by the addition of deoxyadenosine triphosphate (dATP) with Taq polymerase (Life Technologies) at 72℃ for 30 minutes in order to provide the complementary A overhang sequence to the linearized vector. The modified amplicon was purified by the Qiaquik PCR purification kit (Qiagen) and subcloned to the linearized pGEM®T Easy vector (Promega) by T4 DNA ligase (Promega) at 4℃ overnight. The ligation reaction was transformed into MC1061 cells and the positive clone, pGEM® T Easy-Asibi-st, was selected after propagation and purification by the Qiaprep Spin Miniprep kit (Qiagen) followed by the confirmation of nucleotide sequences.

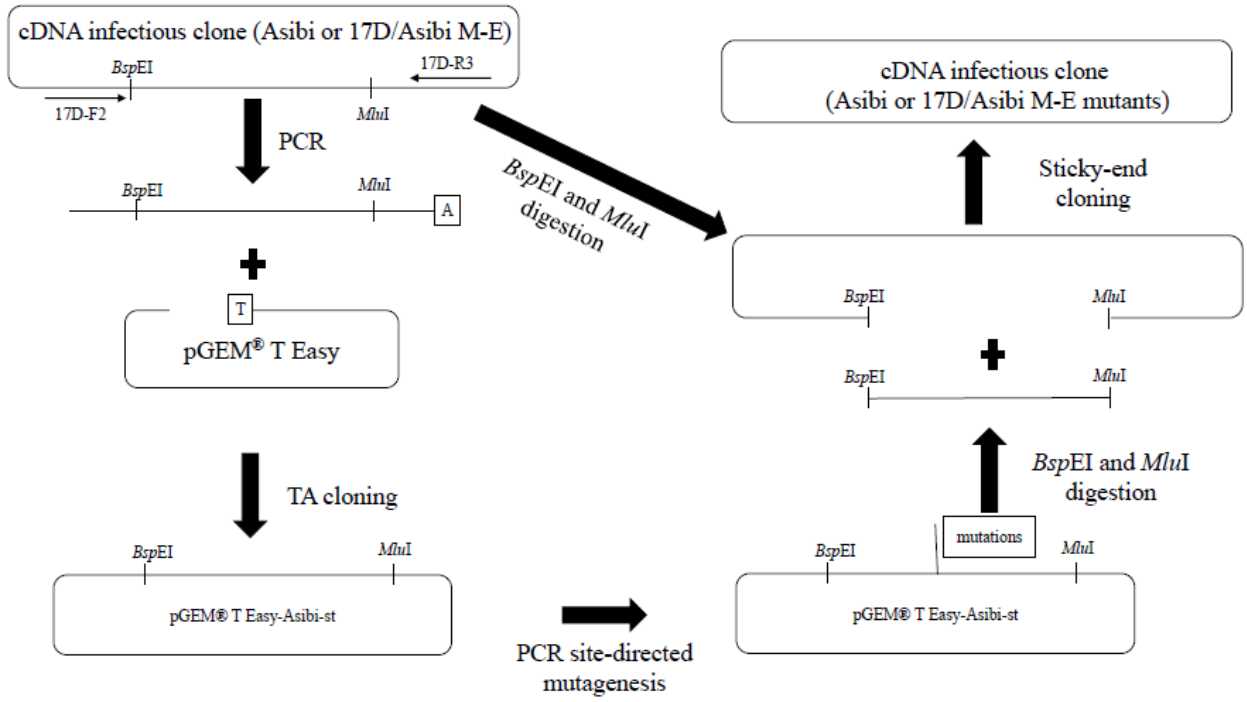

Figure 2.2 Cloning strategies for generating Asibi or 17D/Asibi M-E mutants
The mutations were made by PCR site-directed mutagenesis on the subcloned M and E genes of the Asibi strain to exclude the possibility of additional spontaneous mutations. The full-length mutants of YFV were generated by the ligations between the subcloned fragments and the full-length cDNA infectious clone digested by restriction endonucleases.

The mutations were introduced to the pGEM® T Easy-Asibi-st plasmid by polymerase chain reaction (PCR) site-directed mutagenesis with the Quikchange® II XL kit (Agilent). The

primer sets for each point mutation are summarized in **table 2.1**. Four subcloned mutants contain the single mutations in the E gene of Asibi strain. The G1127A mutation led to the G52R mutation in the E protein. The C1491T mutation led to the T173I mutation in the E protein. The G1870A mutation generated the M299I mutation in the E protein. The C2112G mutation resulted in the T380R mutation in the E protein. The pGEM® T Easy-Asibi-st-G1127A mutant was subjected to a second round of PCR site-directed mutagenesis with the primer set introducing the C1491T mutation to generate the pGEM® T Easy-Asibi-st-G1127-C1491T mutant. The reaction products were digested with the *Dpn*I restriction endonucleasae at 37℃ for 60 minutes to remove the template with the wildtype sequence. The amplicons were transformed to MC1061 cells and propagated in 10 ml 2X YT broth supplemented with ampicillin followed by the miniprep purification method. The mutations were confirmed by nucleotide sequencing.

Primer name	Sequence (5'-3')
17D-F2	ACGGGTGGAGTGACCTTGGTCCGGAAAAACAGATGGTTGC
17D-R3	AAGACTGCGTCCATGTACAC
G1127A-sense	ACTAGAGACAGTAGCCATTGATAGACCTGCTGAGG
G1127A-antisense	CCTCAGCAGGTCTATCAATGGCTACTGTCTCTAGT
C1491T-sense	CTCCCAGGAAGCCGAGTTCATTGGGTATGGAAAAG
C1491T-antisense	CTTTTCCATACCCAATGAACTCGGCTTCCTGGGAG
G1870A-sense	CACTCAAGGGGACATCCTACAAAATATGCACTGACAAAA
G1870A-antisense	TTTTGTCAGTGCATATTTTGTAGGATGTCCCCTTGAGTG
C2112G-sense	ACAGCTACATTATCGTTGGGAGAGGAGATTCACG
C2112G-antisense	CGTGAATCTCCTCTCCCAACGATAATGTAGCTGT

Table 2.1 Primers used for the subcloning of the structural genes of the Asibi strain and PCR site-directed mutagenesis

The subcloned structural genes from the mutants on the pGEM® T Easy-Asibi-st plasmid were released by digestion with the *Bsp*EI (New England Biolabs) and *Mlu*I (New England Biolabs) to generate the insert for cloning into the reciprocal fragments derived from the cDNA infectious clones of the Asibi strain and the 17D/Asibi M-E chimera that were digested with *Bsp*EI and *Mlu*I. Prior to the ligation reaction, the digested subcloned plasmids were separated by the electrophoresis with 0.8% agarose gels. The DNA fragments were excised from the argarose

gels and purified with the Qiaquik purification kit (Qiagen). The plasmids of the cDNA infectious clones were digested with *Bsp*EI and *Mlu*I at 37℃ for 60 minutes to remove the fragments corresponding to the inserts containing the mutations. The digested vectors were separated by electrophoresis with 0.5% agarose gels, removed by the excision of the products with the correct molecular weight and then purified by the Qiaquik purification kit (Qiagen). The inserts and vectors were quantified by $O.D._{260}$ and ligated together at the molar ratio of 9:1 at 4 ℃ overnight with T4 DNA ligase to generate the full-length cDNA infectious clones of YFV mutants and transformed to MC1061 cells. The mutants were selected by propagating individual colonies in 10ml 2X YT broth, purified by the miniprep purification method and confirmed by nucleotide sequencing.

The full-length mutants were transformed to MC1061 cells and propagated in 250 ml terrific broth containing ampicillin at 40 μg/ml. The plasmids were purified by alkaline purification method followed by the cesium chloride (CsCl) gradient purification at UTMB or the QIAfilter Plasmid midi kit (Qiagen) at the Kansas State University.

The detail methods for transformation, plasmid purification and PCR site-directed mutagenesis are listed in the **section 2.2.B**, **2.2.C**, and **2.2.D**, respectively.

B. Transformation and propagation of E. coli MC1061 strain

The transformation of the cDNA infectious clones and the subcloned plasmids was performed by the permeabilization of the bacterial cells treated by calcium chloride ($CaCl_2$) and heatshock transformation.

The starting culture of cells were made by inoculating ~5 μl of the glycerol stock into 5 ml of 2X YT broth propagated at 37℃ for 16 hours at 300 r.p.m. The log phase culture was prepared by transferring 1 ml of the overnight culture to 50 ml of 2X YT broth which was subjected to the shaking culture at 37℃ for 50~60 minutes at 300 r.p.m. Cells were chilled on ice for 10 minutes and pelleted by centrifugation at 4,000 r.p.m. for 10 minutes at 4℃. The cells were suspended in 10 ml ice-cold BF1 buffer and pelleted at 4,000 r.p.m. for 10 minutes at 4℃. The pellet was gently suspended in 10 ml ice-cold BF2 buffer and chilled on ice for at least 20 minutes. The cells were pelleted by centrifugation at 4,000 r.p.m. for 10 minutes at 4℃ and resuspended in 220 μl of BF2 buffer per transformation reaction for up to 10 reactions. Cells for each transformation were aliquoted into a pre-chilled 15 ml conical tubes (BD Biosciences),

mixed with 3 µl of dimethylsulfoxide and 5 µl of plasmid DNA and chilled on ice for 30 minutes. The cell-plasmid DNA mixtures were heatshocked at 43.5℃ for 45 seconds, recovered on ice for 10 minutes, gently suspended in 5 ml of pre-warmed 2X YT broth and incubated at 37 ℃ for 60 minutes at 300 r.p.m. Transformed bacteria were pelleted at 4,000 r.p.m. for 10 minutes and plated on 2X YT agar supplemented with ampicillin.

The plates were incubated at 37℃ overnight until the individual colonies appeared. The individual colonies were transferred to 10 ml of 2X YT broth for the subcloned vectors or terrific broth for the full-length cDNA infectious clones containing appropriate concentrations of ampicillin for overnight 16-hr cultures. The large-scale 250 ml cultures of the cDNA infectious clones were made by inoculating 1 ml of overnight 10 ml cultures to 250 ml terrific broth with ampicillin and culturing at 37℃ for 16 hours at 300 r.p.m.

C. Purification of plasmids

Three methods of alkaline lysis plasmid purification methods were used in the project based on the quantities of plasmid DNA propagated and the availability of equipment. The mini-scale preparation was performed in 10 ml of broth to isolate individual clones from transformed *E. coli* for nucleotide sequencing. The stocks of cDNA infectious clones were made from the purification of 250 ml cultures.

The overnight miniprep cultures were pelleted by centrifugation at 4,000 r.p.m. for 10 minutes. The bacterial pellet was resuspended in 250 µl buffer P1 (50 mM Tris-HCl, 10 mM ethylenediaminetetracetic acid (EDTA) pH 8.0 with 100 µg/ml RNase A) and lysed with 250 µl buffer P2 (200 mM NaOH and 1% sodium dodecylsulfate (SDS)) by gently inverting the tubes for 4-6 times. The bacterial debris was precipitated by adding 350 µl buffer N3 (3 M sodium acetate pH 5.5) and pelleting at 13,500 r.p.m. for 10 minutes. The clear lysate was flown through the spin column at 13,500 r.p.m. for one minute and subsequently washed with 500 µl buffer PB and 750 µl buffer PE at 13,500 r.p.m. for one minute. The plasmid DNA was eluted with 50 µl nuclease-free H_2O at 13,500 r.p.m. for one minute and stored at -20℃.

The supercoiled form of the plasmid DNA was isolated by alkaline lysis followed by CsCl gradient centrifugation. The pellets of the 250 ml cultures of cDNA infectious clones were collected by centrifugation at 6,500 r.p.m. for 10 minutes at 4℃. The bacterial pellet was resuspended in 8 ml BF1 buffer (25 mM Tris-HCl, 100 mM NaCl, and 10 mM EDTA pH 7.5)

and subsequently lysed with 16 ml BF2 buffer (200 mM NaOH and 1% SDS). The plasmids were released into clear lysate by adding 12 ml of BF3 buffer (3 M potassium acetate in 20% acetic acid aqueous solution) and centrifugation at 4,000 r.p.m. for 15 minutes. The debris was removed by filtering the supernatant with sterilized gauzed and the nucleic acids were precipitated with isopropanol in a 50 ml reaction at -20℃ for at least 40 minutes. The pellet of nucleic acids was isolated by centrifugation at 4,000 r.p.m. for 10 minutes at 4℃, dissolved in 2 ml of TE buffer (10 mM Tris-HCl and 1 mM EDTA pH 8.0) and precipitated with 2 ml of 5M LiCl solution on ice for at least 20 minutes. The ribosomal RNA was removed by pelleting the mixture at 4,000 r.p.m. for 10 minutes at 4℃ and the dissolved plasmid DNA was precipitated with 8 ml of ethanol at -20℃ for at least 60 minutes. The plasmid DNA was pelleted at 4000 r.p.m. for 10 minutes at 4℃ and dissolved in 3.3 ml TE buffer containing 4.8 g of $CsCl_2$ and 40 μl of 1% ethidium bromide aqueous solution and subjected the gradient centrifugation in NVP90 rotors (Beckman Coulter) at 65,000 r.pm. for 16 hours. The supercoiled form of plasmid DNA is concentrated in the lower band based on its compact structure and extracted by the aspiration with 1 ml tuberculin syringe needles. The extracted solution was mixed with 1 ml TE buffer and 3.5 ml ethanol, precipitated at -20℃ for 40 minutes, and pelleted at 4,000 r.p.m. for 10 minutes at 4℃. The pellet was dissolved with 400 μl TE buffer and mixed with 400 μl 25:24:1 phenol:chloroform:isoamylalcohol mixture by vortexing at 3,000 r.p.m. for 15 seconds. The aqueous layer was separated by centrifugation at 13,500 r.pm. for 5 minutes at room temperature and mixed with 400 μl 24:1 chloroform:isoamylalcohol mixture by vortexing at 3,000 r.p.m. for 15 seconds. The aqueous layer was collected after centrifugation at 13,500 r.p.m., mixed with 1000 μl ethanol and 100 μl 5M NaCl and precipitated at -20℃ for at least 15 minutes. The purified plasmid was pelleted at 13,500 r.p.m. for 30 minutes at room temperature. The pellet was washed with 500 μl 70% ethanol, centrifuged at 13,500 r.p.m. for 5 minutes, dissolved with 50~100 μl nuclease-free H_2O and stored at -20℃.

The QIAFilter Plasmid Midi kit was used for the purification of plasmids with modified procedures. The bacteria were pelleted at 4,000 r.p.m. for 25 minutes at 4℃ and resuspended in 8 ml BF1 buffer (25 mM Tris-HCl, 100 mM NaCl, and 10 mM EDTA pH 7.5 supplemented with RNase A at a concentration of 100 μg/ml). The lysis reaction was performed with 16 ml BF2 buffer (200 mM NaOH and 1% SDS) and neutralized with 12 ml of BF3 buffer (3 M potassium

acetate in 20% acetic acid aqueous solution). The lysate were obtained by centrifugation at 4,000 r.p.m. for 15 minutes at 4℃ and filtered through the QIAfilter Cartridge. The plasmid DNA was purified by flowing the lysates through the Qiagen-tip 100 resin columns, which were previously activated by applying 4 ml buffer QBT (750 mM NaCl, 50 mM MOPS, 15% isopropanol, and 0.15% Triton X-100 pH 7.0). The columns were washed with 10 ml buffer QC twice and eluted with 4 ml buffer QF. The eluted DNA was precipitated with 3.5 ml at 15,000 g for 30 minutes at 4℃. The pellet was rinsed with 70% ethanol, centrifuged at 15,000 g for 10 minutes, dried for 10 minutes at room temperature, dissolved in 50~100 μl nuclease-free H_2O and stored at -20℃.

D. PCR site-directed mutagenesis

The PCR site-directed mutagenesis was performed with the Quikchange® XL II site-directed mutagenesis kit (Agilent). The template DNA molecules are produced in bacterial competent cells that are competent in methylation enzymatic mechanisms. The reaction required the mutations to be incorporated into the oligonucleotide primer sets, which could tolerate the mismatch between the nucleotides of the wildtype templates and the desired mutations designed in the primers between the primers and the template double-stranded plasmid DNA. The sense and anti-sense primers are complementary to each other and the unmethylated cDNA products are increased in the linear fashion with the high-fidelity DNA polymerases. The unmethylated DNA molecules are protected from the digestion of *Dpn*I restriction endonuclease that reduces the transformation efficiency by digesting the circular plasmid DNA templates to produce linear fragments. The mutants are/were subsequently isolated by the transformation of bacterial competent cells.

In the research described in this dissertation, the subcloned pGEM® T Easy-Asibi-st plasmid was used as the template for PCR site-directed mutagenesis. The reactions were assembled with 500 ng of plasmid DNA as the template, 5 μl of 10X reaction buffer, 125 ng of sense and anti-sense primers, 1 μl of dNTP mix, 3 μl of QuikSolution reagent and 1 μl of *Pfu*Ultra HF DNA polymerase in the 50 μl reactions. The mutants were produced by denaturation at 95℃ for 120 seconds, 18 cycles of denaturation at 95℃ for 30 seconds, primer annealing at 60℃ for 30 seconds and amplification at 68℃ for 7 minutes, and final incubation at 68℃ for 20 minutes. The reactions were chilled on ice briefly and 1 μl of *Dpn*I was added for the

removal of methylated template DNA at 37℃ for 60 minutes. Mutants were transformed to MC1061 and individual clones were isolated for nucleotide sequencing.

E. Linearization of plasmids

The linearization of the cDNA infectious clones was performed to generate the linear form of plasmids which provided the termination site for the transcription of the SP6 DNA-dependent RNA polymerase. The cDNA infectious clones of the 17D-204 strain, 17D/Asibi chimera and its mutants were digested by the *Xho*I restriction endonuclease (New England Biolabs). The cDNA infectious clones of the Asibi strain and its mutants were digested by the *Nru*I restriction endonuclease (New England Biolabs). The digested plasmids were purified by the phenol-chloroform purification and ethanol precipitation methods.

The digestion of plasmids was performed with 2-3 μg of plasmids in 40 μl reactions supplemented with 4 μl of 10X reaction buffer, 4 μl of 10X bovine serum albumin (BSA) and 1 μl of restriction endonuclease at 37℃. The reactions were diluted with 60 μl of nuclease-free H_2O (Life Technologies) and mixed with 100 μl of phenol:chloroform:isoamylalcohol 25:24:1 solution (Life Technologies) by vortexing at 3,000 r.p.m. for 15 seconds and centrifugation at 13,500 r.p.m. for 5 minutes. The aqueous layer was collected and the phenol was removed by mixing with 100 μl of chloroform:isoamylalcohol 24:1 (Amresco) at 3,000 r.p.m. for 15 seconds and centrifugation at 13,500 r.p.m. for 3 minutes. The aqueous layer was collected and mixed with 220 μl of ethanol and 10 μl of 3M sodium acetate pH 4.2. Plasmid DNA was precipitated at -80℃ for at least 20 minutes followed by centrifugation at 13,500 r.p.m. for 20 minutes at ambient temperature. The pellet was collected and washed with 400 μl of 70% ethanol solution by centrifugation at 13,500 r.p.m. for 5 minutes. The pellet was resuspended in 12 μl nuclease-free H_2O and subjected to *in vitro* transcription.

F. In vitro transcription

The *in vitro* transcription of YFV cDNA infectious clones described in the study is regulated by the SP6 promoter sequence prior to the sequences of viral genomes and used to generate the positive-sense viral RNA for the recovery of viruses. All the reactions were performed and modified from the procedures of the mMESSAGE mMACHINE® SP6 Transcription kit (Life Technologies).

The reactions were assembled by combining 12 µl of linearized plasmid DNA, 4 µl of 10X reaction buffer, 4 µl of 20 mM GTP, 20 µl of 2X NTP/CAP mixture and 2.8 µl of SP6 enzyme mix and incubated at 37℃ for 60 minutes. The integrity and the yield of RNA products were examined by separating 1 µl of the reaction collected at 20 minutes after the start of the incubation on 1% agarose gel at 125 volt for 20 minutes. Each reaction was divided into four aliquots and stored at -80℃ for electroporation.

G. Electroporation

The infectious viral RNA was electroporated into BHK-21 cells and incubated at 37 ℃ supplemented with 5% CO_2 for the production and recovery of viruses as detailed below.

BHK-21 cells were seeded in tissue culture-treated T150 flaks (BD Biosciences) and maintained until the cells reach 80-90% confluence. The cells were rinsed with 20 ml of Dulbecco's phosphate buffer saline (DPBS) without Ca^{2+} or Mg^{2+} (Cellgro) and treated with 3 ml of 0.25% trypsin-EDTA (Life technologies) briefly at 37℃ to detach the cells from the surface. The reaction of trypsin was terminated by adding 7 ml of MEM-α supplemented with 10% FBS. The cells were pelleted by centrifugation at 1,200 r.p.m. for 5 minutes at 4℃. The cells were resuspended in 10 ml of ice-cold DPBS and pelleted by centrifugation at 1,200 r.p.m. for 5 minutes at 4℃ for three times to remove the excessive nucleases on the cellular surface.

The cells were suspended in ice-cold DPBS and adjusted to the total volume 400 µl. The cells were chilled on ice and mixed with 10 µl of viral RNA transcripts. The mixtures were immediately transferred to pre-chilled 2 mm electroporation cuvettes (Fisher Scientific) for electroporation on the GenePulser Xcell electroporation system (BioRad). The electroporation was performed at 140V for 25 msec with the preset BHK-21 electroporation protocol. The electroporated cells were placed on ice briefly for recovery and the cuvettes were rinsed with 600µl pre-warmed media for three times. The fluid containing the cells was mixed with 8-10 ml of media and maintained in T75 flasks (Corning). For the Asibi strain and its mutants, the electroporated cells were incubated for five days; whereas, the cells electroporated with the viral RNA of the 17D-204 strain, 17D/Asibi M-E chimera and its mutants were incubated for four days.

2.3 Mosquitoes and *per os* infection

A. Rearing of Ae. aegypti

Ae. aegypti, the urban vector of YFV, was used in the study. The *Ae. aegypti* Red D white-eye laboratory colony was used based on its high susceptibility to YFV and other mosquito-borne viruses (McElroy, Tsetsarkin et al. 2005). The mosquito colony was reared at the rearing facility at the University of Texas Medical Branch and the Arthropod-borne Animal Disease Research Unit of the United States Department of Agriculture.

The eggs of *Ae. aegypti* were maintained on moist paper towels and hatched in tap water at room temperature. The larvae were maintained at the density of ~300 larvae per liter of water and supplied with the mixture of 1:1 fish food and rodent food mixture. At 28℃, the process of the development from the first to forth instar larvae generally requires six to eight days and the pupae stage lasts approximately two days prior to the adult eclosion. The adults were maintained with unlimited amount of 10% sucrose solution in 12"-by-12" collapsible cages (Bioquip) at 28 ℃. For the production of egg-liners, 8-10-day-old adults acquired mammalian blood through anesthetized rodents proved by IACUC at UTMB or artificial glasses feeders and laid eggs on moist paper towels 3~5 days after the blood meals.

For *per os* infections, 6-8-day-old adults were collected from the rearing cages by mechanically aspirators, cold anesthetized and females were sorted from each pool of mosquitoes. Each pint-size carton was used to house 100 female mosquitoes. Mosquitoes were fed with 10% sucrose solution through saturated cotton pellets above the mesh secured on the top of cartons. The sucrose solution was replaced with cotton pellets saturated with water 24 hours prior to the *per os* infection.

B. Procedures of per os infection

All the *per os* infection experiments were performed in the arthropod containment level 3 (ACL-3) laboratories at UTMB's Department of Pathology and at the Biosecurity Research Institute at Kansas State University.

The mosquitoes were transferred from the rearing facilities and the cotton pellets were removed 2~3 hours prior to the *per os* infection. The Hemotek membrane blood feeding apparatus (Discovery Workshop, Lancastershire, England, United Kingdom) was used to orally

administer the blood meals. The freshly harvested YFV was mixed with prewarmed defibrinated sheep blood (Colorado Serum Company) at 1:1 volume ratio. The negative control group received defibrinated sheep blood mixed with tissue culture media. Each blood meal reservoir was covered with rodent skin, secured with O-rings and filled with 3 ml of artificial viremic blood. The reservoirs were fastened to the pre-warmed feeding cones with the rodent skin facing the cartons. The acquisition of blood meals was achieved by probing through the skin and the mosquitoes were allowed to engorge during the 60-minute oral feeding period. The blood meals were collected immediately after the feeding and stored at -80℃ for titration.

Cartons were briefly chilled to cold anesthetize the mosquitoes and the engorged mosquitoes were counted and separated from the pools. For each clone of YFV, three engorged mosquitoes were immediately collected to confirm the intake of virus. The mosquitoes were placed in the cartoons and maintained in the secondary containers. The cotton pellets were saturated with 10% sucrose solution, placed on the mesh of each carton and replaced every two days. The mosquitoes were maintained at 28℃ under the 16hr:8hr light-dark photoperiod for up to 14 days.

C. Viruses used in per os infection

Two cDNA infectious clones, the Asibi strain and the 17D/Asibi M-E chimera, were used in the study to generate mutants for oral infection of *Ae. aegypti* as described in section 2.2. The infectious clones were generated in the previous studies described by McElroy *et al* (McElroy, Tsetsarkin et al. 2005, McElroy, Tsetsarkin et al. 2006). The viruses used in the oral infection studies are listed below. The rationale of the experimental design with the viruses is summarized in **figure 2.3**.

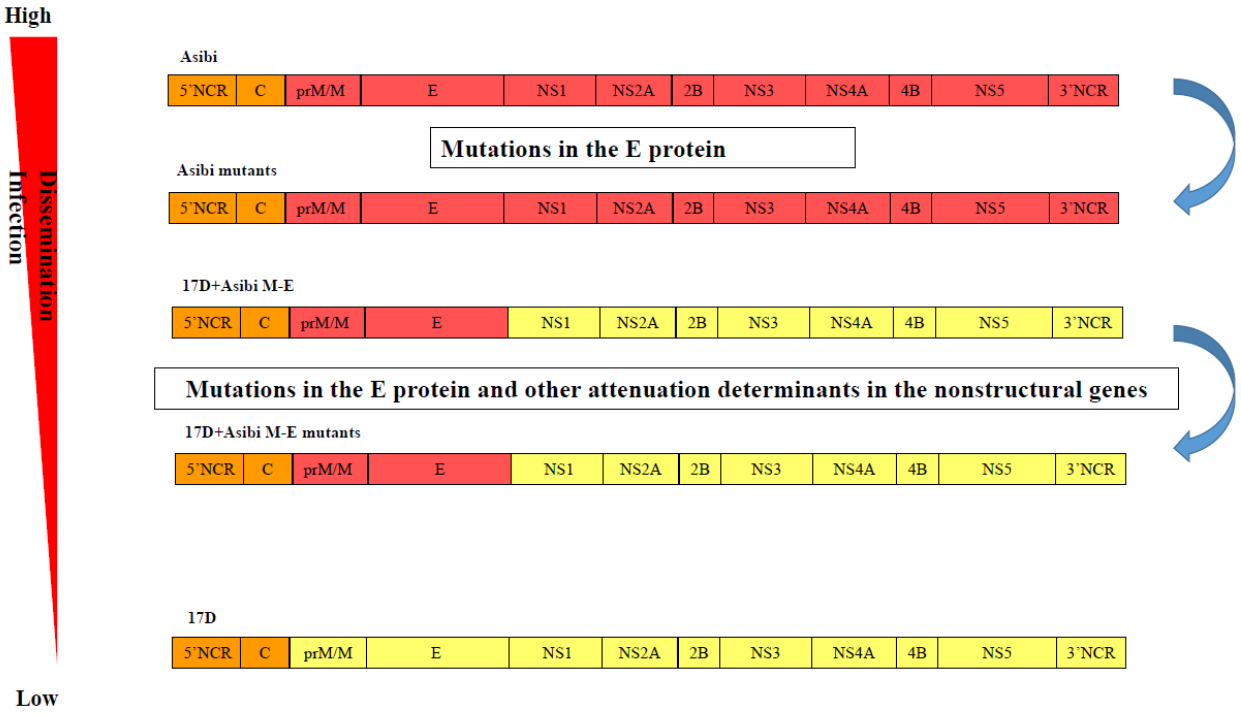

Figure 2.3 The rationale of experimental design with the viruses.
The mutations were introduced to the cDNA infectious clone of the Asibi strain and the 17D/Asibi M-E chimera. The 17D/Asibi M-E chimera was included due to the presence of the attenuation determinants present in the nonstructural proteins. The Asibi mutants were generated to evaluate the attenuation caused by the mutations in the E protein. The 17D/Asibi M-E chimeric mutants were devised to assess the attenuation caused by the mutations in the E protein and the attenuation determinants in the nonstructural proteins. The Asibi and 17D strains were used as the disseminating and non-disseminating controls respectively.

The attenuated YFV 17D strain was use in the study as the control of virus which is defective in viral dissemination in *Ae. aegypti*. The sites of viral replication of YFV 17D strains has been repeatedly found restricted to the midgut of infected mosquitoes (Miller and Adkins 1988, McElroy, Girard et al. 2008).

The YFV Asibi wildtype strain was included as the control for the infectious and disseminating phenotype of virus. The virus was first proved to be disseminating into the heads, wings and legs of infected mosquitoes and transmissible to immunologically naïve primates (Whitman 1937). The characterization of the infection process was further investigated to determine dissemination rates into the secondary tissues such as the fat body, ganglia tissues and

the salivary glands (McElroy, Girard et al. 2008). The viruses containing the mutations in the E protein of Asibi strain were tested to evaluate the phenotypical change due to the mutations.

The 17D/Asibi M-E chimera, which carried the 3' end of capsid gene, the full-length prM and E genes and the 5' portion of NS1 gene, showed a significantly lower infection rate and a insignificantly lower dissemination rates in *Ae. aegypti* (McElroy, Tsetsarkin et al. 2006). The attenuated phenotype was proposed to be attributed to the mutations present in the non-structural genes of 17D strain and the chimerization-induced attenuation. The virus was used as a control group representing the virus with the lowest infectivity and dissemination. The mutants were generated by introducing the mutations to the E protein of 17D/Asibi M-E chimera in the same locations as the Asibi E protein mutants.

D. Collection and dissection of mosquitoes

At 7, 10 and 14 d.p.i., mosquitoes were mechanically aspirated from the cartons and cold anesthetized. All the samples were submerged in 1 ml of L-15 media supplemented with amphotericin B at 1μg/ml and sodium deoxycholate at 0.82μg/ml and stored at -80℃ until tested.

Whole mosquitoes were collected for the assessment of the growth kinetics of individual clones of viruses. The dissection of mosquitoes was performed with electron microscopy forceps and double-edged dissecting needles (Electron Microscopy Sciences, Hatfield, PA) and 10-mm petri dishes on ice. Paired mosquito samples were collected by removing the body containing the abdominal segments from the head, thorax, wings and legs. The body section contained the midgut, where viral infection is initiated. The head, thorax, wings and legs are considered as secondary tissues, which are subsequently infected after the virus disseminates from the infected midgut.

2.4 Quantification and detection of viral antigens *in vitro*

A. Homogenization of mosquito samples

Mosquito samples were disrupted by mechanical homogenization to release the infectious virions from the tissues prior to the viral titration as described by McElroy *et al*.(McElroy et al., 2005) All the manipulations of infectious viruses were performed in the BSL-3 laboratories at the UTMB's Department of Pathology or at K State's Biosecurity Research Institute.

Samples were thawed in 37℃ water bath immediately after being removed from the freezers. The homogenization process was performed at 26.0 Hz for 4 minutes at room temperature on a Tissue Lyser II Homogenizer (Qiagen) placed in a Class IIA biosafety cabinets. The homogenates were cleared by centrifugation at 10,000 r.p.m. for 10 minutes at room temperature and immediately subjected to tissue culture infectious dose 50 ($TCID_{50}$) titration.

B. Tissue culture infectious dose 50 titration

$TCID_{50}$ titrations were performed with homogenates of mosquito tissues on Vero cells seeded in 96-well microtiter plates (Nunc) as described by Higgs *et al* (Crampton, Beard et al. 1997). The limit of detection of the assay was at 1.06 log$TCID_{50}$/ml. The clear homogenates were titrated in two duplicated columns on each plate up to 10^{-6} dilutions. The negative control wells received media and the positive control wells were infected with YFV 17D strain.

Each row from B to H was filled with 90 µl of L-15 media containing Fungizone® at 4µl/ml. The wells in row A received 100 µl of homogenates in duplicate format and titrated by 10-fold serial dilution from row B to G. Plates were temporarily stored on ice prior to the addition of cells. Each T150 flask was rinsed with 20 ml of Mg^{2+}/Ca^{2+}-free DPBS and cells were removed with 4 ml of 0.25% trypsin-EDTA at 37℃ briefly. The cells were resuspended with L-15 media and the volume was adjusted to 65 ml. Each well received 100 µl culture fluid.

The plates were sealed with plastic parafilm and incubated at 37℃ for 7 days. The tissue culture fluid was removed and each well was fixed with 150~200 µl ice-cold acetone:phosphate buffer saline 3:1 mixture for 20 minutes at room temperature. The fixatives were removed and the plates were allowed to dry at room temperature to remove residual fluid. The plates were stored at -20℃ until the staining of viral antigens.

C. Indirect immunofluorescence assay

The lack of cytopathic effect in Vero cells caused by YFV infection necessitates detection of viral antigens by immunostaining methods on acetone-fixed cells. The indirect immunofluorescence assay (IFA) was performed with mouse anti-YFV hyperimmune serum MA93 (provided by S. Higgs) and goat anti-mouse IgG secondary antibodies. The viral antigens were detected from the emission of light provided by the excitation energy from ultraviolet (UV) light.

The microtiter plates were removed from -20℃ and allowed to dry at room temperature to remove the excessive moisture due to condensation. Anti-YFV MA93 hyperimmune serum used as the primary antibody was reconstituted from lyophilized antibodies and stored at -20℃. The primary antibody was thawed at 37℃ and diluted with PBS at 1:200 volume ratio. Each well received 40 µl of diluted MA93 and incubated at 37℃ for 40 minutes. Plates were washed with 200 µl PBS twice and stained with 40 µl of 200-fold diluted Alexa Fluor® 488 goat anti-mouse IgG (H+L) polyclonal antibody (Life Technologies) at 37℃ for 40 minutes. The counter staining compound, tetrasodium (6*E*,6'*E*)-6,6-[(3,3'-dimethylbiphenyl-4,4'-diyl)di(1*E*)hydrazin-2-yl-1-ylidene]bis(4-amino-5-oxo-5,6-dihydronaphthalene-1,3-disulfonate) (Evans Blue), was mixed with the secondary antibody at the concentration (w/v %) of 1%. Excessive antibodies were removed by washing with 200 µl PBS followed by a final wash with 200 µl of deionized water. Each well was stabilized with ~20 µl of stabilizer mixture, which contains 2.5% 1,4-diazobicyclo-2,2,2-octane (DABCO) (Sigma Aldrich) in glycerol:PBS 9:1 mixture, pH 8.6, and stored at 4℃. The stabilizer was made by gently heating 450 ml of glycerol at 53℃ and adding 12.5 g of DABCO and 50 ml of PBS and buffered with 3 ml of hydrochloric acid solution (Fisher Scientific).

The excitation energy was provided by the UV light on the Olympus IX-71 inverted microscope and the green fluorescence was visualized with the filters from fluorescein isothiocyanate (FITC) or green fluorescent protein (GFP). The scoring of the plates was performed by the presence of the positive cytosolic immunofluorescence signal at the highest dilutions.

2.5 Statistical analysis

A. Fisher's exact test

The numbers of positive and negative mosquito samples were recorded at each time point. The infection rate was derived from the percentage of the positive staining from the whole mosquito homogenates and the positive staining from the samples of dissected mosquito bodies or mosquito secondary tissues divided by the total number of mosquitoes orally challenged by the same type of viremic blood meals. The comparison was made between the Asibi strain and

the Asibi mutants as well as the 17D/Asibi M-E chimera and the 17D/Asibi M-E mutants by Fisher's exact test with the Sigmaplot version 12.0 (Systat Software Inc.).

B. Analysis of Variance

The comparison of viral titers among the homogenized whole mosquitoes and mosquito tissue samples derived from the groups of mosquitoes orally infected by wild-type and mutant viruses was performed with one-way analysis of variance (ANOVA) on the Sigmaplot version12.0 (Systat Software Inc.). The post-hoc analysis between two groups was conducted to compare the Asibi strain and the Asibi mutants as well as the 17D/Asibi M-E chimera and the 17D/Asibi M-E mutants with Tukey's test.

C. Non-parametric test

The comparison of viral growth kinetics from the tissue culture supernatants of electroporated BHK-21 cells was performed with non-parametric test on the Sigmaplot version12.0 (Systat Software Inc.). Mann-Whitney *U*-test was used to compare the viral titers of the wildtype and mutant viruses as described by Wang *et al*. (Wang and Bushman 2006)

Chapter 3 - Characterization of T380R mutation in YFV E protein

3.1 Introduction

A. Location and putative function of T380R mutation

Based on the available structure, the T380R mutation in YFV 17D strains is located in the FG loop of the lateral surface in YFV EDIII (Volk, May et al. 2009). The functions of flavivirus EDIIIs have been reported to include mediating receptor binding and stimulation of humoural immunity due to the presence of critical epitopes. It has been shown that several putative molecules that are expressed on the surfaces of arthropod or vertebrate cells, interact with the FG loops of flavivirus EDIIIs prior to clathrin-mediated endocytosis that results in viral entry (Chen, Maguire et al. 1997, Lee and Lobigs 2008). The FG loop is a structure that contains up to six amino acids between the F and G β-strands and is exposed on the lateral surface of EDIII. The lateral surface of EDIII is located in the distal end of the envelope protein dimer and has been suggested for its potential roles in determining the tissue tropisms and antigenicity as the receptor-binding region on the surface of virions (Rey, Heinz et al. 1995). The earlier studies with other flaviviruses closely related to YFV suggested that the FG loop contains residues which interact with negatively charged cellular molecules that are likely to serve as receptors for virus entry (Chen, Maguire et al. 1997, Germi, Crance et al. 2002). Additionally, the importance of the FG loop in determining the viral infectivity into mosquito cells was confirmed in completion assays using synthetic peptides corresponding to the sequence of the FG loop in the EDIII of DENV-2. These peptides prevented the viral entry in C6/36 cells by saturating the cellular receptors (Hung et al., 2004). The complexity of the roles of flavivirus FG loops was supported by the fact that the strong affinity of FG lop sequences for cellular molecules may alter the tropisms or virulence of the viruses. These observations were interpreted as suggesting the importance of FG loops in determining the efficiency of dissemination and pathogenesis (Lee and Lobigs 2000, Lee, Hall et al. 2004, Lee and Lobigs 2008). The putative receptors for YFV and mosquito-borne flaviviruses, the process of viral entry and the structures and functions of EDIIIs will be reviewed in the **section 3.1.B, 3.1.C** and **3.1.D**, respectively.

The T380R mutation in YFV 17D E protein was acquired during the *in vitro* passage of YFV Asibi strain and was first shown to facilitate the adaptation of YFV 17D strains to the *in*

vitro cell cultures. The underlying mechanism of this adaptation is primarily due to increased dissemination into neighboring uninfected cells (van der Most, Corver et al. 1999). The mutation led to the formation of an arginine-glycine-aspartate (RGD) motif that has been characterized as the putative receptor-binding site of flaviviruses for negatively charged integrin molecules (Lee and Lobigs 2000). By utilizing the reverse genetics system of flaviviruses within the JEV serocomplex, it was further demonstrated that such electrostatic interactions also contributed to the interactions with the glycosaminoglycan (GAG) molecules and resulted in both the enhanced viral entry *in vitro* and the attenuation *in vivo* in the serially passaged MVEV, JEV, KUNV and WNV (Lee and Lobigs 2000, Lee and Lobigs 2002, Lee, Hall et al. 2004). GAG molecules ubiquitously exist as the post-translational modifications on the proteins and use the non-template-driven synthesis mechanisms in eukaryotic cells. The synthetic mechanisms of GAG molecules lead to the structural variations that are tissue-specific and require the use of heparan or heparin sulfate as molecules for the assessment of the interactions between the virions and GAG molecules (Shriver, Capila et al. 2012). The further experiments demonstrated that the presence of the RGD motif led to a phenotype with increased binding to the negatively charged heparin sulfate *in vitro* and it was hypothesized to result in the more efficient interaction with the negatively charged molecules on the cell surface such as GAG as shown in **Figure 3.1**. Although the increased binding affinity to heparin sulfate may lead to the enhancement in viral entry, the consequence of such a phenotype may further complicate the mechanisms for disease pathogenesis *in vivo* by increasing the viral clearance through the higher binding affinity between the virions and cellular molecules. More efficient viral clearance reduces the likelihood of systemic infections in the viremic phase, and the progression to viscerotropic diseases during the intoxication phase of the infection. In the experiments using the type-I/II interferon (IFN)-deficient mice, the T380R mutation attenuated the recombinant 17D virus chimerized with the E gene of the Asibi strain by reducing the viral dissemination and viscerotropism. The progeny virions were likely to be retained in the extracellular matrix or readsorbed in the primary target cells prior to the spread to other susceptible organs (Lee and Lobigs 2008). However, the T380R mutation in the YFV 17D E protein had not been tested for the viral infection and dissemination in *Ae. aegypti*. The available genome sequence of *Ae. aegypto* suggested the presence post-translational modification enzymes for the production of proteoglycans in the extracellular matrix and the potential of a common attenuation mechanism of YFV for both the vertebrate

hosts and mosquito vectors by the increased affinity between the 17D virions and the glycosaminoglycans in the extracellular matrix (Kato, Mueller et al. 2005).

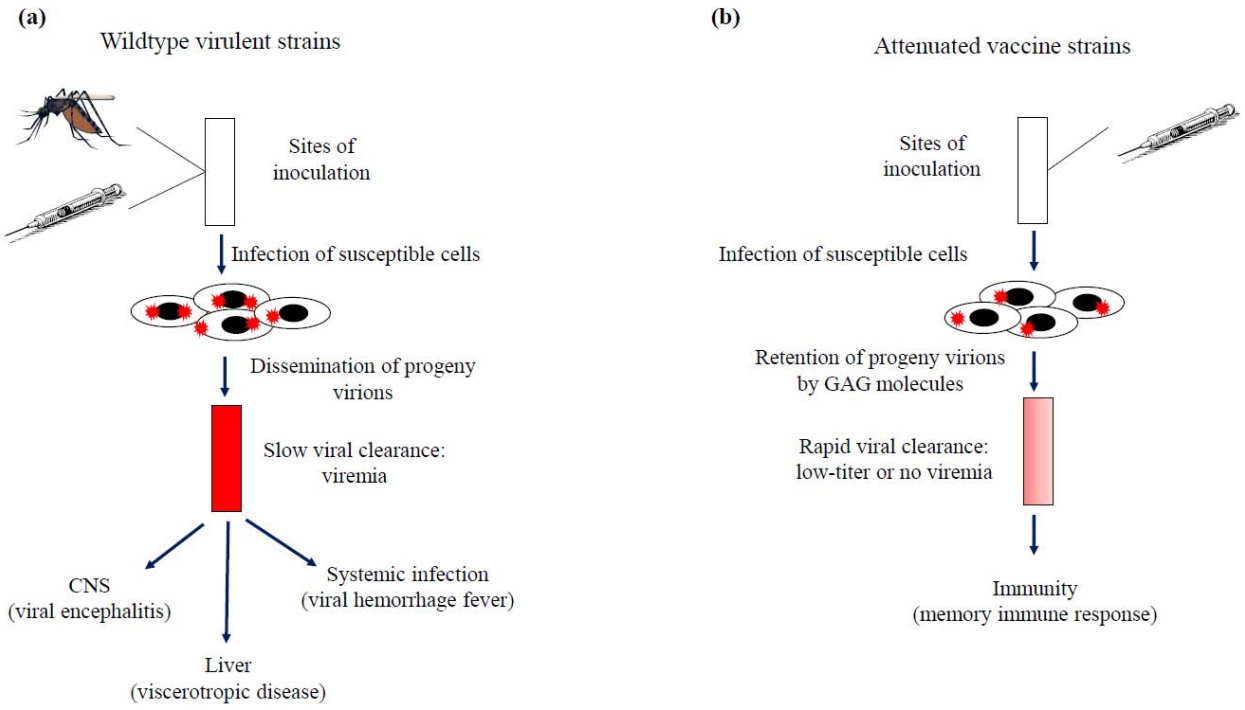

Figure 3.1 Invasion and disease pathogenesis of wildtype virulent strains and attenuated vaccine strains in vertebrate hosts

(a) The infection of the wildtype virulent strains is initiated at the site of inoculation followed by the infection of susceptible cells and subsequent dissemination into the blood stream. The viremia results in the systemic infection or severe clinical disease depending on the tissue tropisms of the viruses. (b) The inoculation of the attenuated vaccine strain lead to the infection of primary target cells and the limited dissemination due to the binding with GAG molecules. The binding with GAG molecules enhances the viral clearance from the blood stream. The resulting low viremia prevents the systemic infection and viral dissemination to target organs. The clearance of virus is followed by the development of the memory immune response.

The alignment of YFV E protein sequences derived from the Asibi strain, the 17D-204 substrain, the 17DD substrain, FVV and FNV indicated that the T380R mutation in the FG loop is only present in the attenuated YFV 17D strains derived from the Asibi strain. It is not found in the virulent and attenuated FVV and FNV strains. All other field isolates in Africa and Latin

America also showed the conserved threonine residue at the corresponding position. It was therefore, proposed that the attenuation was due to the RGD sequence is likely to be specific to 17D strains (Lee and Lobigs 2008). The sequences of the FG loops of YFV strains are summarized in **table 3.1**.

Strain	FG loop sequence (Amino acid residues 379-384)
Asibi	GTGDSR
17D-204	GRGDSR
17DD	GRGDSR
FVV	GTGDSR
FNV	GTGDSR

Table 3.1 The FG loop amino acid sequences of wildtype and vaccine YFV strains

The RGD motif was highlighted by underline.

The comparison of the region of FG loop with other flaviviruses revealed different patterns between the mosquito-borne and tick-borne flaviviruses, and among different serocomplexes of mosquito-borne flaviviruses. Interestingly, in spite of the variation of vectoring species and tissue tropisms, all of the FG loops present in mosquito-borne flavivirus EDIIIs are invariantly longer than the corresponding region in tick-borne flaviviruses. This is due to the absence of four amino acid residues in the tick-borne flaviviruses (Gritsun, Holmes et al. 1995, Rey, Heinz et al. 1995, Volk, Chavez et al. 2006, Volk, May et al. 2009).

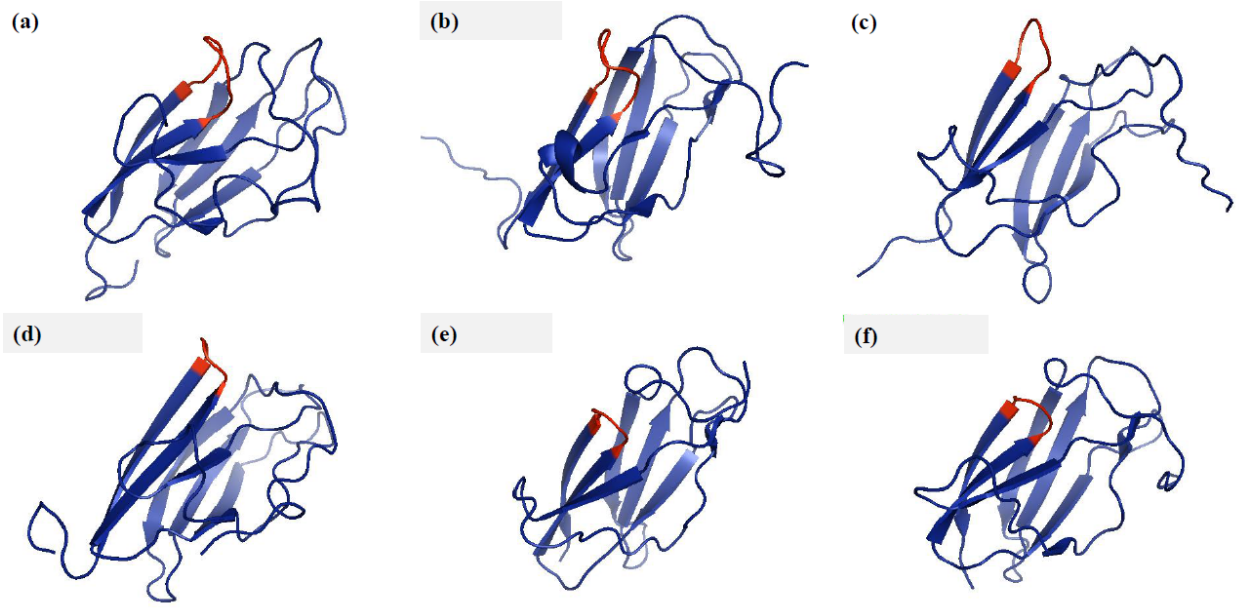

Figure 3.2 NMR structures of flavivirus EDIIIs

The EDIIIs of six flaviviruses are displayed in the order of (a) YFV (PDB: 2JQM), (b) DENV-2 (PDB: 2JSF), (c) JEV (PDB:1PJW), (d) WNV (PDB:1S6N), (e) TBEV (PDB:1Z66) and (f) OHFV (PDB: 1Z3R) with the FG loops labeled in red. The mosquito-borne flaviviruses share the longer FG loops than the tick-borne flaviviruses with the insertion of integrin-binding RGD motif.

The first glycine residue of FG loops is highly conserved among all the mosquito-borne flaviviruses; whereas, the last amino acid is only conserved in a serocomplex-specific manner. The sequences of the four amino acids are conserved in different serocomplexes which were classified based on serological antigenicity and are transmitted by different vector species. Members of JEV serocomplex, which are transmitted mainly by *Culex* mosquitoes, have highly conserved sequences containing the RGD motif in the region. For JEV and MVE within the JEV serocomplex, the RGD sequence is conserved and followed by a lysine residue (Ni, Burns et al. 1994, Hurrelbrink, Nestorowicz et al. 1999). The first functional characterization of the RGD motif in the flaviviruses under the JEV serocomplex demonstrated that the number of the positive charges associated with the RGD motif is direcly correlated with the efficienct of virus entry *in vitro.* However, the addition of the positive charge by substituting the aspartate residue with the histidine residue resulted in the attenuation *in vivo* (Lee and Lobigs 2000). In an NMR-structure study with the JEV monoclonal antibody (mAb) E3.3, the RGD motif was confirmed to determine antigenicity (Wu, Wu et al. 2003). In the two JEV-serocomplex members found in North America, namely SLEV and WNV, the arginine and glycine residues are conserved with the variations in third residue utilizing glutamate in WNV or threonine in SLEV and the forth residue utilizing glutamate in WNV and threonine in SLEV (Jia, Briese et al. 1999, Baillie, Kolokotronis et al. 2008). Whilst the sequence variation exsits in the third residue of the RGD motif, the aspartate, glutamate and threonine share the biochemical property due to the presence of the negatively charged hydroxyl group on the sidechains. The RGD sequence was less conserved under the DENV and YFV serocomplexes, which mainly consists of viruses that are transmitted by *Ae. aegypti* and *Ae. albopictus*. The FG loops of DENV-1, 3 and 4 use a hydrophobic amino acid as the first residue of the RGD motif followed by the conserved glycine and aspartate residues. DENV-2 has the most different sequences in the same region, which consists of the sequence of valine, glutamate, proline and glycine. In spite of the lack of sequence homology in the FG loop of DENV-2, it has been shown that the length of the FG loop

is critical for maintaining viral infectivity of DENV-2. Deletion of the region significantly reduces the infection rate of DENV-2 (Erb, Butrapet et al. 2010). The other viruses that are genetically closely related to YFV also showed a limited degree of sequence homology, especially at the positions of glycine and aspartate residues, in the FG loops. Notably, these viruses including Yokose virus, Sepik virus and Entebbe bat virus were known to be in the no known vector group, being viruses of bats and rodents and transmitted through the contact of excreta (Tajima, Takasaki et al. 2005, Kuno and Chang 2006). The sequences of the FG loops among the different serocomplexes of flaviviruses are summarized in **table 3.2**.

Serocomplex	Virus	Strain	Sequence of FG loop
YFV	YFV	Asibi	GTGDSR
	YFV	17D-204	GRGDSR
	ENTV	UgIL-30	GNGEDR
	SEPV	MK7148	GSGDDK
	YOKV	Oita36	GNGEDR
DENV	DENV-1	Haiwaii	GAGEKA
	DENV-2	New Guinea C	GVEPGQ
	DENV-3	H87	GIGDKA
	DENV-4	H241	GVGDSA
JEV	JEV	SA14	GRGDKQ
	JEV	SA14-14-2	GRGDKQ
	WNV	NY99	GRGEQQ
	KNV	MRM61C	GRGEQQ
	SLEV	MSI-7	GRGTTQ
	MVEV	MVE-1-151	GRGDKQ
TBEV	TBEV	Neudoerfl	G– – – – E
	OHFV	Bogoluvovska	G– – – – E
	KFDV	W-377	G– – – – E

Table 3.2 Amino acid sequences of the FG loop region in different flaviviruses.

The presence of the RGD motif is underlined.

Based upon the available knowledge related to the FG loop, one would predict that it is likely to serve as the determinants for the viral entry of DENV-2 into the mosquito midgut and

the viral dissemination of YFV and other encephalitic flaviviruses in mice. The different virus-vector relationships among the serocomplexes demonstrate that the viruses transmitted by *Culex* mosquitoes within the JEV serocomplex, contain the greatest degree of sequence homology for the RGD motif in the FG loop, whilst the DENV serocomplex and YFV serocomplex transmitted by *Aedes* mosquitoes show a higher diversity of amino acid sequences in the same region. The presence of the RGD motif is largely restricted to the flaviviruses, such as WNV and JEV, that are capable of utilizing a relatively broad number of different mosquito vectors species (Weng, Lien et al. 1997, Goddard, Roth et al. 2002, Capelli, Drago et al. 2011). Additionally, the attenuated JEV SA_{14}-14-2 vaccine strain and KNV, which is an attenuated subtype of WNV, still contain the conserved RGD or RGE sequence in the FG loops (Coia, Parker et al. 1988, Ni, Burns et al. 1994). The JEV SA_{14}-14-2 vaccine strain still retained the capacity of infecting multiple vertebrate hosts and vector species although it is attenuated and immunogenic as a human vaccine (Chen and Beaty 1982, Song, Yun et al. 2012, Calvert, Dixon et al. 2014).

The *per os* infection experiments using YFV T380R mutants in *Ae. aegypti* were designed to characterize the two critical mechanisms related to viral infection and dissemination. Our studies of the mutants will lead to a better understanding of the impact of the introduction of the RGD motif in the FG loop with respect to viral infection in *Ae.aegypti*. Additionally, the dissemination of the mutants will deterimine if the increased binding affinity with cellular GAG molecules might contribute to the retention of progeny virions from the infected midgut.

B. Receptors for YFV and other mosquito-borne flaviviruses

The biology of mosquito-borne flaviviruses requires the binding of infectious virions to cellular receptors of a diverse range of animal types, namely mammalian, avian and arthropod. The definition of viral receptors in the Fields Virology is as follows (Knipe and Howley 2013):

Virus receptors can be defined as cell surface molecules that bind the incoming viruses to the cell, and, in addition, promote entry by (a) inducing conformational changes in the virus that lead to priming, association with other receptors, membrane fusion and penetration; (b) transmembrane signals through the plasma membrane that lead to virus uptake or penetration, and prepare the cell for invasion; or (c) guiding bound virus particles into a variety of endocytic pathways.

The available knowledge suggests that multiple cellular molecules can be used simultaneously or sequentially by flaviviruses during the process of viral entry. Although the alternative route of viral entry through the endocytosis of the partially neutralized viruses bound to the recycled Fcγ receptors has been described, the first cellular component for the binding of YFV identified was the GAG molecules as the post-translational modifications to host proteins (Schlesinger and Brandriss 1981, Germi, Crance et al. 2002). The major cellular targets hypothesized to be the receptors for other related flavivirus described in the available literature will also be discussed in this section. The conservation of amino acid sequences of the ectodomains in the E proteins among many different mosquito-borne flaviviruses suggests the use of the same or similar receptor molecules as viral receptors across a broad range of susceptible host cell types. The identification of receptor molecules is often based on 1) the pre-treatment and competition of biochemically similar molecules with the endogenously expressed molecules in the susceptible cells, 2) the depletion or blockade of functional receptor molecules by the addition of chemical compounds and specific antibodies, and 3) the overlay assays of viral structural components with cell lysates separated electrophoretically. The major types of cellular receptors are summarized in **table 3.3**.

Molecules	Viruses	Cell type	Experimental approaches
Glycaosaminoglycans (GAG)	YFV	Vero	Heparin sulfate inhibition (Germi et al., 2002)
	DENV-1	Huh-7	Viral overlay binding (Hilgard & Stockert, 2000) (Hilgard et al. 2000)
	DENV-2	CHO Vero	Heparin sulfate inhibition (Yaping Chen et al., 1997; Germi et al., 2002) Genetically deficient cells (Yaping Chen et al., 1997)
	DENV-4	HUVEC	Heparinase III treatment (Dalrymple & Mackow, 2011)
	JEV	CHO	Heparin sulfate inhibition, sulfation inhibition, genetic deficient cells, immobilized heparin beads (Su, Liao, Lee, & Lin, 2001)

Integrins	WNV	Vero BHK CEF Neuro2a HeLa	Anti-$\alpha_5\beta_3$ integrin antibody (Chu and Ng 2004)
	MVEV	BHK-21 SW13 Vero	Heparin sulfate treatment(E Lee & Lobigs, 2000a)
Heatshock proteins	DENV-2	HepG2 U937	Viral overlay protein binding assay and chromatography purification (Jindadamrongwech, Thepparit, & Smith, 2004; J. R. Valle, Chávez-Salinas, Medina, & Angel, 2005)
	DENV-4	C6/36 *Ae. aegypti* tissues	Viral overlay protein binding assay (Mendoza, Salas-Benito, Lanz-Mendoza, Hernández-Martínez, & Angel, 2002; J. S. Salas-Benito & Angel, 1997, p. -)
	JEV	Neuro2a Huh7	Viral overlay protein binding assay, cell membrane fractionation, and computational prediction (Soma Das, Laxminarayana, Chandra, Ravi, & Desai, 2009; Zhu et al., 2012)
Laminin receptors	DENV-1	HepG2	Anti-laminin receptor antibody and lamin inhibition (Thepparit & Smith, 2004)
	DENV-1,2,3	Porcine kidney cells	Viral overlay protein binding assay (Tio, Jong, & Cardosa, 2005)
	WNV	Vero	Soluble lamin treatment(J. J. Chu & Ng, 2004)
C-type lectin	WNV	*Ae. aegypti* *Cx. quinquefasciatus*	RNAi in mosquitoes (Cheng et al., 2010) L-SIGN-expressing K562 cells (Davis et al., 2006)

		K562	
	DENV-2	3T3	Expression of DC-SIGN in 3T3 cells(J. L. Miller et al., 2008)
TIM/TAM proteins	DENV-2	293T	Expression of TIM and TAM molecules in 293T cells (Meertens et al., 2012)
	YFV	293T	Expression of TIM and TAM molecules in 293T cells (Meertens et al., 2012)
	WNV	293T	Expression of TIM and TAM molecules in 293T cells (Meertens et al., 2012)

Table 3.3 Summary of the cellular receptors utilized by mosquito-borne flaviviruses

Similar to other mosquito-borne flaviviruses that are able to cause viremia and hemorrhagic fever, especially DENV, the capacity of YFV in establishing infections in Fcγ-receptor-bearing leukocytes of human peripheral blood has been demonstrated and the infection of the YFV 17D strain was augmented *in vitro* by the presence of IgG antibodies through the Fcγ receptors (Schlesinger and Brandriss 1981). However, *in vivo* experiments have demonstrated that the increase in viral entry of wild-type YFV strains through antibody-dependent enhancement only took place in specific combinations between virus strains and antibodies. The mechanisms of viral entry remained unidentified (Barrett and Gould 1986, Gould and Buckley 1989).

Glycosaminoglycans

By introducing mutations to the RGD motif in the envelope protein of the 17D strain, viral dissemination into neighboring uninfected cells was abolished in the human SW13 cells but the mutants remained infectious to other mammalian and insect cells (van der Most, Corver et al. 1999). The results suggested that the binding to the integrins through the RGD motif may not be critical for virus entry, however, the use of integrin as receptors by YFV still cannot be excluded (Ruoslahti 1996). In Vero and BHK-21 cells, the YFV 17D strain was further shown to be sensitive to inhibition caused by the treatment with highly sulfated polysaccharides such as heparan sulfate or heparin sulfate. Such observation suggested that the receptor-binding motif of the E protein probably interacts with the heparan/heparin sulfate or other related GAG molecules as the initial receptors for viral entry (Germi, Crance et al. 2002, Lee and Lobigs 2008). The

disruption of RGD motif by the substitution of a TGD sequence in the wild-type YFV E protein led to a phenotype that was resistant to heparin sulfate treatment. As such, the motif has also been mapped as the potential GAG binding region of mosquito-borne flaviviruses (Hung, Hsieh et al. 2004). It therefore follows, that the GAG molecules on the cell surface are likely to be the receptors favored by YFV vaccine 17D strains, but not by other natural isolates. The passage of the Asibi strain in naturally non-susceptible mouse and avian cells resulted in the adaptation of viruses by utilizing GAG molecules as receptors. The change in the choice of cellular receptors is the consequence of the removal of the negative charges on the receptor binding motif by the amino acid substutions with positively charged or neutral side chains. This has been reported not only in flaviviruses but also for other enveloped RNA viruses. The adaptation of MVEV, JEV and WNV in tissue culture showed the consensus removal of the negative charge at the aspartate residue of the RGD motif and the increase affinity to GAG molecules (Lee and Lobigs 2000, Lee and Lobigs 2002, Lee, Hall et al. 2004). The GAG-binding phenotype of passaged attenuated viruses may contribute to the viral attenuation by promoting the more rapid viral clearance and preventing the systematic infection *in vivo*. Data using the immunocompromised mouse challenge model suggested that the potential mechanisms for the attenuation can be potentially achieved by the more efficient readsorption of progeny virions onto the primary target cells prior to the release into the blood stream. Altentatively, attenuation may also be achieved by the retention of virions in the extracellular matrix (ECM) through the interactions between the RGD motif and GAG molecules, which are ubiquitously expressed on the cellular surface (Lee and Lobigs 2008). The details of the mechanisms leading to the attenuation due to the increase electrostatic interactions among the vaccine or attenuated strains will be discussed in **section 3.1.E**. Another class of newly identified molecules as YFV receptors is human T-cell immunoglobulin and mucin-domain containing proteins (TIM-1,3 and 4) which mediate the phosphatidylserine-dependent phagocytosis for the cellular materials. The expression of TIM-1 in 293T cells was found to enhance the infectivity of YFV 17D strain and other mosquito-borne flaviviruses (Meertens, Carnec et al. 2012). However, this class of molecules is only encoded in the genomes of vertebrate hosts and the major viral receptors for YFV in the vectors remain unknown.

With the similar structures and amino acid sequences in the FG loop of E proteins, the interactions between GAG and flavivirus E proteins have also been reported as potential receptor

binding mechanisms for viral entry in multiple combinations of viruses and target tissues. By utilizing heparan disaccharides that vary in the concentrations of the sulfate modification and Vero cells, DENV-2 was found to interact with disaccharide units that were modified with the sulfate moieties. The disaccharide units are the minimal structural units required for the interaction with the E protein. The mutant CHO cells that are deficient in the sulfation mechanisms, also exhibited reduced binding efficiency to the virions (Chen, Maguire et al. 1997, Germi, Crance et al. 2002). Further supportive evidence was also provided by experiments that were based on Huh7 human hepatocytes exposed to DENV-1, as well as endothelial cells challenged with DENV-4 (Hilgard and Stockert 2000, Dalrymple and Mackow 2011). Both cell types are regarded as susceptible tissues that support the productive infection of DENV in human. Although variations in the sensitivity of the antiviral effect have been reported in different sulfated disaccharides and serotypes of DENV, multiple sulfated saccharides have been evaluated as inhibitors for the entry of DENV for use as antiviral treatments (Lin, Lei et al. 2002, Kato, Era et al. 2010, Vervaeke, Alen et al. 2013). Although the crystal structures and sequences of DENV E proteins suggested the presence of potential heparin binding motifs in EDI and EDIII, respectively, the *in vitro* experimental evidence demonstrated that the heparin sulfate binding motif is likely to be located in the FG loop region. For YFV, this is also where the RGD motif in the EDIII is located (Chen, Maguire et al. 1997, Hung, Hsieh et al. 2004, Lee and Lobigs 2008). In contrast to the observations for YFV, for JEV it was demonstrated that both virulent and attenuated strains, which shared the conserved RGD motif of the EDIII FG loop, interact with GAGs during the early stage of infection *in vitro* (Su, Liao et al. 2001). However, the variants of JEV and other viruses within the JEV serocomplex showed that multiple motifs in the E protein may be responsible for such interactions and that these motifs may differ from those identified in YFV and DENV (Lee, Hall et al. 2004, Liu, Chiou et al. 2004, Chiou, Liu et al. 2005). Interestingly, experiments utilizing TBEV have demonstrated that an increase in the binding of heparan sulfate among the variant viruses can be frequently caused by the mutations that accumulated during the process of *in vitro* passage, and that led to a gain of positive charges in the E protein (Mandl, Kroschewski et al. 2001). The capacity of establishing productive infection by TBEV in heparan sulfate-deficient cell lines further suggested the involvement of other non-GAG molecules serving as the receptors for flaviviruses.

Together, the experimental evidence suggests that the GAG molecules are likely to function as viral receptors or as the docking molecules that create the concentrated distribution of virions prior to the binding other viral receptors. However, the conclusions should be made carefully based on the fact that the mutants with the higher affinity to the GAG molecules can be artificially selected after the serial passage of viruses *in vitro*, especially in cell lines derived from naturally non-susceptible hosts (Kroschewski, Allison et al. 2003).

Integrins

The other class of molecules abundantly expressed in both vertebrate hosts and arthropod vectors are integrin molecules. These are involved in the interactions between cells and the scaffold of the ECM, and have been identified as receptors for arboviruses and other small enveloped RNA viruses (Gavrilovskaya, Shepley et al. 1998, La Linn, Eble et al. 2005). Interestingly, the viral protein regions proposed to interact with integrin molecules may overlap with the GAG-binding region in the flavivirus E proteins, primarily in the RGD motif in EDIII (van der Most, Corver et al. 1999, Chu and Ng 2004, Lee and Lobigs 2008). However, the subsequent competition binding assays with the recombinant RGD peptide suggested that WNV may use a non-classical integrin-binding motif that does not contain the RGD sequence in these interactions (Chu and Ng 2004). For MVEV which was the first virus proposed to utilize integrins as cellular receptors, it was found that the virus was resistant to heparin sulfate treatment. This lack of the sensitivity to heparin sulfate treatment, supported the importance of molecules other than GAG molecules in the viral entry process because the receptor-binding domain of the virions was able to interact with the viral receptors despite of the high concentration of heparin sulfate (Lee and Lobigs 2000, Hurrelbrink and McMinn 2001). In contrast to MVEV, DENV-2 which requires the presence of GAGs on the cellular surface is resistant to the depletion of divalent cations such as Ca^{2+} and Mg^{2+}, which disrupt the structure and function of cellular integrin molecules (Stuiver, Ruggeri et al. 1996, Bielefeldt-Ohmann, Meyer et al. 2001). The reverse genetics system for MVEV allowed the evaluation of the integrin-interacting RGD sequences (that are conserved across the members of JEV serocomplex) and were proposed to interact with integrin molecules among flaviviruses by van der Most *et al* (van der Most, Corver et al. 1999). By selectively mutating the aspartate residue in the RGD motif to glycine or histidine, the mouse neurovirulence of MVEV was significantly reduced, however, the mutant viruses remained resistant to heparin sulfate treatment.

Unfortunately, experiments to evaluate the physical interaction between the virions and the integrins or the effects of depletion of functional integrins were not performed (Lee and Lobigs 2000). Further supporting a role of integrin as a receptor, are results with specific antibodies to block $\alpha_5\beta_3$ integrin, which resulted in the inhibition of WNV and JEV infection. The elevated expression of the $\alpha_5\beta_3$ integrin in the variant CS-1β_3 cells also led to the increase of virus entry of WNV in contrast to the lack of the permissiveness to WNV in the CS-1 cells (Chu and Ng 2004). Interestingly, discrepancies between the experiments based on the genotype I and genotype II of WNV suggested that $\alpha_5\beta_3$ integrin-mediated viral entry may be genotype specific (Medigeshi, Hirsch et al. 2008). The β_3 integrins exhibited the capacity of modulating the permissiveness of WNV infection *in vitro* (Schmidt, Keller et al. 2013). A specific β_3 integrin molecule, CD61, has been proposed to be associated with the DENV antigens in the platelets of patients (Noisakran, Onlamoon et al. 2012). Together, the evidence based on blocking and expression experiments has generally supported the possibility that integrin molecules play a role as the receptors for flaviviruses. The actual/specific roles of integrins as receptors for flaviviruses remain obscure and can be complicated by the fact that integrins may be involved in various parts of virus infection.

Heatshock proteins

Multiple types of data suggest that the family of heat shock proteins (HSP) encoded in genomes of both vertebrate hosts and mosquitoes may be receptors of mosquito-borne flaviviruses. These include: viral overlay protein binding assay (VOPBA) data from DENV-2 infection of HepG2 cells, mass spectrometry data and antibody inhibition results which identified the glucose regulated protein 78 GRP78 (Bip) under the family of HSP as a potential DENV-2 receptor in humans (Jindadamrongwech, Thepparit et al. 2004). Purified cellular lysates interacting with DENV-2 E protein through chromatography also suggested that the other two other heat shock proteins HSP70 and HSP90 may be receptors in monocytic U937 cells (Reyes-Del Valle, Chavez-Salinas et al. 2005). Similar VOPBA methods were also used to identify DENV-4 receptors in C6/36 cells leading to the discovery of two glycoproteins, gp40 and gp45, which were subsequently identified in other permissive tissues in *Ae. aegypti* for DENV-4 (Salas-Benito and del Angel 1997, Yazi Mendoza, Salas-Benito et al. 2002). The gp45 protein was also identified in the experiments using DENV-2, together with the other heat shock protein Hsp74 (Salas-Benito, Reyes-Del Valle et al. 2007). Subsequently, HSP70 was identified as a

receptor for JEV in Neuro2a and Huh7 cells through the potential interaction of the RGD motif in the E protein based on the bioinformatics analysis (Das, Laxminarayana et al. 2009, Zhu, Cao et al. 2012).

Laminin receptors

The other class of molecules identified as the potential receptors for flaviviruses based on the VOPBA experiments was laminin receptors. Laminin receptors are molecules expressed on the cellular surface for the binding of the basement membrane and have been reported to mediate the entry of members under the Flaviviridae and Togaviridae (Nelson, McFerran et al. 2008). DENV-1 was also demonstrated to interact with the 37 kDa/67 kDa high-affinity laminin receptor in HepG2 cells. Antibodies targeting the laminin receptors and the soluble laminin treatments led to the reduced viral titer potentially by reducing the viral entry (Thepparit and Smith 2004). The same receptor derived from porcine kidney cells also interacted with DENV-1, 2 and 3 (Tio, Jong et al. 2005). Laminin receptors reactive to anti-37 kDa/67 kDa antibodies were also found to interact with DENV-3 and DENV-4 in C6/36 cells (Sakoonwatanyoo, Boonsanay et al. 2006). The interactions between the laminin receptors and JEV were also observed with similar methods and the pretreatment of soluble laminin inhibited the virus entry (Boonsanay and Smith 2007). In the experiments devised to test the hypothesis that WNV utilizes receptors molecules other than $\alpha_5\beta_3$ integrin, the physical interaction was observed between the laminin binding protein and the recombinant polypeptide of WNV E protein. The atomic force spectroscopy data further suggested EDIIs of flaviviruses are the conserved region which interact with the laminin receptors (Bogachek, Protopopova et al. 2008).

C-type lectins

The studies on the three groups of C-type lectin receptors indicated such mechanisms are conserved in vertebrate hosts, especially among the myeloid cells which express other homologous proteins. The glycosylation sites conserved across flaviviruses have been shown to complex with the carbohydrate recognition domain (CRD) of the dendritic cell-specific intracellular adhesion molecule-3grabbing non-integrin (DC-SIGN) in the immature dendritic cells, which may act as the primary target cells for viral infections in humans (Pokidysheva, Zhang et al. 2006). As the primary susceptible cells at the locations for the initiation of arbovirus infection, the identification of DC-SIGN as the viral receptors supports the importance of

dendritic cells as the susceptible cells in human (Wu, Grouard-Vogel et al. 2000). The other similar molecule, liver/lymph node-specific ICAM-3 grabbing non-integrin (L-SIGN), has also been proposed to enhance the infection of WNV (Davis, Nguyen et al. 2006). Similarly, the mannose receptor which also belongs to the family of C-type lectin receptor has also been demonstrated as a receptor of DENV-2 in various cell types that are involved in DENV disease pathogenesis (Taylor, Gordon et al. 2005, Miller, de Wet et al. 2008).

Although it has only been found for WNV, the galactose-specific binding C-type lectin serves as the bridging factor which anchors the virions to the cellular receptor, mosPTP-1 tyrosine phosphatase in mosquitoes (Cheng, Cox et al. 2010). The hemocytes of hematophagus arthropods, including *Ae. aegypti,* exhibit the lectin binding activity and have been found susceptible to the infection of arboviruses. This suggests the possibility that the C-type lectin receptors may also function as virus receptors for mosquitoes (Sriurairatna and Bhamarapravati 1977, Yamamoto, Kimura et al. 1987, Hillyer and Christensen 2002, Parikh, Oliver et al. 2009). Although the importance of C-type lectins to assist the binding between virions and hemocytes has been recognized, the receptors for flaviviruses on the midgut epithelial cells remains unknown.

T cell immunoglobulin domain and mucin domain

In mammalian hosts of flaviviruses, the recycling machinery for the apoptotic cells through the T-cell immunoglobulin domain and mucin domain (TIM) proteins may directly facilitate viral entry through direct interactions between TIM-1,3 and 4 with the virion of flaviviruses. Similarly, the class of TAM receptors consist of the family of surface protein tyrosine TYRO3, AXL and MER kinases also increases the virus entry via the binding through their natural ligands as the bridging molecules (Meertens, Carnec et al. 2012). The recognition of virions by both classes of the receptors is achieved by the recognition of the phosphatidylserin derived from the cell membrane of the hosts.

In conclusion, the research to identify receptors for YFV and other mosquito-borne flaviviruses has suggested the virus entry may be achieved by multiple molecules and pathways. Although the extensive research has identified several molecules in the vertebrate hosts and the arthropod vectors, there was no confirmative evidence showing YFV and other related flaviviruses rely on a specific class of molecules as receptors. Such information is critical for its application in the development of antiviral inhibitors targeting at the virus entry for humans and

other vertebrate hosts. On the other hand, the mapping of the viral determinants for receptor binding can contribute to the goal of rationale-based vaccine design that limits the infectivity of live-attenuated vaccines in both vertebrate hosts and arthropod vectors.

C. The process of viral entry

It is generally accepted that members in the family of *Flaviviridae* and other arboviruses enter cells through endocytosis pathways. The specific knockdown and blockade of genes required for the different subsets of endocytosis mechanisms through molecular biological or pharmacological approaches have been used to determine the specific routes of viral entry, and the cellular compartments that are responsible for the trafficking of viral components prior to the formation of replication complex in the perinuclear space in the infected cells. Lysosomotropic weak bases such as chloroquine were first demonstrated to suppress the infection by 10-fold of YFV in murine macrophage $P388D_1$ cell line at early stage of infection, and suggested that the endocytosis pathways shared by other mosquito-borne flaviviruses can mediate virus entry of YFV (Brandriss and Schlesinger 1984). Subsequent experiments utilizing other weak bases such as ammonium chloride, or the depletion of the V-ATPase by RNA interference, showed that the gradual decrease of pH in the endocytosis pathway is critical for DENV-2 and WNV (Krishnan, Sukumaran et al. 2007). Although clathrin-mediated endocytosis is considered to be the predominant pathway for the entry of flaviviruses, additional pathways including macropinocytosis, caveolae-dependent endocytosis, and lipid-raft have also been reported in different combinations of flaviviruses and cell types.

Clathrin-mediated endocytosis

In the clathrin-mediated endocytosis pathway, the virions of flaviviruses are transported by endosomes that are exposed to the gradient of acidic conditions prior to reaching the perinuclear space of the infected cells, where the viral replication complex is formed (Welsch, Miller et al. 2009, Mercer, Schelhaas et al. 2010). Clathrin protein was first found in the coat of vesicles that contain KUNV (Ng and Lau 1988). Treatment of chlorpromazine inhibited the clathrin-mediated endocytosis and also resulted in reduced numbers of infected Vero and HeLa cells challenged with JEV and WNV respectively (Nawa, Takasaki et al. 2003, Krishnan, Sukumaran et al. 2007). The evidence suggesting that flaviviruses enter the host cells through clathrin-mediated endocytosis, followed by the transportation in the early endosomes, is based on

the reduced viral replication of DENV-2 and WNV in the HeLa cells with the depletion of Rab5 GTPase and Eps15 adapter protein functions. Both the enzyme and the protein have been found as two critical components of clathrin-mediated endocytosis (Krishnan, Sukumaran et al. 2007). The silencing of clathrin genes also led to a reduced number of DENV-2 infected cells and a reduced extracellular viral load in Huh7 cells, HepG2 cells and primary monocyte cultures (Ang, Wong et al. 2010, Alhoot, Wang et al. 2011, Alhoot, Wang et al. 2012). The expression of anti-clathrin antibodies and the dominant negative mutant of Eps15 also effectively suppressed the WNV and DENV-2 entry in C6/36 cells and supports the importance of the clathrin-mediated endocytosis in viral entry of flaviviruses (Lee, Chu et al. 2006, Mosso, Galvan-Mendoza et al. 2008). The inhibitor treatment further demonstrated that clathrin-mediated endocytosis is required for the viral entry of DENV-1, DENV-3 and DENV-4 into C6/36 cells (Acosta, Castilla et al. 2011). Together, it is likely that the entry of flaviviruses may utilize the conserved clathrin-mediated endocytosis pathways in both vertebrate hosts and arthropod vectors. Subsequently, the adapter protein such as AP2 and its homologous molecules interact with Eps15 will lead to the formation of clathrin-coated pits that contain the virions under the outside-in endocytosis signaling via the focal adhesion kinase (FAK) (Benmerah, Lamaze et al. 1998, Chu, Leong et al. 2006). The switching of the Rab5 GTPase to the Rab7 GTPase in the late endosomes containing viral antigens was also observed in HeLa cells. The acidic environment of late endosomes triggers the fusion process mediated by the exposed fusion peptide in the EDII of flaviviruses (Miller, de Wet et al. 2008). In C6/36 cells, the colocalization of the early endsome marker EEA1 and the late endosome markers MRP-1 and the antigens indicated that the same endocytosis pathways and subset of endosomes may be conserved in infected vertebrates hosts (Chu, Leong et al. 2006). However, the sequestering of functional Rab7 GTPase by the overexpression of dominant negative Rab7 mutant did not affect the virus internalization of two serotypes of DENV and WNV *in vitro* (Krishnan, Sukumaran et al. 2007, Acosta, Castilla et al. 2012). The Rab22 GTPase majorly localized in the recycling endosomes has also been implicated as an alternative route for viral endocytosis (Acosta, Castilla et al. 2012). There have been at least three types of cytoskeletal structures, microfilaments, microtubules and vimentin, reported for the post-entry trafficking processes (Chu, Leong et al. 2006, Acosta, Castilla et al. 2008, Chen, Gao et al. 2008).

Macropinocytosis

Although the blockade of clathrin-mediated endocytosis resulted in the significant reduction in viral infection, DENV-2 antigens were still detected in a subset of HepG2 cells suggesting that alternative pathways may contribute to viral entry. The growth-factor mediated macropinocytosis pathway has also been described as an additional endocytosis pathway used by microorganisms (Mercer, Schelhaas et al. 2010). Similar to other growth-factor-mediated signal transduction pathways, the macropinocytosis is subjected to the regulation of phosphoinositol 3-kinase (PI 3-kinase) at the step of endocytosis vesicle formation (Murray, Wilson et al. 2000). Simultaneous inhibition of the clathrin-mediated endocytosis and macropinocytosis by RNA interference and the PI 3- kinase inhibitor wortmannin led to the more profound reduction in the quantities of viral antigens than the monovalent inhibition of both pathways. The observation is also consistent with the result that cytochalasin D led to a minor reduction of JEV infection in Vero cells (Nawa, Takasaki et al. 2003). Macropinocytosis may therefore act as an alternative mechanism for the entry of flaviviruses (Suksanpaisan, Susantad et al. 2009). Alternatively, the knockdown of caveolin-1 also led to the reduction of JEV infection in neuroblastoma cells and the same study also showed the dynamin GTPase that is required for the scission of endocytosis vesicles is also required for viral entry. However, whether the macropincytosis or the caveolae-dependent endocytosis of flaviviruses acts as alternative viral entry mechanisms for other flaviviruses in other tissues in either vertebrate hosts or in arthropod vectors has not been determined.

Lipid Raft-dependent entry

Another critical structure that has been reported to be involved in the viral entry on the cell surface is the cholesterol-dependent lipid raft. The significance of the local lipid raft for flavivirus entry was established by the experimental observation that the withdrawal of cholesterol is often assicuated with the inhibition of viral entry. The lipid raft-mediated the viral entry requires the early and late endosomes with ER as an alternative destination of the uncoating of viral genetic material.The process is less well characterized because the removal of cholesterol can also subsequently impair the clathrin-mediated endocytosis pathway (Mercer, Schelhaas et al. 2010). The importance of lipid raft for virus entry was first demonstrated by treatment of U937 cells with methyl-β-cyclodextrin (MβCD) which suppressed DENV-2 infection. The lipid raft structures were co-purified with the putative receptors Hsp70 and Hsp90 suggesting that lipid rafts act as a platform for the enrichment of viral receptors on the cell

membrane (Salas-Benito, Reyes-Del Valle et al. 2007). The cholesterol-rich membranous structures were demonstrated to be required for the entry of WNV but were independent from α5β3 integrin (Medigeshi, Hirsch et al. 2008). Depletion of cholesterol by MβCD also disrupted the lipid raft structure and simultaneously suppressed JEV infection in the porcine kidney epithelial PK15 cell line (Yang, He et al. 2013). The lipid raft, which may act as the platform for various viral receptors, was first found to be associated with the JEV infection in the neural stem/progenitor cells by the colocalization of the lipid-raft marker Cholera toxin B (Das, Chakraborty et al. 2010). Although it was not tested in the cells derived from its naturally susceptible tissues, the observation was further expanded to an association between the putative JEV receptor Hsp70 and the lipid raft of HepG2 cells s. The infection with JEV led to the migration of Hsp70 into the lipid raft and triggered the signaling of the PI3K/Akt signaling pathway (Zhu, Cao et al. 2012).

Although the various endocytosis mechanisms identified for the viral entry of flaviviruses suggested that multiple pathways may be used by individual viruses, the virions are ultimately transported to the late endosome, where the acidic environment triggers the conformational change of the E proteins. All the flaviviruses share similar mechanisms triggering the conformational changes, which lead to the exposure of the fusion peptides in the E proteins and its insertion into the cellular membranes. The details of membrane fusion process and mechanisms will be described in **section 4.1**.

D. Structures and functions of YFV and flavivirus EDIIIs

The available structure information of flavivirus EDIIIs including YFV has been determined by the nuclear magnetic resonance (NMR) spectroscopy. The structure of YFV EDIII was obtained by the recombinant EDIII of YFV Asibi strain and NMR spectroscopy (Volk, May et al. 2009). Although the mature infectious form of YFV particles has not been characterized in cryoelectron microscopy (cryoEM), the immature virus particles of YFV resemble those of DENV-2 suggesting high homology of the mature particles of YFV and DENV-2 and also high similarity after the removal of the pr peptide from the prM protein prior to the release into extracellular space (Zhang, Corver et al. 2003). The EDIIIs project away from the surface of the virion to enable binding of cellular receptors, and form the pore-like structure under the 5-fold axes of symmetry (Kuhn, Zhang et al. 2002). Each monomeric unit of EDIII is anchored to the

lipid membrane by the transmembrane region in the C terminus of E protein. The transmembrane region consists of three perimembrane helical structures at its N-terminal region and two helical structures spanning the viral membrane at its C-terminal region connected by the loop structures. The perimembrane helices are the transition amphipathic regions with hydrophilic amino acids arranged outwards and hydrophobic amino acids located at the bottom within the close proximity of viral membrane. The two transmembrane helical structures are stabilized by the formation of the coiled-coil structural unit with the hydrophobic residues exposed outwards and the hydrophilic amino acids facing inward (Zhang, Chipman et al. 2003, Zhang, Ge et al. 2013). The structures and arrangement of EDIIIs on the virion surface among other flaviviruses are also highly similar (Zhang, Kaufmann et al. 2013, Kostyuchenko, Chew et al. 2014).

The overall structure of YFV EDIII resembles the IgG-like β-barrel structure consisting of nine β-strands arranged in three β-sheets. The permembrane and transmembrane helices were not included in the available NMR structure derived from the soluble portion of EDIII (Volk, May et al. 2009). The detailed annotated structure of YFV EDIII is displayed as **Figure 3.1**.The first β-sheet is composed of four β-strands, β-strand A from Ser305 to Asp312, β-strand B from Val318 to Lys323, β-strand D from Ile348 to Leu349, and β-strand E Glu362 to Asn368. (**Figure 3.1 (a)**) The ABED β-sheet faces EDI via the linker region between EDI and EDIII. Two short β-strands, β-strand Cx from Cys330 to Lys331 and β-strand Dx from Ile355 to Ala356, form the second β-sheet. The third β-sheet consists of three β-strands, β-strand C from Val334 to Ala337, β-strand F from Gly372 to Val378 and β-strand G from Leu385 to Lys391. The CFG β-sheet is exposed in the outer lateral surface of the dimeric structure of E protein. (**Figure 3.1 (b)**) The conservide disulfide bond is formed between Cys300 in the N-terminal loop structure and Cys330 in the β-strand Cx. There are four surface exposed loop structures connecting the β-strands between different β-sheets or within the same β-sheet. DE loop exists between β-strand D and β-strand E within the first β-sheet. The BC loop is comprised of the amino acids between β-strand B in the first β-sheet and β-strand C in the third β-sheet. Similarly, the CD loop structure connects the β-strand C in the third β-sheet and the β-strand D of the first β-strand. The FG loop is located between the β-strand F and β-strand G within the third β-sheet.

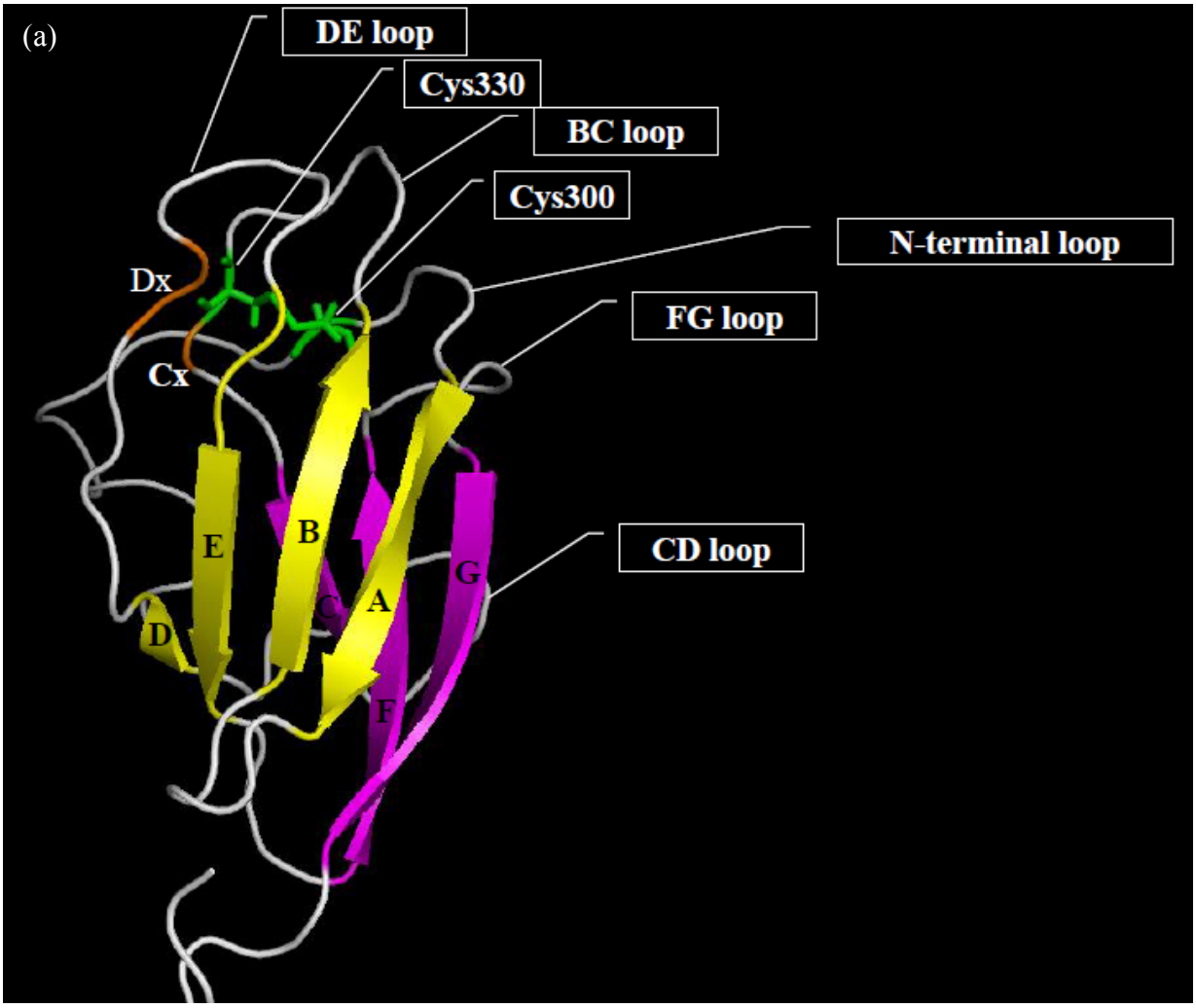
(a)
DE loop
Cys330
BC loop
Cys300
N-terminal loop
FG loop
CD loop
Dx
Cx
E
B
C
A
G
D
F

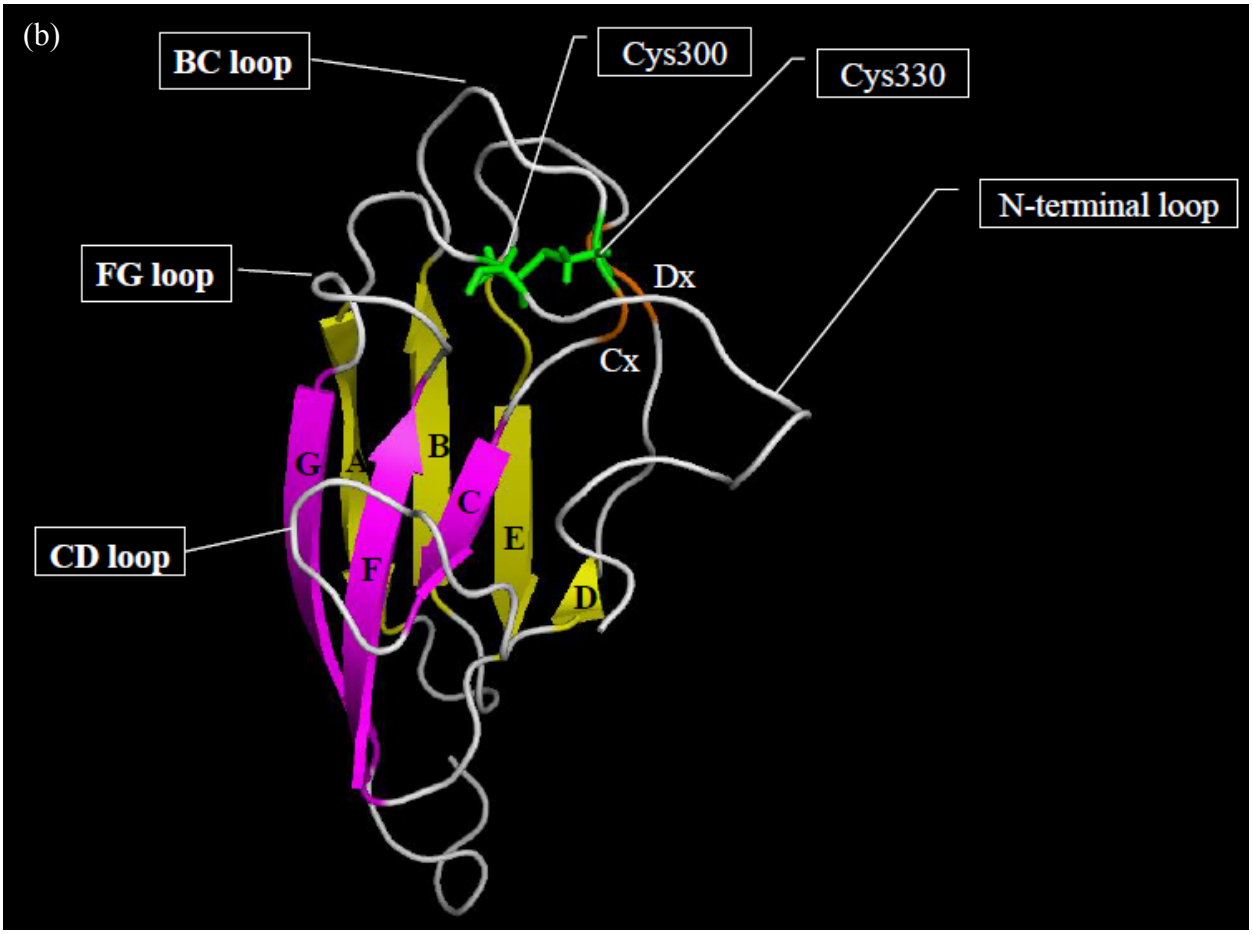

Figure 3.3 NMR 3D structure of recombinant YFV EDIII is displayed and annotated. (a)The inner ABED β-sheet is colored in yellow. Cys300 and Cys330 that contribute to the formation of the disulfide bond are colored in green. (b) The lateral surface portion formed by the third CFG β-sheet is colored in magenta. The second β-sheet formed by the two short Cx and Dx β-strands is colored in orange.

With respect to YFV, there have been four amino acid substitutions identified in the ectodomain of EDIII between the Asibi and 17D strains. The M299I mutation is located in the N-terminal loop, which is part of the linker region between EDI and EDIII. The region accommodates the mechanical force generated due to the pH-dependent conformational changes during the virus entry and the exocytosis of progeny virions (Modis, Ogata et al. 2004, de Wispelaere and Yang 2012). The details of the conformational changes and the phenotypes associated with the mutations in the N-terminal loop will be discussed in **section 5.1**. The S305F mutation in the A β-strand is located in the inner face of EDIII formed by the ABED β-sheet.

The ABED β-sheet faces the region between the C β-strand and the D β-strand of EDI and interacts with the cd loop structure of EDII from the other subunit. The P325F mutation is part of the BC loop structure in the upper portion of EDIII that has been found variable among different serocomplexes of flaviviruses. The conservative K331R mutation exists in the small Cx β-strand as part of the second β-sheet structure of the two-layer sandwich IgG-like structure. The T380R mutation is located in the FG loop between the F and G β-strands of the third β-sheet. The sequence diversity and the phenotypes associated with the mutations within the FG loop are listed in the **section 3.1.a**.

The detail functions and antigenicities of YFV and flavivirus EDIIIs were characterized with the mutant viruses or recombinant proteins carrying specific mutations. The mutations that present in YFV 17D strain EDIIIs have been found related to the protective humoral immune responses or the changes in the electrostatic interactions with the host cellular proteins. The S305F mutation on the A β-strand and the P325S mutation in the BC loop of YFV are the B-cell epitopes for the 17D strains identified by the neutralization escapes of the monoclonal antibody (MAb) Mab864 (Despres, Ruiz-Linares et al. 1990, Ryman, Ledger et al. 1998). The substitution of Phe305 with valine was found associated with the increase of neurovirulence and neuroinvasiveness in the escape mutants and the mouse-neuroadapted strains of YFV, respectively (Ryman, Ledger et al. 1998, Nickells and Chambers 2003). The immunogenic properties of the A β-strand region neighboring to the S305 mutation in YFV EDIII were also supported by the mapping of B-cell epitopes in other flaviviruses. The regions in the A β-strand of DENV-2 and WNV EDIIIs have also been demonstrated to contain the epitopes for the subcomplex-specific neutralizing MAbs and the neutralizing MAbs, respectively (Beasley and Barrett 2002, Sukupolvi-Petty, Austin et al. 2010).

The wildtype YFV Asibi and attenuated 17DD strains showed the Pro325 residue forcing the BC loop turning towards the C β-strand and created the unique structure of the N-terminus of BC loop by substituting the conserved tyrosine or phenylalanine residues among all flaviviruses with the valine for YFV BC loop (Volk, May et al. 2009, Zhang, Bovshik et al. 2010). The use of proline residue forces the turn of BC loop towards the C β-strand. Interesting, the Pro325 residue was mutated to serine in YFV 17D-204 strains and identified as the substrain-specific epitope for YFV 17D-204 strains (Ryman, Ledger et al. 1998, Stock, Boschetti et al. 2012). Interestingly, the P325S mutation of the 17D-204 strand led to the smaller BC loop structure than the other

strains of YFV and all other mosquito-borne flaviviruses without altering the valine residue present in the first residue of the BC loop. In addition to the alteration of the conserved tyrosine or phenylalanine to valine in the N-terminus of BC loop, the unique structure of YFV BC loop also led to the amino acid substitution of the conserved phenylalanine to methionine at the last residue of the N-terminal loop due to the molecular interactions with the first residue of the BC loop (Volk, May et al. 2009).

As the exposed structure in the upper portion of YFV EDIII, the BC loop is associated with a change of GAG-binding affinity due to the amino acid substitutions at the Lys326 residue in a mouse neuroadapted 17D strain. The K326E mutation led to the higher neuroinvasiveness resembling the mouse-neuroadapted 17D strain (Nickells, Cannella et al. 2008). Although the T380R and K326E mutations are located in distinct locations in the upper portion of YFV EDIII, the experimental results suggested that an accumulation of the positive charges on the exposed surface of EDIII is likely to determine viral dissemination in mammals. The E327G mutation in the BC loop of DENV-4 also led to the predicted gain of net positive charges on the virion surface through the structural rearrangement and reduced the infectivity and immunogenicity in rhesus monkeys (Anez, Men et al. 2009). The other additional region that has been extensively reported to confer the determinants for GAG binding affinity, exists in the N-terminal loop region (Chen, Her et al. 2010, Watterson, Kobe et al. 2012, Roehrig, Butrapet et al. 2013). However, the results were obtained from the binding of recombinant proteins of EDIII or the rescued mutants that contain the secondary compensatory mutations. Althought the G304K mutation in the N-terminal loop of DENV-2 E protein was characterized as an additional GAG-binding determinant, the G304K mutant also contains the G330D compensatory mutation located in the BC loop, which was reported to change the GAG binding affinity in YFV and DENV-4.(Añez et al., 2009; J. Nickells et al., 2008; Roehrig et al., 2013).

The K331R mutation in the short Cx β-strand was also found in both the lethal and non-lethal viscerotropic strain of hasmster-passaged YFV Asibi strain (McArthur, Xiao et al. 2005). The tolerance between the lysine and arginine residues may be explained by the similar chemical and physical properties, and suggested a lack of the short Cx β-strand involvement in either attenuation or virulence.

E. Viral attenuation due to the increased electrostatic interactions through negatively charged cellular molecules

The attenuation of virulent viruses has often been achieved by the serial passages *in vitro* in order to increase the interactions between the virions and the negatively charged molecules on the cellular surface. The gain of positive charges on such locations has been hypothesized to be the consequence of the adaptation made by the various viruses to the environment of non-natural hosts or tissue cultures. Although the post-translation modification of GAG has been considered as the potential underlying mechanism that mediates viral entry *in vitro* through the electrostatic interactions, the GAG molecules are also likely to cause the attenuation of virulent strains in the experimental models of vertebrate hosts predominantly through the retention of progeny virions after the processes of morphogenesis and virion secretion are completed. The attenuated GAG-binding variant viruses exhibit a higher affinity to heparin or heparan molecules that may be used as the approach for phenotype characterization (Klimstra, Ryman et al. 1998, Perera-Lecoin, Meertens et al. 2014).

The attenuation of YFV being attributed to the positive charges on the E protein has been reported in two experimental models. The first involves the T380R mutation that was described in the section 3.1.A and which shares a similar phenotype with the GAG-binding variants of flaviviruses (Lee and Lobigs 2008). The second involves the characterization of the K326E mutation in the neuroadapted 17D strain which implicated the BC loop as a potential locus for the binding with negatively charged cellular molecules and the neurovirulence of the virus (Nickells, Cannella et al. 2008).

The attenuation caused by the mutations in the GAG-binding region of EDIII was first observed in MVEV. The RGD motif in MVEV EDIII was found to be critical for the growth kinetics *in vitro* and the virulence *in vivo*. The conservative mutation from aspartate to glutamate resulted in the minor reduction in the viral titers and the virulence; whereas, the non-conservative glycine, histidine, and tyrosine mutations attenuated the virus and led to the lower mortality rates among the outbred Swiss mice. Interestingly, the gain of positive charge by the histidine mutation not only was responsible for the most significant attenuation by causing no or negligible mortality among intraperitoneally challenged mice, but it also increased the inhibition of viral entry caused by heparin sulfate treatment (Lee and Lobigs 2000). In the other independent study characterizing the hinge region and the RGD motif of MVEV E protein, the

non-conservative mutation of the aspartate residue to asparagine or tyrosine significantly reduced both the neurovirulence and neuroinvasiveness in intracranially or intraperitoneally inoculated outbred Swiss mice. Whilst the growth kinetics showed that the non-conservative mutations impaired the viral replication, the pH-dependent conformational change was not altered as the optimal pH of hemagglutination activity remained the same. The lower viral titers in the brains of intracranially challenged mice further supported the attenuation caused by the mutations (Hurrelbrink and McMinn 2001). The RGD motif is therefore likely to harbor the determinant for viral attenuation by enhancing the interactions with negatively charged cellular materials.

The serial passage experiments of other flaviviruses within the JEV serocomplex in naturally nonsusceptibile tissues further identified additional locations in the E protein associated with viral attenuation. The additional three amino acid substitutions were identified as the lysine substitutions in the glutamate 49, 138, and 306 of the envelope proteins of viral variants which were shown to have higher GAG binding affinity (Lee, Hall et al. 2004). However, the results still support the importance of mutations in RGD motif of EDIII which was previously tested in the mutants generated by the reverse genetics systems for viral attenuation. The mutations still appeared in the regions corresponding to the RGD motif in the EDIIIs of KUNV MRM61C strain and JEV SA14 strain after the wildtype viruses were serially passaged in human adenocarcinoma SW13 cells. The mutation of Glu390, which shares the biochemical properties of the aspartate in the RGD motif, to glycine in KUNV EDIII has been identified in three plaque-purified variants. Experimentally, the Asp389 in the EDIII of JEV SA14 strain was substituted with glycine in one of the five JEV variants. Both of the mutations in KUNV and JEV were considered as the non-conservative mutations with the replacement of the acidic electrically charged side chains of glutamate and aspartate with the small side chain of glycine. Both variants favored the binding of GAG molecules *in vitro* and significantly reduced the neuroinvassiveness in the intraperitoneally challenged Swiss mice. In addition to the mutations in the FG loops of EDIII, the glutamate→lysine mutation at the residue 38 of WNV E protein and JEV E protein was detected after the five serial passages in SW13 cells. Both of the mutations are located in the E_0 β-strand in EDI of WNV and JEV as part of the external sheet structure of EDI exposed on the surface of flavivirus virions (Rey, Heinz et al. 1995). The increase of the binding to the heparin was observed among the mutants *in vitro* and the LD_{50} for intracerebral and intraperitoneal inoculation was higher by 50 and 200 fold in Swiss mice when the mutation was

tested with the WNV cDNA infectious clone (Lee, Hall et al. 2004). The glutamate → lysine mutation at the residue 49 in the EDI of JEV also increased the affinity of heparin binding but only led to the partial attenuation by the reduction of mortality by 80%. The mutants of KUNV and WNV that caused the increase of heparin binding and the attenuation in mice were removed more efficiently from the blood circulation. Together, the amino acid substitutions with basic amino acid residues among encephalitic mosquito-borne flaviviruses are the consequences of the viral adaptation after the serially passage *in vitro*. The mutants favored the binding to the negatively charged molecules in the vertebrate hosts and led to the viral attenuation through the higher efficiency of viral clearance in the blood stream. The available one-plasmid reverse genetics system of JEV further supported the role of the lysine substitution at the residue 138 and revealed the retention of progeny virions in the infected cells, which was consistent with the proposed model of the attenuation of the GAG-binding variant of recombinant YFV described by Lee et al (Zhao, Date et al. 2005, Lee and Lobigs 2008). On the other hand, the lysine substitution at the residue 306 also occurred in variants of the T1P1 strain isolated from *Armigeres subalatus* and purified based on the difference in plaque morphologies and led to the delay in the peak viral titer in the brain of intracranially inoculated ICR mice confirming its potential contribution to the attenuation (Chiou and Chen 2007).

The dependence of utilizing GAG molecules for the retention of variant viruses was further tested in different strains of DENV-2, which have a different history of passage *in vitro*. The mouse neurovirulent New Guinea C strain acquired the lysine substitution at the residue 126 of the envelope protein and this led to the higher affinity of GAG binding, which differs from other natural isolates of DENV-2. The gain of positive charges due to the lysine substitutions at the residue 120 and the arginine substitutions at the residue 227 led to the attenuation in AG129 mice; whereas the lysine substitution at the residue 202 resulted in the phenotypic instability without the attenuation. Also, the compensatory mutation at asparagine 124 is required for the stabilization of the structure (Lee, Wright et al. 2006). Although the gain of positive charges in DENV-2 E proteins also led to the attenuation, the locations of the mutations were found in the surface of EDII and differ from the flaviviruses in the JEV serocomplex.

Although TBEV is listed under the other distinct category of tick-borne flaviviruses and predominantly utilizes ticks as its vectors, its attenuation *in vivo* was associated with the phenotype of increased GAG binding after the serial passage *in vitro* (Mandl, Kroschewski et al.

2001, Kroschewski, Allison et al. 2003). The adaptation of TBEV by serial passage in BHK-21 cells resulted in the substitutions with predominantly positively charged basic amino acids on the upper and lateral surface of virions across the three domains of the E protein. Three mutants, E201K, E122G and S158R-G159R, exhibited the higher sensitivity of soluble heparin inhibition and shared the phenotype of the reduced infectivity and neuroinvasiveness in Swiss mice model.

The evidence has suggested that the tropism and disease pathogenesis characteristic of different flaviviruses are likely altered due to the mutations causing the different GAG-binding properties. In addition to the phenotypic changes in the binding affinity with the GAG molecules and virulence associated with the mutations in the FG loop of the flavivirus EDIII, the structural and sequence homology between the E2 glycoprotein of alphaviruses and the E protein of flaviviruses suggested the presence of a secondary structure similar to the FG loop of flaviviruses in the domain A of the E2 glycoprotein of alphaviruses. Such structure consists of the linear polypeptide between the E and F β-stands of alphavirus E2 glycoprotein (Pierro, Powers et al. 2008, Voss, Vaney et al. 2010). The same region has been found to harbor the glutamate→lysine substitution in the epizootic strains of VEEV IE subtype and associated with the GAG-binding affinity (Brault, Powers et al. 2002, Wang, Brault et al. 2003). However, there has not been any clear association identified between the enzootic and epizootic types of VEEV that utilize different vector species.

Together, the gain of positive charges on the E protein of flaviviruses has led to the attenuation in mice. Although the mutations are found in various locations clustered in the serocomplex-specific manner, the consequences of serial passage *in vitro* is likely to lead to the lysine or arginine substitutions that increase the GAG- binding affinity, which in turn results in the rapid viral clearance from the blood circulation. Similar negatively charged homologs are also synthesized by the mosquitoes as the post-translational modifications of cellular proteins (Kato, Dasgupta et al. 2002, Kato, Mueller et al. 2005). The evaluation of the GAG-binding variants of flaviviruses in its infectivity and disseminability in the vector mosquitoes will provide the mechanistic understanding in the role of such a conserved class of molecules in the vertebrate hosts and insect vectors in determining the vector competence for arboviruses.

3.2 Results

A. Infection and dissemination of YFV E T380R mutants in Ae. aegypti

The titers of viremic blood meals and the infection rates of wildtype and mutant YFV are summarized in **Table 3.4**. The infection rates of the Asibi strain, the 17D strain and the 17D+Asibi M-E chimera followed the pattern described previously by McElroy et al suggesting the Asibi strain is the most infectious strain among the three viruses orally administered. Although the Asibi strain was administered at the lower titer, the infection rates of *Ae. aegypti* exposed to the Asibi strain were consistently higher than those exposed to the 17D strain at 7 (p=0.01) and 14 d.p.i. (p=0.01) but similar at 10 d.p.i. (p=0.47). The infection rates of 17D+Asibi M-E chimera were comparable to the Asibi strain at 7 (p=0.20), 10 (p=1.00) and 14 (p=1.00) d.p.i. The exposure of 17D+Asibi M-E chimera also led to the higher infection rates than the 17D strain at 7 (p=0.78) and 14 (p=0.01) d.p.i. except for 10 d.p.i., where both viruses led to the similar infection rates (p=0.72).

Viremic blood meal ($logTCID_{50}$/ml)	7 d.p.i.		10 d.p.i.		14 d.p.i.	
Defibrinated sheep blood (N.A.)	0/30	(0.0%)	0/24	(0.0%)	0/35	(0.0%)
17D (6.24)	9/25	(36.0%)	8/12	(66.7%)	8/32	(25.0%)
17D+Asibi M-E (5.77)	12/29	(41.4%)	13/24	(54.2%)	21/39	(53.8%)
17D+Asibi M-E E T380R (5.85)	21/23	(91.3%)†	10/12	(83.3%)	14/16	(87.5%)†
Asibi (3.99)	20/33	(60.6%)	9/18	(50.0%)	21/38	(52.6%)
Asibi E T380R (4.21)	32/48	(66.7%)	21/36	(58.3%)	21/39	(53.8%)

Table 3.4 Infection rates of YFV mutants and control strains in *Ae. aegypti* at 7, 10 and 14 d.p.i.

† indicates the statistical significance between the 17D/Asibi M-E E T380R mutant and the 17D/Asibi M-E chimera by Fisher's exact test.

The introduction of the T380R mutation caused the increase in the infection rates of the Asibi strain at 7 (60.6% vs. 66.7%, p= 0.64), 10 (50.0% vs. 58.3%, p=0.58) and 14 (52.6% vs. 53.8%, p=1.00) d.p.i. without reaching the statistical significance. Interestingly, the infection rates of 17D+Asibi M-E E T380R mutant was significantly higher than those of 17D+Asibi M-E chimera at 7 (41.4% vs 91.3%, p=0.0003) and 14 (54.2% vs. 87.5%, p=0.03) d.p.i. although the higher infection rate of the 17D+Asibi M-E E T380R mutant at 10 d.p.i. was not significant from the 17D+Asibi M-E chimera (54.2% vs. 83.3%, p=0.14).

The dissemination rates of wildtype and mutant YFV are summarized in **Table 3.5**. Although the 17D strain was orally challenged with the highest average titer, the control virus failed to disseminate from the infected midguts to the secondary tissues among the infected mosquitoes except for one disseminated infection detected at 10 d.p.i. The dissemination was observed among mosquitoes that were infected by the control Asibi strain and the 17D+Asibi M-E chimera at 7 (47.1% vs. 33.3%, p=0.66), 10 (80.0% vs. 37.5%, p=0.27) and 14 (60.0% vs. 50.0%, p=0.72) d.p.i. Although the dissemination rates remain higher in the dissected mosquitoes infected by the Asibi strain, the dissemination rates were not significantly different between the Asibi strain and the 17D+Asibi M-E chimera.

The Asibi E T380R mutant was equally disseminating as the Asibi strain at 7 (47.1% vs. 79.0%, p=0.08), 10 (80.0% VS. 64.3%, p=1.00) and 14 (60.05 VS. 66.7%, p=1.00) d.p.i. Similarly, the dissemination of 17D+Asibi M-E E T380R mutant was comparable to the 17D+Asibi M-E chimera (7 d.p.i.:33.3% vs. 21.4% , p=0.61; 10 d.p.i.: 37.5% vs. 16.7, p=0.58; 14 d.p.i. 50.0% vs. 62.5%, p=0.67)

	7 d.p.i.		10 d.p.i.		14 d.p.i.	
17D	0/3	(0.0%)	1/5	(20.0%)	0/12	(0.0%)
17D+Asibi M-E	2/6	(33.3%)	3/8	(37.5%)	7/14	(50.0%)
17D+Asibi M-E E T380R	3/14	(21.4%)	1/6	(16.7%)	5/8	(62.5%)
Asibi	8/17	(47.1%)	4/5	(80.0%)	9/15	(60.0%)
Asibi E T380R	15/19	(79.0%)	9/14	(64.3%)	10/15	(66.7%)

Table 3.5 Dissemination rates of YFV mutants and control strains in *Ae. aegypti* at 7, 10 and 14 d.p.i.

B. Viral titers of whole mosquitoes, bodies and secondary tissues

The growth kinetics of YFV mutants were assessed in the homogenates of whole-mosquitoes to the wildtype YFV. The whole-mosquito titers of the Asibi strain and the Asibi E T380R mutant and the 17D+Asibi M-E chimera and the 17D+Asibi M-E E T380R mutant are compared in **Figure 3.4**.

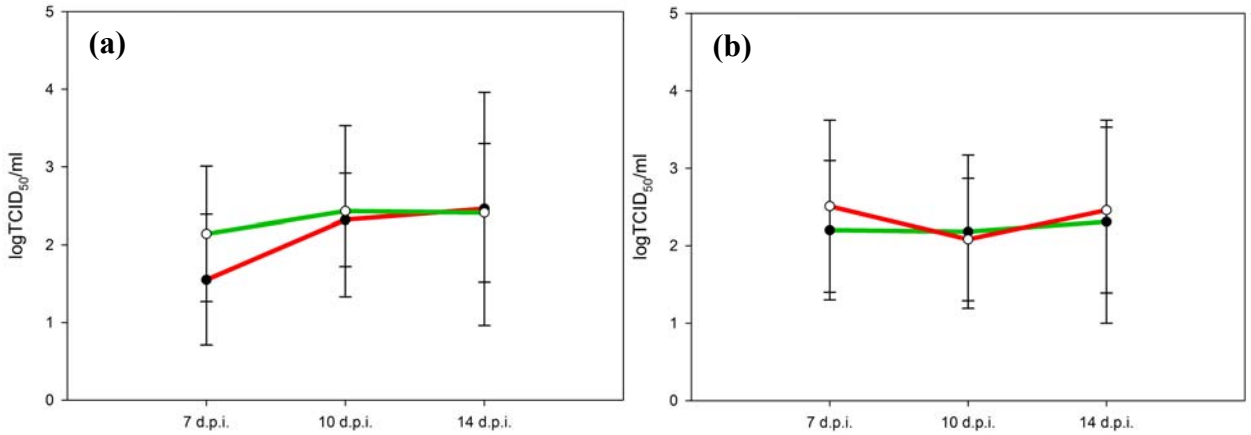

Figure 3.4 Titers of the whole mosquitoes infected by YFV at 7, 10 and 14 d.p.i. (a) The Asibi strain and the Asibi E T380R strain are labeld in red and green, respectively. (b) The 17D+Asibi M-E chimera and the 17D+Asibi M-E E T380R mutant are labeled in red and green, respectively.

Although the infection of the Asibi E T380R mutant did not lead to the significant higher infection and dissemination rates, the titers of whole mosquitoes infected by the Asibi E T380R mutant were consistently higher than the Asibi strain at 7 (1.55 $logTCID_{50}$/ml, n=14 vs. 2.14 $logTCID_{50}$/ml, n=3, p>0.05) and 10 (2.32 $logTCID_{50}$/ml, n=4 vs. 2.43 $logTCID_{50}$/ml, n=7, p>0.05) d.p.i. At 14 d.p.i., the infection of the Asibi strain resulted in the higher titer among whole mosquitoes than the Asibi E T380R mutant (2.46 $logTCID_{50}$/ml, n=5 vs. 2.41 $logTCID_{50}$/ml, n=6, p>0.05). The 17D+Asibi M-E E T380R mutant replicated to the higher viral titers in whole mosquitoes at 7 (2.20 $logTCID_{50}$/ml, n=5, vs. 2.51 $logTCID_{50}$/ml, n=9) and 14 (2.31 $logTCID_{50}$/ml, n=6 vs. 2.46 $logTCID_{50}$/ml, n=10) d.p.i. but not at 10 (2.18 $logTCID_{50}$/ml, n=3 vs. 2.08 $logTCID_{50}$/ml, n=10) d.p.i. However, the titers between the wildtype and mutant viruses did not differ significantly throughout the timecourse of the experiments.

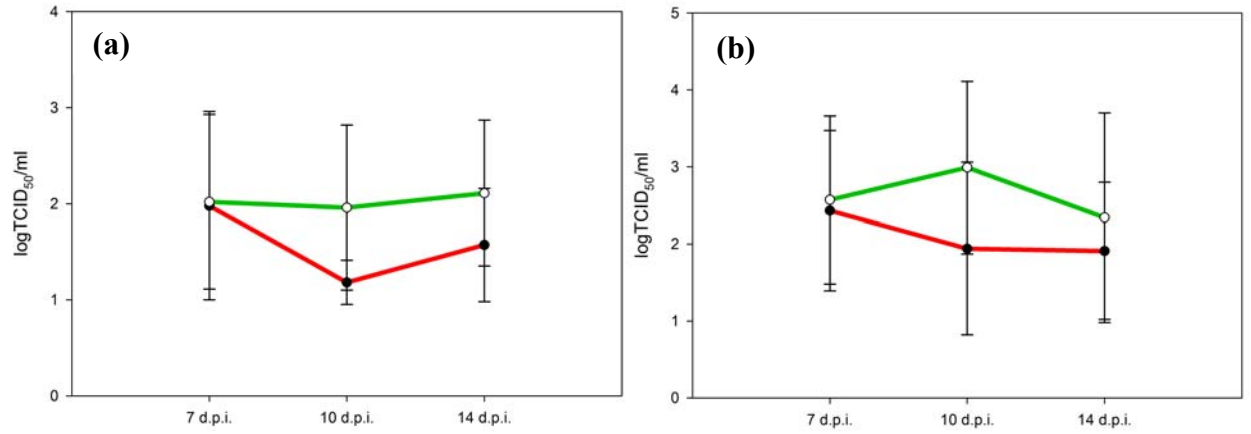

Figure 3.5 Titers of dissected mosquito bodies infected by YFV at 7, 10 and 14 d.p.i
(a) The Asibi strain and the Asibi E T380R strain are labeled in red and green, respectively. (b) The 17D+Asibi M-E chimera and the 17D+Asibi M-E E T380R mutant are labeled in red and green, respectively.

Although the titers of the dissected bodies containing the abdomen section of mosquitoes did not differ significantly based on the ANOVA test, the T380R mutation led to the constantly higher titer in the mosquito bodies than the wildtype sequence. (**Figure 3.5**) The body titers of mosquitoes infected by the 17D+Asibi M-E E T380R mutant were higher at 7 (2.43 $\log TCID_{50}$/ml, n=6 vs. 2.57 $\log TCID_{50}$/ml, n=11, p>0.05), 10 (1.94 $\log TCID_{50}$/ml, n=7 vs. 2.99 $\log TCID_{50}$/ml, n=7, p>0.05) and 14 (1.91 $\log TCID_{50}$/ml, n=14 vs. 2.43 $\log TCID_{50}$/ml, n=10, p>0.05) d.p.i. than those infected by the 17D+Asibi M-E chimera. The Asibi E T380R mutant also led to the higher body titers than the Asibi strain at 7 (1.98 $\log TCID_{50}$/ml, n=11 vs. 2.02 $\log TCID_{50}$/ml, n=13), 10 (1.18 $\log TCID_{50}$/ml ,n=4 vs. 1.96 $\log TCID_{50}$/ml, n=8) and 14 (1.57 $\log TCID_{50}$/ml, n=12 vs. 2.11 $\log TCID_{50}$/ml, n=14) d.p.i.

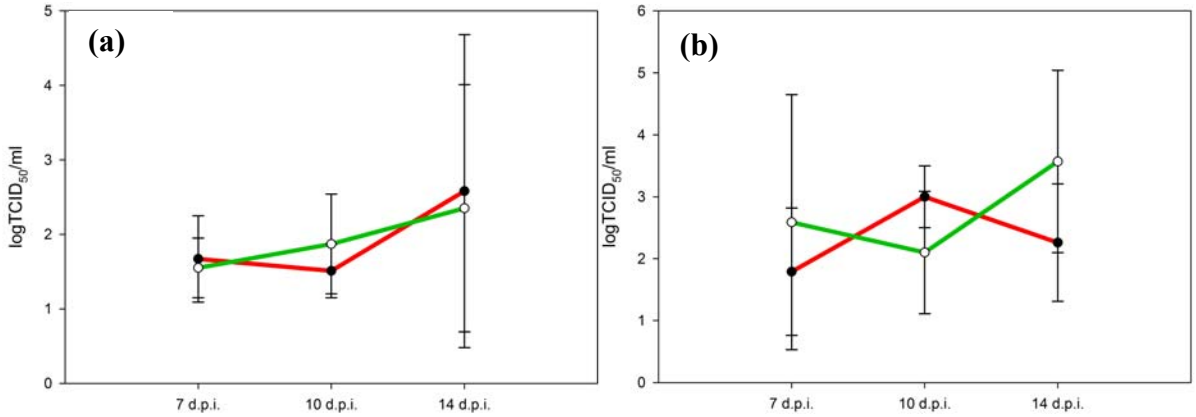

Figure 3.6 Titers of dissected mosquito secondary tissues infected by YFV at 7, 10 and 14 d.p.i.
(a) The Asibi strain and the Asibi E T380R strain are labeld in red and green, respectively. (b) The 17D/Asibi M-E chimera and the 17D/Asibi M-E E T380R mutant are labeled in red and green, respectively.

The titers of the homogenized secondary tissues did not show the consistent patterns between the wildtype and mutant YFV or identify any statistically significant difference in viral titers. The Asibi E T380R mutant disseminated into the secondary tissues and resulted in the

higher viral titers at 10 (1.51 $logTCID_{50}$/ml, *n*=4 vs. 1.87 $logTCID_{50}$/ml, *n*=9) d.p.i. than the Asibi strain, which led to the higher average viral titers in the infected secondary tissues at 7 (1.67 $logTCID_{50}$/ml, *n*=8 vs. 1.55 $logTCID_{50}$/ml, *n*=15) and 14 (2.58 $logTCID_{50}$/ml, *n*=9 vs. 2.35 $logTCID_{50}$/ml, *n*=9) d.p.i. The dissemination of 17D+Asibi M-E E T380R mutant resulted in the higher average titers at 7 (1.79 $logTCID_{50}$/ml, *n*=2 vs. 2.59 $logTCID_{50}$/ml, *n*=4) and 14 (2.26 $logTCID_{50}$/ml. *n*=7 vs. 3.57 $logTCID_{50}$/ml, *n*=5) d.p.i. than the 17D+Asibi M-E chimera. At 10 d.p.i., the 17D+Asibi M-E chimera replicated to the higher viral titer in the secondary tissues than the 17D+Asibi M-E E T380R mutant (3.00 $logTCID_{50}$/ml, *n*=3 vs. 2.10 $logTCID_{50}$/ml, *n*=5)

3.3 Conclusions

Our results in *Ae. aegypti* demonstrated that the YFV E T380R mutants still maintain the viral infectivity and disseminability *in vivo*. The presence of the T380R mutation may further enhance the viral infectivity of the 17D+Asibi M-E chimera as the 17D+Asibi M-E E T380R mutant resulted in significantly higher infection rates at 7 and 14 d.p.i. and the marginal increase of the infection rate at 10 d.p.i. The insignificant gain of viral infectivity was also observed in *Ae. aegypti* which were orally challenged with the Asibi E T380R mutant and showed higher infection rates throughout the time course.

The gain of viral infectivity could also potentially result in the higher average titers of the homogenates of bodies infected with the Asibi E T380R mutant and the 17D+Asibi M-E E T380R mutant with no demonstrable difference. However, the insignificantly higher average viral titers in the bodies did not lead to the higher average titers of whole mosquitoes in both the Asibi E T380R mutant and the 17D+Asibi M-E E T380R mutant. Similarly, the propagation of viruses in the secondary tissues did not show the demonstrable difference in viral titers in the secondary tissues between the wildtype controls and the E T380R mutants.

The T380R mutation in the E protein of the Asibi strain and the 17D+Asibi M-E chimera failed to prevent the viruses from disseminating into the secondary tissues. The similar dissemination rates and the average titers of the secondary tissues suggested that the mutants based on the Asibi strain and the 17D+Asibi chimera are equally capable of disseminating as the wildtype virus controls. Neither the single amino acid substitution in the E protein nor the combination of the mutation in the E protein and the other additional attenuation determinants in the nonstructural genes did not lead to the non-disseminating phenotype of the 17D strains.

In conclusion, the results suggested that the gain of the positive charge in the FG loop of the wildtype Asibi E protein enhanced viral infectivity and maintained the capacity of viral dissemination. The infectivity of the 17D+Asibi M-E T380R mutant was significantly higher than the 17D+Asibi M-E chimera. The Asibi E T380R mutant showed a marginal increase in the viral infectivity compared to the Asibi strain. The T380R mutation in YFV E protein is not an attenuation determinant between the virulent Asibi strain and the attenuated 17D strains.

3.4 Discussion

A. The increase of viral infectivity by the T380R mutation

In spite of the same amino acid sequences present in the E protein of both the Asibi strain and the 17D+Asibi M-E chimera, the significant enhancement in the viral infectivity was only observed in the 17D+Asibi M-E E T380R mutant but not for the Asibi E T380R mutant. The previously published characterization on the 17D+Asibi M-E chimera suggested that the virus only retained the partial infectivity of the Asibi strain even though the envelope protein of the Asibi strain was present (McElroy, Tsetsarkin et al. 2006). Therefore, it is likely that the T380R mutation only resulted in the observed marginal increase of the infectivity in the Asibi strain since this strain is already highly infectious in *Ae. aegypti*.

Additionally, the Asibi strain and the Asibi E T380R mutant, which were only able to propagate to the relatively lower viral titer *in vitro*, were administered at the concentration of 3.99 and 4.21 log$TCID_{50}$/ml; whereas, the 17D+Asibi M-E chimera and its mutant, which shared the high capacity of growth *in vitro*, were administered at titers of at 5.77 and 5.85 log$TCID_{50}$/ml, respectively. The different titers in the viremic blood meals may also result in the differences in the results of the experiments.

The observations suggested the attenuation caused by the T380R mutation in the envelope protein in IFN-α/γ-$R^{-/-}$ mice model through the retention of virions due to the increase in the GAG-binding capacity at the step of viral dissemination into the secondary tissues was not conserved in the mosquitoes (Lee and Lobigs 2008). Although the experimental evidence suggested that the gain of positive charges in the structural proteins is likely to lead to the attenuation *in vivo*, there have been at least two reports for arboviruses to show higher infectivity among the mutants carrying the amino acid substitutions with positively charged amino acids in the structure genes. Both the flaviviruses and the alphaviruses utilize class II fusion proteins as

the mechanisms of the viral entry (Harrison 2008).(Harrison, 2008) The structural and sequence homologies have also been reported between the structural genes of both classes of viruses (Pierro, Powers et al. 2008). The positively charged mutations in the E2 protein acquired in the process of the *in vitro* adaptation of SINV resulted in higher morbidity and mortality in intracranially challenged CD-1 mice (Ryman, Gardner et al. 2007). The positive charges on the E2 protein of naturally isolated strains of EEEV were also found to associate with the heparan sulfate binding and the neurovirulence in CD-1 mice. The neurovirulent strains of EEEV also caused higher numbers of the infected cells among the intracranially challenged mice (Gardner, Ebel et al. 2011). The general gain of positive charges has also been reported to associate with a gain of infectivity in other unrelated virus, adeno-associated viruses (Lerch and Chapman 2012). In addition to the attenuation effects that are frequently reported among viruses, the gain of the positive charges on the structural proteins can also potentially serve as the mechanism for the gain of infectivity.

B. GAG molecules in mosquitoes

In contrast to the extensive characterization of the interactions between various viruses and the GAG molecules in vertebrate hosts (Samreen, Khaliq et al. 2012, Tiwari, Maus et al. 2012), the knowledge in the interactions between the viruses and GAG molecules in arthropod vectors remains limited (Smith 2012). The presence of the GAG molecules in arthropod vectors originated from the characterization of *Anopheles* mosquitoes, which are vectors for malarial parasites (Sinnis, Coppi et al. 2007). The available genomic sequences further suggested that the enzymes required for the synthesis of GAG molecules are also present in the genome of *Ae. aegypti* (Altschul, Madden et al. 1997). To the best of our knowledge, the results described in this dissertation are the first available evidence that the increase of the GAG-binding affinity would likely favor the establishment of viral infection in arthropod vectors. The higher infectivity of YFV E T380R mutants is consistent with the characterization of the GAG-binding variant of MVEV in mammalian cells, which showed that the addition of positive charges in the FG loop of EDIII favors the virus intake (Lee and Lobigs 2008). A knowledge gap remains with respect to the identity of which types of GAG molecules are responsible for the higher viral infectivity in *Ae. aegypti.* Mosquito GAG molecules differ in chemical and structural properties in a tissue-specific manner. It is noteworthy that a relatively minor structural difference can

cause the difference in the binding between flavivirus virions and the GAG molecules. For example, the different sulphation patterns of chondroitin sulfate are associated with the different inhibitory effect on JEV infection (Kim, Okumura et al. 2011). Additionally, as with the argument proposed by Perera-Lecoin *et al*., the conclusive mechanistic evidence to demonstrate that GAG molecules function in mosquitoes as viral receptors or as attachment factors that enrich the local virion concentrations prior to the binding of viral receptors is still missing (Perera-Lecoin, Meertens et al. 2014).

The establishment of arbovirus infection in mosquitoes takes place in the midgut. Therefore, the higher viral infectivity of YFV E T380R mutants might be achieved by the higher binding affinity with the GAG molecules present on the apical surface of mosquito midgut epithelial cells, which is exposed to the viremic blood after the ingestion of the blood meal. The GAG molecules in the apical surface of midgut cells mainly consists of chondroitin sulfate, which is synthesized by the pathway with peptide-*O*-Xylosyltransferase in *An. gambiae* and *Ae. aegypti* (Altschul, Madden et al. 1997, Dinglasan, Alaganan et al. 2007). The interaction between flaviviruses and chondroitin sulfate has been found in DENV and JEV (Kato, Era et al. 2010, Kim, Okumura et al. 2011). It is highly likely that the higher binding affinity of YFV E T380R mutant can arise from electrostatic interactions between the positively charged arginine in the FG loop and the negatively charge chondroitin sulfate. One approach that could be employed to identify the specific GAG molecules responsible for viral entry into the midgut of *Ae. aegypti* would be to use RNAi targeting to selectively knockdown specific genes that encode for expression of enzymes involved in GAG synthesis. Another significant gap in our knowledge is our understanding of how the differences in the quantities of YFV E T380R mutants and the wildtype viruses which entered the midgut epithelial cells, may influence infection Since the efficiency of infection of arboviruses in mosquitoes is dose-dependent, the quantity of viruses that enters susceptible midgut epithelial cells may be a critical factor to determine the infection rate of arboviruses (Gubler and Rosen 1976). It remains unclear as to whether or not the higher viral infectivity of the YFV E T380R mutants is mediated by the increase in the affinity with GAG molecules and subsequently the viral entry into the primary target cells in the midgut of *Ae. aegypti*. Alternatively, the higher-binding affinity between the GAG molecules and the YFV E T380R mutants could potentially result in a more efficient attachment to the epithelial cells and subsequently a higher number of infected cells than the wildtype controls.

The other source of GAG molecules in the mosquito midgut lumen is the peritrophic matrix. The peritrophic matrix has been known to be secreted after the blood meal and abundant in the chintin proteins modified with GAG molecules. The chitins of the type I peritrophic matrix have previously been shown to be sequentially modified to the negatively charged β-(1,4)-*N*-acetyl-D-glucosamine structure polymers (Hegedus, Erlandson et al. 2009). Unlike the malarial parasites, which secret chitnases to distrupt the physical barrier created by peritrophic matrix, the formation of the peritrophic matrix takes place after the arboviruses encounters the susceptible cells in the midgut. Therefore, the timing limits the likelihood of the GAG molecules in peritrophic matrix retaining the infectious virions in viremic blood. The lack of the retention of YFV T380R mutants and 17D strains regardless of the increase electrostatic interactions with GAG molecules agreed with the earlier observation that the manipulation of the thickness of peritrophic matrix with RNAi mechanisms did not change the infectivity and dissemination of DENV-2 in *Ae. aegypti* (Kato, Mueller et al. 2008).

The proteins on the basal surface of the mosquito midgut epithelial cells have been known to be frequently modified by the heparan sulfate molecules in *Ae. aegypti* and *An. gambiae* (Sinnis, Coppi et al. 2007). Under the hypothesis that viral escape and dissemination from the basal surface of the midgut epithelial cells takes place in the basal lamina followed by the subsequent infection of cells and tissues in the hemocoels, for example fat bodies, muscles and nerve tissues, the heparin sulfate on the basal surface of the midgut epithelial cells is unable to retain the progeny virions of YFV E T380R mutants in the vicinity of midgut. Subsequently, the YFV E T380R mutants disseminate into the secondary tissues. The similar dissemination rates between the wildtype and mutant viruses suggested the T380R mutation did not serve as a attenuation determinant that contribute to the lack of dissemination in *Ae. aegypti* infected by YFV 17D strains. The observation for *Ae. aegypti* is strikingly different from the observation in immunocompromised mice. In the study described by Lee *et al*., the progeny virions that were released into the vertebrate's blood stream were efficiently removed by the binding with the GAG molecules in the extracellular matrix. This process is conserved as the critical mechanism for viral attenuation as the progeny virions are readsorbed in the extraceullar matrix (Lee and Lobigs 2008). Clearly, the mechanism, which the increased affinity with the GAG molecules attenuates YFV, only contributes to the viral attenuation in vertebrate hosts but not in the mosquito vectors.

C. Public health significance and potential application

The results of the increased infectivity due to the T380R mutation can potentially create a concern that the increase of the positive charge in the FG loop of YFV E protein may result in the viral transmission. However, the advantage created by the higher infectivity of the YFV E T380R mutants should not be considered as representing an attempt to increase the potential for the transmission of YFV 17D vaccine strains used in the field. The characterization of the mutation was performed in the context of the E protein encoding the sequence of the Asibi strain.

The other mutations present in the structural genes of YFV 17D strains have also been characterized as the attenuation determinants and together ensure the significant reduction in the viral infection and dissemination (McElroy, Tsetsarkin et al. 2006). The chance of the simultaneous amino acid substitutions at multiple genetic loci for the reversion back to the virulent and infectious phenotypes is highly unlikely. In such an extremely unlikely scenario, the single T380R mutation have only been found to the increase in the viral infectivity without significantly enhance the disseminability, which is essential for the viral transmission in nature. Other evidence also indicates that vaccine viruses remain attenuated in the non-human primates in the presence of other amino acid substitutions in the nonstructural genes of YFV. The attenuated viruses have been known to cause the reduced viremia by greater than 1,00 fold compared to the virulent Asibi strain when 10^4 $TCID_{50}$ of viruses were used in the challenge experiments (McGee, Lewis et al. 2008). Additionally, the viremic phase of YFV 17D strains has been characterized to be low in the quantities of virions and transient after the vaccination. The vaccination with YFV 17D vaccines only resulted in the transient and low-titer viremia below 10^3 viral RNA copies per ml in humans (Miller, van der Most et al. 2008). The oral challenge of YFV 17D-204 strain in our experiments demonstrated low infectivity of the vaccine strains in spite of the high viral titers between 10^6 and 10^7 $TCID_{50}$/ml. In such an unlikely event where the amino acid substitutions in the E protein undergo the significant reversions, the attenuated phenotype and the low viremic titers limit the chance of initiating further transmissions. Together, the other attenuation determinants may synergistically contribute to the attenuated phenotype in both vertebrate hosts and mosquitoes.

The use of a threonine residue in the E protein FG loop of the 17D strains to limit the viral infectivity in mosquitoes is not a practical approach because the T380R mutation is likely to be the determinant for viral dissemination in vertebrate hosts. Our observation on YFV in *Ae.*

aegypti can potentially be applied towards the attenuation of JEV-serocomplex members. In comparison to other mosquito-borne flaviviruses, which share the elongated structure of the FG loops, the T380R mutation resulted in the formation of the RGD motif, which is present in the genomes of flaviviruses within the JEV serocomplex. The available sequences suggest the RGD motif is conserved between the virulent SA_{14} strain and other attenuated vaccine strains. The JEV 2-8 vaccine strain showed the lower infectivity and caused the lower percentage of dissemination in orally infected *Cx. tritaeniorhynchus* mosquitoes than the wildtype SA_{14} strain (Chen and Beaty 1982). Together with our observations, it is clear that the presence of the RGD motif, which has been previously characterize to increase the binding between the viruses and the GAG molecules of the hosts, has a limited impact for the infection and dissemination of flaviviruses in mosquitoes. This may also explain why the RGD motif and its similar sequences have been detected among the naturally isolated strains of other flaviviruses under the JEV serocomplex without compromising the transmission by mosquito vectors. It is also consistent with the observation that the length of the FG loop is more critical for the vector competence of *Ae. aegypti* in DENV-2 than the actual sequences. This may also be the plausible explanation that the sequences of the FG loops among all four serotypes of DENV are not strictly conserved (Erb, Butrapet et al. 2010). The sequences of the FG loops of the mosquito-only flaviviruses also suggested that the RGD motif is likely to be dispensable for the infection and the dissemination in mosquitoes. The alignment of at least six known mosquito-only flaviviruses that infect either *Aedes* or *Culex* mosquitoes did not identify strictly conserved or any similar sequences of the RGD motif (Cammisa-Parks, Cisar et al. 1992, Crabtree, Sang et al. 2003, Cook, Moureau et al. 2009, Crabtree, Nga et al. 2009, Farfan-Ale, Lorono-Pino et al. 2009, Haddow, Guzman et al. 2013). Together, the dispensable role of the FG loop for the attenuation in mosquitoes allows the variations in the sequences and also agrees with the previously published study on SINV, which selectively mutated the region resembling the RGD motif downstream of the PPFGDS sequence but did not result in the significant reduction in the infection of *Ae. aegypti* (Pierro, Powers et al. 2008).

However, by comparing the vector and host species in nature, the members of JEV serocomplex has been described to have a broader spectrum of competent vectors and susceptible vertebrate hosts. It is unclear if the RGD motif increases the host range of YFV. As demonstrated using the model of YFV 17D+/Asibi M-E chimera in *Ae. aegypti*, the RGD motif

increased the viral infectivity of YFV. It will be interesting to evaluate whether or not the mutation would result in the successfully infection of, and transmission by less competent vectors or incompetent mosquito species in the laboratory. Future experiments that are designed to delineate the mechanisms should also focus on mutating the conserved RGD motif of EDIII among the flaviviruses under the JEV serocomplex to the sequences of the corresponding regions of other flaviviruses under the DENV and YFV serocomplexes. The experimental results will provide the knowledge in understanding the mechanisms that JEV-serocomplex members are able to infect multiple species of mosquitoes.

Previous experimental evidence with the peptides with the RGD sequence has excluded the possibility that the RGD motif of the WNV mediates the integrin-dependent viral entry (Chu and Ng 2004). However, such observations did not exclude the potential increase of viral infectivity in the vertebrate hosts due to the presence of the RGD motif in EDIII. The members of the JEV serocomplex have been shown to infect multiple types of vertebrate hosts. This is especially true for JEV and WNV, which contain the conserved RGD or RGE sequences (Gould and Solomon 2008). Both viruses are able to establish the CNS infection after the intradermal challenge in immunocompetent rodent model such as the C57BL/6 and C3H/NeH mice, which are not considered as natural hosts of flaviviruses. Other flaviviruses under the DENV and YFV serocomplex, which do not contain the conserved RGD motif, are unable to establish the infection and cause comparable morbidity and mortality with the same route of challenge at the comparable concentration of inoculated viruses in the same model (Kimura, Sasaki et al. 2010). Furthermore, the mosquito-only flaviviruses, which are unable to infect any known vertebrate hosts, also showed the lack of the RGD motif in the corresponding region. With the history of passages in the non-natural chicken embryo host system, the T380R mutation may be the consequence of tissue adaptation due to the relative advantage in viral uptake in the non-natural vertebrate hosts of YFV. The mutation further caused the attenuation by the stronger affinity to the GAG molecules that ultimately led to the ideal phenotype of a live-attenuated vaccine. However, the mutation alone also unexpectedly favors the establishment of infection in *Ae. aegypti* by mehcanisms that still require further characterization. Therefore, it will be critical to identify other genetic mutations in the genome of YFV 17D strains which suppress the gain of the infectivity in mosquitoes due to the T380R mutation.

Chapter 4 - Characterization of Two Point Mutations in YFV EDI and EDII

4.1 Introduction

McElroy *et al.* (2006a) demonstrated that the substitution of YFV 17D EDI and EDII into the full-length YFV Asibi genome resulted in a significant reduction of infection rates in *Ae. aegypti* at 14 d.p.i. The results therefore suggested that the presence of the determinants for the infectivity of YFV in *Ae. aegypti* in these domains (McElroy, Tsetsarkin et al. 2006). A comparison of the amino acid sequences identified five mutations between the parental Asibi strain and the passaged 17D strains. **(Table 4.1)** For the current studies, two point mutations, G52R and T173I, were selected for the characterization. They were chosen due to the predicted locations in the three-dimensional structure, and their association with neurovirulent and attenuated phenotypes in mice (Hahn, Dalrymple et al. 1987, Gould and Buckley 1989, Rey, Heinz et al. 1995, Schlesinger, Chapman et al. 1996, Ryman, Xie et al. 1997, Kuhn, Zhang et al. 2002). The details regarding the predicted locations of these mutations in the three-dimensional structures and the sequences in the corresponding regions of the other strains of YFV and other flaviviruses will be provided in **section 4.1.A**. The functional and the structural importance of flavivirus EDI and EDII have been shown to be related to structural rearrangement due the pH-dependent conformational change that occurs during viral envelope fusion with the host cell membrane. The details of the structural rearrangement of flavivirus E proteins during fusion will be described in **section 4.1.B**. The information of the phenotypes associated with the G52R and T173I mutations in YFV E protein or the corresponding regions in the E proteins of other flaviviruses will be discussed in **section 4.1.C** and **4.1.D**.

Mutation (Asibi/17D)	Location
G52R	EDI-EDII molecular hinge
A56V	A β-strand of EDII
A170V	G_0 β-strand of EDI
T173I	G_0H_0 loop of EDI
K200T	FG loop of EDII

Table 4.1 Amino acid mutations in EDI and EDII of 17D strains

There is evidence supporting the functional importance of the G52R and T173I mutations in determining the virulence of YFV and other flaviviruses in mice. However, the characterization of the two mutations in the *Ae. aegypti* mosquito vector has not yet been performed.(Schlesinger, Chapman et al. 1996, Ryman, Xie et al. 1997) Characterization studies described in this chapter represent the first attempt to investigate the relationship between the G52R and T173I mutations in YFVE protein and viral phenotype in *Ae. aegypti.* The purpose of the studies was to provide mechanistic understanding that could assist in the rationale attenuation of arboviruses in mosquito vectors, based on the homology of the amino acid sequences and the conserved secondary structures among the E proteins of flaviviruses.

A. Location and putative function

The two point mutations, G52R and T173I, are located in two separate positions in the YFV E protein. Although the crystal structure of YFV E protein has not been described, based on the homology of the amino acid sequences among flaviviruses, the G52R mutation is considered to be part of the molecular hinge structures between EDI and EDII. **(Table 4.2)** There are four molecular hinge peptides (designated as H1-H4) which exist as loosely packed structures in the junctions between EDI and EDII of flavivirus E proteins (Rey, Heinz et al. 1995, Modis, Ogata et al. 2004). The sequences of the four amino acids in the H1 region which harbors the G52R mutation of YFV 17D strain show a high degree of variation in the first and second amino acid residues among flaviviruses. Regardless of the virus serocomplex and vector type, the last two amino acids of the hinge region, are characterized by having high hydrophobic sidechains. The third amino acid residue is predominantly composed of proline and leucine, although DENV-4 utilizes valine. The fourth amino acid residue typically is the small hydrophobic alanine except for the use of proline or threonine in three flaviviruses (ENTV, SEPV, YOKV) that have not been isolated from arthropod vectors but are classified under the YFV serocomplex based on the genetic homology.

Serocomplex	Virus	strain	Sequence of H1 peptide (E 51-54)
YFV	YFV	Asibi	DGPA
	YFV	17D	DRPA
	ENTV	UgIL-30	NGPP

	SEPV	MK7148	DTPT
	YOKV	Oita36	NNPP
DENV	DENV-1	Hawaii	TNPA
	DENV-2	New Guinea C	KQPA
	DENV-3	H87	TQLA
	DENV-4	H241	KEVA
JEV	JEV	SA_{14}	SQLA
	JEV	SA_{14}-14-2	SQLA
	WNV	NY99	ANLA
	KNV	MRM61C	ANLA
	SLEV	MS1-7	TELA
	MVEV	MVE1-151	TNLA
TBEV	TBEV	Neudoerfl	ENPA
	OHFV	Bogluvovska	ENPA

Table 4.2 Sequences of the molecular hinge H1 peptide between flavivirus EDI and EDII The hydrophobic amino acids are labeled by underline.

Although the four molecular hinge peptides are often displayed as four distinct regions in the alignment of full-length E proteins, due to the discontinuous nature of the numbering of the residues of EDI and EDII, the peptides are consistently located in close proximity to the three-dimensional structure of flavivirus E proteins. The location and overall structure of the molecular hinge region is displayed in the crystal structure of the DENV-2 E protein dimer as shown in **Figure 4.1**. The G52R mutation exists in the H1 molecular hinge between the β-strand D_0 of EDI and β-strand a of EDII. The region has been hypothesized to accommodate the conformational change between EDI and EDII during viral membrane fusion. The detail mechanisms of viral membrane fusion and the crystal structure and functional characterization of four peptides in the molecular hinge will be discussed in **section 4.1.B** and **4.1.C**.

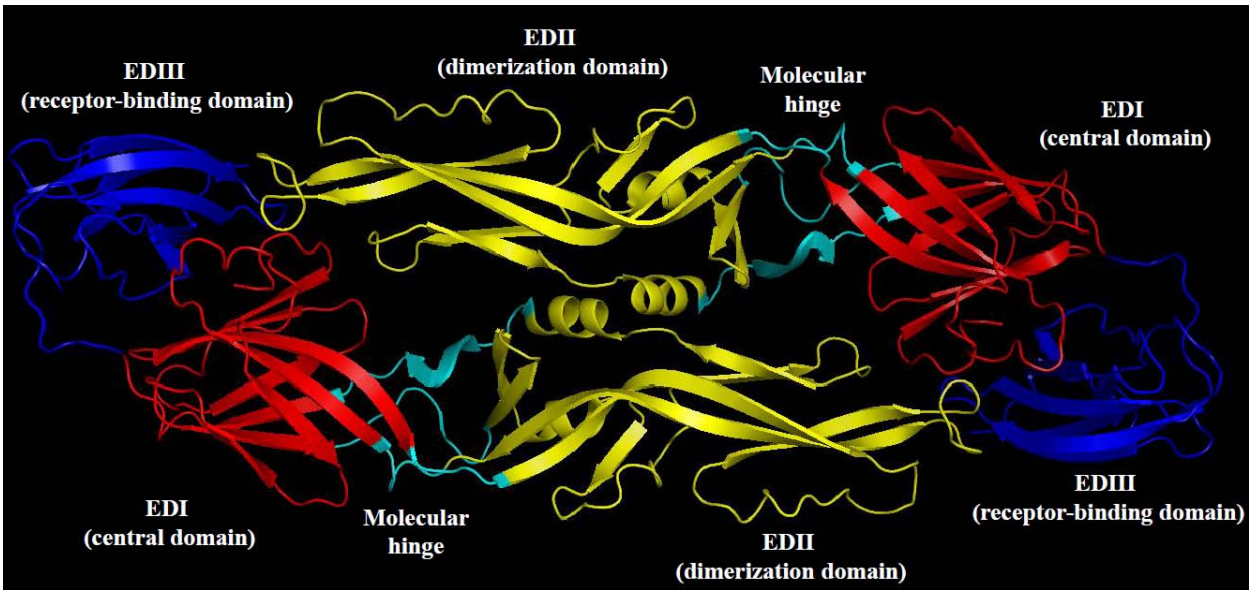

Figure 4.1 The location of the molecular hinge region in the crystal structure of DENV-2 E protein dimer (PDB ID: 1OAN)

The individual domains of DENV-2 E protein are coded in red for EDI, yellow for EDII and blue for EDIII. The four short peptides consist of the molecular hinge region are labeled in cyan.

The G52R mutation is a conserved between the 17D-204 and 17DD substrains used for vaccine production. The H1 molecular hinge of the FNV strain showed conservatation of the mutation at the forth amino acid residue compared to the parental FVV. The sequence alignment of the YFV E proteins is summarized in **table 4.3**.

Strain	Sequence of H1 molecular hinge
Asibi	DGPA
17D-204	DRPA
17DD	DRPA
FVV	DGPA
FNV	DGPV

Table 4.3 Sequences of H1 molecular hinge region in YFV E proteins of the wildtype virulent strains and the attenuated vaccine strains

The T173I mutation is located in the G_0H_0 loop structure between the G_0 and H_0 β-strands of YFV EDI. The G_0H_0 loop structure is composed of the conserved "glycine-tyrosine-glycine" tripeptidic sequences facilitating the turn of the polypeptide chain that contributes to the

formation of G_0 and H_0 β-strands observed in all flavivirus E proteins. The relative location of the G_0H_0 loop structure of flavivirus EDI is displayed in the crystal structure of DENV-2 E protein dimer in **Figure 4.2**.

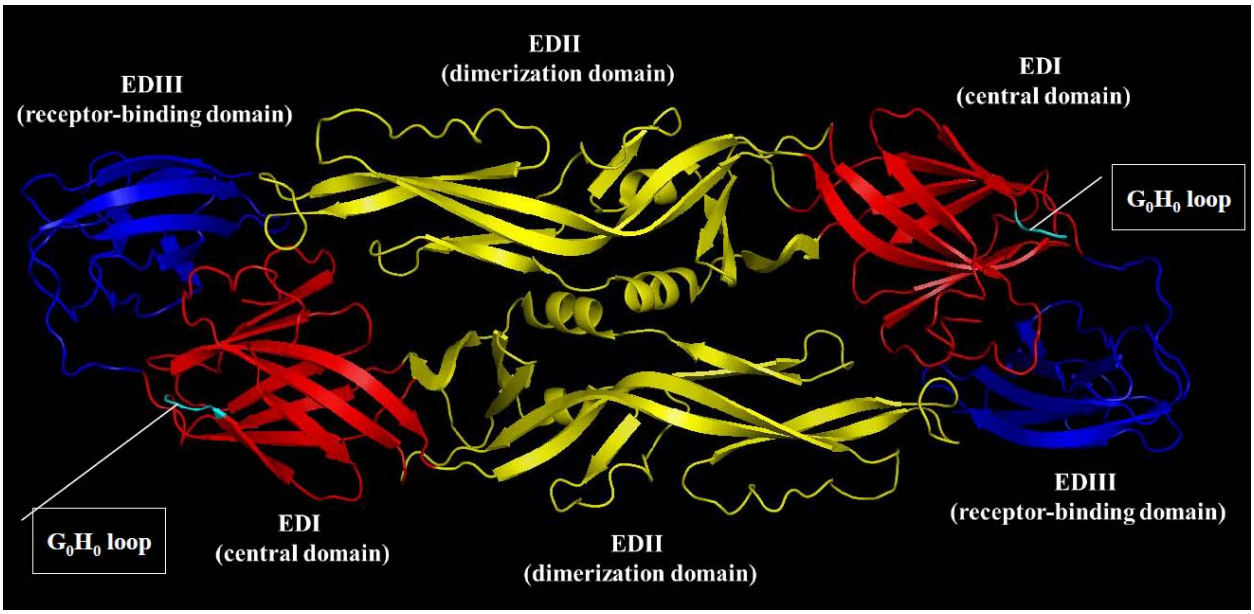

Figure 4.2 The relative location of the G_0H_0 loop in the crystal structure of DENV-2 E protein dimer (PDB ID: 1OAN)

The three domains are labeled in red for EDI, yellow for EDII and blue for EDIII. The G0H0 loop structure is labeled in cyan.

The flavivirus EDI serves as a structurally central domain which connects EDII and EDIII. EDI contains two β-sheets that contributes to the formation of the overall β-barrel structure. The G_0H_0 loop is located between the neighboring antiparallel G_0 and H_0 β-strands as displayed in **Figure4.3**. With the additional B_0 and I_0 β-strands, the inner $B_0I_0G_0H_0$ β-sheet faces the viral membrane underneath the outer $A_0C_0D_0E_0F_0$ β-sheet. The two β-sheet structures are stabilized by the interactions of the tightly packed hydrophobic interactions.

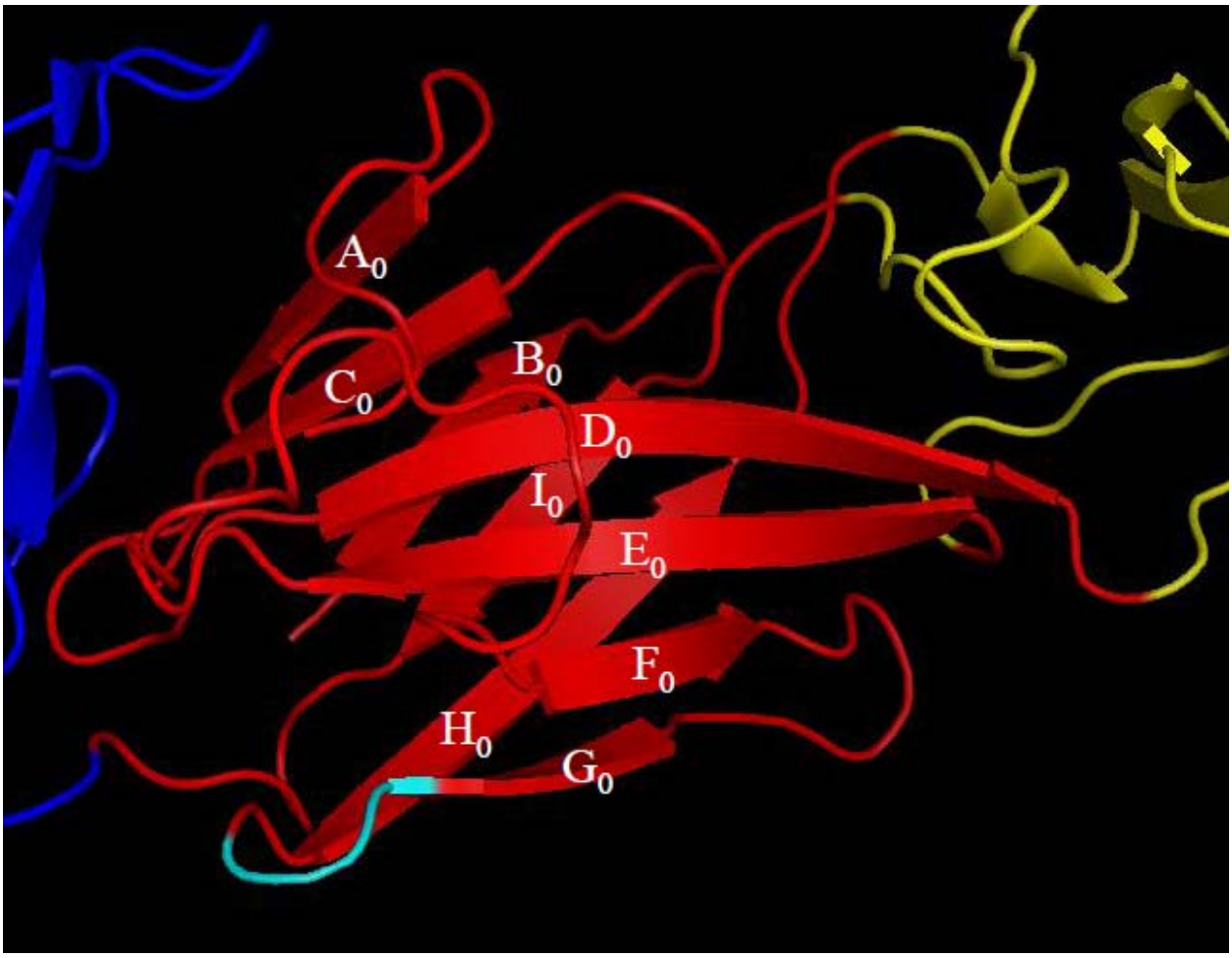

Figure 4.3 The relative location of the G_0H_0 loop structure in the crystal structure of DENV-2 E protein monomer (PDB ID: 1TG8)

EDI is labeled in red with two neighboring domains, EDII in yellow and EDIII in blue. The β-barrel structure of DENV-2 EDI consists of two β-sheets structures. The $B_0I_0G_0H_0$ β-sheet faces the viral membrane and contains the G_0H_0 loop labeled in cyan. Five β-strands form the $A_0C_0D_0E_0F_0$ β-sheet forms as the external surface.

The structurally central domain, EDI does not undergo extensive structure rearrangement during the fusion process. In addition to the presence of several B-cell epitopes that have been reported on the G_0H_0 loop in EDI of wildtype YFV and DENV, the YFV EDI is different from the DENV EDI due to the absence of the Asn67 glycosylation site that has been characterized as the binding site of DC-SIGN (Gould, Buckley et al. 1989, Pokidysheva, Zhang et al. 2006, Lai, Goncalvez et al. 2007, Fibriansah, Tan et al. 2014). The details of the B-cell epitopes in the G_0H_0 loop of EDI will be discussed in **section 4.4**. The sequences of the G_0H_0 loop in flavivirus EDI,

suggested that YFV uses amino acid residues that are largely conserved among other flaviviruses as summarized in **table 4.4**.

Serocomplex	Virus	Strain	Sequence of G_0H_0 loop
YFV	YFV	Asibi	EAEFTGYGK
	YFV	17D	EVEFIGYGK
	ENTV	UgIL-30	VVVFTGYGT
	SEPV	MK7148	TVTFTGYGN
	YOKV	Oita36	VIGFAGYGT
DENV	DENV-1	Hawaii	EIQLTDYGA
	DENV-2	New Guinea C	EAELTGYGT
	DENV-3	H87	EAILPEYGT
	DENV-4	H241	EVKLPDYGE
JEV	JEV	SA_{14}	TLKLGDYGE
	JEV	SA_{14}-14-2	ALKLGDYGE
	WNV	NY99	TLKLGEYGE
	KNV	MRM61C	TLKLGEYGE
	SLEV	MS1-7	TANMGEYGT
	MVEV	MVE1-151	TAKMGDYGE
TBEV	TBEV	Neudoerfl	ILTMGEYGD
	OHFV	Bogluvovska	ILTMGEYGD

Table 4.4 Sequences of the G_0H_0 loops in EDI of flaviviruses

The amino acid residues in the G_0H_0 loops are underlined based on the available three-dimensional structures and the sequence homologies.

The consistent use of glycine or proline as the amino acid residues in the flavivirus G_0H_0 loop structure follows the biochemical properties of the secondary turn structures (Lodish 2013). However, minor structural difference remains in flaviviruses in YFV serocomplex, DENV-1 and DENV-2. The G_0H_0 loops of YFV-serocomplex flaviviruses, DENV-1, DENV-2 and DENV-3 are consistently shorter than the loops of members of the JEV and TBEV serocomplexes. The elongated structure of JEV- and TBEV-serocomplex flaviviruses is due to the insertion of an aspartate or glutamate residue following the first turn made by the glycine residue, and an

aspartate or glutamate residue prior to the H_0 β-strand. The comparison was made utilizing the available crystal structures of DENV-2, DENV-3, JEV and TBEV E proteins. **(Fig. 4.4)**

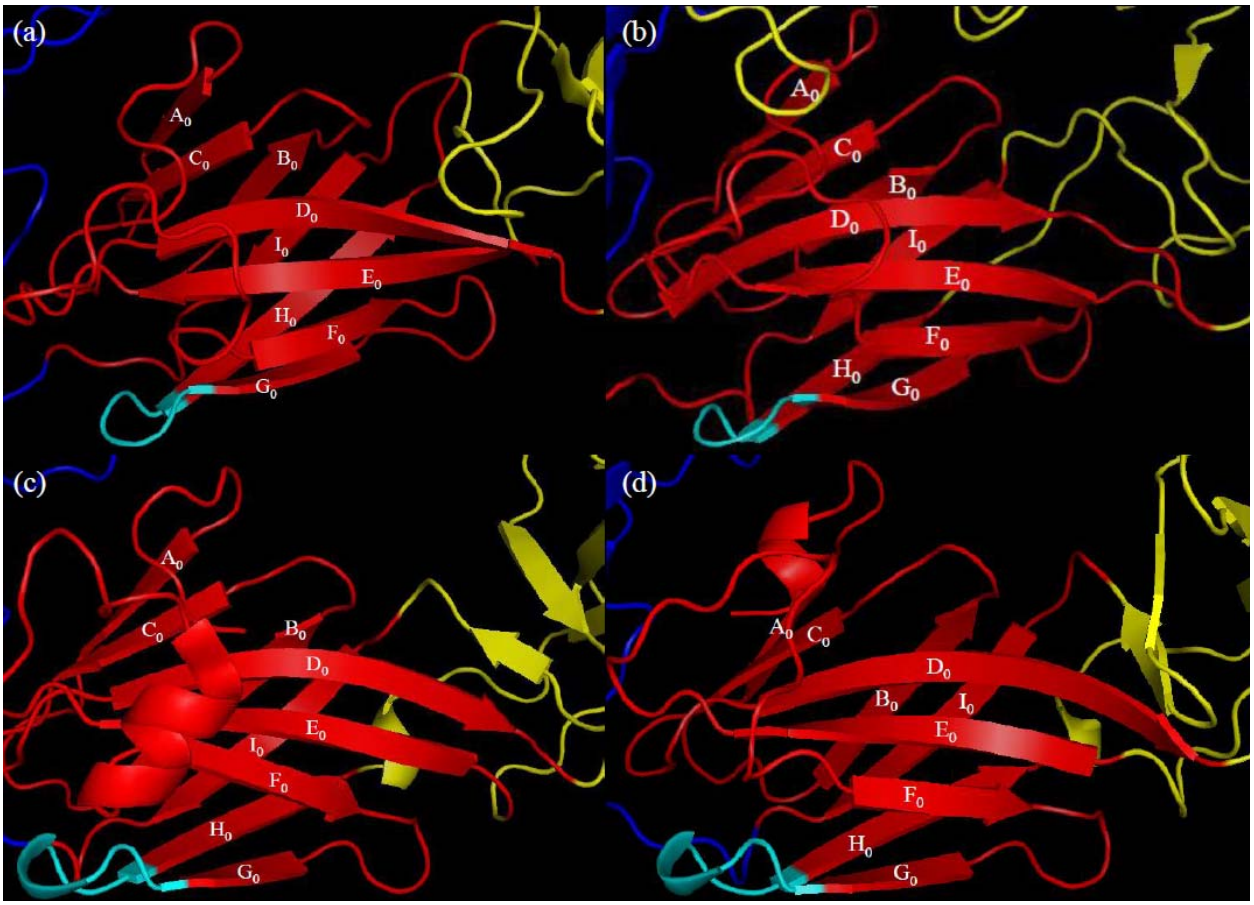

Figure 4.4 The G_0H_0 loop structure in flavivirus EDI

EDI of four different flaviviruses are displayed in (a) DENV-2 (PDB ID: 1TG8), (b) DENV-3 (PDB ID: 1UZG), (c) JEV (PDB ID: 3P54), and (d) TBEV (PDB ID: 1SVB). The G0H0 loop structure is labeled in cyan with residues from EDI in red, EDII in yellow and EDIII in blue.

The T173I mutation is a conserved mutation between the 17D-204 and 17DD vaccine substrains. As the wildtype YFV-specific B-cell epitope, the threonine residue is conserved among natural isolates of YFV. The plaque purification of the 17D-204 substrain demonstrated maintenance of a minor viral population that use a threonine residue in the G_0H_0 loop structure. This was recognized by the wildtype-specific mAb 117 (Gould, Buckley et al. 1989). The details regarding to the phenotype of the mAb 117-reactive variants *in vivo* will be discussed in **section 4.1.D**.

B. Viral membrane fusion mediated by flavivirus E proteins

The pH-dependent energy-driven fusion between the viral envelope and host membranes allows the release of the genetic materials of enveloped viruses into the host cellular compartment (Helenius, Kartenbeck et al. 1980). Based on structural characteristics, there are three distinct mechanisms of pH-dependent viral membrane fusion (Knipe and Howley 2013). The conformational changes in each class of the fusion proteins are listed in **figure 4.5** and reviewed by Harrison *et al* (Harrison 2008). The E proteins of flaviviruses and the E1 glycoproteins of alphaviruses are considered as class II fusion proteins which undergo dimer-to-trimer structural rearrangement during the process of viral membrane fusion. The details of the conformational change will be described in the following paragraph. The family of class I fusion proteins is exemplified by the hemagglutinin (HA) protein of influenza virus and the gp41 protein of human immunodeficiency virus type 1 (HIV-1). Class I fusion proteins consist of mostly α-helical structures and they maintain the trimeric conformation before and after t fusion. The protonation-initiated structure rearrangement is followed by the insertion of the fusion peptide into the host membrane and then the refolding of the trimeric structure to produce a stable rod-like conformation. The only available structural information is derived from the crystal structures of the pre- and post-fusion conformations of vesicular stomatitis virus (VSV) G protein. Class III fusion proteins retain the trimeric conformation throughout the fusion process. The acidic environment results in the extended intermediate structure and the insertion of the fusion peptide. Finally, the carboxy-terminal segment folds back towards the fusion peptide to create the post-fusion conformation.

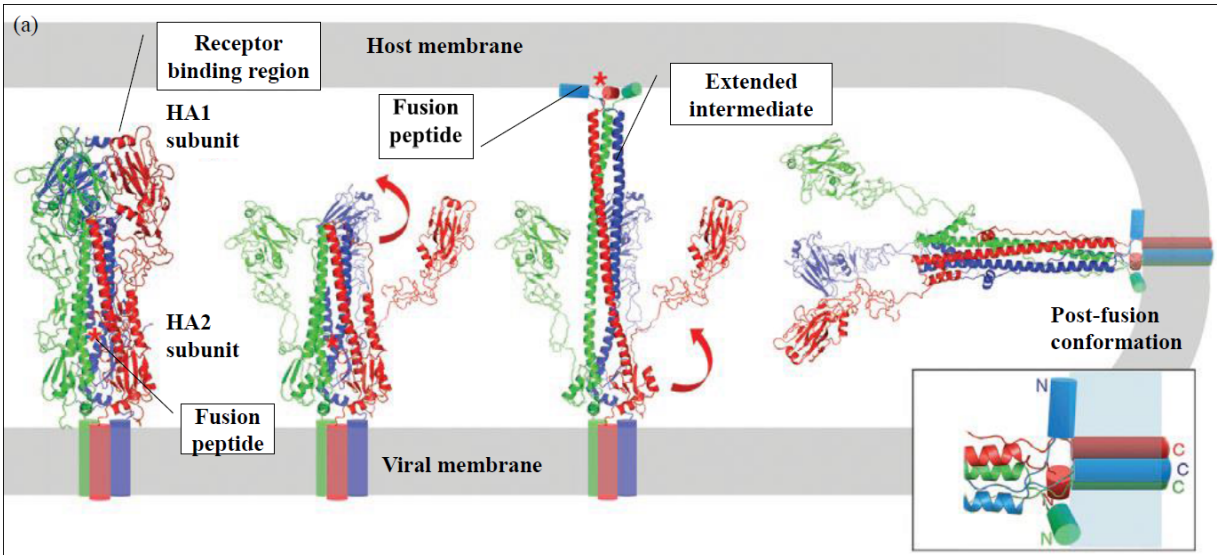

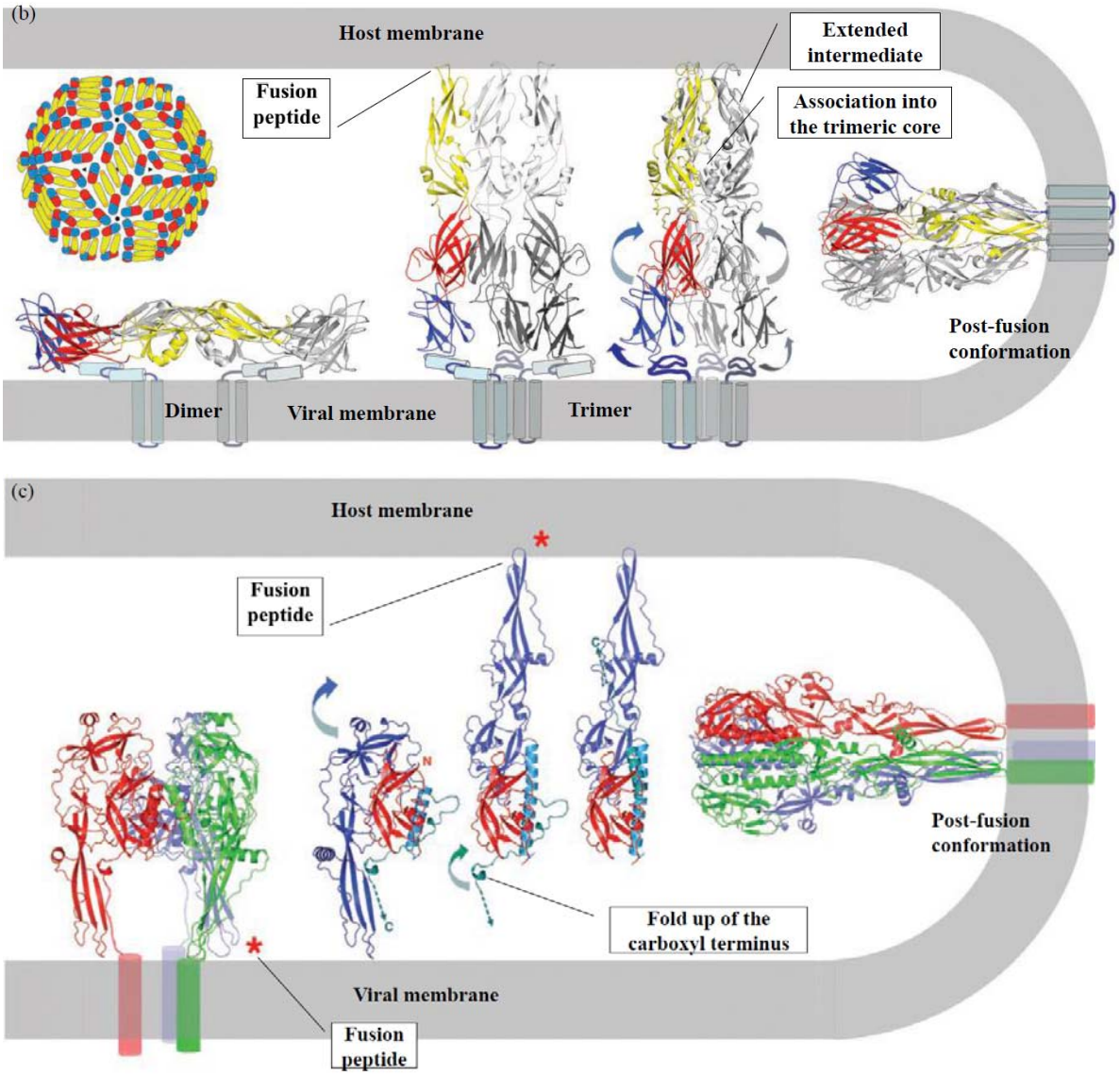

Figure 4.5 Viral membrane fusion process (modified from Harrison *et al*. 2008)

The pre-fusion and post-fusion conformational changes are displayed at the left and right of each figure with the extended intermediate structure in the middle. (a) The influenza virus HA protein is used as an example of class I fusion protein. Each color represent a monomer of the HA protein. The receptor binding region is located at the tip of the individual monomer. The protonation leads to the dissociation of the HA1 subunit and the insertion of the fusion peptide into the host membrane. The carboxyl terminus folds back on the outside of the trimer. (b) The class II fusion protein is arranged in the dimeric conformation on the surface of virion as the flavivirus displayed in the figure. The acidic environment triggers the outward movement of EDI (red) and EDII (yellow) followed by

the insertion of the fusion peptide into the host membrane. The trimmers were formed by the physical association among three monomers and stabilized by the fold back of EDIII (blue) to form the post-fusion conformation. (c) VSV G protein is used as an example for class III fusion proteins. The fusion peptide is packed to face viral membrane in the pre-fusion conformation. Each color is used to label each monomer of the trimeric structure. The insertion of the fusion peptide is induced by the exposure to the acidic environment. The carboxyl terminus folds back towards the fusion peptide to form the post-fusion conformation.

The release of the positive-sense genomes of flaviviruses requires fusion between viral envelope and host membranes. All flavivirus E proteins are classified as class II fusion protein and share the β-strand structures that are characteristic of other class II fusion proteins (Modis, Ogata et al. 2004, Zhang, Zhang et al. 2004, Roussel, Lescar et al. 2006). The E protein dimers are stabilized by the interactions between two neighboring EDIIs and converted to the trimeric structure in the fusion. **(Figure 4.5)** The conformational change from the dimeric structure to the trimeric structure has been confirmed by the observation that soluble monomers of DENV-2 E protein were associated into the trimeric structures and inserted into the membrane of liposomes with an acidic environment (Modis, Ogata et al. 2004). The insertion of the fusion peptide was achieved by the extended intermediate structure, followed by molecular interactions between the EDII of each of the monomers. The E protein trimer is stabilized by molecular interactions at the tip and the base of EDII, and the foldback of EDIII. At the base of the post-fusion trimer, the interaction between EDI and EDIII further stabilizes its structure (Modis, Ogata et al. 2004). The fused viral and host membranes form the fusion pore which is the channel for release of viral genetic material. As shown in the **Figure 4.6**, using the available DENV-2 E protein crystal structure as a model, the acidic environment in the endosomes triggers the destabilization of the structure and the conformational changes by the protonation of conserved four histidine residues, which are His^{144}, His^{244}, His^{282}, and His^{317}, among all the known flaviviruses. The His^{244} and His^{282} are located in the junction between EDI and EDII. The His^{144} and His^{317} are located between EDI and EDIII (Stiasny, Fritz et al. 2011). It is still unclear if the protonation process is completed simultaneously or initiated at specific residues in a sequential order.

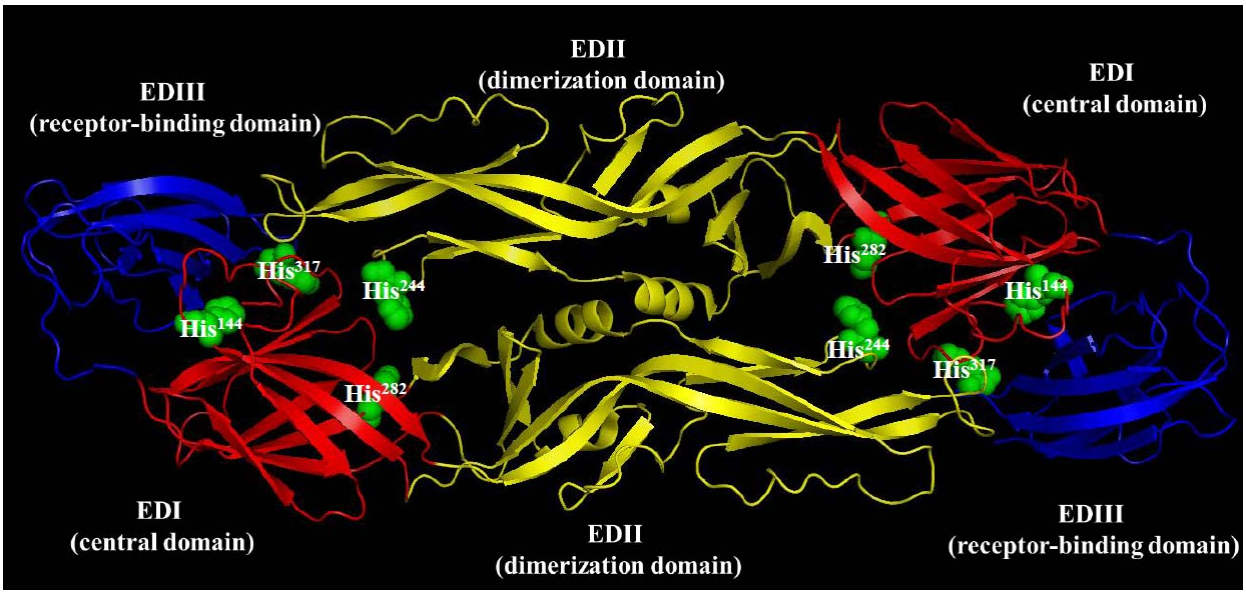

Figure 4.6 The conserved histidine residues subjected to protonation in the DENV-2 E protein (PDB: 10AN)

The four conserved histidine residues are showed in the green sphere structure. The His^{244} and His^{282} residues are located in the interface between EDI (red) and EDII (yellow). The His^{144} and His^{317} residues are located in the junction between EDI (red) and EDIII (blue).

The destabilized structure results in the relative rotations of EDII and EDIII towards the structurally central domain. The available crystal structures of the pre- and post-fusion monomers of DENV-2 E protein are used as examples to illustrate the conformational change of the flavivirus E protein in **Figure 4.7**. The first step of the conformational change is a 30˚ rotation of EDII with respect to EDI (Modis, Ogata et al. 2004, Zhang, Zhang et al. 2004). The movement is tolerated because of the stability created by the hydrophobic properties of the amino acids in the molecular hinge region at the interface between EDI and EDII (Modis, Ogata et al. 2004, Luca, Nelson et al. 2013). The relative location between EDI and EDII at the post-fusion state is further stabilized by the hydrogen bonds created between the D_0 β-strand of EDI and the 1 β-strand of EDII (Modis, Ogata et al. 2004). The refolding of the EDIII is the consequence of the displacement created by the 70˚ degree rotation with respect to EDII and its original location. The displacement reduces the distance between the center of mass of EDIII and EDII to 36Å by the distortion of the linear structure between EDI and EDIII (Modis, Ogata et al. 2004).

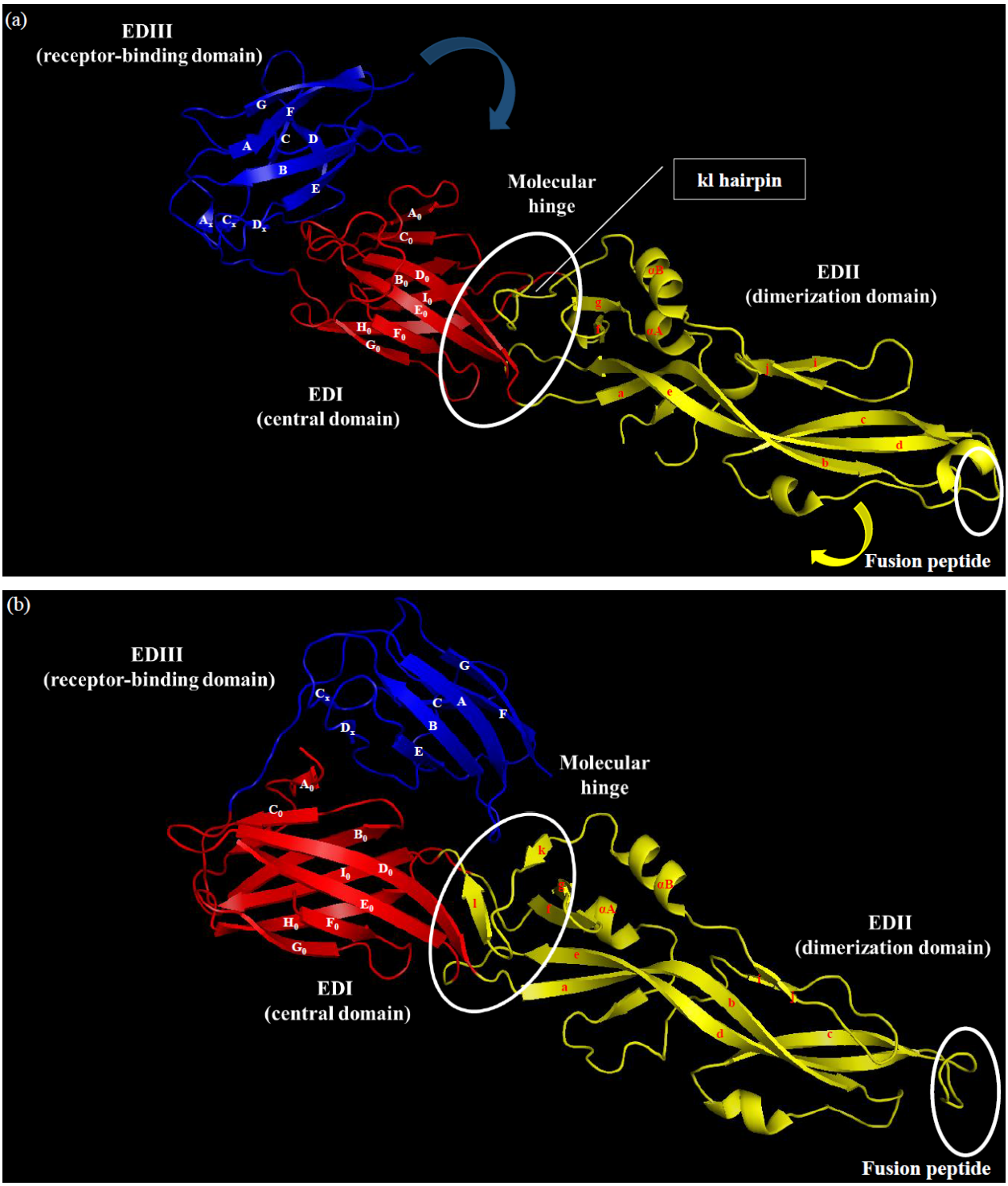

Figure 4.7 Pre- and post-fusion conformation of DENV-2 E protein monomer (PDB ID: (a) 1TG8 and (b) 10K8)

EDI, EDII and EDIII are labeled in red, yellow, and blue, respectively. The molecular hinge region and the fusion peptide are highlighted in the ovals. (a) the pre-fusion conformation of DENV-2 E protein monomer at physiological pH (b) the post-fusion conformation of DENV-2 E protein monomer The relative locations of EDII and EDIII are altered with respect to EDI. The EDII undergoes the 30˚ rotation which disrupted the kl hairpin structure to form the hydrogen bonds between the neighboring D_0 β-strand of EDI and l β-strand in EDII. The refolding of EDIII results in the shorter distance between EDII and EDIII and the elongated structure of the linear structure between EDI and EDIII.

The conformational change of flavivirus E proteins during viral membrane fusion has implicated that, because of their location in the three-dimensional structure, at least two point mutations in YFV 17D strains may result in a phenotypic change. The G52R mutation in the molecular hinge region between EDI and EDII is considered as a non-conservative mutation due to the modification of the sidechain by the increase of the positive charge. The phenotypes of YFV and flavivirus mutants related to the amino acid substitutions in the molecular hinge region will be discussed in **section 4.1.C**. The characterization of the M299I mutation in the linear structure between EDI and EDIII will be described in **chapter 5**.

C. Molecular hinge region of flavivirus E protein

The molecular hinge region (H1-H4) of flavivirus E proteins is composed of four peptides at the interface between EDI and EDII. Although the four peptides are located in the distinct locations in the full-length sequences, due to the discontinuous nature of EDI and EDII, the H1-H4 peptides are located in close proximity to the interface between EDI and EDII. The G52R mutation in the H1 peptide has been described in **section 4.1.A** and the sequence homology of H1 peptides among flaviviruses has been summarized in **table 4.2**. The sequences of H2, H3 and H4 of flaviviruses are listed in **table 4.5**, **4.6** and **4.7**, respectively.

The second peptide, H2, exists between the E_0 β-strand of EDI and e β-strand of EDII. The sequences of H2 peptide among flaviviruses show conserved hydrophobicity at both ends of the peptides because hydrophobic amino acids present at the amino-terminus and carboxy-terminus. The amino-terminus of the H2 peptide of different mosquito-borne flaviviruses shares the use of hydrophobic amino acids. YFV and DENV use valine as the first residue. The flaviviruses under the JEV serocomplex and other flaviviruses under the YFV serocomplex with

no known vectors utilize isoleucine as the first residue. The last residue of the H2 peptide is also composed of the hydrophobic isoleucine or leucine. For WNV, KUNV, MVEV and SLEV, the third residue still remain hydrophobic due to the consistent presence of leucine.

Serocomplex	Virus	Strain	Sequence of H2 peptide (E 130-135)
YFV	YFV	Asibi	VDQTKI
	YFV	17D	VDQTKI
	ENTV	UgIL-30	IGQDKV
	SEPV	MK7148	IDSTKI
	YOKV	Oita36	IDQNKI
DENV	DENV-1	Hawaii	VQYENL
	DENV-2	New Guinea C	VQPENL
	DENV-3	H87	VQHENL
	DENV-4	H241	VQIENL
JEV	JEV	SA_{14}	IQPENI
	JEV	SA_{14}-14-2	IQPENI
	WNV	NY99	ILKENI
	KNV	MRM61C	ILKENI
	SLEV	MS1-7	ILRENI
	MVEV	MVE1-151	ILPEDI
TBEV	TBEV	Neudoerfl	YDANKI
	OHFV	Bogluvovska	YDANKI

Table 4.5 Sequences of the molecular hinge H2 peptide between flavivirus EDI and EDII The hydrophobic amino acids are labeled by underline.

For the H3 peptide of YFV E protein, hydrophobic amino acids are present in the Val^{184}, Ala^{187}, Val^{188} and Phe^{190}. In the corresponding region of the YFV E Val^{184} residue, the use of hydrophobic amino acids is conserved by the presence of proline in other mosquito-borne flaviviruses and valine in tick-borne flaviviruses. The biochemical property of the Val^{188} residue in YFV E protein is also maintained in tick-borne flaviviruses or in other flaviviruses by the use of leucine or isoleucine in other mosquito-borne flaviviruses. The hydrophobicity of the E Phe^{190} residue in YFV is also conserved in the DENV or TBEV serocomplex by the conserved sequence of phenylalanine or the substitution with leucine, respectively. The carboxy terminus of

the H3 peptide in the E proteins of DENV- and JEV-serocomplex flaviviruses also contains the hydrophobic amino acids.

Serocomplex	Virus	Strain	Sequence of H3 peptide (E 183-193)
YFV	YFV	Asibi	QVQTAVDFGNS
	YFV	17D	QVQTAVDFGNS
	ENTV	UgIL-30	NLKTTMDLGNY
	SEPV	MK7148	HVQMMVDLGNS
	YOKV	Oita36	NLKTSMDLNNY
DENV	DENV-1	Hawaii	SPRTGLDFNEM
	DENV-2	New Guinea C	SPRTGLDFNEM
	DENV-3	H87	SPRTGLDFNEM
	DENV-4	H241	EPRSGIDFNEM
JEV	JEV	SA_{14}	EPRSGLNTEAF
	JEV	SA_{14}-14-2	EPRSGLNTEAF
	WNV	NY99	EPRSGIDTNAY
	KNV	MRM61C	EPRSGIDTSAY
	SLEV	MS1-7	EARSGINTEDY
	MVEV	MVE1-151	EPRSGLNTEAY
TBEV	TBEV	Neudoerfl	RVASGVDLAQT
	OHFV	Bogluvovska	RVASGVDLAQT

Table 4.6 Sequences of the molecular hinge H3 peptide between flavivirus EDI and EDII The hydrophobic amino acids are labeled by underline.

The fourth hydrophobic H4 peptide in the molecular hinge region shows the greatest sequence and structure diversity. The H4 molecular hinge of YFV E protein is invariantly longer than other flaviviruses due to the presence of four amino acids between Asn^{268} and Asn^{271}. However, the distribution of the hydrophobic amino acids shows clustering at both amino and carboxy termini of the H4 peptide. The first cluster consists of Ala^{261}, Met^{262}, and Val^{264} in YFV. The corresponding region of Ala^{261} is conserved among all flaviviruses except for TBEV, which contains a valine substitution. The Met^{262} also shows the conserved biochemical properties in the flaviviruses within the JEV- and TBEV-serocomplex by the use of isoleucine and proline respectively. The hydrophobic Val^{264} in YFV is conserved in JEV serocomplex and shares the

similar biochemical properties with the isoleucine and alanine in DENV- and TBEV serocomplex respectively. The second cluster of the hydrophobic amino acids shows the greater diversity by the use of two or three hydrophobic amino acids in different serocomplexes. YFV E protein contains three hydrophobic residues Leu^{273}, Tyr^{274} and Leu^{276} with the positively charged Lys^{275}. The Leu^{273} is conserved by the use of leucine or valine in JEV serocomplex and tyrosine in TBEV serocomplex. The Leu^{276} is identified as the conserved residue in the corresponding region of JEV- and TBEV-serocomplex flaviviruses. In the DENV serocomplex, three hydrophobic amino acids are located together at the corresponding region between the Leu^{277} and Phe^{279} in DENV-2. At the carboxy terminus, all the flaviviruses share the use of hydrophobic valine or leucine at the corresponding position of Val^{281} in YFV E protein.

Serocomplex	Virus	Strain	Sequence of H3 peptide (E 259-281)
YFV	YFV	Asibi	TGAMRVTKDTNDNNLYKLHGGHV
	YFV	17D	TGAMRVTKDTNDNNLYKLHGGHV
	ENTV	UgIL-30	SGATRLQLSSGK---NVLKGGHA
	SEPV	MK7148	SGAMVVEVSSNR---YTLKGGHV
	YOKV	Oita36	VGATKISYSENK---YHIKGGHA
DENV	DENV-1	Hawaii	TGATEIQTSG----TTKIFAGHL
	DENV-2	New Guinea C	TGATEIQMSS----GNLLFTGHL
	DENV-3	H87	TGATEIQTSG----GTSIFAGHL
	DENV-4	H241	TGATEVDSGD----GNHMFAGHL
JEV	JEV	SA_{14}	AGAIVVEYSS----SVKLTSGHL
	JEV	SA_{14}-14-2	AGAIVVEYSS----SVMLTSGHL
	WNV	NY99	AGAIPVEFSSN---TVKLTSGHL
	KNV	MRM61C	AGAIPVEFSSN---TVKLTSGHL
	SLEV	MS1-7	AGAIPATVSSS---TLTLQSGHL
	MVEV	MVE1-151	AGAIPVEFSSS---TLKLTSGHL
TBEV	TBEV	Neudoerfl	AGVPVAHIEG---TKYHLKSGHV
	OHFV	Bogluvovska	AGAPLAHIEG---TKYHLKSGHV

Table 4.7 Sequences of the molecular hinge H4 peptide between flavivirus EDI and EDII The hydrophobic amino acids are labeled by underline.

In conclusion, the molecular hinge region of different viruses displays sequence variations but contains conserved hydrophobic amino acids at specific locations in four different peptides. The biochemical properties and sequence homologies contributes to the loosely packed structure of the peptides, which not only accommodates the pH-dependent conformational change but also the sequence variation (Modis, Ogata et al. 2004). Mutations reported in the molecular regions of various flaviviruses are primarily associated with changes in the threshold of optimal fusion pH (Lee, Weir et al. 1997, Modis, Ogata et al. 2003). The importance of such regions in disease pathogenesis in mice and the replication of virus in mosquitoes has been demonstrated in YFV, JEV, DENV-2 and MVEV (Schlesinger, Chapman et al. 1996, Hurrelbrink and McMinn 2001, Monath, Arroyo et al. 2002, Butrapet, Childers et al. 2011).

The G52R mutation is a conserved substitution in both of the attenuated 17D-204 and 17DD vaccine substrains (Stock, Boschetti et al. 2012). The R52G reversion was discovered in the neurovirulent YFV Porterfield strain variant. This neurovirulent Porterfield strain was derived from the serial passage of YFV 17D in the brain of sucking mice. The genetic and phenotypic characterization demonstrated that the YFV Porterfield strain, replicated to consistent higher viral titers in the central nervous system. It contained two mutations that resulted in the R52G and T173I reversions resembling the E protein sequence of the virulent Asibi strain (Schlesinger, Chapman et al. 1996). The chimerization of the genetic materials by introducing the R52R, I173T, F305V, and I462M mutations in the E protein, the L228Q and S239G mutations in the NS1 protein and the M17L and F79L mutations in the NS2A protein to the genome of the genome of YFV 17D strain increased the neurovirulence of YFV 17D strain in CD1 mice (Schlesinger, Chapman et al. 1996). The results suggested that the mutations at multiple genetic loci in the E, NS1 and NS2A protein were able to increase the virulence of YFV 17D strain. However, whether the R52G reversion in the H1 region of YFV E protein alone is able to increase the virulence remains unclear.

The functional characterization of the molecular hinge region of MVEV E protein was performed by introducing the mutations into the H4 peptide by the selection of neutralization escape mutants and mutants generated by the reverse genetics system (McMinn, Lee et al. 1995, Hurrelbrink and McMinn 2001). The MVEV neutralization escape mutants of mAb 4B6C-2 demonstrated that the H4 peptide within the molecular hinge region in the E protein contains the MVEV-specific neutralization epitope for mAb 4B6C-2. The two selected neutralization escape

mutants, BHv1 and BHv2, contain the S277I and S277N mutations, respectively. Whilst both mutants were only neutralized in the presence of concentrated mAb 4B6C-2 and showed the high neurovirulence in outbred Swiss mice, the significant reduction of neuroinvasiveness only occurred in the non-conservative S277I mutant (Hurrelbrink and McMinn 2001). Characterization of the escape mutants was further performed using the reverse genetics system of MVEV. The neutral Ser^{277} residue was substituted with the hydrophobic amino acids, isoleucine and valine, or the hydrophilic amino acid, proline. The other mutant was generated by conservative substitution with asparagine. The S277I mutation was able to reproduce the phenotype associated with the low neuroinvasiveness observed in the neutralization escape S277I mutant. The conclusion of the studies provided the first evidence that the molecular hinge region can simultaneously serve as both a component of the conformational B-cell epitope and a determinant of neurovirulence. Unfortunately, the mutant was not further characterized for the infection and dissemination in mosquitoes.

For JEV, the H4 molecular hinge contains the virulence determinant that was identified in the passaged chimeric YFV/JEV vaccine candidate (ChimeriVax-JE) in fetal rhesus lung cells (Monath, Arroyo et al. 2002). The single M279K reversion in the H4 peptide to the sequence of the wildtype E protein was associated with an increase of neurovirulence in mice. In contrast to the increase in neurovirulence, the viscerotropism of the virus was further reduced resembling the serially passaged YFV *in vitro* (Theiler and Smith 1937, Barrett, Monath et al. 1990).

The serial passage of DENV-3 in mouse brain led to A54E and F277S mutations in the H1 and H4 peptide, respectively. By performing the fusion-from-within (FFW) assay in C6/36 cells, the mutants with the amino acids substitutions in the H1 and H4 peptides showed a requirement for higher activation energy. This is explained by the decrease of the optimal pH for fusion because the viral membrane fusion process is driven by the energy provided by the acidification of the late endosome (Chernomordik and Kozlov 2003, Harrison 2008). The optimal pH for fusion of the A54E mutant decreased by 0.2. The F277S mutation further resulted in the decrease of the optimal pH for fusion by 0.7 (Lee, Weir et al. 1997).

The H1-H4 peptides of the molecular hinge region in DENV-2 E protein have also been tested using a the reverse genetics system (Butrapet, Childers et al. 2011). Mutations were introduced to all four peptides. The recovery of mutants was first performed on Vero cells and mutants that were lethal in Vero cells were recovered by passage in C6/36 cells. The non-

conservative substitutions in the H1 and H3 peptides led to the production of mutants in Vero cells except for the introduction of the F193R mutation which resulted in mixed population of the F193L and F193R mutants. Two non-conservative mutations, G52R and A54E identified in YFV 17D strain and the serially passaged DENV-3, respectively, in the H1 peptide led to a minor reduction in the peak viral titer in C6/36 cells. The higher optimal pH for the FFW assay suggested that the energy required for the viral membrane fusion is lower in both mutants. The G190F, G190W and F193A mutations in the H3 peptide showed comparable peaked viral titers in C6/36 cells; whereas the non-conservative F193R mutation rescued from C6/36 cells had a lower peaked titer in C6/36 cells. The non-conservative mutations in the H2 and H4 peptides were lethal and precluded recovery of the mutants in Vero cells, although electroporation into C6/36 cells enabled recovery of the F279A and T280Y mutants. The L135W, L135G and L135K mutations in the H2 peptide led to the lower peaked viral titer in C6/36 cells and the significantly lower infection rates in intrathoracically inoculated *Ae. aegypti* mosquitoes. Furthermore, the L135G mutation abolished the viral fusogenic capacity. The F279A and T280Y mutations resulted in a minor reduction of peak viral titer in C6/36 cells and the comparable optimal pH for the fusogenic activity. With respect to vector infectivity, the results obtained for DENV-2 provide a partial understanding of the importance of the molecular hinge region of the flavivirus E proteins. Viral infectivity can potentially be impaired by the single non-conservative mutation in the molecular hinge region. However, the evidence was derived from the L135G mutation in the DENV-2 H2 peptide, and this mutation does not exist in the YFV 17D strain. The DENV-2 G52R mutation that resembles the mutation in the envelope protein of YFV 17D strains showed no demonstrable difference in the peaked viral titers and the activation energy required for viral membrane fusion. Whether the G52R mutation of DENV-2 impairs the viral infectivity in *Ae. aegypti* remains unclear.

In summary, the molecular hinge has been repeatedly demonstrated to control the neurovirulence or neuroinvasiveness of flaviviruses in mice. Mutations in the molecular hinge region generated by the serial passage of YFV and JEV were identified as attenuation determinants for neurovirulence although the mutations are located in the H1 and H4 peptides, respectively (Schlesinger, Chapman et al. 1996, Monath, Arroyo et al. 2002). It has been shown that the fusogenic capacity can be altered due to the mutations in the molecular hinge region in DENV-2 and DENV-3. These observations support the structural evidence that the molecular

hinge region accommodates a conformational change required for viral membrane fusion of flaviviruses (Lee, Weir et al. 1997, Butrapet, Childers et al. 2011). It is still unclear whether or not the mutations in the molecular hinge region can lead to the attenuation of flaviviruses in orally infected arthropod vectors. We propose that the characterization of the G52R mutation in the E protein of YFV 17D strains by the oral infection of the mutant viruses may provide the mechanistic knowledge for the viral attenuation created by the mutations in the molecular hinge region.

D. The T173I mutation as the YFV wildtype-specific epitope

Monoclonal antibodies were originally used to detect and characterize the variants of vaccine seed viruses among the 17D strains and the FNV strain (Buckley and Gould 1985, Gould, Buckley et al. 1985). The mAb117 was first found reactive to wildtype YFV and subsequently mapped to recognize the epitope containing the Thr^{173} residue (Gould, Buckley et al. 1989, Ryman, Ledger et al. 1998). This epitope is conserved across all genotypes of naturally isolated YFV, and the reported acquisition of the wildtype-specific epitope by the 17D(+wt) variant was associated with the loss of the antigenic structure specifically recognized by vaccine-specific mAbs (Gould, Buckley et al. 1989). Indirect immunofluorescence staining with the wildtype YFV-specific mAb 117 on the Vero cells infected by the 17D-204 strain demonstrated the presence of a minor viral population that contains the wildtype-specific epitope. The plaque purification of the 17D-204 strain resulted in the isolation of at least eight variants and demonstrated that a variant virus, later designated as 17D(+wt), contained the epitope recognized by mAb117, and had lost the epitope recognized by the vaccine-specific mAb411 (Gould, Buckley et al. 1989). The characterization of the eight YFV variants by the intracerebral challenge of newborn and weanling mice further identified the 17D(-wt) variant, which was found to be avirulent despite producing the highest viral yield in the brain homogenates up to 10 d.p.i. (Gould, Buckley et al. 1989).

Intracerebral challenge by 17D(+wt) in various outbred and inbred mouse models as summarized in **table 4.8,** demonstrated that the attenuated phenotype of the 17D(+wt) variant was maintained despite the presence of the wildtype-specific epitope (Ryman, Xie et al. 1997, Ryman, Ledger et al. 1998). Intracerebral challenge of the outbred or inbred mice with the 17D-204 strain resulted in a nearly 100% mortality rate in six mouse model systems tested. The

plaque-purified variant 17D(+wt) showed attenuation resulting in 85.0% mortality rate in the outbred TO mice, and 0% mortality in the inbred Balb/C mice although there was 100.0% mortality in four other mouse strain models. In contrast, the 17D(-wt) variant was demonstrated to have the significant attenuation and led to 17.7% and 0% mortality rate in the TO and Balb/C mice, respectively.

	17D-204-UK		17D(+wt)		17D(-wt)	
T0	10/10	(100.0%)	17/20	(85.0%)	8/45	(17.7%)
NIH Swiss	20/20	(100.0%)	10/10	(100.0%)	2/45	(4.4%)
C3H	8/8	(100.0%)	8/8	(100.0%)	12/18	(66.7%)
DBA/2	18/18	(100.0%)	Not tested		8/17	(17.0%)
C57BL/6	10/10	(100.0%)	10/10	(100.0%)	9/10	(90.0%)
Balb/C	26/27	(96.3%)	0/7	(0.0%)	0/16	(0.0%)

Table 4.8 Mortality of mice intracerebrally challenged with the 17D-204 strain and its variants derived from Ryman *et al*. (1997)

The nucleotide sequencing of the prM and E gene identified two genetic mutations among the 17D-204 substrains and two variants listed in **table 4.9**. The 17D(+wt) and 17D(-wt) share the A240V mutation from the 17D-204 substrains, 17D-204-UK and 17D-204-WHO. This mutation attenuated the 17D(+wt) and 17D(-wt) and did not caused the 100% mortality as seen with the two 17D-204 substrains that have the consensus sequence of the Ala^{240} residue in the E protein. The Thr^{173} and Ile^{173} residues in the E protein of the 17D(+wt) and 17D(-wt) variants distinguished by the binding of mAb 117 in two different subpopulations in the 17D-204 strain. The presence of the wild-type YFV-specific epitope by the reversion of the isoleucine residue to threonine in the E protein of 17D(+wt) led to increased neurovirulence in intracerebrally challenged adult mice (Ryman, Ledger et al. 1998).

Strains	Mortality rate in intracerebrally challenged mice	E-153	E-173	E240
17D-204-UK	10/10 (100.0%)	N	I	A
17D-204-WHO	8/8 (100.0%)	T	I	A
17D(+wt)	17/20 (85.0%)	N	T	V
17D(-wt)	8/45 (17.7%)	N	I	V

Table 4.9 The neurovirulence and the genetic mutations distinguish YFV17D-204 substrains and the variants modified from Ryman *et al*. (1998)
The intracerebral challenge was performed in adult outbred mice intracerebrally challenged with 10^4 plaque forming unit. (P.F.U.) The amino acid substitutions were observes at the residues 153, 173 and 240 in the E protein of the 17D-204 substrains and variants.

In summary, the binding of mAb117 is specific to the E proteins of wildtype YFV and the variant of the 17D-204 substrain with the I173T reversion in the E protein. The I173T reversion enhanced the neurovirulence, suggesting that the T173I mutation is likely to be an attenuation determinant. The mechanism distinguishing the neurovirulence in mice between the 17D(+wt) and 17D(-wt) remains unclear.

The antigenicity of the corresponding G_0H_0 loop structure of EDI containing the T173I mutation has also been observed in at least three other flaviviruses, TBEV, DENV-1 and DENV-4. By selecting the variant of TBEV in the presence of mAb i2, the K171E mutation was identified in the variant Vi2 and confirmed as a B-cell epitope for TBEV in mice (Heinz, Berger et al. 1983, Mandl, Guirakhoo et al. 1989). The fusion-from-without assay performed with mAb i2 (50μg/ml) and TBEV Neudoerfl strain in C6/36 cells demonstrated that the binding of the mAb i2 completely abolished the fusion activity at the step of viral entry. The optimal pH for the fusogenic activity of the TBEV Vi2 variant was significantly lower than that for the wildtype TBEV Neudoerfl strain, thereby indicating that the K173E mutation results in the requirement for higher energy for viral membrane fusion (Guirakhoo, Heinz et al. 1991). The epitope mapping of a chimpanzee anti-DENV-4 mAb also suggested that the G_0H_0 loop of EDI is part of the interdomain conformational epitope (Lai, Goncalvez et al. 2007). Recently, the G_0H_0 loop of EDI was also demonstrated to be recognized by a DENV-1-specific human mAb 1F4. The Thr^{176} residue in the G_0H_0 loop region was recognized by the complementarity-determining regions of the heavy chain in mAb (Fibriansah, Tan et al. 2014).

In conclusion, the current understanding in the G_0H_0 loop structure is derived from studies with variants of flaviviruses that demonstrate the different binding affinities with mAb. B-cell epitopes have been repeatedly identified within the G_0H_0 loop structure of the E proteins among YFV, TBEV, DENV-1 and DENV-4. For YFV 17D strain, the T173I mutation was identified as an attenuation determinant leading to the low neurovirulence phenotype in mice

(Ryman, Ledger et al. 1998). The putative function of the region may be related to the fusogenic activity of the flavivirus E proteins in the process of viral membrane fusion during viral entry. The fusion-from-without experiments in C6/36 cells with a TBEV E K171E mutation provided an understanding of the function of the G_0H_0 loop in flavivirus E proteins (Guirakhoo, Heinz et al. 1991). The actual functional importance of the T173I mutation in the E protein of YFV 17D strain for the viral infection and dissemination in *Ae. aegypti* still remains unknown.

4.2 Results

Clearly, the G52R mutation in the molecular hinge between EDI-EDII and the T173I mutation in EDI have been extensively tested *in vitro* and in mice. In spite of the experimental evidence that suggests the functional importance of both regions in the E protein of YFV and other flaviviruses, it is still unclear how the G52R and T173I mutations might lead to the phenotypic changes of YFV in orally infected *Ae. aegypti*. The characterization of the mutations was first performed by introducing single G52R or T173I mutations into the Asibi strain and the 17D+Asibi M-E chimera. This approach was used to assess the attenuation associated with the single mutations in the E protein alone, and the attenuation caused by the single mutations in the E protein and the attenuation determinants in the nonstructural proteins, respectively. The YFV E G52R-T173I double mutants were also characterized.

A. Infection and dissemination of YFV E G52R mutants

The YFV 17D E protein G52R mutation was introduced into the cDNA infectious clone of the Asibi strain and the 17D/Asibi M-E chimera to evaluate the role of the G52R mutation as an attenuation determinant. The infection and dissemination rates of the YFV wildtype controls and E G52R mutants at 7, 10 and 14 d.p.i. are summarized in **Table 4.10 and 4.11**, respectively.

Viremic blood meal (titer in log$TCID_{50}$/ml)	7 d.p.i.		10 d.p.i.		14 d.p.i.	
Mock (N.A.)	0/24	(0.0%)	0/18	(0.0%)	0/24	(0.0%)
17D (4.24)	9/24	(37.5%)	3/6	(50.0%)	4/16	(25.0%)
17D+Asibi M-E (7.02)	16/20	(80.0%)	4/7	(57.1%)	11/24	(45.8%)
17D+Asibi M-E G52R (7.14)	5/24	(20.8%)*	3/15	(20.0%)	4/24	(16.7%)
Asibi (6.11)	17/24	(70.8%)	12/15	(80.0%)	15/24	(62.5%)
Asibi E G52R (5.52)	7/24	(29.2%)†	3/9	(33.3%)‡	5/16	(31.3%)

Table 4.10 Infection rate of YFV wildtype controls and E G52R mutants in *Ae. aegypti* at 7, 10 and 14 d.p.i.

† and ‡ indicate the statistically significant difference by Fisher's exact test compared to the infection rates of the Asibi strain at 7 and 10 d.p.i., respectively. ($p<0.05$)

*** indicates the statistically significant difference by Fisher's exact test compared to the infection rate of the 17D+Asbi M-E chimera at 7 d.p.i., respectively. ($p<0.05$)**

The average titer of the viremic blood meals containing the Asibi strain and the Asibi E G52R mutant were 6.11 and 5.52 $logTCID_{50}$/ml, respectively. The infection rate of the Asibi E G52R mutant was consistently lower than that observed for the Asibi strain at 7 (70.8% vs. 29.2%, p=0.0087) and 10 (80.0% vs. 33.3%, p=0.0361) d.p.i. At 14 d.p.i., the infection rate of the Asibi E G52R mutant remained lower than the Asibi strain without significant difference (62.5% vs. 31.3%, p=0.10).

The 17D+Asibi M-E chimera and the 17D+Asibi M-E E G52R mutant were orally administered at 7.02 and 7.14 $logTCID_{50}$/ml, respectively. The infection rate of the 17D+Asibi M-E E G52R mutant was significantly lower than the 17D+Asibi M-E chimera (80.0% vs. 20.8%, p=0.0001) at 7 d.p.i. There was no demonstrable difference in the infection rates of the 17D+Asibi M-E chimera and 17D+Asibi M-E E G52R mutant at 10 (57.1% vs. 20.0%) and 14 (45.8% vs. 16.7%) d.p.i.

Viremic blood meal (titer in $logTCID_{50}$/ml)	7 d.p.i.		10 d.p.i.		14 d.p.i.	
17D (4.24)	0/5	(0.0%)	0/1	(0.0%)	0/3	(0.0%)
17D+Asibi M-E (7.02)	1/10	(10.0%)	1/2	(50.0%)	3/8	(37.5%)
17D+Asibi M-E G52R (7.14)	1/6	(16.7%)	0/1	(0.0%)	0/3	(0.0%)
Asibi (6.11)	3/10	(30.0%)	6/9	(66.7%)	8/10	(80.0%)
Asibi E G52R (5.52)	1/3	(33.3%)	0/2	(0.0%)	1/1	(100.0%)

Table 4.11 Dissemination rate of YFV wildtype controls and E G52R mutants in *Ae. aegypti* at 7, 10 and 14 d.p.i.

There was no significant difference in viral dissemination observed between the YFV wildtype strains and the E G52R mutants. The dissemination rate of the Asibi E G52R mutant was comparable but not significantly higher than the Asibi strain at 7 (30.0% vs. 33.3%, p=1.00) and 14 (100.0% vs. 80.0%, p=1.00) d.p.i. At 10 d.p.i., there was no dissemination observed in

the dissected *Ae. aegypti* infected by the Asibi E G52R mutant, whilst the infection of the Asibi strain led to the dissemination rate at 66.7% (6/9, p=0.18). The dissemination rate of the 17D+Asibi M-E E G52R mutant was lower with no demonstrable difference at 7 (10.0% vs. 16.7%, p=1.00) , 10 (50.0% vs. 0.0%, p=1.00) and 14 (37.5% vs. 0.0%, p=0.49) d.p.i.

In summary, the infection rate of the Asibi E G52R and 17D+Asibi M-E E G52R mutants was significantly lower at 7 d.p.i. The infection rate of the Asibi E G52R mutant remained significantly lower than the Asibi strain at 10 d.p.i. At, 14 d.p.i., the infection rate of the wildtype and mutant viruses showed no significant difference. The infection of the Asibi E G52R and 17D+Asibi M-E E G52R mutants led to the comparable dissemination rates at 7, 10 and 14 d.p.i. compared to YFV wildtype controls. The results suggested that the infectivity of the Asibi strain and the 17D+Asibi M-E chimera is significantly impaired at 7 d.p.i. The reduced infectivity was further observed in the Asibi E G52R mutant at 10 d.p.i., when the 17D+Asibi M-E E G52R mutant did not show a demonstrable difference in the infection rate from the 17D+Asibi M-E chimera. The dissemination of the Asibi E G52R mutant was still observed at 14 d.p.i. implicating the G52R mutation in the E protein did not impair viral dissemination in *Ae. aegypti*. In conclusion, the G52R mutation should be considered as a determinant for the infectivity of YFV in *Ae. aegypti*.

B. Viral titers of whole mosquitoes, bodies and secondary tissues infected by YFV E G52R mutants

The titers of the whole mosquitoes infected by the Asibi E G52R and the 17D/Asibi M-E E G52R are summarized in **Figure 4.8**. The titers between the Asibi E G52R mutant and the Asibi strain or between the 17D/Asibi M-E chimera and the 17D/Asibi M-E E G52R mutant did not show any significant difference (p>0.05). The engorgement of viremic blood containing the Asibi E G52R mutant and the Asibi strain resulted in the average titer of 1.92 and 2.83 $logTCID_{50}$/ml at 0 d.p.i. The whole-mosquito titers of the Asibi E G52R mutant and the Asibi strain remain similar at 7 (2.25 $logTCID_{50}$/ml, n=7 vs. 2.23 $logTCID_{50}$/ml, n=4) and 10 (2.16 $logTCID_{50}$/ml, n=3 vs. 2.52 $logTCID_{50}$/ml, n=1) d.p.i. At 14 d.p.i., the Asibi E G52R mutant and the Asibi strain replicated to 2.56 (n=4) $logTCID_{50}$/ml and 3.89 $logTCID_{50}$/ml (n=5), respectively. The whole-mosquito titers of the 17D+Asibi M-E chimera and the 17D+Asibi M-E E G52R mutant were comparable at 7 (2.99 $logTCID_{50}$/ml, n=5 vs. 1.51 $logTCID_{50}$/ml, n=2), 10

(3.52 logTCID$_{50}$/ml, *n*=2 vs. 2.51 logTCID$_{50}$/ml, *n*=2) and 14 (2.58 logTCID$_{50}$/ml, *n*=3 vs. 2.95 logTCID$_{50}$/ml, *n*=1) d.p.i.

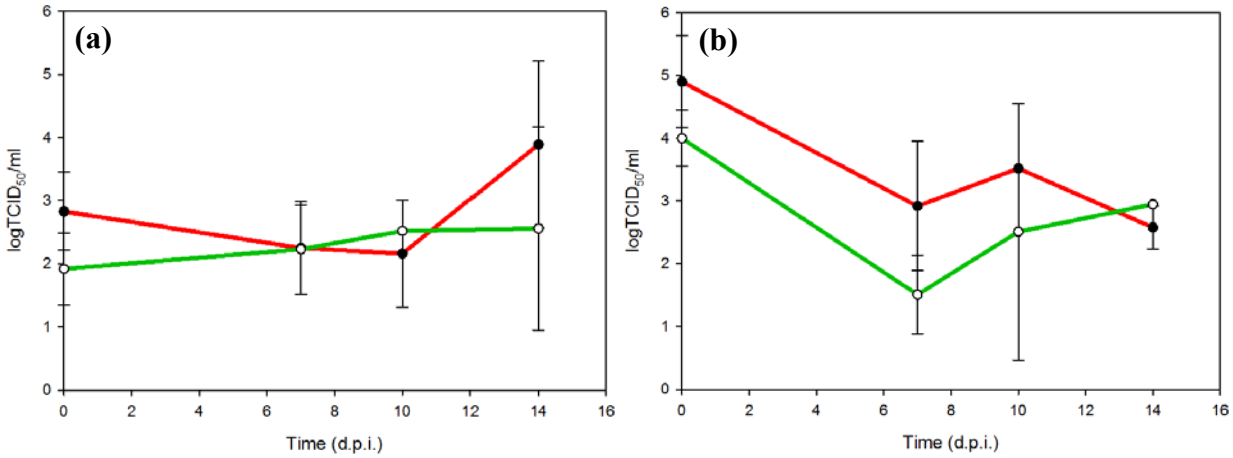

Figure 4.8 Average titers of whole mosquitoes infected by YFV wildtype controls and E G52R mutants

(a) Titers of whole mosquitoes infected by the Asibi strain (red) and the Asibi E G52R mutant (green) (b) Titers of whole mosquitoes infected by the 17D+Asibi M-E chimera (red) and the 17D+Asibi M-E E G52R mutant (green)

The Asibi E G52R mutant and the 17D+Asibi M-E E G52R mutant was able to replicate to the similar level as the Asibi strain and the 17D+Asibi M-E chimera (p>0.05). The results are shown in **Figure 4.9**. The average body titer of *Ae. aegypti* infected by the Asibi E G52R mutant was insignificantly lower than the Asibi strain at 7 (2.44 logTCID$_{50}$/ml, *n*=10 vs. logTCID$_{50}$/ml, *n*=2) and 10 (2.17 logTCID$_{50}$/ml, *n*=8 vs. 1.77 logTCID$_{50}$/ml, *n*=2) d.p.i. There was no positive body sample among the *Ae. aegypti* dissected at 14 d.p.i. as the average body titer of *Ae. aegypti* infected by the Asibi E G52R mutant. The average body titer of the Asibi strain increased to 2.68 logTCID$_{50}$/ml (*n*=8). The infection of the 17D+Asibi M-E chimera and the 17D+Asibi M-E E G52R mutant resulted in the similar average body titer at 7 d.p.i. (2.41 logTCID$_{50}$/ml, *n*=10 vs. 2.51 logTCID$_{50}$/ml, *n*=5) The average body titer of the 17D+Asibi M-E E G52R mutant was lower with no significant difference from the 17D+Asibi M-E chimera at 10 (3.52 logTCID$_{50}$/ml, *n*=1 vs. 1.95 logTCID$_{50}$/ml, *n*=1) and 14 (2.32 logTCID$_{50}$/ml, *n*=8 vs. 1.83 logTCID$_{50}$/ml, *n*=3) d.p.i.

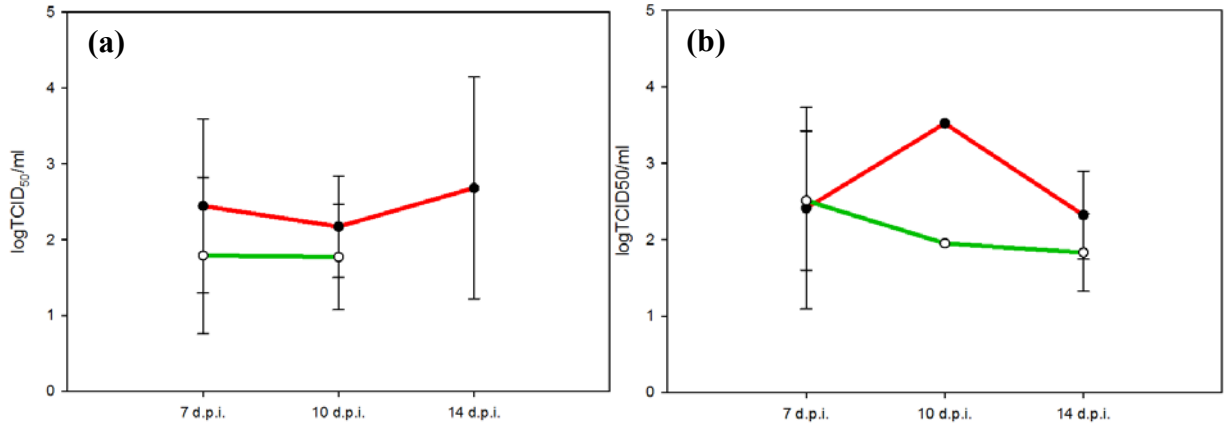

Figure 4.9 Average body titers of *Ae. aegypti* infected by YFV wildtype controls and E G52R mutants

(a) Average body titers of the Asibi strain (red) and the Asibi E G52R mutant (green) (b) Average body titers of the 17D+Asibi M-E chimera (red) and the 17D+Asibi M-E E G52R mutant (green)

The average titers of the secondary tissues are summarized in **Figure 4.10**. There was no statistically significance in the difference of viral titers between the Asibi strain and the Asibi E G52R mutant or between the 17D+Asibi M-E chimera and the 17D+Asibi M-E E G52R mutant. The titers of the secondary tissues in *Ae. aegypti* infected by the Asibi E G52R mutant were lower without demonstrable difference at 7 (3.00 $\log TCID_{50}$/ml, n=3 vs. 2.52 $\log TCID_{50}$/ml, n=1) and 14 (2.50 $\log TCID_{50}$/ml, n=8 vs. 1.06 $\log TCID_{50}$/ml, n=1) d.p.i. The disseminated 17D+Asibi M-E E G52R mutant resulted in the lower titer (2.95 $\log TCID_{50}$/ml, n=1 vs. 1.95 $\log TCID_{50}$/ml, n=1) than the 17D+Asibi M-E chimera at 7 d.p.i.

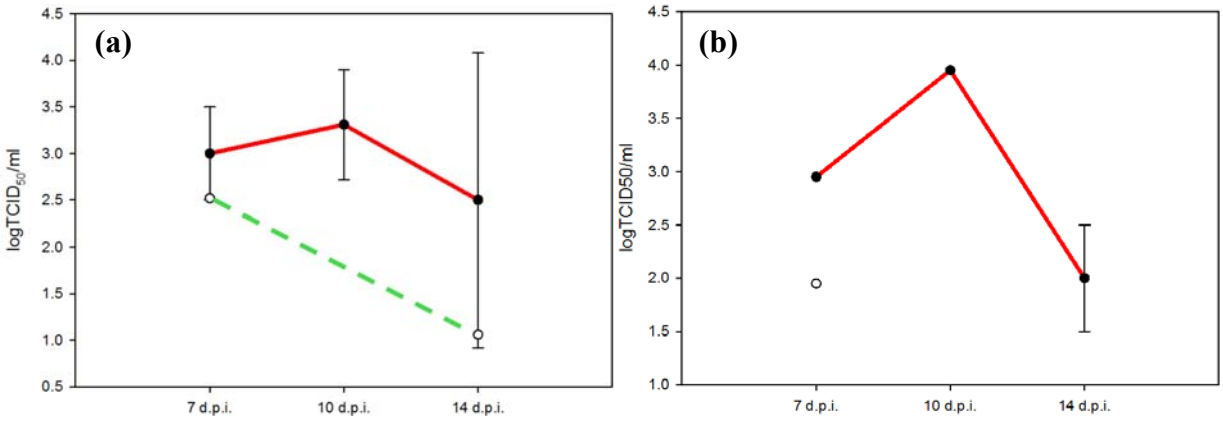

Figure 4.10 Average secondary tissue titers of *Ae. aegypti* infected by YFV wildtype controls and E G52R mutants

(a) Average secondary tissue titers of the Asibi strain (red) and the Asibi E G52R mutant (green) The green dash line was used to represent the average secondary tissue titers of the Asibi E G52R mutant between 7 and 14 d.p.i. due to the lack of positive secondary tissues derived from the dissected mosquitoes, which were previously exposed to the blood meal containing the Asibi E G52R mutant. (b) Average body titers of the 17D+Asibi M-E chimera (red) and the 17D+Asibi M-E E G52R mutant (open circle)

In summary, the average titers of samples derived from the whole mosquitoes, the bodies and the secondary tissues showed no statistical significance between the Asibi strain and the Asibi E G52R mutant or between the 17D+Asibi M-E chimera and the 17D+Asibi M-E E G52R mutant. Although the significantly lower infection rates caused by the G52R mutation have been observed and described in **section 4.2.B**, the dissemination and the average titers of homogenized mosquito samples did not show the significant difference between the YFV E G52R mutants and the wildtype controls. Presumably, the G52R mutation contributes to the attenuated phenotype of the 17D strains by lowering the infection rate but not preventing the viral dissemination into the secondary tissues.

C. Infection and dissemination of YFV E T173I mutants

The Asibi E T173I mutant and the 17D+Asibi M-E E T173I mutant were produced to characterize the potential phenotypic effects of the T173I mutation in the E protein. The infection and dissemination rates of the YFV wildtype controls and E T173I mutants are summarized in **Table 4.12** and **4.13**.

Viremic blood meal (titer in log$TCID_{50}$/ml)	7 d.p.i.		10 d.p.i.		14 d.p.i.	
Mock (N.A.)	0/24	(0.0%)	0/18	(0.0%)	0/24	(0.0%)
17D (4.24)	9/24	(37.5%)	3/6	(50.0%)	4/16	(25.0%)
17D+Asibi M-E (7.02)	16/20	(80.0%)	4/7	(57.1%)	11/24	(45.8%)
17D+Asibi M-E T173I (7.14)	14/24	(58.3%)	10/16	(62.5%)	10/24	(41.7%)
Asibi (6.11)	17/24	(70.8%)	12/15	(80.0%)	15/24	(62.5%)
Asibi E T173I (6.24)	10/24	(41.7%)	14/24	(58.3%)	8/24	(33.3%)

Table 4.12 Infection rate of YFV wildtype controls and E T173I mutants in *Ae. aegypti* at 7, 10 and 14 d.p.i

The infection rate of the Asibi E T173I mutant was not significantly different to the Asibi strain at 7 (41.7% vs. 70.8%, p=0.08), 10 (58.3% vs. 80.0%, p=0.43) and 14 (33.3% vs, 62.5%, p=0.08) d.p.i. Similarly, there was no significant difference in the infection rate of the 17D+Asibi M-E E T173I mutant from the 17D+Asibi M-E chimera at 7 (80.0% vs. 58.3%, p=0.19), 10 (57.1% vs. 62.5%, p=1.00) and 14 (45.8% vs. 41.7%, p=1.00) d.p.i.

Viremic blood meal (titer in log$TCID_{50}$/ml)	7 d.p.i.		10 d.p.i.		14 d.p.i.	
17D (4.24)	0/5	0.0%	0/1	0.0%	0/3	0.0%
17D+Asibi M-E (7.02)	1/10	10.0%	1/2	50.0%	3/8	37.5%
17D+Asibi M-E T173I (7.14)	2/10	20.0%	1/7	14.3%	4/6	66.7%
Asibi (6.11)	3/10	30.0%	6/9	66.7%	8/10	80.0%
Asibi E T173I (6.24)	4/8	50.0%	3/11	27.3%	3/4	75.0%

Table 4.13 Dissemination rate of YFV wildtype controls and E T173I mutants in *Ae. aegypti* at 7, 10 and 14 d.p.i

The dissemination rate showed no significant difference between the Asibi strain and the Asibi E T173I mutant at 7 (30.0% vs. 50.0%, p=0.63), 10 (66.7% vs. 27.3%, p=0.17) and 14 (80.0% vs. 75.0%, p=1.00) d.p.i. The infection of the 17D+Asibi M-E chimera and the 17D+Asibi M-E E T173I mutant resulted in the similar infection rate at 7 (10.0% vs. 20.0%, p=1.00), 10 (50.0% vs. 14.3%, p=1.00) and 14 (37.5% vs. 66.7%, p=0.59) d.p.i.

In summary, the T173I mutation in the E protein of YFV 17D strains caused no demonstrable attenuation. The infection rate and the dissemination rate of the Asibi E T173I and 17D+Asibi M-E E T173I mutants were comparable to the Asibi strain and the 17D+Asibi M-E chimera.

D. Viral titers of whole mosquitoes, bodies and secondary tissues infected by YFV E T173I mutants

The average titers of the whole mosquitoes infected by the YFV wildtype controls and E T173 mutants are shown in **Figure 4.11**. The titers between the Asibi strain and the Asibi E T173I mutant remain comparable (p>0.05) at 7 (2.25 log$TCID_{50}$/ml, n=7 vs. 1.06 log$TCID_{50}$/ml, n=1), 10 (2.16 log$TCID_{50}$/ml, n=3 vs. 2.25 log$TCID_{50}$/ml, n=3) and 14 (3.89 log$TCID_{50}$/ml, n=5 vs. 2.62 log$TCID_{50}$/ml, n=4) d.p.i. There was no significant difference in the average titers of

whole mosquitoes infected by the 17D+Asibi M-E chimera and the 17D+Asibi M-E E T173I mutant at 7 (2.99 logTCID$_{50}$/ml, *n*=5 vs. 1.89 logTCID$_{50}$/ml, *n*=4), 10 (3.52 logTCID$_{50}$/ml, *n*=2 vs. 2.51 logTCID$_{50}$/ml, *n*=3) and 14 (2.58 logTCID$_{50}$/ml, *n*=3 vs. 3.42 logTCID$_{50}$/ml, *n*=4) d.p.i.

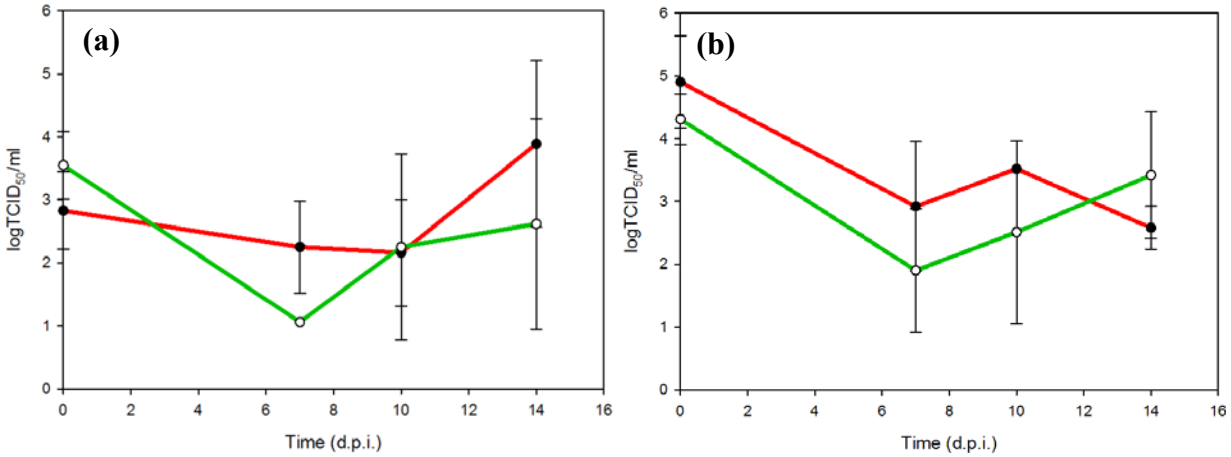

Figure 4.11 Average titers of whole mosquitoes infected by YFV wildtype controls and E T173I mutants

(a) Titers of whole mosquitoes infected by the Asibi strain (red) and the Asibi E T173I mutant (green) (b) Titers of whole mosquitoes infected by the 17D+Asibi M-E chimera (red) and the 17D+Asibi M-E E T173I mutant (green)

The comparison of the average body titers did not identify any significant difference between the Asibi strain and the Asibi E T173I mutant or the 17D+Asibi M-E chimera and the 17D+Asibi M-E E T173I mutant as summarized in **Figure 4.12**. The average titers of the bodies infected by the Asibi E T173I mutant were comparable to those infected by the Asibi strain at 7 (2.44 logTCID$_{50}$/ml, *n*=10 vs. 2.60 logTCID$_{50}$/ml, *n*=7), 10 (2.17 logTCID$_{50}$/ml, *n*=8 vs. 2.49 logTCID$_{50}$/ml, *n*=11) and 14 (2.68 logTCID$_{50}$/ml, *n*=8 vs. 2.38 logTCID$_{50}$/ml, *n*=4) d.p.i. There was no significant difference in the average titers of the bodies infected by the 17D+Asibi M-E chimera and the 17D+Asibi M-E E T173I mutant at 7 (2.41 logTCID$_{50}$/ml, *n*=10 vs. 2.50 logTCID$_{50}$/ml, *n*=9), 10 (3.52 logTCID$_{50}$/ml,*n*=1 vs. 2.71 logTCID$_{50}$/ml, *n*=1) and 14 (2.32 logTCID$_{50}$/ml, *n*=8 vs. 2.46 logTCID$_{50}$/ml, *n*=6) d.p.i.

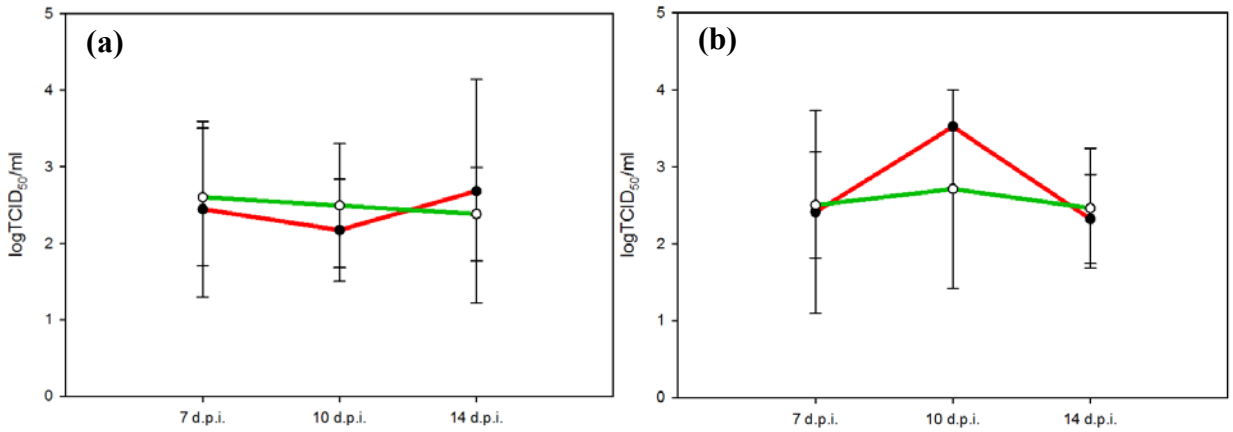

Figure 4.12 Average body titers of *Ae. aegypti* infected by YFV wildtype controls and E T173I mutants

(a) Average body titers of the Asibi strain (red) and the Asibi E T173I mutant (green) (b) Average body titers of the 17D+Asibi M-E chimera (red) and the 17D+Asibi M-E E T173I mutant (green)

The average titers of secondary tissues among the disseminated form of infection showed no significant difference between the Asibi strain and the Asibi E T173I mutant or between the 17D+Asibi M-E chimera and the 17D+Asibi M-E E T173I mutant (p>0.05) in **Figure 4.13**. The dissemination of the Asibi E T173I mutant resulted in similar average titers of homogenized secondary tissues to the Asibi strain at 7 (3.00 logTCID$_{50}$/ml, n=3 vs. 3.49 logTCID$_{50}$/ml, n=4), 10 (3.31 logTCID$_{50}$/ml, n=6 vs. 4.00 logTCID$_{50}$/ml, n=3) and 14 (2.50 logTCID$_{50}$/ml, n=8 vs. 3.66 logTCID$_{50}$/ml, n=2) d.p.i. The average titers of the secondary tissues infected by the 17D+Asibi M-E chimera and the 17D+Asibi M-E T173I mutant remained similar at 7 (2.95 logTCID$_{50}$/ml, n=1 vs. 2.29 logTCID$_{50}$/ml, n=2), 10 (3.95 logTCID$_{50}$/ml, n=1 vs. 1.52 logTCID$_{50}$/ml, n=1) and 14 (2.00 logTCID$_{50}$/ml, n=3 vs. 3.09 logTCID$_{50}$/ml, n=4) d.p.i.

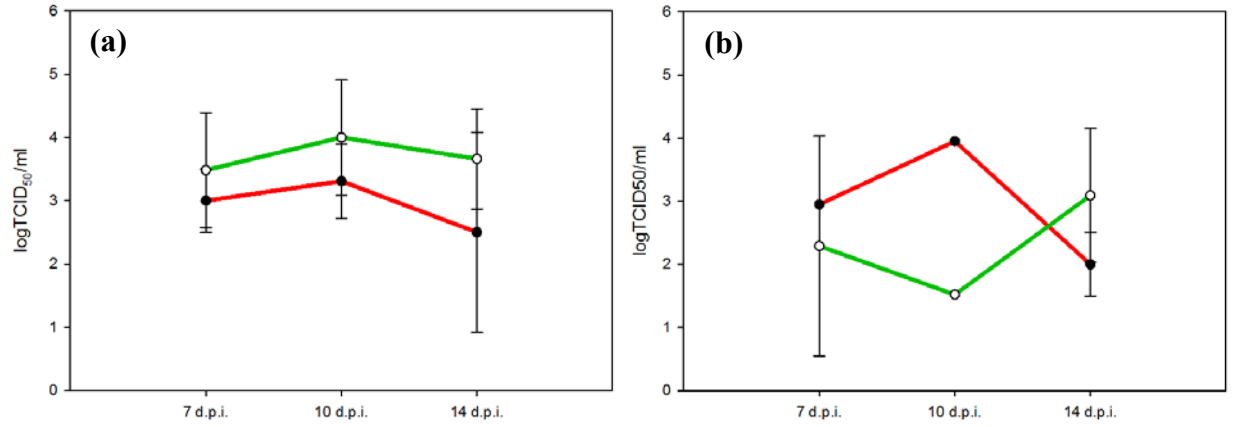

Figure 4.13 Average secondary tissue titers of *Ae. aegypti* infected by YFV wildtype controls and E T173I mutants

(a) Average body titers of the Asibi strain (red) and the Asibi E T173I mutant (green) (b) Average body titers of the 17D+Asibi M-E chimera (red) and the 17D+Asibi M-E E T173I mutant (green)

Similar to the no demonstrable difference in the infection and dissemination rates observed in the Asibi E T173I and the 17D+Asibi M-E E T173I mutants. The replication of both mutants resulted in the comparable average titers to the wildtype controls in the homogenized whole mosquitoes, bodies and secondary tissues.

E. Infection and dissemination of YFV E G52R-T173I double Mutants

It is clear that the attenuation of the Asibi strain requires multiple genetic mutations in the structural genes. The significant impairment in viral infectivity for mosquitoes was achieved by the substitution of 17D EDI and EDII into the Asibi strain. (McElroy et al., 2006b) Based on the significant attenuation caused by the single G52R mutation, the YFV E G52R-T173I double mutants were generated in order to determine the the potential synergistic effect of two point mutations. The infection rate and dissemination rate of the YFV E G52R-T173I double mutants and wildtype controls are summarized in **Table 4.14 and 4.15**, respectively.

Ae. aegypti exposed to the Asibi strain and the Asibi E G52R-T173I mutant at 3.66 and 2.52 log$TCID_{50}$/ml showed comparable infection rates at 7 (72.7% vs. 67.7%) d.p.i. The infection rate of the Asibi E G52R-T173I mutant was consistently lower than the Asibi strain at 10 (100.0% vs. 61.1%, p=0.0076) and 14 (76.3% vs. 32.3%, p=0.0005) d.p.i. The infectivity of the 17D+Asibi M-E E G52R-T173I mutant was significantly lower than that of the 17D+Asibi M-E chimera at 7 (62.1% vs. 30.8%, p=0.0139) and 14 (65.6% vs. 25.6%, p=0.0009) d.p.i.; whereas, the infection rate of the 17D+Asibi M-E E G52R-T173I mutant was similar to the 17D+Asibi M-E chimera at 10 d.p.i. (45.5% vs. 64.4%, p>0.05).

Viremic blood meal (titer in log$TCID_{50}$/ml)	7 d.p.i.		10 d.p.i.		14 d.p.i.	
Mock (N.A.)	0/30	(0.0%)	0/24	(0.0%)	0/35	(0.0%)
17D (6.19)	15/25	(60.0%)	11/12	(91.7%)	12/32	(37.5%)
17D+Asibi M-E (5.77)	18/29	(62.1%)	5/11	(45.5%)	21/32	(65.6%)

17D+Asibi M-E E G52R-T173I (4.69)	12/39	(30.8%)†	29/45	(64.4%)	10/39	(25.6%)‡
Asibi (3.66)	24/33	(72.7%)	18/18	(100.0%)	29/38	(76.3%)
Asibi E G52R-T173I (2.52)	23/34	(67.7%)	11/18	(61.1%)*	10/31	(32.3%)**

Table 4.14 Infection rate of YFV wildtype controls and E G52R-T173I mutants in *Ae. aegypti* at 7, 10 and 14 d.p.i

*** and ** indicate the significant difference by Fisher's exact test between the Asibi strain the Asibi E G52R-T173I mutant at 10 (p=0.0076) and 14 (p=0.00035)d.p.i., respectively.**

† and ‡ indicate the significant difference by Fisher's exact test between the 17D+Asibi M-E chimera and the 17D+Asibi M-E E G52R-T173I mutant at 7 (p=0.0139) and 14 (p=0.0009)d.p.i., respectively.

Although a significant reduction in the infection rate was observed in the group orally challenged by the Asibi E G52R-T173I mutant at 10 and 14 d.p.i., the dissemination rate of the Asibi E G52R-T173I mutant remained similar (p>0.05) to that of the Asibi strain at 7 (82.4 vs. 87.5%), 10 (83.3% vs. 85.7%) and 14 (70.0% vs. 16.7%) d.p.i. Similarly, there was no significant difference in the dissemination rate between the 17D+Asibi M-E chimera and the 17D+Asibi M-E E G52R-T173I mutant at 7 (50.0% vs. 80.0%), 10 (25.0% vs. 63.16%) and 14 (50.0% vs. 20.0%) d.p.i.

Viremic blood meal (titer in log$TCID_{50}$/ml)	7 d.p.i.		10 d.p.i.		14 d.p.i.	
17D (6.19)	0/12	(0.0%)	0/8	(0.0%)	1/9	(11.1%)
17D+Asibi M-E (5.77)	6/12	(50.0%)	1/4	(25.0%)	6/12	(50.0%)
17D+Asibi M-E G52R-T173I (4.69)	8/10	(80.0%)	12/19	(63.16%)	1/5	(20.00%)
Asibi (3.66)	14/17	(82.4%)	10/12	(83.3%)	14/20	(70.0%)
Asibi E G52R-T173I (2.52)	14/16	(87.5%)	6/7	(85.7%)	1/6	(16.7%)

Table 4.15 Dissemination rate of YFV wildtype controls and E G52R-T173I mutants in *Ae. aegypti* at 7, 10 and 14 d.p.i

The YFV E G52R-T173I double mutants showed consistently lower infection rates at 14 d.p.i. between the Asibi strain and the Asibi E G52R-T173I mutant and between the 17D+Asibi M-E chimera and the 17D+Asibi M-E E G52R-T173I mutant. The Asibi E G52R-T173I mutant and the 17D+Asibi M-E E G52R-T173I mutant also showed the significantly lower infection rate at 10 and 7 d.p.i., respectively. The lower infection rates observed in the YFV E G52R-T173I

double mutants suggest the mutations together caused the impairment of viral infectivity that were observed in the YFV E G52R mutants.

F. Viral titers of whole mosquitoes, bodies and secondary tissues infected by YFV E G52R-T173I double mutants

The viral replication in whole mosquitoes resulted in no demonstrable difference (p>0.05) between the Asibi strain and the Asibi E G52R-T173I mutant or between the 17D+Asibi M-E chimera and the 17D+Asibi M-E E G52R-T173I mutant. The average titers are summarized in **Figure 4.14**.The average titers of homogenized whole mosquitoes infected by the Asibi E G52R-T173I mutant were lower than the Asibi strain without any statistical significance at 7 (1.87 logTCID$_{50}$/ml, n=7 vs. 1.66 logTCID$_{50}$/ml, n=7), 10 (2.53 logTCID$_{50}$/ml, n=6 vs. 1.06 logTCID$_{50}$/ml, n=1) and 14 (3.09 logTCID$_{50}$/ml, n=8 vs. 2.37 logTCID$_{50}$/ml, n=4) d.p.i. The whole-mosquito homogenates derived from *Ae. aegypti* infected by the 17D+Asibi M-E E G52R-T173I mutant had the comparable titers with *Ae. aegypti* infected by the 17D+Asibi M-E chimera at 7 (2.46 logTCID$_{50}$/ml, n=6 vs. 1.79 logTCID$_{50}$/ml, n=2), 10 (1.06 logTCID$_{50}$/ml, n=1 vs. 1.71 logTCID$_{50}$/ml, n=10) and 14 (2.47 logTCID$_{50}$/ml, n=8 vs. 1.51 logTCID$_{50}$/ml, n=5) d.p.i.

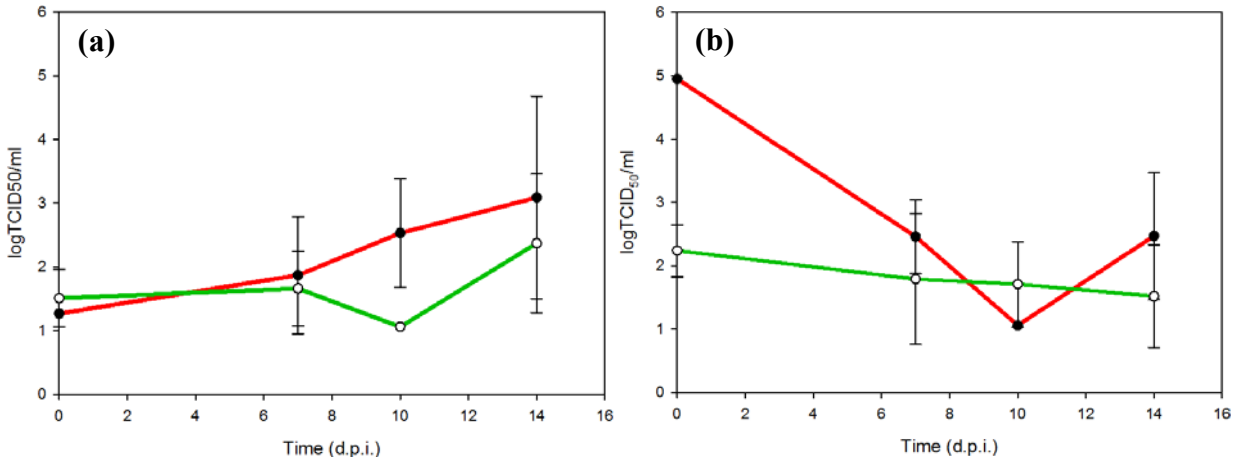

Figure 4.14 Average titers of whole mosquitoes infected by YFV wildtype controls and E G52R-T173I mutants

(a) Average body titers of the Asibi strain (red) and the Asibi E G52R-T173I mutant (green) (b) Average body titers of the 17D+Asibi M-E chimera (red) and the 17D+Asibi M-E E G52R-T173I mutant (green)

The comparison in the body titers did not identify any significant difference in the average body titers between the Asibi strain and the Asibi E G52R-T173I mutant or between the 17D+Asibi M-E chimera and the 17D+Asibi M-E E G52R-T173I mutant (p>0.05) as summarized in **Figure 4.15**. The average body titers of *Ae. aegypti* infected by the Asibi E G52R-T173I mutant were similar to those infected by the Asibi strain at 7 (2.91 logTCID$_{50}$/ml, n=12 vs. 2.03 logTCID$_{50}$/ml, n=14), 10 (2.31 logTCID$_{50}$/ml, n=11 vs. 1.56 logTCID$_{50}$/ml, n=4) and 14 (1.70 logTCID$_{50}$/ml, n=16 vs. 1.83 logTCID$_{50}$/ml, n=5) d.p.i. The comparable average body titers were also observed between the 17D+Asibi M-E chimera and the 17D+Asibi M-E E G52R-T173I mutant at 7 (3.24 logTCID$_{50}$/ml, n=10 vs. 1.49 logTCID$_{50}$/ml, n=7) , 10 (2.48 logTCID$_{50}$/ml, n=4 vs. 1.43 logTCID$_{50}$/ml, n=10) and 14 (2.28 logTCID$_{50}$/ml, n=11 vs. 2.12 logTCID$_{50}$/ml, n=4) d.p.i.

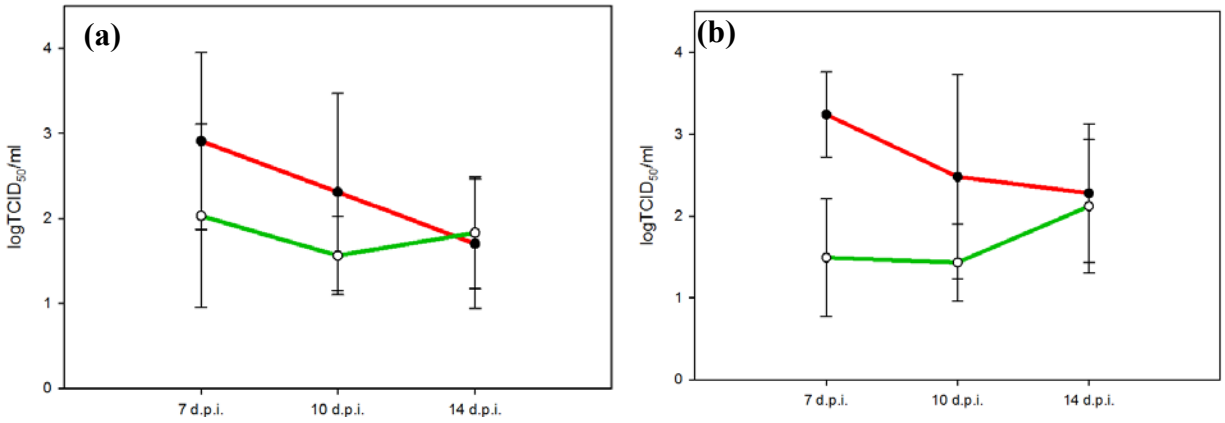

Figure 4.15 Average body titers of *Ae. aegypti* infected by YFV wildtype controls and E G52R-T173I mutants

(a) Average body titers of the Asibi strain (red) and the Asibi E G52R-T173I mutant (green) (b) Average body titers of the 17D+Asibi M-E chimera (red) and the 17D+Asibi M-E E G52R-T173I mutant (green)

Among the disseminated form of infection, the average titers of the secondary tissues did not show any significant difference between the Asibi strain and the Asibi E G52R-T173I mutant or between the 17D+Asibi M-E chimera and the 17D+Asibi M-E G52R-T173I mutant (p>0.05). The results are shown in **Figure 4.16**. The average titers of the secondary tissues infected by the Asibi E G52R-T173I mutant were similar to those infected by the Asibi strain at 7 (1.75 logTCID$_{50}$/ml, n=15 vs. 2.19 logTCID$_{50}$/ml, n=11), 10 (2.19 logTCID$_{50}$/ml, n=10 vs. 1.36 logTCID$_{50}$/ml, n=6) and 14 (2.69 logTCID$_{50}$/ml, n=14 vs. 2.95 logTCID$_{50}$/ml, n=1) d.p.i. The

dissemination of the 17D+Asibi M-E E G52R-T173I mutant resulted in the comparable average titers in the secondary tissues as the 17D+Asibi M-E chimera at 7 (1.60 $logTCID_{50}$/ml, *n*=6 vs. 2.37 $logTCID_{50}$/ml, *n*=8), 10 (2.95 $logTCID_{50}$/ml, *n*=1 vs. 1.49, *n*=13 $logTCID_{50}$/ml) and 14 (2.33 $logTCID_{50}$/ml, *n*=6 vs. 2.52 $logTCID_{50}$/ml, *n*=1) d.p.i.

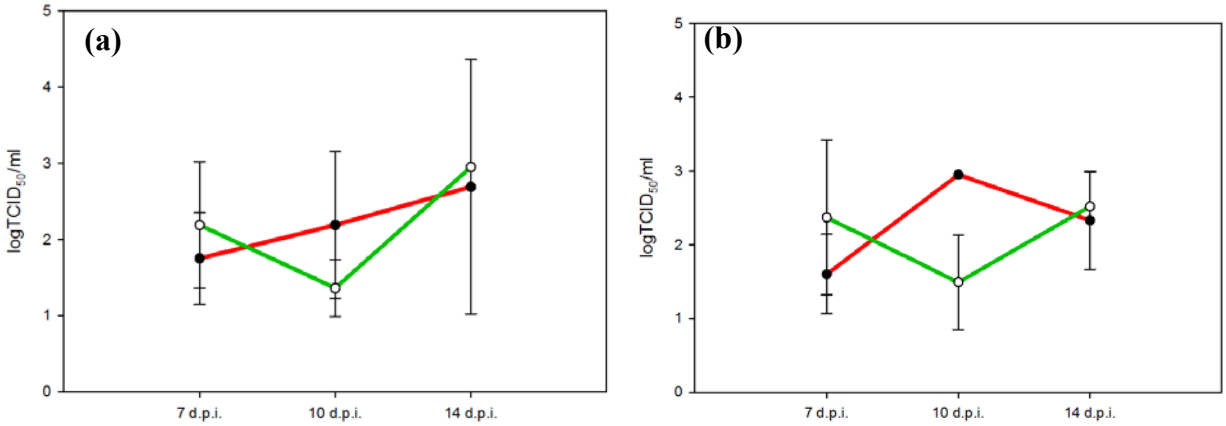

Figure 4.16 Average secondary tissue titers of *Ae. aegypti* infected by YFV wildtype controls and E G52R-T173I mutants

(a) Average body titers of the Asibi strain (red) and the Asibi E G52R-T173I mutant (green) (b) Average body titers of the 17D+Asibi M-E chimera (red) and the 17D+Asibi M-E E G52-T173I mutant (green)

In conclusion, the YFV E G52R-T173I double mutants did not show reduced replication in comparison to the YFV wildtype controls. Although the infection rates of the YFV E G52R-T173I mutants showed the consistently lower infection rate at 14 d.p.i., there was no demonstrable difference in the average titers of homogenized whole mosquitoes, bodies and secondary tissues between the YFV wildtype controls and the E G52R-T173I mutants.

4.3 Conclusions

A. Attenuation caused by the G52R single mutation and the G52R-T173I double mutations

Our results demonstrated that the single G52R mutation in YFV E protein was sufficient to cause a significant reduction in the infection rate, especially between 7 and 10 d.p.i. The Asibi E G52R mutant was associated with consistently lower infection rates at 7 and 10 d.p.i. Although there was no demonstrable difference at 14 d.p.i., a low infection rate of the Asibi E G52R mutant was consistently observed. The exposure of the 17D+Asibi M-E E G52R mutant resulted

in a significantly lower infection rate at 7 d.p.i. At 10 and 14 d.p.i., the infection rate remained lower but did not show any statistical significance in *Ae. aegypti* challenged by the 17D+Asibi M-E E G52R mutant. The dissemination of the Asibi E G52R mutant at 7 and 14 d.p.i. and the 17D+Asibi M-E G52R mutant at 7 d.p.i. suggested that the single YFV 17D G52R mutation when introduced into YFV Asisbi was unable to achieve the complete blockade of viral dissemination. The attenuation caused by the 17D G52R mutation in the E protein correspondingly caused a substantial reduction of the viral infectivity when cloned into the wildtype Asibi control. Therefore, the G52R mutation should be considered as a potential target to incorporate when designing biologically non-transmissible live-attenuated flavivirus vaccine candidates.

The single T173I mutation in the E protein did not lead to significant attenuation of the Asibi strain and the 17D+Asibi M-E chimera. The infection rate between the Asibi strain and the Asibi E T173I mutant or between the 17D+Asibi M-E chimera and the 17D+Asibi M-E E T173I mutant remained comparable at 7, 10 and 14 d.p.i. The dissemination of the YFV E T173I mutants also support the minor effect contributed by the T173I mutation in the E protein.

The infection with the YFV Asibi E 17D G52R-T173I mutant resulted in the similar attenuated phenotype associated with the single G52R mutation. The E G52R-T173I double mutants did not lead to the more attenuated phenotype by causing the consistently lower infection rate than wildtype controls. The infection rate of the YFV E G52-T173I mutants remained significantly lower for at least two of the three time points of collection. The infection rate of the Asibi E G52R-T173I mutant at 10 and 14 d.p.i. and the 17D+Asibi M-E E T173I mutant at 7 and 14 d.p.i was significantly lower than the wildtype controls. The non-dissemination phenotype was also not achieved by the simultaneous presence of the G52R and T173I mutations.

In summary, the YFV E G52R mutants and the YFV E G52R-T173I double mutants showed an attenuated phenotype with respect to significantly lower infection rates of mosquitoes. However, the mutations were unable to cause the non-disseminating phenotype of the YFV 17D strains. The results are consistent with the observation described by McElroy *et al*. (2006) that the genetic determinants for the viral infectivity of YFV in *Ae. aegypti* are likely to exist in EDI and EDII (McElroy, Tsetsarkin et al. 2006). The single and double mutants

characterized in the study also reproduced the disseminating phenotype that was observed in the Asibi+17D EDI-EDII chimera.

B. Viral titers of homogenized mosquito tissues

In spite of the significant loss of the infectivity in the YFV E G52R mutants and the YFV E G52R-T173I double mutants, the comparison of the average titers did not show any significant reduction between the wildtype controls and the mutants. The results are similar to the earlier observation that the Asibi strain and the Asibi+17D EDI-EDII chimera did not show any significant difference in the average titers of homogenized whole mosquitoes (McElroy, Tsetsarkin et al. 2006).

4.4 Discussion and future directions

To the best of our knowledge, the characterization of the YFV E G52R mutants is the first report that the single point mutation located in the molecular hinge region of the structure gene is sufficient to cause a significant viral attenuation of arboviruses in orally infected mosquito vectors. The presence of the T173I mutation caused a minor but non-statistically significant decrease in the infection rate. There was no additive effect by the simultaneous presence of the G52R and T173I mutations in the E protein of the Asibi strain. Therefore, it is likely the G52R mutation contributes to the attenuation independently. The observation does not exclude the possibility that three other additional mutations, A56V, A170V and K200T, in EDI and EDII of YFV can also result in significant attenuation.

The capacity of efficient viral dissemination that is characteristic of YFV Asibi was not impaired due to the introduction of the single YFV 17D G52R mutation. The disseminated form of infection was observed in *Ae. aegypti* infected by the Asibi E G52R mutants at 7 and 14 d.p.i. Although there was no disseminated form of infection observed in *Ae. aegypti* infected by the 17D+Asibi M-E E G52R mutant at 10 and 14 d.p.i., it is likely to be the consequence of the further attenuated phenotype when the G52R mutation in the E protein is coupled with known attenuation determinants in the nonstructural proteins. The mutations in the NS2A and NS4B genes of YFV 17D strains have been described to contribute to the significant reduction of dissemination in comparison to the highly disseminating phenotype of the Asibi strain (McElroy, Tsetsarkin et al. 2006). The 17D+Asibi M-E E G52R mutant contains the I95M mutation in the YF 17D NS4A protein, which has been described as the attenuation determinant which

significantly impairs the viral dissemination by McElroy *et al* (McElroy, Tsetsarkin et al. 2006). Therefore, the lack of dissemination of the 17D+Asibi M-E E G52R mutant is likely to be the results of the combined effect of attenuation among the G52R mutation in the E protein and the other additional attenuation determinants in the nonstructural proteins.

The average titers of the whole-mosquitoes, bodies and secondary tissues infected by the YFV E G52R or the YFV E G52R-T173I mutant did not show a significant difference from those infected by the YFV wildtype controls. The result was similar to the observation made by McElroy *et al*. that the chimerization of the 17D EDI and EDII with the Asibi strain did not lead to the significant reduction of average titers of homogenized whole mosquitoes (McElroy, Tsetsarkin et al. 2006).

A. Attenuation of YFV and flaviviruses by the mutations in the molecular hinge region

Our results not only have identified at least one attenuation determinant in the region of YFV EDI and EDII but also confirmed that the introduction of point mutations in the molecular hinge region is a feasible approach to reduce the infectivity of mosquito-borne flaviviruses. As the only mutation which exists in the molecular hinge region between EDI and EDII of YFV 17D strains, the characterization of the G52R mutation was only able to lead to the conclusion that the mutations in the H1 peptide can be a potential target for mutagenesis in order to generate biologically nontransmissible live-attenuated vaccine candidates for mosquito-borne flaviviruses. The attenuation of flaviviruses due to the mutations in the molecular hinge region has also been described in the H2 peptide of DENV-2 E protein and the H4 peptide of MVEV (Hurrelbrink and McMinn 2001, Butrapet, Childers et al. 2011). More complete characterization can be achieved by orally administering the mutants described by Butrapet *et al*. and McMinn *et al*. to competent vector species, or selectively mutatating the corresponding residues in the E protein of the Asibi strain. Although it has been shown that the mutations in all four peptides of the molecular hinge region in DENV-2 E protein can be associated with the viral attenuation *in vitro* in the study published by Butrapet *et al*., the evaluation of the viral infectivity was only performed with the mutants derived from the mutations which substitute the Leu^{135} residue of the H2 peptide. The experimental approach of intrathoracic inoculation of mosquitoes in their study to assess the infection rate has been used to characterize a challenge method that promotes the infection and dissemination of flaviviruses in mosquitoes but is of course unnatural since it does not include

the important process of midgut infection. Therefore, the attenuation caused by the mutations evaluated in the study can potentially be underestimated by artificially forcing the establishment of infection among the attenuated mutant viruses. The *per os* challenge of DENV-2 mutants generated in the same study should be conducted to provide the information generated by the experimental approach which resembles the natural route of infection (McElroy, Tsetsarkin et al. 2006, Butrapet, Childers et al. 2011).

It is still unclear how the single G52R mutation was able to result in the significant viral attenuation. The G52R mutation is structurally isolated from the known receptor-binding region of the flavivirus E protein as shown in **Figure 4.1**. The plausible mechanism for the viral attenuation may be the impairment of the viral membrane fusion process (Chen, Maguire et al. 1997, Modis, Ogata et al. 2004). The earlier experimental evidence derived from the analysis of virus-mediated fusion in C6/36 cells suggested that the mutations in the molecular hinge regions of flavivirus E proteins may result in the change of the optimal pH required for the fusogenic activity (Lee, Weir et al. 1997, Butrapet, Childers et al. 2011). Such observations are consistent with the knowledge derived from the comparison of the crystal structures of pre- and post-fusion flavivirus E proteins, which require the molecular hinge region to accommodate the structure rearrangement between EDI and EDII during the viral membrane fusion (Modis, Ogata et al. 2003). The process of the viral membrane fusion is driven by the energy generated during the acidification of the endosomes. Although, the assay provides the functional characterization on the fusogenic capacity, the biochemical nature of the membrane fusion process renders the assay on the virus-mediated cell fusion in insects highly specific to the osmotic pressures of culture media in the experimental system (Higgs and Gould 1991). The fusion process can also be spontaneously initiated due to the confluence in some insect cell culture (Maramorosch and McIntosh 1994). Therefore, the development of a more standardized method to analyze the fusogenic activity of arboviruses in insect culture or cell-free system is needed in order to fully characterize the phenotypic changes associated with the mutations in the molecular hinge region at the cellular level. It is less likely to adopt the full-length DENV-2 E protein and liposome platform described by Modis *et al.* although the study successfully reproduced the dimer-to-trimer conformational change. The observation of the process requires electron microscopy studies which requires specific techniques and knowledge for operation (Modis, Ogata et al. 2004).(Modis et al., 2004) The use of the DENV replicon system described by Ansarah-Sobrino

et al. may be a feasible approach since the platform has been successfully coupled with the reporter gene. The amino acid substitutions in the molecular hinge region can be introduced and the quantification of viral entry by the expression of the reporter genes in the cellular compartment should provide the quantitative analysis to mechanistically characterize the viral attenuation at the molecular level.(Ansarah-Sobrinho, Nelson, Jost, Whitehead, & Pierson, 2008)

B. Characterization of the T173I mutations

The characterization of the YFV E T173I mutants in *Ae. aegypti* showed that there was no demonstrable difference in the infection and dissemination from the wildtype controls. Although the insignificant reduction in the infection rate occurred, the conclusion of the statistical analysis suggest the significant attenuation did not occur.

The plaque purification of the 17D-204 substrain suggested the presence of the viral population 17D(+wt) which contains the reversion from the isoleucine to threonine in the E protein and exists at the minor quantity in the viral population of the vaccine pool.(E A Gould et al., 1989) The comparison of the neurovirulence between the 17D(+wt) and (17D(-wt) suggested that the I173T reversion can be a neurovirulence determinant in mice.(K D Ryman et al., 1997a) It is still unknown if the single YFV Asibi I173T reversion introduced into YFV 17D would increase the viral infection and dissemination in *Ae. aegypti*. The better understanding can be gained by characterize the 17D(+wt) variant or the YFV E I173T mutants by the *per os* infection of *Ae. aegypti*.

It was also reported that the acquisition of the wildtype epitope in the 17D(+wt) variant is also associated with the change of the antigenic structure by the A240V mutation in the E protein.(E A Gould et al., 1989; K D Ryman et al., 1998) Therefore, in addition to the assessment in the phenotype of the naturally occurring 17D(+wt) variant in *Ae. aegypti*, the complete understanding will be achieved by characterizing the additional A240V mutation, which has previously been shown as a known cause of the attenuation in mice.(K D Ryman et al., 1998) The result is expected to provide the knowledge for the unlikely, but worst case scenario, that whether the simultaneous presence of the I173T reversion and the A240V mutations will maintain the attenuated phenotype when the I173T reversion becomes the major genetic component in the 17D strains.

The importance of characterizing the phenotypes of viruses associated with the mutations in the G_0H_0 loop of EDI, where the T173I mutation is located, can also further contribute to the evaluation of the safety of utilizing the type-specific anti-flavivirus mAb as potential therapies or the rationale-based design of the vaccine candidates eliciting the antibody responses targeting the G_0H_0 loop.(Cockburn et al., 2012) Similar to the B-cell epitope present in the G_0H_0 region of YFV E protein, two potent primate anti-DENV type-specific mAb that are the chimpanzee anti-DENV-4 5H2 and the human anti-DENV-1 4F1 both recognize the G_0H_0 region of the EDI as part of the epitope based on the inter-domain quaternary structures.(Fibriansah et al., 2014; C.-J. Lai et al., 2007) The characterization of the neutralization escape mutants of the 5H2 mAb suggested that potential mutations can potentially accumulate in the G_0H_0 region. It is still unknown if the selective pressure created by the application of antibodies targeting the G_0H_0 loop of EDI will result in the change of phenotypes of flaviviruses in vector mosquitoes.

C. Locations of YFV 17D mutations in EDI and EDII

The observation is consistent with the currently available structures of flavivirus E proteins. Based on the available knowledge in the structures of flavivirus E proteins, it is likely that the two point mutations located in the two distinct regions of YFV E protein as shown **Figure 4.1 and 4.2**. Therefore, the interactions between the two point mutations are likely to be limited and the G52R-T173I double mutants were not able to substantiate the attenuation caused by the G52R single mutation.

The results suggested that the more significant role of the G52R mutation in molecular hinge region of YFV E protein for the viral attenuation, can potentially provide critical information for future characterization on other mutations in the YFV E protein. As shown in the available crystal structure of the structurally similar DENV-2 E protein, the K200T mutation is located in the close proximity of the molecular hinge region at the interface between EDI and EDII as shown in **Figure 4.17**.

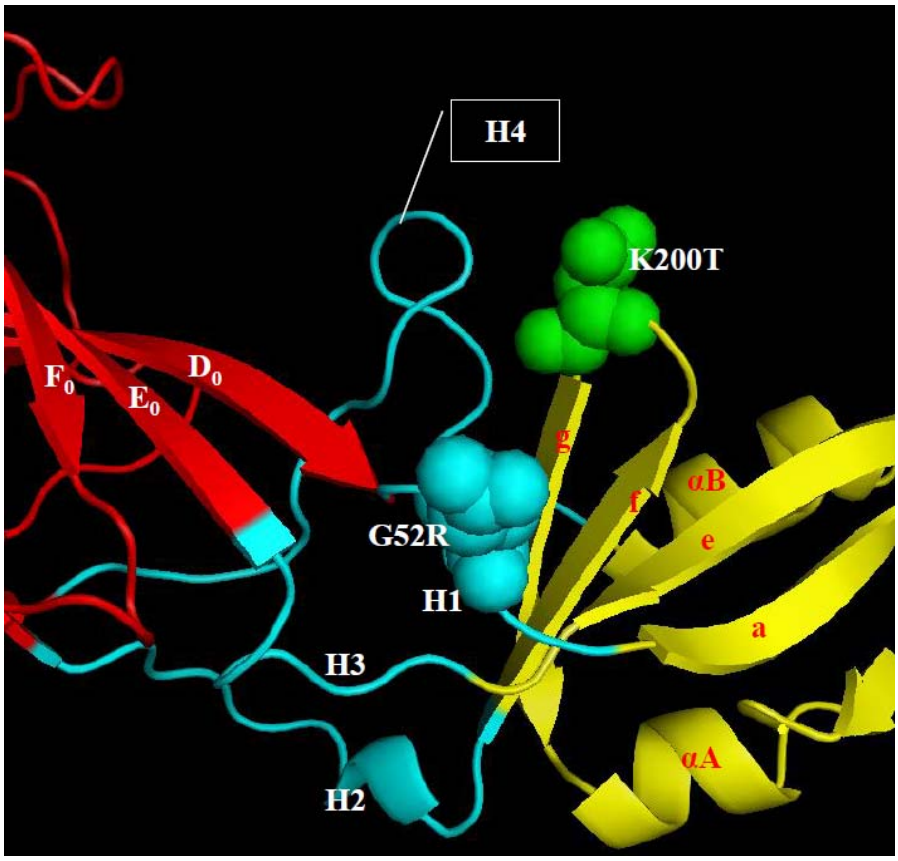

Figure 4.17 Relative locations of the molecular hinge region and the YFV 17D K200T mutation in the corresponding region of structurally similar DENV-2 E protein (PID ID: 1TG8)

EDI and EDII are labeled in red and yellow, respectively. The four peptides (H1-H4) are color in cyan and the G52R mutation is displayed in spheres. The K200T mutation is displayed in spheres and colored in green.

It is still unclear whether or not the K200T mutation in YFV E protein contributes to any attenuation in vertebrate hosts and vector mosquitoes. The K200T mutation is part of the fg loop region between the f and g β-strands of EDII. Structurally, the fg loop of EDII among mosquito-borne flaviviruses is consistently shorter than the corresponding region of the tick-borne flavivirus E proteins due to the presence of additional six amino acids in the carboxy terminus.(Rey et al., 1995) The region is in the neighboring region of the H4 peptide of the molecular hinge region, which consists of the k and l β-strand of EDII. The k and l β-strand forms the hairpin structure which are stabilized by hydrophobic interactions among amino acids in the pre-fusion and dissociated in the post-fusion conformation as shown in **Figure 4.6**.(Modis

et al., 2004) The characterization of the YFV E K200T mutant and the YFV E G52R-K200T double mutant might be able to provide a more comprehensive understanding in not only the attenuation caused by mutations in the molecular hinge and its neighboring region but also the potential difference in the structures and functions of the mosquito-borne and tick-borne flavivirus E proteins.

In summary, the YFV E G52R mutants have been determined as an attenuation determinant for infection in mosquitoes whilst the T173I mutation did not contribute to the significant attenuation. The knowledge derived from the YFV mutants and other attenuated phenotypes associated with the mutations in the molecular hinge region of the E proteins highlights the possibility that the attenuation in both the vertebrate hosts and the arthropod vectors. The understanding of the mechanisms for viral attenuation can provide the critical knowledge for the design of the biologically non-transmissible live-attenuated flavivirus vaccines.

Chapter 5 - Characterization of the M299I Mutation in the EDI-EDIII Linker

5.1 Introduction

The importance of mutations in EDIII of the YFV 17D strains has been demonstrated by the significantly lower infection and dissemination rate among *Ae. aegypti* when orally challenged by the Asibi+17D EDIII chimera. In the ectodomain of EDIII, there are five amino acid mutations identified between the Asibi strain and the 17D-204 substrain as summarized in **Table 5.1** (Hahn, Dalrymple et al. 1987). The comparison between the 17D-204 substrain and the 17DD substrain demonstrated that the P325S mutation is only present in the E protein of the 17D-204 substrain (dos Santos, Post et al. 1995). Therefore, the potential attenuation determinants that resulted in the attenuated phenotype of YFV 17D strains are likely to exist in the other four amino acid mutations.

Mutation (Asibi/17D)	Location
M299I	EDI-EDIII linker
S305F	A β-strand
P325S*	BC loop
K331R	C_x β-strand
T380R	FG loop of EDIII

Table 5.1 Amino acid mutations in EDIII between the YFV Asibi strain and 17D strains
*** indicates the P325S as the 17D-204 substrain-specific mutation.**

The characterization of the T380R mutation has been performed and described in **Capter 3** indicating that the T380R mutation probably promotes the propagation of the virus *in vitro,* and has a limited contribution to the attenuated phenotype in *Ae*. *aegypti* (Huang, Nuckols et al. 2014). The K331R mutation is likely to be tolerated by YFV due to the minor biological change associated with what is regarded as a relatively conservative amino acid substitution. The conserved presence of the K331R in the two hamster-passage variants of the YFV Asibi strain that caused distinct pathological characteristics in the livers of intraperitoneally challenged hamsters, suggested that the mutation is less likely to result in the significant phenotypic change (McArthur, Xiao et al. 2005). The characterization of the M299I mutation was performed and described in this chapter based on its critical location in the linker region at the interface of EDI

and EDIII, and the conserved sequences of the corresponding region in the E proteins of the flaviviruses.

A. Conserved sequences and biochemical properties of EDI-EDIII linker region

The M299I mutation is located in the carboxy-terminus of the EDI-EDIII linker region of YFV 17D E protein. The EDI-EDIII linker region in flavivirus E proteins is a polypeptide which consists of 12 amino acid residues between the I_0 β-strand of EDI and the N-terminal loop of EDIII. An alignment of the sequences shows that the conserved sequences or biochemically similar amino acids are present in either the pan-flavivirus manner or the serocomplex-specific manner as shown in **Table 5.2**. The region consists of at least four highly hydrophobic leucine or methionine amino acids with other additional residues conserved among flaviviruses or within specific serocomplexes.

Serocomplex	Virus	strain	Sequence of EDI-EDIII linker region (290-300)
YFV	YFV	Asibi	LTLKGTSYKMC
	YFV	17D	LTLKGTSYKIC
	ENTV	UgIL-30	LTLKGKTYAMC
	SEPV	MK7148	LTLKGSTYPMC
	YOKV	Oita36	LTMKGSTYTMC
DENV	DENV-1	Hawaii	LTLKGMSYVMC
	DENV-2	New Guinea C	LQLKGMSYSMC
	DENV-3	H87	LKLKGMSYAMC
	DENV-4	H241	LRIKGMSYTMC
JEV	JEV	SA_{14}	LALKGTTYGMC
	JEV	SA_{14}-14-2	LALKGTTYGMC
	WNV	NY99	LQLKGTTYGVC
	KNV	MRM61C	LQLKGTTYGVC
	SLEV	MS1-7	VKIKGTTYGMC
	MVEV	MVE1-151	LKLKGTTYGMC
TBEV	TBEV	Neudoerfl	LKMKGLTYTMC
	OHFV	Bogluvovska	LKMKGLTYTMC

Table 5.2 Sequences of the EDI-EDIII linker region in the flavivirus E proteins

There are at least five amino acids, Met^{299}, Lys^{293}, Gly^{294}, Tyr^{297} and Cys^{300}, which are conserved among flaviviruses, or only allow minor variation. The Ile^{299} residue in the EDI-EDIII linker region of YFV 17D strains, which was characterized in our study, is unique. Other flaviviruses, largely use the Met^{299} residue with the exception of a V^{299} residue in the E proteins of WNV and KUNV. The other four amino acid residues that are universally conserved across all the known flaviviruses are Lys^{293}, Gly^{294}, Tyr^{297}, and Cys^{300}.

Although the corresponding positions in all other flaviviruses at the Leu^{290}, Leu^{292} and Ser^{296} residues of YFV E protein vary, the biochemical properties of these positions are generally conserved by conservative amino acid substitutions. The Leu^{290} residue is conserved across flaviviruses except that the biochemically conserved valine was observed in the corresponding position by SLEV. The hydrophobic nature of the Leu^{292} residue in YFV E protein is universally conserved in the mosquito-borne flaviviruses and is biochemically similar to the methionine residue in the corresponding region of the TBEV-serocomplex flaviviruses. The Ser^{296} is shared by YFV and all four serotypes of DENV and shows the conservative biochemical property associated with the presence of threonine in other flaviviruses in the corresponding positions. The Thr^{295} residue in the YFV E protein is conserved in the serocomplex-specific manner. YFV and the members of the JEV serocomplex show the consensus use of threonine. The DENV-serocomplex and TBEV-serocomplex flaviviruses utilize the hydrophobic methionine and leucine, respectively.

In addition to the pan-flavivirus and serocomplex-specific conserved residues described above, the residue 291 in the EDI-EDIII linker region allows for variation of sequences among different flaviviruses. The neutral polar Thr^{291} residue is specific to YFV-serocomplex and DENV-1 and shows the highest diversity in sequences and biochemical properties. The neutral polar glutamine residue is present in the corresponding position of DENV-2, WNV, and KUNV. The positively charged lysine and arginine residues, which contain polar sidechains, are shared in the corresponding region of DENV-3, DENV-4, SLEV, MVEV and the tick-borne

á □ Í □ á □ · □

r alanine residue in contrast to the other flaviviruses, which use largely polar residues.

There has been no known function assigned to the YFV EDI-EDIII linker region. The EDI-EDIII linker region of flavivirus E proteins initially has been proposed as a potential binding site for GAG molecules in DENV-2 due to the high density of positively charged lysine

and arginine (Chen, Maguire et al. 1997). The evaluation of the GAG-binding capacity was further investigated using recombinant EDIII of DENV-2 and it was reported to act as a viral entry mechanism into mammalian cells (Watterson, Kobe et al. 2012). Furthermore, the residues responsible for the GAG binding in the EDI-EDIII linker region have recently been identified observing that removal of the positively charged residues abolished viral entry of DENV-2 mutants (Roehrig, Butrapet et al. 2013). With the availability of flavivirus EDIIIs NMR structures, it was clearly demonstrated that the two proposed and characterized GAG-binding motifs, (i.e. the EDI-EDIII linker region and the FG loop of EDIII), are located in the same region of EDIII (Huang, Lee et al. 2008, Volk, May et al. 2009). **(Figure 5.1)**

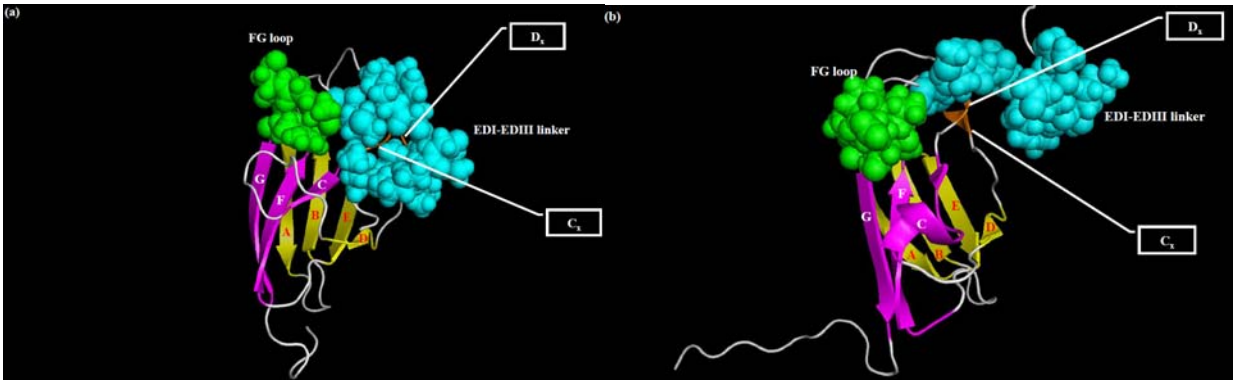

Figure 5.1 Locations of the two GAG-binding, the EDI-EDIII linker region and the FG loop, motifs in YFV EDIII and DENV-2 EDIII (PDB ID: 2JQM; 2JSF)

(a) YFV EDIII is labeled based on the secondary structure. The EDI-EDIII linker and the FG loop are shown in spheres and labeled in cyan and green, respectively. The ABDE β-sheet is labeled in yellow. The CxDx β-sheet is labeled in orange. The CFG β-sheet is labeled in magenta. (b) DENV-2 EDIII is labeled based on the secondary structure. The EDI-EDIII linker and the FG loop are shown in spheres and labeled in cyan and green, respectively. The ABDE β-sheet is labeled in yellow. The CxDx β-sheet is labeled in orange. The CFG β-sheet is labeled in magenta.

The crystal structures of the pre- and post-fusion DENV-2 E protein soluble monomer suggests that the structure of EDI-EDIII is critical for the displacement of the EDIII, which results in the stabilized structure with a lower free energy state in the fused viral and cell lipid bilayers (Harrison 2008). The pre-fusion conformation of DENV-2 E protein contains the disordered linear structure in the EDI-EDIII linker region. The displacement of the EDIII is achieved by the refolding of the EDIII with respect to EDI which leads to the elongated structure

of the EDI-EDIII linker region. Therefore, the EDI-EDIII linker region has long been hypothesized to be the critical region for the viral membrane fusion (Modis, Ogata et al. 2004). The pre-fusion and post-fusion structure of the EDI-EDIII linker region is displayed in DENV-2 E protein and shown in **Figure 5.2**. Similar sequences and structures have also been reported to exist in the other two class II fusion proteins; namely the E1 protein of alphaviruses and the E2 protein of hepatitis C virus (HCV) (Albecka, Montserret et al. 2011, Zheng, Sanchez-San Martin et al. 2011). The details of the conformational change that occurs during viral membrane fusion has been discussed in **section 4.1.B**. The structure of the similar linker region in the available crystal structures of alphavirus E1 protein will be discussed in **section 5.1.B**.

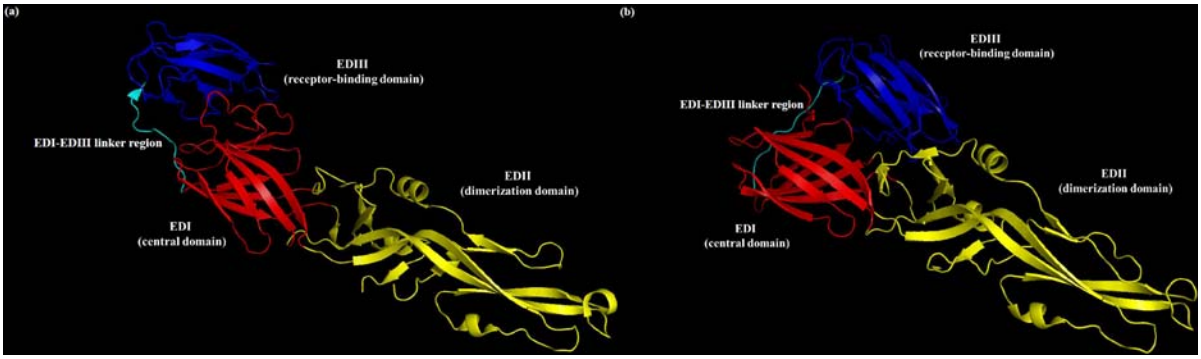

Figure 5.2 EDI-EDIII linker region in the pre-fusion (a) and post-fusion (b) conformation of DENV-2 E protein. (PDB ID: 1OAN; 1OK8)

The three distinct domains of DENV-2 E protein are labeled in red (EDI), yellow (EDII) and blue (EDIII). The EDI-EDIII linker region is highlighted in cyan.

In contrast to the proposed importance based on the currently available crystal structures of flavivirus E protein, the characterization of the EDI-EDIII linker region in DENV-2 suggested that the mutations in such regions did not show the anticipated impairment of viral entry but rather led to a defective phenotype in for virion assembly (de Wispelaere and Yang 2012). The details of the virion particle assembly and the structural change of the E protein during the maturation of virions will be reviewed in **section 5.1.C**. The phenotypic changes associated with the mutations in the DENV-2 EDI-EDIII linker region will be discussed in **section 5.1.D**.

B. The linker region in alphavirus E1 protein

Although the surface of alphavirus (Togaviridae) virions are coated with the trimeric units composed of the E1, E2 and E3 proteins, they utilize similar entry mechanisms to those of flaviviruses that have E proteins (Mancini, Clarke et al. 2000, Kielian 2006, Zhang, Hryc et al.

2011). For alphaviruses, the key initiation step for viral entry requires the binding of cellular receptors mediated by the E2 protein. The E1 protein of alphaviruses mediates the membrane fusion and is categorized under the class II fusion proteins. Both the alphavirus E1 proteins and the flavivirus E proteins undergo an extended intermediate structure in order to insert the fusion peptides into the host membranes. The acidification in the endosomes provides the energy that leads to the extended structure of the trimers of E1 protein, and the subsequent insertion of the fusion peptides into the host cell membrane (Fuller, Berriman et al. 1995, Harrison 2008). By encoding the receptor-binding domain separately in the E2 gene, the E1 protein of alphaviruses functionally resembles the flavivirus EDII because of the presence of the hydrophobic region in the domain II of the E1 proteins (Smith, Cheng et al. 1995, Lescar, Roussel et al. 2001). The domain I and domain III of the E1 proteins are responsible for the central restructure and the tethering of the entire E1 protein to the viral membrane through the transmembrane domain, respectively (Lescar, Roussel et al. 2001). At the interface between the structurally central DI and the transmembrane DIII, the DI-DIII linker region was found to tolerate the displacement of DIII in the membrane fusion process and resembles the structure and function of the flavivirus EDI-EDIII linker region (Zheng, Sanchez-San Martin et al. 2011).

Using the pre-fusion soluble monomer of the SFV E1 protein and the post-fusion homotrimer of the SFV E1 protein as a model, the relatively movement of DII and the displacement of DIII were described. The different conformations of the DI-DIII linker region are highlighted in **Figure 5.3**. At physiological pH, the three copies of the E1 monomer form the trimeric structure in each spike on the surface of the virion and share the more extended conformation displayed in **Figure 5.3(a)** (Lescar, Roussel et al. 2001, Gibbons, Vaney et al. 2004). The DI-DIII exists as the disordered structure between the I_0 β-strand of EDI and the A β-strand of EDIII (Gibbons, Vaney et al. 2004). The movement of DIII relative to the location of DI is the most significant overall change of the architecture of E1 in the post-fusion conformation. After the insertion of the fusion loop into the host membrane, the extended intermediate structure of EDI is pulled down due to the stacking of the α-helical structure. Similar to the displacement of the flavivirus EDIII relative to EDI, the DIII of alphavirus E1 protein approaches the tip of DII by 37Å and creates the extended structure of the DI-DIII linker. In addition to the conserved mechanisms of structural displacement, the sequences of the DI-DIII linker region of E1 protein show a high degree of sequence homology among alphaviruses

similar to the sequence homology in the EDI-EDIII linker region observed among the flaviviruses.

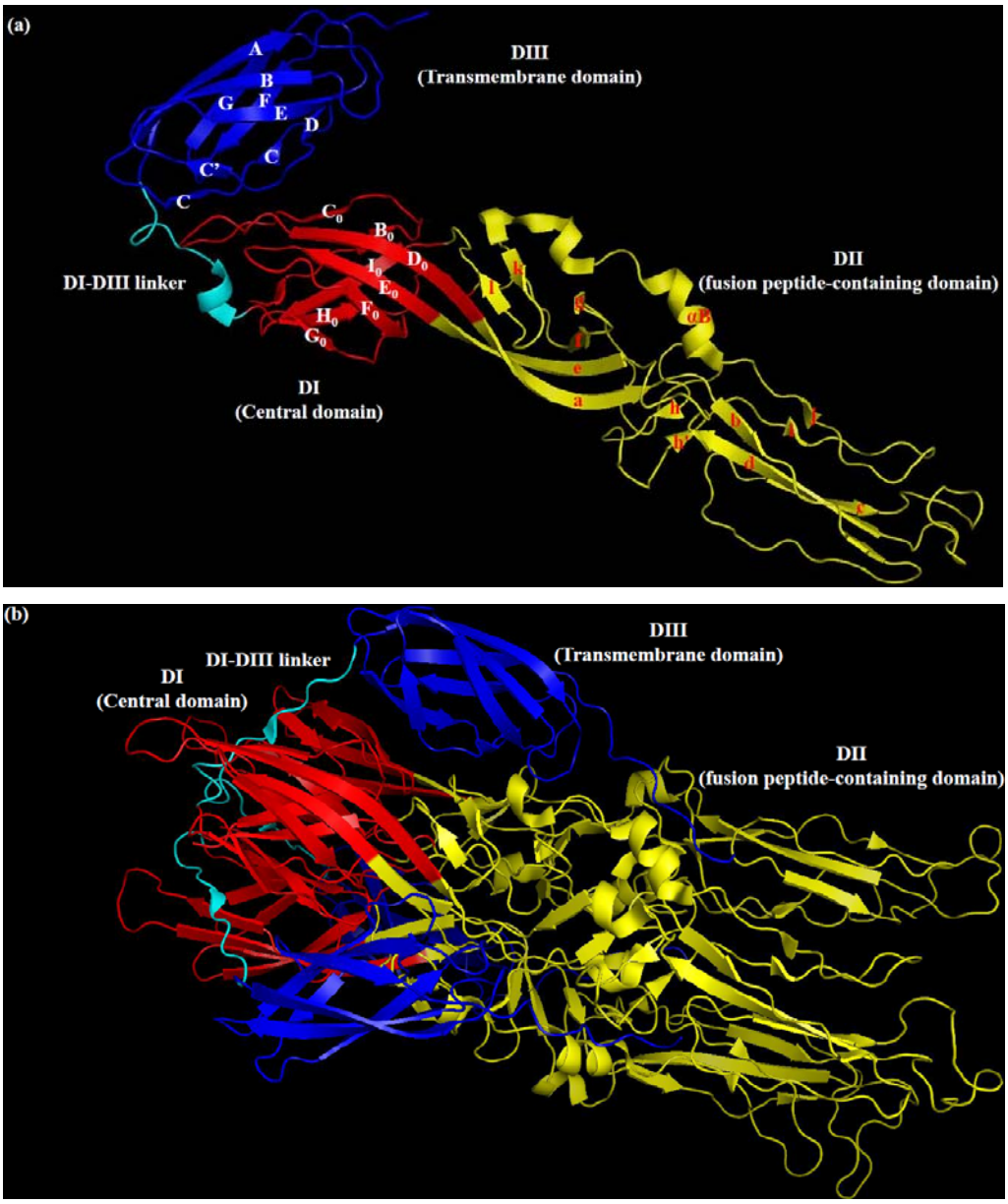

Figure 5.3 The relative locations of three distinct domains, DI, DII, and DIII of SFV E1 protein and the conformational change of the DI-DIII linker region during viral membrane fusion (PDB ID: 2ALA; 1RER)

(a) The pre-fusion conformation of the SFV E1 glycoprotein is displayed in the monomeric form. The DI, DII, and DIII are labeled in red, yellow and blue, respectively. The disorder structure of DI-DIII linker region at the pre-fusion stage is highlighted in cyan. (b) The post-fusion conformation of SFV E1 glycoprotein is displayed in the homotrimeric form.

The DI, DII, and DIII are labeled, in red, yellow and blue, respectively. The DI-DIII linker region is elongated due to the displacement of DIII and highlighted in cyan.

In contrast to the frequent use of the hydrophobic leucine and methionine by the EDI-EDIII linker region of flaviviruses, the hydrophobic nature of DI-DIII reflects the frequent presence of alanine and valine, which have small hydrophobic sidechains, and also phenylalanine which contains a sidechain with an aromatic ring structure. Based on the numbering of SFV E1 protein, the considered sequences of alphavirus D1-DIII linker region are summarized on **Table 5.3**.

Serocomplex	Clade	Virus	Sequence of EDI DI-DIII linker (283-294)
SFV	Old world	SFV	PDSAFTRIVEAP
		RRV	PDSAFTRVVDAP
		CHIKV	PEAAFTRVVDAP
		ONNV	PDAAFTRVTDAP
	New world	MAYV	ADSAFTRLTDAP
BFV	Old world	BFV	PDSAFTRVVDAP
WEEV	Old world	SINV	PNAAFIRTSDAP
	New world	WEEV	PDAAFVRSSESP
EEEV	New world	EEEV	PDAAFTRISETP
VEEV	New world	VEEV	PDALFTRVSETP
WEEV-like	Old world	ELV	PDASFTRSFDAP

Table 5.3 Sequences of the EDI-EDIII linker region in the alphavirus E1 proteins

The hydrophobic amino acids Ala[286] and Phe[287] are highly conserved in various serocomplexes under the *Alphavirus* genus, with the exception of VEEV and the mosquito-only Eilat virus (ELV). VEEV and ELV utilize leucine and serine at the corresponding region of Ala[286]. The hydrophobic Ile[290] in the SFV E1 protein is conserved by the presence of hydrophobic valine or leucine in SFV and BFV serocomplex members in the old world clade, and isoleucine or valine in EEEV and VEEV serocomplex in the new world clade. The neighboring Val[291] residue allows the variation of the sequence due to the presence of threonine in ONNV and MAYV and serine in WEEV, EEEV and VEEV. However, the hydrophobic nature is still maintained by the conserved valine in the corresponding region of RRV, CHIKV and BFV, and phenylalanine in the corresponding region of ELV. Notable, the new world

WEEV complex members, and SINV from the old world clade do not contain amino acids that share the comparable hydrophobicity in the same region of DI-DIII linker as other alphaviruses. Finally, the Ala^{293} is largely conserved among alphaviruses except for the new world WEEV, EEEV and VEEV.

Similar to the positively charged basic nature of Lys^{293} in the flavivirus EDI-EDIII linker, the Arg^{289} residue is conserved in all known alphaviruses. The consistent presence of charged amino acids is also observed in the corresponding positions of Asp^{284} and Glu^{292}. The Asp^{284} is largely conserved in all known alphaviruses except for CHIKV which contains the biochemically conserved glutamate, and SINV which uses asparagine in the corresponding region. The biochemical property of the Glu^{292} residue is conserved by the presence of aspartate or glutamate in the corresponding positions among all known flaviviruses. Both the amino- and carboxy termini of the DI-DIII linker contain the conserved proline residue except for the amino-terminus of MAYV in which the DI-DIII linker contains the hydrophobic alanine.

In summary, the flavivirus E protein EDI-EDIII linker region, and the alphavirus E1 protein DI-DIII linker region, both display high similarity in the structure of the polypeptide during the rearrangement of the overall architecture of the flavivirus E protein and the alphavirus E1 protein. The structures of both regions switch from the disordered conformation in the pre-fusion state to the elongated structures in the post-fusion conformation. The flavivirus EDI-EDIII linker region and the alphavirus DI-DIII linker region have been characterized using reverse genetics systems of DENV-2 and SFV, respectively. The details of the characterization will be discussed in **Section 5.1.C**.

C. Characterization of the linker regions in flavivirus E protein and alphavirus E1 protein

The characterization of the linker regions in flavivirus E protein and alphavirus E1 protein has been performed for DENV-2 and SFV, respectively (Zheng, Sanchez-San Martin et al. 2011, de Wispelaere and Yang 2012). Based on the sequence homologies and the conserved mechanisms for the structure rearrangement of both proteins during viral membrane fusion, it was first hypothesized that the mutations in the linker regions would likely impair viral entry (Gibbons, Vaney et al. 2004, Modis, Ogata et al. 2004).

In the study published by de Wispelaere *et al*., mutations in the EDI-EDIII linker region were introduced by alanine screening performed on the cDNA infectious clone and replicon of DENV-2 (de Wispelaere and Yang 2012). The mutants were designed to carry the alanine mutations at the corresponding position of $Gly^{294}$and Ser^{296} in the EDI-EDIII linker region of YFV, as well as the phenylalanine substitution at the corresponding position of Tyr^{297} in the EDI-EDIII linker region of YFV. Gly^{294} and Tyr^{297} represent the amino acids that are conserved in the pan-flavivirus manner; whereas, Ser^{296} is uniquely conserved between YFV and DENV. Regardless of the locations of the alanine or phenylalanine substitution, the mutants exhibited a similar phenotype *in vitro*. The importance of the conserved sequences of the EDI-EDIII linker region was supported by the lack of viable mutants being recovered after the electroporation of infectious viral RNA in Huh-7 cells. The presence of individual antigen positive cells was observed in all three mutants and suggested that the mutants were capable of replicating *in vitro* and may share the impairment of viral dissemination that requires the production of infectious progeny virions. The characterization of the mutations in the replicon system, coupled with the luciferase reporter gene, further excluded the possibility that the mutations in the EDI-EDIII linker region of DENV-2 may interfere with the viral entry mechanism, while the mutant replicons were infectious and able to enter the cells and produce the luminance *in vitro*. The characterization based on the separation of the intracellular membrane organelles derived from the electroporated Huh-7 cells suggested a dysfunctional assembly and secretion process that prevents production and release of progeny virions. The mutants showed a high degree of retention of E protein in the ER without advancement to the Golgi apparatus, which is required to accomplish the final steps of morphogenesis of infectious virion by removing the pr peptide from the prM protein. These observations emphasize the complexity in the roles of the flavivirus EDI-EDIII linker regions. In addition to the anticipated impairment of viral membrane fusion, the assembly and maturation of flaviviruses may also require a functional EDI-EDIII linker region. The flavivirus E proteins also undergo an extensive conformational change since the different cellular compartments in the exocytosis pathway exhibit different pH. The details of the mechanisms and conformations of flavivirus E proteins will be discussed in **Section 5.1.C**.

In contrast to the phenotypic change solely associated with viral assembly due to the mutations in the DENV-2 EDI-EDIII linker region, mutations in the DI-DIII linker region of SFV E1 protein have been reported to result in altered fusogenic capacity and the efficiency of

viral particle assembly (Zheng, Sanchez-San Martin et al. 2011). It was first demonstrated that mutations in the DI-DIII linker region of alphavirus E1 proteins exist as the compensatory mutations in the presence the mutations in the B_0 β-strand of DI. The post-fusion conformation of SFV E1 protein suggested that the interactions between the DI-DIII linker and the B_0 β-strand of DI are likely to exist in a network format among the Glu^2, His^3 and Tyr^{15} in the B_0 β-strand of DI and the Phe^{287} and Arg^{289} of the DI-DIII linker region. Similarly to the DENV-2 mutants reported by de Wispelaere *et al*., the SFV F287A mutant had significantly lower viral titers when compared with the wildtype parental virus and a correspondingly lower efficiency in viral particle assembly and secretion into the culture media (de Wispelaere and Yang 2012). The SFV R289A mutant showed an expected phenotype which had a lower optimal pH for fusion as reported for the DI-DIII linker of DI that undergoes the pH-dependent conformational change. The lower pH implicates the higher energy required for the mutant to accomplish the viral membrane fusion. Both the F287A and R289A SFV mutants showed the lower fusogenic capacity as the optimal pH for both mutants resulted in the lower fusion index than the wildtype virus.

In addition to the flavivirus E proteins and the alphavirus E1 proteins, the presence of the structurally similar linker region has also been suggested for the E2 glycoprotein of hepatitis C virus (HCV), which is also classified under the family of *Flaviviridae* and is widely recognized as being of high public health importance. Following the conserved translation strategy to produce the polyprotein which contains the structural and nonstructural proteins in the family of *Flaviviridae*, the envelope structure of the HCV virion consists of two structural proteins E1 and E2, which are both tethered to the viral membrane through the transmembrane regions in the carboxy-terminus (Reed and Rice 2000). The research on, and characterization of HCV were largely limited due to the lack of an efficient *in vitro* propagation platform (Kolykhalov, Agapov et al. 1997). With the newly available molecular virology tools including development of cDNA infectious clones, use of pseudoviral particles based on retroviral vectors, and a recombinant expression system in *Drosophila* cells has led to the characterization of the E2 glycoprotein and the subsequent prediction of its secondary structure based on the sequence homologies with alphavirus E1 proteins (Kolykhalov, Agapov et al. 1997, Bartosch, Dubuisson et al. 2003, Krey, d'Alayer et al. 2010). Although the crystal structure of HCV E2 glycoprotein is not yet available, the predicted structure of recombinant HCV E2 protein has suggested that the protein is rich in

the β-sheet structure and resembles the alphavirus E1 protein (Krey, d'Alayer et al. 2010). The HCV E2 glycoprotein is predicted to consist of three discontinuous domains similar to those of the flavivirus E proteins and the alphavirus E1 proteins. The proposed tertiary organization suggested that the domain I (DI) of HCV E2 protein is composed of eight β-strands similar to the structurally central flavivirus EDI and that it connects to the domain II (DII) containing the fusion loop and the transmembrane domain III (DIII). The domain II of HCV E2 protein is located between discontinuous sequences of two β-sheets in DI and contains the proposed fusion loop, which is rich in the hydrophobic amino acids. Finally, the carboxy-terminus of DI and the transmembrane DIII are connected by the linker region specifically named as the intergenotypic variable region (IgVR). The proposed three-dimensional structure of HCV E2 protein is shown in **Figure 5.4**.

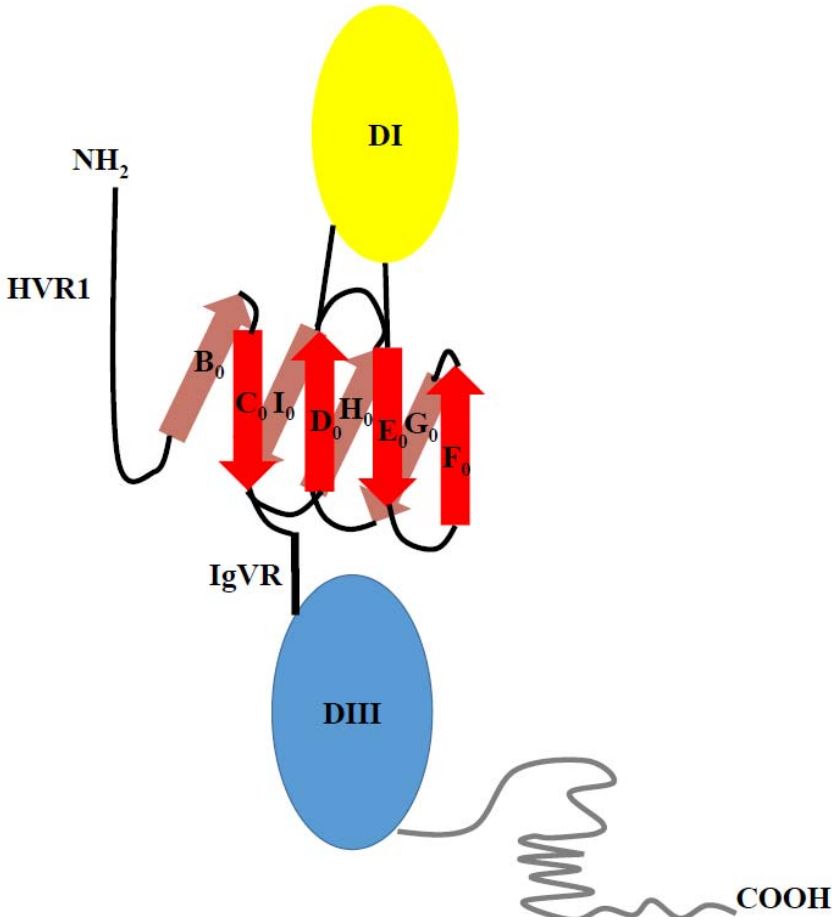

Figure 5.4 The proposed tertiary organization of HCV E2 protein modified from Krey *et al.* (2011)

The DI, DII and DIII are labeled in red, yellow and blue, respectively. The organization of the three domains resembles the other class II fusion proteins. The predicted eight β-strands are labeled according to the standard nomenclature of class II fusion proteins.

Similar to the conserved sequences observed within the serocomplexes of flaviviruses and alphaviruses, the IgVR region of HCV E2 glycoprotein contains high sequence homology within seven different genotypes of HCV, i.e. the intergenotypic sequence diversity (Hijikata, Kato et al. 1991). Subsequently, the IgVR region of HCV E2 glycoprotein, which resembles the structure of the linker region of flavivirus E proteins and alphavirus E1 glycoproteins, was shown to confer intergenotypic incompatibility among different genotypes. Experiments performed with chimeric HCV genotypes 1a and 2a demonstrated that the substitution of the amino acid residues in the IgVR region of the genotype-2a HCV with the residues derived from the IgVR region of the genotype-1a HCV abolished the viral infectivity of the resulting pseudoviral particle that was produced by presentation of HCV E1 and E2 glycoproteins with a retroviral vector system. By the chimerization of the IgVR region from the HCV genotype-1a variant with the HCV genotype-2a variant in the infectious clones of HCV, it was demonstrated that the lack of infectivity observed in the pseudoviral particle system was a consequence of impaired viral particle assembly (Albecka, Montserret et al. 2011).

In conclusion, the structure of the flavivirus EDI-EDIII linker region is conserved in two other categories of enveloped small RNA viruses. The sequences of the linker regions showed high sequence homology among flaviviruses and alphaviruses. Although the IgVR region of the HCV E2 protein shows the diversity in the sequences of different genotypes, the phenotypic change associated with the mutations in the IgVR region is also similar to the phenotypic changes associated with the mutations in the flavivirus EDI-EDIII linker region and the alphavirus DI-DIII linker region. The mutations in the DENV-2 EDI-EDIII linker region resulted in the defects in viral particle assembly, which was also observed in SFV E1 F287A mutant and the genotype-2a HCV chimera containing the IgVR sequence of the genotype-1a HCV variant (Albecka, Montserret et al. 2011, Zheng, Sanchez-San Martin et al. 2011, de Wispelaere and Yang 2012). Therefore, the M299I mutation in YFV EDI-EDIII linker region is likely to result in the consensus impairment in viral particle assembly and subsequently cause the attenuation *in vivo*.

D. Viral particle assembly and virion maturation of flaviviruses

Based on the homologous genomic structures and the conserved translational strategies among flaviviruses, YFV and other flaviviruses apparently share common mechanisms for viral particle assembly and virion maturation prior to the secretion into the extracellular space (Chambers, Hahn et al. 1990). The matured virions of flaviviruses consist of the three structural proteins assembled upon the lipid bilayers derived from the host cells and the encapsidated viral RNA. Using immunogold labeling and the thin-section transmission electron microscopy, the assembly of the structural proteins and the encapsidation of viral RNA have been demonstrated to take place in the rough ER near the nuclear envelope membrane (Welsch, Miller et al. 2009).

The conformation of mature flaviviruses virions share the smooth surface structure which is formed by the dimerized E protein monomers. Prior to the completion of the pH-dependent maturation process, 180 copies of the E protein monomers are arranged in the trimeric conformation leading to the presence of 60 spike structures that consists of three E protein monomers. Maturation requires the extensive quaternary structure rearrangement of the ectodomain of the E protein (Kuhn, Zhang et al. 2002, Zhang, Chipman et al. 2003). The original trimeric conformation of each spike upon the assembly of the immature virions of YFV and DENV-2 is shown in **Figure 5.5**.

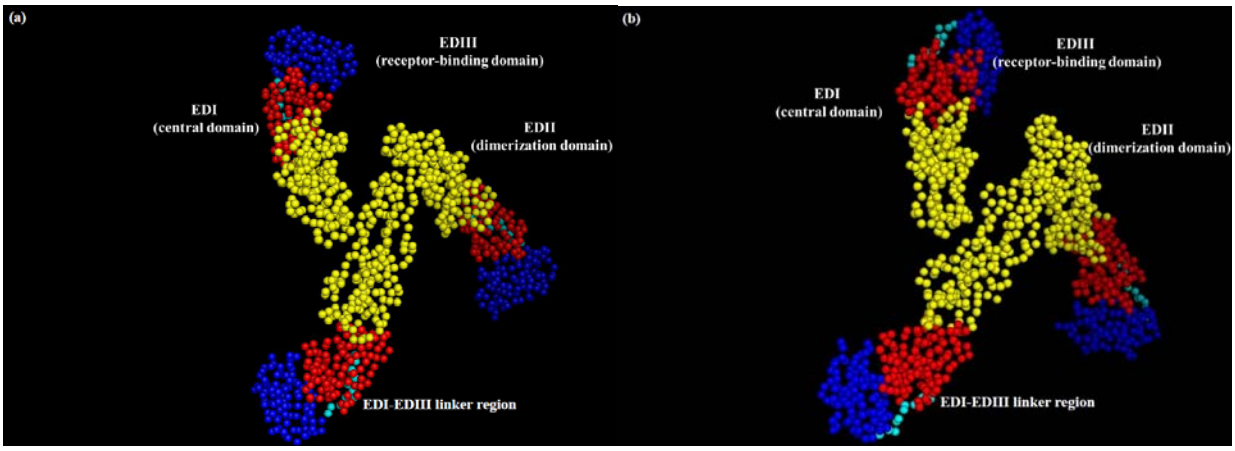

Figure 5.5 The trimeric conformation of E protein monomers in the immature virion of flaviviruses (PDB ID: 1NA4;1TGE)

(a) The spike structure consists of three YFV E protein monomers in the immature virion. (b) The spike structure consists of three DENV-2 E protein monomers in the immature virion. The EDI, EDII and EDIII are labeled in red, yellow and blue, respectively. The EDI-EDIII linker region is highlighted in cyan.

Due to the nature of the pH-dependent maturation process, the immature virions of flaviviruses can be obtained by the treatment of infected cells with NH_4Cl (Heinz, Stiasny et al. 1994). The transition from the trimeric conformation of E proteins in the immature virions to the dimeric conformation of E proteins in the mature virions occurs by the decrease of pH between ER and the Golgi network as shown in **Figure 5.6**. The presence of spike structures on the immature virions were was confirmed by cryo-EM reconstructed virion structures that appear as a spiky image with a larger diameter than seen with the matured virions of flaviviruses (Zhang, Corver et al. 2003). During the process of virion maturation in infected cells, the trimeric spike structure of immature virions undergoes a structural rearrangement to form the dimer which results in the smooth surface of mature virions in the acidic compartment of the *trans* Golgi network. In contrast to the relative rotation between EDI and EDII in each monomer of the E protein during the viral membrane fusion by 37˚ in the cryo-EM fitted structures, the structural rearrangement that occurs during virion maturation has been reported to lead to the swing of the EDI-EDII molecular hinge region by 27˚ based on the comparison of the fitted pre-mature E monomer in the cryo-EM reconstituted structure and the available structure of the soluble E monomer (Zhang, Zhang et al. 2004). According to the models from both the cryo-EM fitted structures and the soluble recombinant monomers, the maturation of virions does not involve reorientation between EDI and EDIII (Modis, Ogata et al. 2004, Zhang, Zhang et al. 2004).

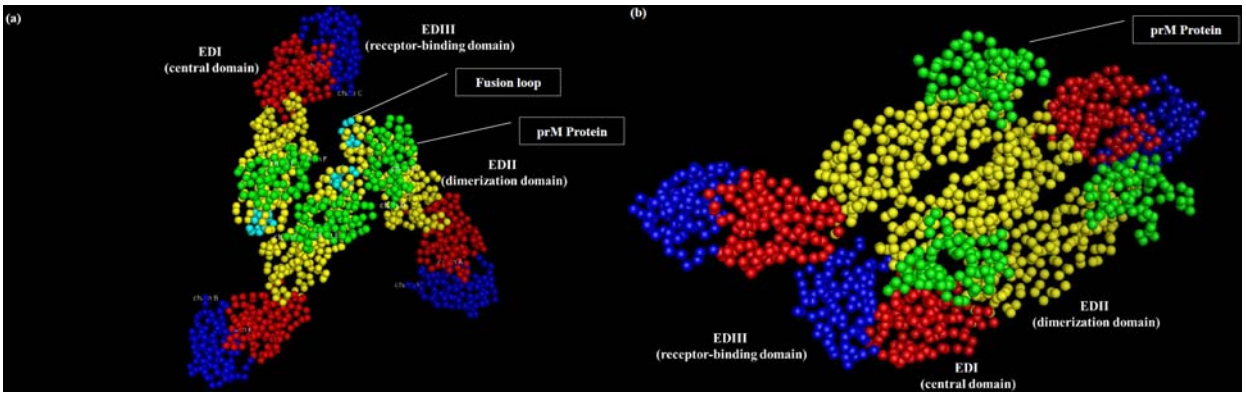

Figure 5.6 The conformational changes of flavivirus E protein during the process of virion maturation (PDB ID: 3C6D;3C6R)

(a) The trimeric conformation of DENV-2 E protein monomers in the immature virion assembled in the rough ER. The residues of the cryo-EM-fitted structure is displayed in spheres. Three monomers are arranged in the trimeric conformation with EDI, EDII and EDIII labeled in red, yellow and blue, respectively. The pr peptide of the prM protein is

colored in green and docks on the fusion loop in EDII colored in cyan. (b) The dimeric conformation of DENV-2 E protein monomers in the immature virion from the *trans* Golgi network prior to the furin cleavage. The residues of the cryo-EM-fitted structure is displayed in spheres. The envelope protein domain I, II and III are labeled in red, yellow and blue, respectively. The pr peptide colored in green remains docked on the fusion loop to prevent the premature membrane fusion in the acidic compartment of the *trans* Golgi network.

Prior to the formation of the fully matured dimeric structure which is capable of mediating viral membrane fusion via the exposed fusion loop structure, the fusion loop is protected in the immature dimers due to the continued docking of the pr peptide above the fusion loop (Yu, Zhang et al. 2008). The relative locations of the pr peptide and the envelope protein are shown in **Figure 5.7**. The removal of the pr peptide of the flavivirus prM proteins from the E protein is achieved by the host furin protease after the release of the immature virions from the *trans* Golgi network in order to obtain the full fusogenic capacity which is essential for the viral infectivity (Stadler, Allison et al. 1997).

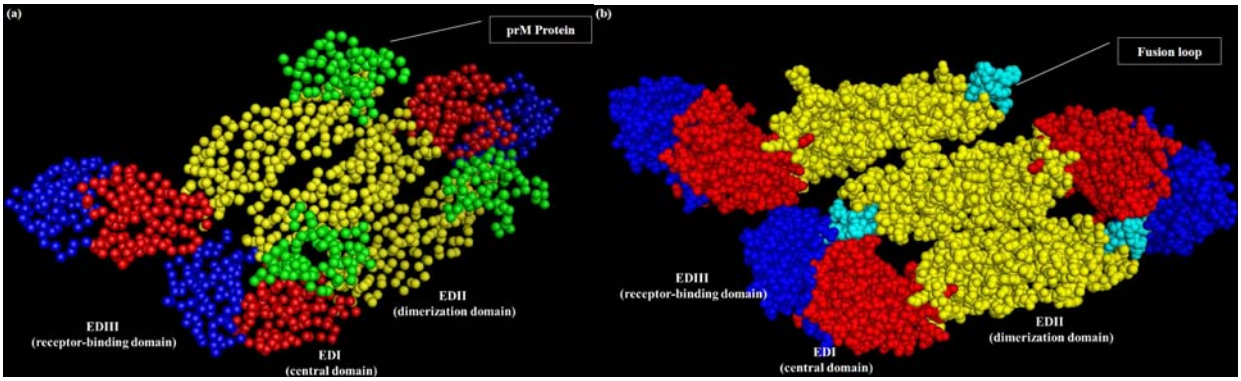

Figure 5.7 The removal of the pr peptide prior to the exocytosis of matured flavivirus virions

(a) The immature dimer of DENV-2 E protein exist in the immature virions released from the *trans* Golgi network with EDI, EDII and EDIII labeled in red, yellow and blue, respectively. The pr peptide remains attached to the E protein by docking above the fusion loop and is labeled in green. (b) The cleavage of furin protease removes the pr peptide and leads to the exposed fusion loop (cyan) at the tip of two neighboring EDII labeled (yellow).

The efficiency of the removal of the pr peptide from the prM protein is determined by the sequence at the junction between the pr peptide and the M protein (Keelapang, Sriburi et al.

2004). It was clearly demonstrated that the inefficient removal of DENV pr peptide results in the retention of the pr peptide on a subset of 180 copies of envelope protein monomers (Keelapang, Sriburi et al. 2004, Plevka, Battisti et al. 2011). For DENV, the incomplete removal of the pr peptide resulted in the production of immature-like non-infectious virions. The presence of anti-pr peptide antibodies in response to a primary infection of DENV may lead to more efficient viral entry in a subsequent infection due to an antibody-dependent enhancement mechanism. The anti-pr peptide antibodies fail to neutralize the virions in the secondary infection by another heterologous serotype of DENV and the severity of the disease is augmented by the increase uptake of virus through the internalization of Fcγ receptors, which are associated with the anti-pr antibodies and non-neutralized virions (Dejnirattisai, Jumnainsong et al. 2010).

In summary, the process of viral particle assembly and virion maturation contain multiple steps, about which we still lack complete understanding. Although the ultrastructural studies suggested that the site of virion assembly resides in close proximity to the rough ER, the details of the encapsidation mechanism for viral RNA are still unknown (Welsch, Miller et al. 2009). It is clear that the maturation of flavivirus virions occurs within the pH gradient from ER to the Golgi complex, and is characterized by the conformational transition of the E proteins from the trimeric to the dimeric form. Observation based on the reconstituted structures from cryo-EM images suggested that the quaternary organization of the flavivirus E protein monomers is rearranged from the trimeric spikes to the anti-parallel dimers, although the actual process is unknown (Kuhn, Zhang et al. 2002, Zhang, Corver et al. 2003, Zhang, Zhang et al. 2004). The comparison between the available crystal structures of flavivirus E proteins resembling the conformations on the mature virions and the cryo-EM-fitted structures of immature virions suggested that the majority of the structural rearrangement take place at the molecular hinge region between EDI and EDII and the relative movement in the EDI-EDIII linker region is limited (Kuhn, Zhang et al. 2002). Therefore, the observations derived from the structural biology studies are contradictory to the characterization of the class II fusion proteins based on the molecular virological tools, which suggest the phenotypes associated with the EDI-EDIII linker region are associated with the deficiency in viral particle assembly or virion maturation (Albecka, Montserret et al. 2011, Zheng, Sanchez-San Martin et al. 2011, de Wispelaere and Yang 2012).

The characterization of the M299I mutation in the YFV EDI-EDIII linker region based upon approaches and experiments described in chapter 2 was expected to provide the information for the further understanding in the function of flavivirus EDI-EDIII linker region.

5.2 Results

In spite of the experimental evidence suggesting the importance of the EDI-EDIII linker region in the flavivirus E proteins and its homology with the linker regions in the alphavirus E1 glycoproteins, the conclusions have largely been derived from *in vitro* experimental models based on Huh7 and BHK-21 cells (Zheng, Sanchez-San Martin et al. 2011, de Wispelaere and Yang 2012). The lack of the characterization of mutants *in vivo* creates a gap in our knowledge on how mutations in the EDI-EDIII linker or other regions which resemble the EDI-EDIII linker impair the lifecycle of arboviruses in susceptible hosts and arboviruses. To assess the phenotypic changes associated with the M299I mutation in the YFV E protein, three mutants were evaluated by orally infecting *Ae. aegypti* mosquitoes. The single M299I mutation was introduced into both the Asibi strain and the 17D+Asibi M-E chimera in order to produce the Asibi E M299I mutant and the 17D+Asibi M-E E M299I mutant, respectively. The I299M reversion was introduced into the 17D strain. The 17D E I299M revertant was evaluated for the infection and dissemination in *Ae. aegypti*.

A. Infection and dissemination of YFV E M299I mutantsin mosquitoes

The characterization of the M299I mutation in the YFV EDI-EDIII linker region is characterized by the Asibi E M299I mutant and the17D+Asibi M-E E M299I mutant. The infection and dissemination rates of the YFV wildtype controls and the E M299I mutants as determined at 7, 10 and 14 d.p.i. are summarized in **Table 5.4** and **Table 5.5**, respectively. The Asibi strain and the Asibi E M299I mutant were administered at 4.44 and 4.07 log$TCID_{50}$/ml, respectively. The challenge with the 17D+Asibi M-E chimera and the 17D+Asibi M-E E M299I mutant was performed with average titers of 5.91 and 6.77 log$TCID_{50}$/ml, respectively.

Viremic blood meal (titer in log$TCID_{50}$/ml)	7 d.p.i.		10 d.p.i.		14 d.p.i.	
DSB (N.A.)	0/29	(0.0%)	0/22	(0.0%)	0/37	(0.0%)
17D (5.47)	20/37	(54.1%)	16/34	(47.1%)	13/26	(50.0%)
17D+Asibi M-E (5.91)	36/44	(81.8%)	25/28	(89.3%)	28/34	(82.4%)
17D+Asibi M-E E M299I (6.77)	31/33	(93.9%)	49/53	(92.5%)	19/23	(82.6%)

Asibi (4.44)	31/38	(81.6%)	26/39	(66.7%)	31/42	(73.8%)
Asibi E M299I (4.07)	18/38	(47.4%)*	19/24	(79.2%)	32/43	(74.4%)

Table 5.4 Infection rate of YFV wildtype controls and E M299I mutants in *Ae. aegypti* at 7, 10 and 14 d.p.i.

*** indicates the statistically significant difference by Fisher's exact test compared to the infection rate of the Asibi strain at 7 d.p.i., respectively. ($p<0.05$)**

The infection rate of the Asibi E M299I mutant (47.4%) was significantly lower than the parental Asibi strain (81.6%) at 7 d.p.i. (p=0.0036) However, the infection rate of the Asibi strain and the Asibi E M299I mutant became indistinguishable at 10 (66.7% vs. 79.2%, p=0.39) and 14 (73.8% vs. 74.4%, p=1.00) d.p.i. The infection rates of the 17D+Asibi M-E chimera and the 17D+Asibi M-E E M299I mutant were not significantly different at 7 (81.8% vs. 93.9%, p=0.17), 10 (89.3% vs. 92.5%, p=0.69) and 14 (82.4% vs. 82.6%, p=1.00) d.p.i.

Viremic blood meal (titer in log$TCID_{50}$/ml)	7 d.p.i.		10 d.p.i.		14 d.p.i.	
17D (5.47)	0/13	(0.0%)	0/11	(0.0%)	1/9	(11.1%)
17D+Asibi M-E (5.91)	10/24	(41.7%)	7/16	(43.8%)	9/19	(47.4%)
17D+Asibi M-E E M299I (6.77)	5/22	(22.7%)	9/35	(25.7%)	7/13	(53.9%)
Asibi (4.44)	12/21	(57.1%)	11/18	(61.1%)	12/24	(50.0%)
Asibi E M299I (4.07)	10/21	(47.6%)	6/11	(54.6%)	14/24	(58.3%)

Table 5.5 Dissemination rate of YFV wildtype controls and E M299I mutants in *Ae. aegypti* at 7, 10 and 14 d.p.i.

Similar dissemination rates were observed for the Asibi strain and the Asibi E M299I mutant at 7 (57.1% vs. 47.6%, p=0.76), 10 (61.1% vs. 54.6%, p=1.00) and 14 (50.0% vs. 58.3%, p=0.77) d.p.i. The 17D+Asibi M-E chimera and the 17D+Asibi M-E E M299I mutant showed a lower but not significantly different dissemination rate at 7 (41.7% vs. 22.7%, p=0.29) and 10 (43.8% vs. 25.7%, p=0.24) d.p.i. At 14 d.p.i., there was no significant difference in the dissemination rate of the 17D+Asibi M-E chimera (47.4%) and the 17D+Asibi M-E E M299I mutant (53.9%) (p=1.00).

In summary, the infection rate of the Asibi E M299I mutant was significantly lower than that of the Asibi strain only at 7 d.p.i. The infection rate of the Asibi strain and the Asibi E M299I mutant were similar at 10 and 14 d.p.i. Similarly, there was no significant difference in the infection rate of the 17D+Asibi M-E chimera and the 17D+Asibi M-E E M299I mutant at 7 and 14 d.p.i. The M299I mutation in the E protein of the Asibi strain and the 17D+Asibi M-E

chimera did not result in to the demonstrable difference in the dissemination rate between 7 and 14 d.p.i.

B. Viral titers of whole mosquitoes, bodies and secondary tissues infected by YFV M299I mutants

The average titers of whole mosquitoes infected by the YFV wildtype controls and the E M299I mutants showed no significant difference at 7, 10 and 14 d.p.i. and the results are summarized in **Figure 5.8**.

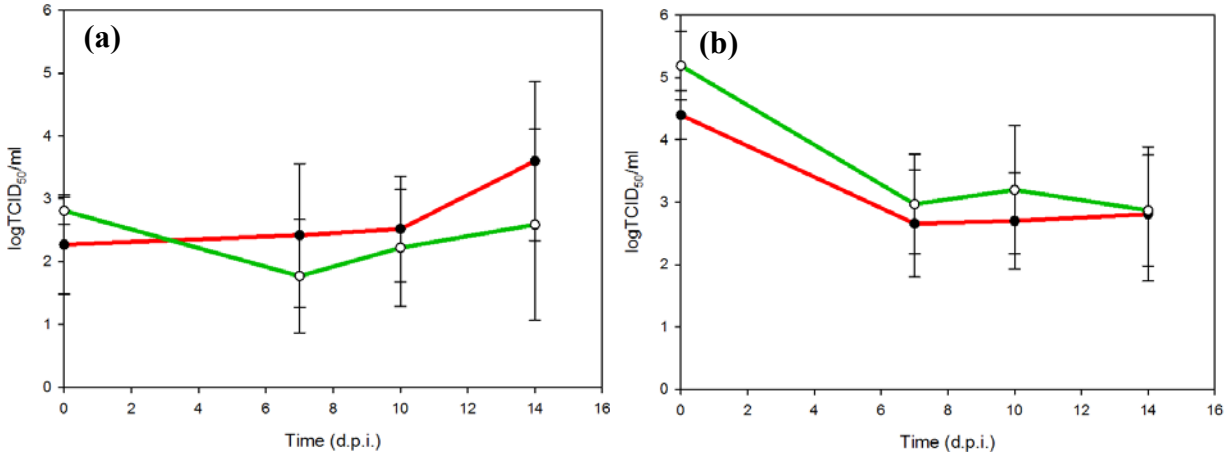

Figure 5.8 Average titers of whole mosquitoes infected by YFV wildtype controls and E M299I mutants

(a) Average whole-mosquito titers of the Asibi strain (red) and the Asibi E M299I mutant (green) (b) Average whole-mosquito titers of the 17D+Asibi M-E chimera (red) and the 17D+Asibi M-E E M299I mutant (green)

The engorgement of the viremic blood meals containing the Asibi E M299I mutant (2.80 $\log TCID_{50}$/ml) led to the relatively higher titers in the whole-mosquito homogenates than the Asibi strain (2.27 $\log TCID_{50}$/ml) collected at 0 d.p.i. Similarly, the engorgement of the 17D+Asibi M-E E M299I mutant (5.19 $\log TCID_{50}$/ml) resulted in the relatively higher titers of the whole-mosquito homogenates than the 17D+Asibi M-E chimera (4.40 $\log TCID_{50}$/ml).

The average titers in the whole mosquitoes infected by the Asibi strain and by the Asibi E M299I mutant did not show a significant difference at 7 (2.42 $\log TCID_{50}$/ml, n=10 vs. 1.77 $\log TCID_{50}$/ml, n=5, p>0.05), at 10 (2.52 $\log TCID_{50}$/ml, n=8 vs. 2.22 $\log TCID_{50}$/ml, n=8, p>0.05) and at 14 (3.60 $\log TCID_{50}$/ml, n=7 vs. 2.59 $\log TCID_{50}$/ml, n=8, p>0.05) d.p.i. There was no demonstrable difference in the average titers in the whole mosquito homogenates between the

17D+Asibi M-E chimera and the 17D+Asibi M-E E M299I mutant at 7 (2.66 logTCID$_{50}$/ml, *n*=11 vs. 2.97 logTCID$_{50}$/ml, *n*=9, *p*>0.05), 10 (2.70 logTCID$_{50}$/ml, *n*=8 vs. 3.20 logTCID$_{50}$/ml, *n*=14, *p*>0.05) and 14 (2.81 logTCID$_{50}$/ml, *n*=9 vs. 2.87 logTCID$_{50}$/ml, *n*=8, *p*>0.05) d.p.i.

The average titers of the bodies derived from *Ae. aegypti* showed no demonstrable difference between the Asibi strain and the Asibi E M299I mutant or between the 17D+Asibi M-E chimera and the 17D+Asibi M-E E M299I mutant. The results are summarized in **Figure 5.9**.

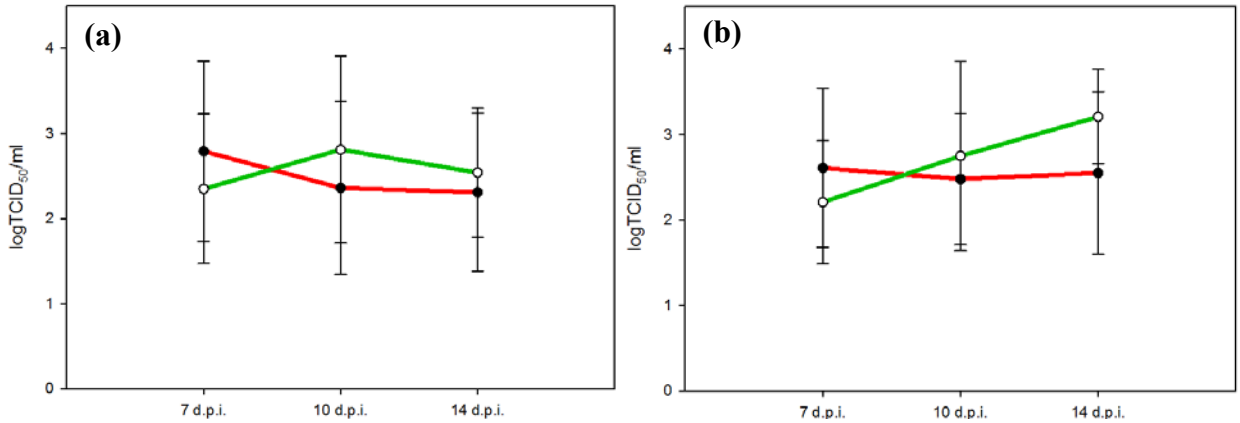

Figure 5.9 Average body titers of mosquitoes infected by YFV wildtype controls and E M299I mutants

(a) Average body titers of the Asibi strain (red) and the Asibi E M299I mutant (green) (b) Average body titers of the 17D+Asibi M-E chimera (red) and the 17D+Asibi M-E E M299I mutant (green)

At 7 d.p.i., the infection of Asibi strain (2.79 logTCID$_{50}$/ml, *n*=20) resulted in a similar average body titer to that recorded for the Asibi E M299I mutant (2.35 logTCID$_{50}$/ml, *n*=18) (*p*>0.05). The Asibi strain and the Asibi E M299I mutant had comparable average body titers at 10 (2.36 logTCID$_{50}$/ml, *n*=17 vs. 2.81 logTCID$_{50}$/ml, *n*=9, *p*>0.05) and 14 (2.31 logTCID$_{50}$/ml, *n*=24 vs. 2.54 logTCID$_{50}$/ml, *n*=22, *p*>0.05) d.p.i. Similarly, the 17D+Asibi M-E chimera (2.61 logTCID$_{50}$/ml, *n*=23) resulted in the insignificantly higher average body titer than the 17D+Asibi M-E E M299I mutant (2.43 logTCID$_{50}$/ml, *n*=22) at 7 d.p.i. (*p*>0.05) The average body titers of *Ae. aegypti* infected by the 17D+Asibi M-E chimera and the 17D+Asibi M-E E M299I mutant were comparable at 10 (2.48 logTCID$_{50}$/ml, *n*=15 vs. 2.75 logTCID$_{50}$/ml, *n*=33, p>0.05) and 14 (2.55 logTCID$_{50}$/ml, *n*=17 vs. 3.21 logTCID$_{50}$/ml, *n*=33, *p*>0.05) d.p.i.

The dissemination of YFV E M299I mutants did not lead to any significant difference in the average titers of homogenized secondary tissues between the Asibi strain and the Asibi E

M299I mutant or between the 17D+Asibi M-E chimera and the 17D+Asibi M-E E M299I mutant. The average titers of the secondary tissues are shown in **Figure 5.10**.

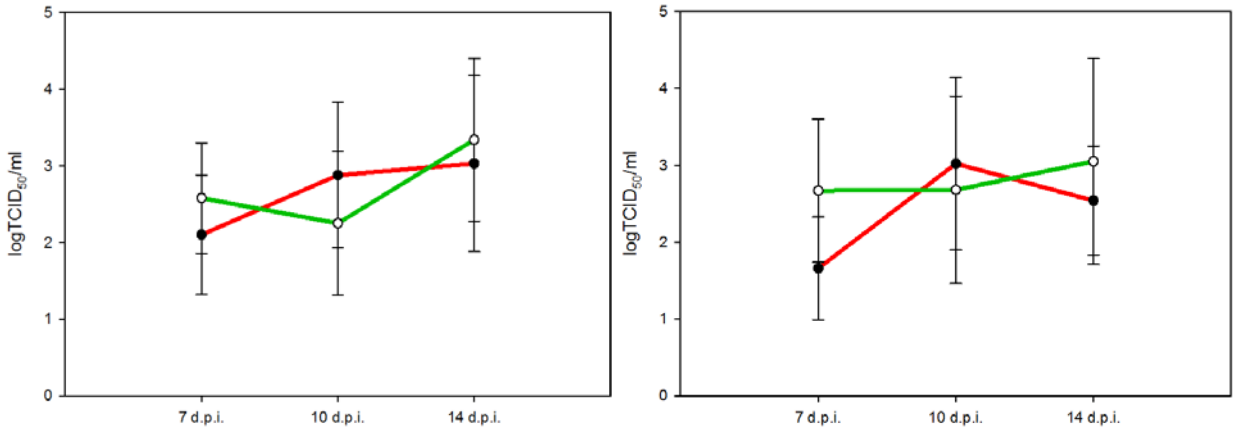

Figure 5.10 Average secondary-tissue titers of mosquitoes infected by YFV wildtype controls and E M299I mutants

(a) Average secondary-tissue titers of the Asibi strain (red) and the Asibi E M299I mutant (green) (b) Average secondary-tissue titers of the 17D+Asibi M-E chimera (red) and the 17D+Asibi M-E E M299I mutant (green)

The average titers of the secondary tissues containing the Asibi E M299I mutant was insignificantly higher than those containing the Asibi strain at 7 (2.10 $\log TCID_{50}$/ml, n=12 vs. 2.58 $\log TCID_{50}$/ml, n=10, p>0.05) and 14 (3.03 $\log TCID_{50}$/ml, n=12 vs. 3.34 $\log TCID_{50}$/ml, n=16, p>0.05) d.p.i.; whereas, the average secondary-tissue titer of the Asibi strain was not significantly different to that of the Asibi E M299I mutant at 10 (2.88 $\log TCID_{50}$/ml, n=11 vs. 2.25 $\log TCID_{50}$/ml, n=6, p>0.05) d.p.i. The dissemination of the 17D+Asibi M-E E M299I mutant also led to the insignificantly higher average secondary-tissue titer than the 17D+Asibi M-E chimera at 7 (1.66 $\log TCID_{50}$/ml, n=10 vs. 2.67 $\log TCID_{50}$/ml, n=5, p>0.05) and 14 (2.54 $\log TCID_{50}$/ml, n=9 vs. 3.05 $\log TCID_{50}$/ml, n=7, p>0.05) d.p.i. At 10 d.p.i., the insignificantly higher average secondary-tissue titer was observed in the mosquitoes infected by the 17D+Asibi M-E chimera (3.02 $\log TCID_{50}$/ml, n=7 vs. 2.68 $\log TCID_{50}$/ml, n=9, p>0.05)

In conclusion, the comparison of the average titers of the whole mosquitoes, bodies and secondary tissues did not show the significant difference in the corresponding type of samples collected at the same time points between the Asibi strain and the Asibi E M299I mutant or between the 17D+Asibi M-E chimera and the 17D+Asibi M-E E M299I mutant. Based upon our data, the M299I mutation in the E protein led to the change of phenotype in the Asibi strain at 7

d.p.i. The amino acid at position E 299 can potentially be a determinant at the early stage of YFV infection in *Ae. aegypti*.

C. Infection and dissemination of YFV E I299M revertant

The I299M reversion in the E protein of the YFV 17D strain was tested for infection and dissemination. The infection and dissemination rates of the YFV wildtype controls and the 17D E I299M revertant are summarized in **Table 5.6** and **Table 5.7**, respectively. The average titers of the viremic blood meals of the 17D strain, the 17D E I299M revertant and the 17D+Asibi M-E chimera are 5.47, 5.78 and 5.91 $logTCID_{50}$/ml, respectively. The Asibi strain as the disseminating control was administered at the relatively lower titer at 4.44 $logTCID_{50}$/ml.

Viremic blood meal (titer in $logTCID_{50}$/ml)	7 d.p.i.		10 d.p.i.		14 d.p.i.	
DSB (N.A.)	0/29	(0.0%)	0/22	(0.0%)	0/37	(0.0%)
17D (5.47)	20/37	(54.1%)	16/34	(47.1%)	13/26	(50.0%)
17D E I299M (5.78)	21/33	(63.6%)	15/31	(48.4%)†	13/24	(54.2%)‡
17D+Asibi M-E (5.91)	36/44	(81.8%)	25/28	(89.3%)	28/34	(82.4%)
Asibi (4.44)	31/38	(81.6%)	26/39	(66.7%)	31/42	(73.8%)

Table 5.6 Infection rate of YFV wildtype controls and E M299I mutants in *Ae. aegypti* at 7, 10 and 14 d.p.i.

† and ‡ indicate the statistically significant difference by Fisher's exact test compared to the infection rates of the Asibi strain at 7 and 10 d.p.i., respectively. ($p<0.05$)

The I299M reversion in the E protein of the 17D strain failed to significantly increase the infection rate of the live-attenuated 17D vaccine strain. There was no demonstrable difference in the infection of the 17D strain and 17D E I299M revertant at 7(54.1% vs. 63.6%, p=0.47), 10 (47.1% vs. 48.4%, p=1.00) and 14 (50.0% vs. 54.2%, p=0.79) d.p.i. The blood meal of the 17D E I299M revertant resulted in the lower but comparable infection rate that was not significantly different from the 17D+Asibi M-E chimera at 7 d.p.i. (81.8% vs. 63.6%, p=0.11) The infection rate of the 17D E I299M revertant was consistently lower than the 17D+Asibi M-E chimera at 10 (89.3% vs. 48.4%, p=0.0009) and 14 (82.4% vs. 54.2%, p=0.04) d.p.i.

Viremic blood meal (titer in $logTCID_{50}$/ml)	7 d.p.i.		10 d.p.i.		14 d.p.i.	
17D (5.47)	0/13	(0.0%)	0/11	(0.0%)	1/9	(11.1%)
17D E I299M (5.78)	5/11	(45.5%)	0/10	(0.0%)†	4/9	(44.4%)
17D/Asibi M-E (5.91)	10/24	(41.7%)	7/16	(43.8%)	9/19	(47.4%)
Asibi (4.44)	12/21	(57.1%)	11/18	(61.1%)	12/24	(50.0%)

Table 5.7 Dissemination rate of YFV wildtype controls and E I299M mutants in *Ae. aegypti* at 7, 10 and 14 d.p.i.

† indicates the significant difference by Fisher's exact test from 17D/Asibi M-E chimera (*p*=0.02) and Asibi strain (*p*=0.0016) at 10 d.p.i.

The I299M mutation resulted in the dissemination into the secondary tissues at 7 and 14 d.p.i.; whereas no dissemination was observed at 10 d.p.i. The dissemination rate of the 17D E I299M revertant was significantly higher than the 17D strain at 7 d.p.i. (0.00% vs. 45.5%, p=0.01) but showed no statistically significant difference at 10 (0.0% vs. 0.0%, p=1.00) and at 14 d.p.i. (11.1% vs. 44.4%, p=0.29) The comparison in the dissemination rate between the 17D+Asibi M-E chimera and the 17D E I299M revertant showed that the infection of the 17D+Asibi M-E chimera led to the comparable dissemination rate with the 17D E I299M revertant at 7 (41.7% and vs. 45.5%, p=0.24) and 14 (47.4% vs. 44.4%, p=1.00) d.p.i. The 17D+Asibi M-E chimera had a significantly higher dissemination rate than the 17D E I299M mutant at 10 d.p.i. (43.8% vs. 0.0%, p=0.02) Although the Asibi strain was administered at the relatively lower titer, the comparable dissemination rate was observed at 7 (57.1% vs. 45.5%, p=0.72) and 14 (50.0% vs. 44.4%, p=1.00) d.p.i. At 10 d.p.i., the dissemination rate of the Asibi strain was significantly higher than the 17D E I299M mutant (61.1% vs. 0.0%, p=0.0016).

In conclusion, the I299M mutantation in the E protein of the 17D strain failed to significantly increase the infectivity of the 17D strain. The infection of the 17D E I299M revertant did not show the significant higher infection rate than the 17D strain between 7 and 14 d.p.i. Additionally, the 17D E I299M revertant showed the significantly lower infection rate than the 17D+Asibi M-E chimera at 10 and 14 d.p.i. Although the dissemination of the 17D E I299M revertant was observed at 7 and 14 d.p.i., the dissemination rate of the 17D E I299M revertant remained lower than the Asibi strain and the 17D+Asibi M-E chimera. The dissemination rate of the 17D E I299M revertant was insignificantly lower than that of the Asibi strain and the 17D+Asibi M-E chimera at 7 and 14 d.p.i. and significantly lower than that of the Asibi strain and the 17D+Asibi M-E chimera at 10 d.p.i.

D. Viral titers of whole mosquitoes, bodies and secondary tissues infected by YFV I299M revertant

The evaluation of the viral replication based upon titration of the whole mosquitoes infected by the YFV wildtype controls and the 17D E I299M revertant did not identify the significant difference in the average titers of whole mosquitoes. These average whole-mosquito titers are summarized in **Figure. 5.11**.

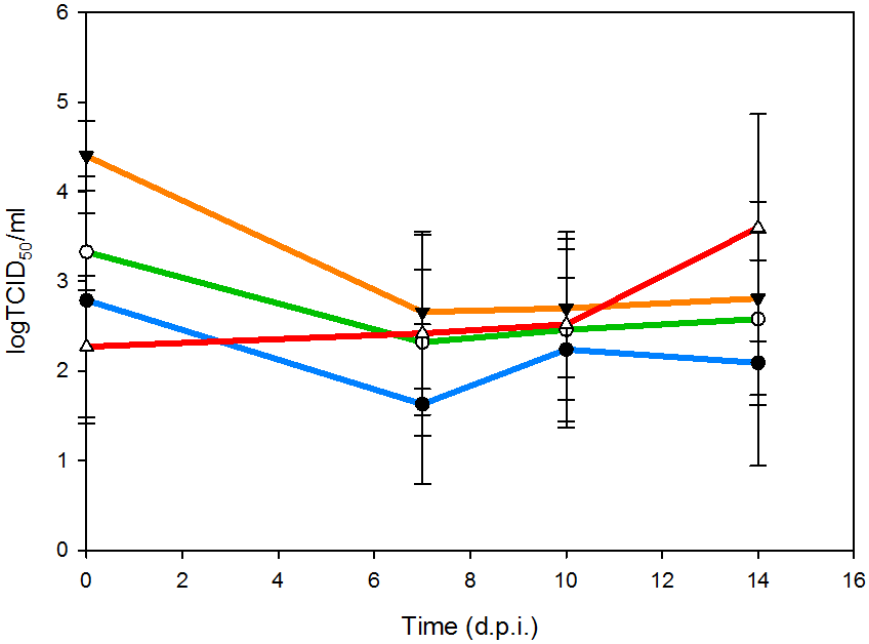

Figure 5.11 Average titers of whole mosquitoes infected by the Asibi strain, the 17D+Asibi M-E chimera, the 17D strain, and the 17D E I299M revertant

The curves representing the average titers of the whole-mosquito homogenates infected by the 17D strain, the 17D E I299M mutant, the 17D+Asibi M-E chimera and the Asibi strain are labeled in blue, green, orange and red, respectively.

Although the initial engorgement of the viremic blood meal containing the Asibi strain resulted from a relatively lower input of virus than the 17D E I299M revertant (2.27 $logTCID_{50}$/ml vs. 3.33 $logTCID_{50}$/ml), the average whole-mosquito titers of the Asibi strain were insignificantly higher than the 17D E I299M revertant at 7 (2.42 $logTCID_{50}$/ml, n=10 vs. 2.32 $logTCID_{50}$/ml, p>0.05, n=10),10 (2.52 $logTCID_{50}$/ml, n=8 vs. 2.46 $logTCID_{50}$/ml, n=6, p>0.05) ,14 (3.60 $logTCID_{50}$/ml, n=7 vs. 2.58 $logTCID_{50}$/ml, n=5, p>0.05) d.p.i. Similarly, the infection of the 17D+Asibi M-E chimera resulted in an insignificantly higher whole-mosquito titers at 7 (2.66 $logTCID_{50}$/ml, n=11 vs. 2.32 $logTCID_{50}$/ml, n=10, p>0.05), 10 (2.70

logTCID$_{50}$/ml, n=8 vs. 2.46 logTCID$_{50}$/ml, n=6, p>0.05) and 14 (2.81 logTCID$_{50}$/ml, n=9 vs. 2.58 logTCID$_{50}$/ml, n=5, p>0.05) d.p.i. The average whole-mosquito titers between the 17D strain and the 17D E I299M revertant remained indistinguishable at 7 (2.79 logTCID$_{50}$/ml, n=7 vs. 3.30 logTCID$_{50}$/ml, n=10, p>0.05), 10 (1.63 logTCID$_{50}$/ml, n=5 vs. 2.32 logTCID$_{50}$/ml, n=6, p>0.05) and 14 (2.09 logTCID$_{50}$/ml, n=4 vs. 2.58 logTCID$_{50}$/ml, n=5, p>0.05) d.p.i.

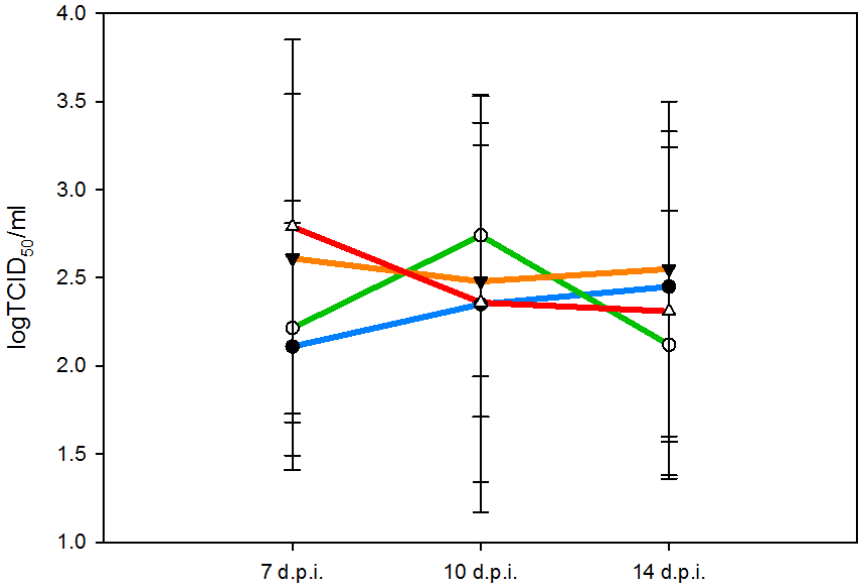

Figure 5.12 Average body titers of mosquitoes infected by the Asibi strain, the 17D+Asibi M-E chimera, the 17D strain and the 17D E I299M revertant The curves representing the average body titers of *Ae. aegypti* infected by the 17D strain, the 17D E I299M revertant, the 17D+Asibi M-E chimera and the Asibi strain are labeled in blue, green, orange and red, respectively.

The comparison of the average body titers is summarized in **Figure. 5.12**. There was no demonstrable difference in the average body titers between the 17D I299M revertant and any of the control infectious clones. The average body titers of *Ae. aegypti* infected by the Asibi strain were indistinguishable from those infected by the 17D E I299M mutant at 7 (2.79 logTCID$_{50}$/ml, n=20 vs. 2.21 logTCID$_{50}$/ml, n=10, p>0.05), 10 (2.36 logTCID$_{50}$/ml, n=17 vs. 2.74 logTCID$_{50}$/ml, n=9, p>0.05) and 14 (2.31 logTCID$_{50}$/ml, n=24 vs. 2.12 logTCID$_{50}$/ml,n=8 , p>0.05) d.p.i. Similarly, there was no significant difference in the average body titers of *Ae. aegypti* infected by the 17D+Asibi M-E chimera and the 17D I299M revertant at 7 (2.61 logTCID$_{50}$/ml, n=23 vs. 2.21, n=10 logTCID$_{50}$/ml, p>0.05), 10 (2.48 logTCID$_{50}$/ml, n=15 vs. 2.74 logTCID$_{50}$/ml, n=9 p>0.05) and 14 (2.55 logTCID$_{50}$/ml, n=17, vs. 2.12, n=8, logTCID$_{50}$/ml,

p>0.05) d.p.i. The average body titers of *Ae. aegypti* infected by the 17D strain did not show any significant difference from those infected by the 17D E I299M revertant at 7 (2.11 logTCID$_{50}$/ml, *n*=13 vs. 2.21 logTCID$_{50}$/ml, *n*=10, *p*>0.05), 10 (2.35 logTCID$_{50}$/ml, *n*=11 vs. 2.74 logTCID$_{50}$/ml, *n*=9, *p*>0.05) and 14 (2.45 logTCID$_{50}$/ml, *n*=9, vs. 2.12 logTCID$_{50}$/ml, *n*=8, p>0.05) d.p.i.

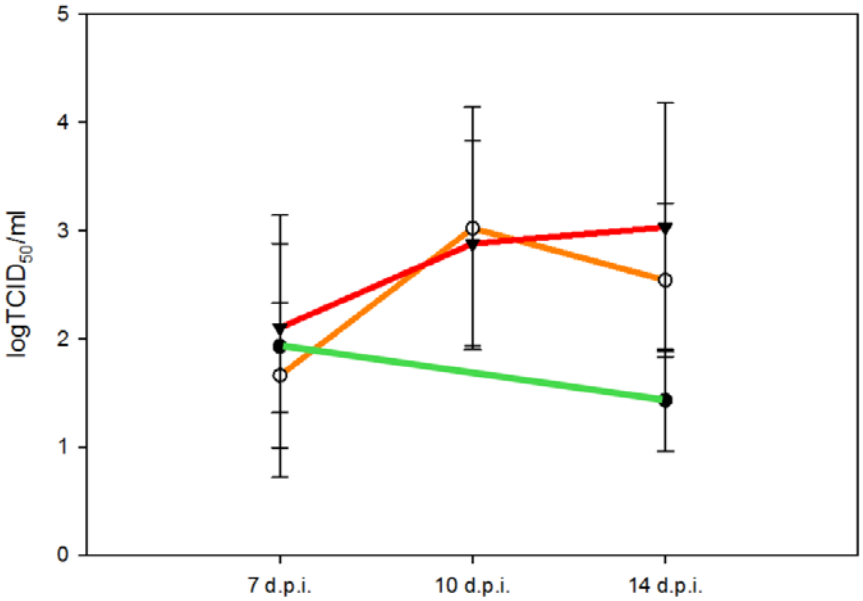

Figure 5.13 Average secondary-tissue titers of mosquitoes infected by the Asibi strain, the 17D+Asibi M-E chimera, the 17D strain and –the 17D E I299M mutant

The curves representing the average secondary-tissue titers of *Ae. aegypti* infected by the 17D strain, the 17D E I299M mutant, the 17D+Asibi M-E chimera and the Asibi strain are labeled in blue, green, orange and red, respectively.

The average titers of secondary tissues infected by the 17D E I299M revertant and the wildtype controls did not show any significant difference at 7 and 14 d.p.i. The average secondary-tissue titers of the 17D E I299M revertant remained insignificantly lower than the Asibi strain at 7 (2.10 logTCID$_{50}$/ml, *n*=12 vs. 1.93 logTCID$_{50}$/ml, *n*=5) and 14 (3.30 logTCID$_{50}$/ml, *n*=12 vs. 1.43, *n*=3 logTCID$_{50}$/ml) d.p.i. The average titers of secondary tissues infected by the 17D+Asibi M-E chimera and the 17D E I299M revertant were indistinguishable at 7 (1.66 logTCID$_{50}$/ml, *n*=10 vs. 1.93 logTCID$_{50}$/ml, *n*=5) and 14 (2.54 logTCID$_{50}$/ml, *n*=9 vs. 1.43 logTCID$_{50}$/ml, *n*=3) d.p.i.

In summary, when compared with the control infectious clones, the cloning of the Asibi E I299M reversion into the YFV 17D strain did not result in an elevation in the average titers of the homogenized whole mosquitoes, bodies and secondary tissues. .

5.3 Conclusions

A. Attenuation caused by the M299I mutation

The incorporation of the single YFV 17D E M299I mutation into the E protein of the Asibi strain resulted in a significantly lower infection than in the wild type Asibi strain at 7 d.p.i. However, the infection rate of the Asibi strain and the Asibi E M299I mutant became comparable at 10 and 14 d.p.i. The similar attenuation was not observed in the comparison between the 17D+Asibi M-E chimera and the 17D+Asibi M-E E M299I mutant. The infection rate remained indistinguishable between the 17D+Asibi M-E chimera and the 17D+Asibi M-E E M299I mutant between 7 and 14 d.p.i. I It is plausible that the observed attenuation caused by the M299I mutation characteristic of the YFV 17D E protein may contribute to the restriction of the infection through delayed or reduced establishment during the early stage of viral infection.

Importantly, the dissemination of the Asibi strain failed to be impaired by the substitution of the 17D M299I mutation. The Asibi E M299I mutant still possessed the disseminating phenotype between 7 and 14 d.p.i. Although the insignificantly reduction of the dissemination rate was observed in *Ae. aegypti* challenged by the 17D+Asibi M-E E M299I mutant at 7 and 10 d.p.i., the statistical analysis suggested the significant attenuation was not achieved.

There was no demonstrable increase of viral infectivity due to the Asibi wild type I299M sequence into the E protein of the 17D strain. There was no significant difference in the infection rate between the 17D+Asibi M-E chimera and the 17D E I299M revertion. Additionally, the infection rate of the 17D E I299M revertant remained significantly lower than the 17D+Asibi M-E chimera, which was challenged at the comparable viral titer, at 10 and 14 d.p.i.

The 17D E I299M revertant showed the restoration of the disseminating capacity whilst the positive secondary tissues infected by the 17D E I299M revertant were identified at 7 and 14 d.p.i. The dissemination rate of the 17D E I299M mutant remained insignificantly lower with a restricted phenotype at 7 and 14 d.p.i. in comparison to the 17D+Asibi M-E chimera and the Asibi strain.

In summary, the YFV 17D M299I mutation was able to cause the viral attenuation at the early stage of infection but did not show a significant contribution to the non-disseminating phenotype that is characteristic of the 17D strain. The genetic reversion by the single Asibi I299M introduction into 17D did not result in the highly infectious and disseminating phenotype of the Asibi strain. The I299M mutation insignificantly increased the infectivity of the 17D strain without reaching the comparable infectivity of the 17D+Asibi M-E chimera. Additionally, the viral dissemination that is only present in the virulent strains of YFV is likely to be partially restored by the I299M mutation. Although the dissemination was observed at 7 and 14 d.p.i., the dissemination rate still remained insignificantly different to that of the Asibi strain and the 17D+Asibi M-E chimera.

B. Viral titers of homogenized mosquito tissues

There was no demonstrable difference in the average titers of the homogenized whole-mosquitoes, bodies and secondary tissues infected by the wildtype controls and the E M299I mutants. Similarly, no significant difference in the average titers of the homogenized whole-mosquitoes, bodies and secondary tissues infected by the wildtype controls and the E I299M mutants was identified. The comparable titers of all three types of samples between the wildtype controls and the mutants are consistent with the observation reported by McElroy *et al*. (McElroy, Tsetsarkin et al. 2006).

5.4 Discussion and future directions

Our observation suggests the phenotypic change, i.e. non-disseminating 17D in the mosquito, caused by the E M299I mutation when introduced into the Asibi strain is at best, only limited to the early stage of the infection. In our experimental model using the reverse genetics system of YFV and *Ae. aegypti*, the significant attenuation was only observed at 7 d.p.i. It is the first available evidence to suggest that the mutations in the EDI-EDIII linker region may contribute to the attenuation *in vivo*. In contrast to the lethality to DENV-2 caused by the alanine substitutions in the EDI-EDIII linker region, the comparable average titers of the viremic blood meals and the similar infection and dissemination rates among *Ae. aegypti* between the YFV wildtype controls and E M299I mutants, YFV E M299I mutants were found viable *in vitro* and infectious to *Ae. aegypti* (de Wispelaere and Yang 2012).

It remains unclear as to how the intitial attenuation observed in our experiments during the early phase of viral infection is achieved by the M299I mutation in the YFV EDI-EDIII linker region. The most plausible explanation based on the *in vitro* experiments of DENV-2, SFV and HCV is that the M299I mutation in YFV E protein also impairs the viral particle assembly (Albecka, Montserret et al. 2011, Zheng, Sanchez-San Martin et al. 2011, de Wispelaere and Yang 2012). According to the available evidence that the binding of the receptors is mediated predominantly by the lateral surface of EDIII, which was not subjected to the mutagenesis in this study, the viral entry is less likely to be inhibited (Chen, Maguire et al. 1997, Hung, Hsieh et al. 2004). Additionally, the replicon experiment described by de Wispelaere *et al*. demonstrated the mutations in the DENV-2 EDI-EDIII linker region did not significantly abolish the viral entry *in vitro* (de Wispelaere and Yang 2012). Although the deficiency in the viral particle assembly is not known to impair the viral entry, the process of the establishment of the infection by the arboviruses can still be potentially interfered. The establishment of the infection by YFV and other arboviruses in the midgut of mosquitoes has been repeatedly demonstrated to be initiated in individual infected epithelial cells followed by the replication and spread to the neighboring cells (Salazar, Richardson et al. 2007, McElroy, Girard et al. 2008, Smith, Adams et al. 2008). The observations suggest the successful establishment of arbovirus infection in mosquitoes potentially requires multiple steps, which are the viral entry in the primary target cells and the spread of infectious progeny virions to neighboring susceptible cells and ultimately other additional susceptible tissues in other body parts of the infected mosquitoes. The limited number of cells which are initially infected by the arboviruses often results in the so-called eclipse phase, when the viral titers of whole mosquitoes or infected tissues may decrease to the level which is below the input titer of the originally engorged virus or the limit of detection of specific assays, in the early stage of infection. The eclipse phase eventually is terminated by the propagation of the virus and the increase in the numbers of infected cells. Such kinetics in viral titer was described by the quantitative analysis of *Ae. aegypti* infected by YFV and DENV-2 (McElroy, Tsetsarkin et al. 2006, Richardson, Molina-Cruz et al. 2006). The examination of infected tissues also supported the observation based on the quantitative analysis. The earliest detection of YFV antigens by the immunohistochemistry staining in the mosquito midguts was reported to occur at 3 d.p.i. and was predominantly localized in the posterior midgut followed by the spread to the anterior midgut between 3 and 7 d.p.i (McElroy, Girard et al. 2008). Similarly, among *Ae.*

aegypti that ingested a viremic blood containing DENV-2, the quantity of viral antigen in the infected midguts did not reach the detectable level of the immunofluorescence staining by anti-DENV human pAb and anti-DENV-2 mouse 3H5 mAb until 3 d.p.i followed by the subsequent spread to the susceptible tissues in the legs, wings and head of the infected mosquitoes (Salazar, Richardson et al. 2007). In this study, the infection rates were calculated by the percentage of mosquitoes, which showed the detection of infectious virions in the homogenized tissues by $TCID_{50}$ assay, among all the mosquitoes assayed. The lowest detectable titer of the assay was 1.06 log$TCID_{50}$/ml. Therefore, it is likely that the potentially impaired progeny viral particle assembly by the M299I mutation significantly delayed the spread of the virions to the neighboring cells in order to achieve the higher titers above the limit of detection. As a consequence of the delay in reaching the level above the limit of detection, the infection rate of the Asibi E M299I mutant was significantly lower than the wildtype control at 7 d.p.i. The continuous propagation and spread of the virus resulted in the similar infection rate between the Asibi strain and the Asibi E M299I mutant at the later time points, 10 and 14 d.p.i. In contrast to the Asibi strain which showed a transient and short eclipse phase between 0 and 3 d.p.i. in the study described by McElroy *et al*., it is likely that a subset of *Ae. aegypti* infected by the Asibi E M299I mutant experienced a significant longer eclipse phase prior to reaching the level of detection (McElroy, Tsetsarkin et al. 2006).

Because the average titers of the 17D+Asibi M-E chimera and the 17D+Asibi M-E E M299I mutant in the viremic blood meals are relatively higher than the average titer of the Asibi strain and the Asibi E M299I mutant, the potential dose effect may result in the higher infection rate among *Ae. aegypti* exposed to the 17D+Asibi M-E chimera and the 17D+Asibi M-E E M299I mutant. Therefore, the comparison should only be made between the Asibi strain and the Asibi E M299I mutant or between the 17D+Asibi M-E chimera and the 17D+Asibi M-E E M299I mutant. Additionally, the high-titer viremic blood meals may also lead to the similar infection rate between the 17D+Asibi M-E chimera and the 17D+Asibi M-E E M299I mutant. As the infection rates of arboviruses are proportionate to the concentration of viremic blood meals, the viremic blood meals containing the 17D+Asibi M-E M299I mutant could potentially infect a larger number of susceptible cells or result in the higher quantity of viral entry into the susceptible cells in the mosquito midguts (Hurlbut 1956, Gubler and Rosen 1976, Tsetsarkin, Vanlandingham et al. 2007, Oviedo, Romoser et al. 2011). Therefore, the eclipse phase required

for the viral titers of the homogenized tissues to exceed the limit of detection may be shorter and resulted in the comparable infection rate at 7 d.p.i. between the 17D+Asibi M-E chimera and the 17D+Asibi M-E E M299I mutant.

Although the reversion of the sequence of the EDI-EDIII linker region in YFV 17D strain to the Asibi strain by the M299I mutation restored some capacity of viral dissemination, the infectivity of the 17D E M299I mutant remained similarly to that of the 17D strain and significantly lower than the 17D+Asibi M-E chimera. Therefore, the occurrence of the genetic reversion at the Ile^{299} residue of the EDI-EDIII linker should not be considered as a potential mechanism for the increase spread of the YFV vaccine strain and the phenotypic reversion to the virulent wildtype virus. In the presence of other attenuation determinants in the nonstructural genes, the complete reversion of the mutations in the structural genes of the 17D strain to the amino acid sequences of the Asibi strain by chimerizing the structural genes of the Asibi strain and the nonstructural genes of the 17D strain did not lead to the increase in the viremic titers and the incidence of viscerotropic diseases in the non-human primates (McGee, Lewis et al. 2008).

In summary, the assessment of the attenuation caused by the M299I mutant in the E protein demonstrated its potential role as an attenuation determinant particularly by significantly reducing the infection rate of *Ae. aegypti* at the early stage of the study. The experimental design used in our study defined the disseminated form of infection by the presence of the infectious virion in the homogenized secondary tissues, which contain the head, wings and legs of the infected mosquitoes. As described by Miller *et al.*, the disseminated form of infection in *Ae. aegypti* may necessarily not lead to the transmission of YFV to suckling mice (Miller and Adkins 1988). Additionally, the presence of the virions of the YFV Asibi strain in the salivary glands took place after the viral dissemination into the thorax and head of the infected mosquitoes (McElroy, Girard et al. 2008). Therefore, prior to the viral dissemination into the salivary glands, it is likely that the virus undergoes multiple cycles of propagation and dissemination among the susceptible tissues in the midgut, thorax and head of the infected mosquitoes. Although there was no demonstrable difference in the dissemination rate between the Asibi strain and the Asibi E M299I mutant and between the 17D+Asibi M-E chimera and the 17D+Asibi M-E E M299I mutant, it is unclear if the M299I mutation will prolong the extrinsic incubation period of the wildtype virus. The identification of the key mutations governing the period required for the extrinsic incubation period will provide the strategy for the design of biologically non-

transmissible live-attenuated vaccines as the definition of incubation period is defined as the interval between the acquisition of the microorganisms and the ability of transmission in arthropod vectors.

A. Mutations and sequence variations in the EDI-EDIII linker region

Our study contributes towards the more comprehensive functional analysis of the EDI-EDIII linker region of flaviviruses. To the best of our knowledge, the Asibi E M299I mutant contains the first non-lethal single point mutation reported in the flavivirus EDI-EDIII linker region. In contrast to the lethality to the virus caused by the alanine and phenylalanine substitutions in the DENV-2 EDI-EDIII linker region, the M299I mutation in YFV EDI-EDIII linker region resulted in the minor attenuation in the early stage of viral infection (de Wispelaere and Yang 2012).

For vertebrate hosts, the largely prevailing theory is that the highly conserved amino acid sequences of protein products are the products of selection during the process of evolution (Boffelli, Nobrega et al. 2004, Gross 2007). The highly conserved amino acid sequences also present in the indispensable enzymatic components of flaviviruses (Valle and Falgout 1998, Zou, Chen et al. 2011). Therefore, the conserved sequences of the flavivirus EDI-EDIII linker region suggests that the region may potentially provide the critical function for the envelope proteins, although the region has only been known to exist in the disordered or linear structure in all the known available crystal structures of flavivirus E proteins in the pre- and post-fusion conformations (de Wispelaere and Yang 2012).

With the available information from the DENV-2 and YFV mutants, the Gly^{294}, Ser^{296} and Tyr^{297} residues in the YFV EDI-EDIII linker region are likely to be the critical residues for the viability of the viruses. The conservative mutations in the corresponding regions in DENV-2 EDI-EDIII linker region were still unable to allow the recovery of mutant viruses. Hence, the lack of the naturally occurring mutations or mutations associated with the attenuated strains of the virus will diminish the actual need for characterization of the mutations in the corresponding residues in other flaviviruses. The Met^{299} residue allows the presence of the conservative mutation utilizing isoleucine or valine in the YFV 17D strains and WNV. Currently, whether the M299I mutation causes any demonstrable attenuation in mammalian hosts of YFV still remains unknown. The complete understanding in the potential attenuation mechanisms of the M299I

mutation can potentially be achieved by the challenge of the Asibi E M299I mutant to the immunocompromised A129 or STAT1 mice model (Meier, Gardner et al. 2009).

The future characterization of the EDI-EDIII linker region may focus on the assessment of phenotypic change associated with the mutations at the Lys^{293} and Cys^{300} residues, which are the other two conserved amino acids among all the flaviviruses. The other potential target for mutagenesis analysis can potentially be the Leu^{292} residue, which is highly conserved among mosquito-borne flaviviruses but is substituted with methionine in the tick-borne flaviviruses. Whilst the structurally similar IgVR segment in the HCV E2 protein suggested the intergenotypic incompatibility, which abolished the viral particle assembly, the screening of mutations in the flavivirus EDI-EDIII linker region to partially or significantly abolish the viral particle assembly will offer another potential mechanism to produce candidates for live-attenuated flavivirus vaccines (Albecka, Montserret et al. 2011).

B. FG loop of EDIII located in the close proximity of the EDI-EDIII linker region

Although the EDI-EDIII linker region and the FG loop are located at the carboxy- and amino-terminus of flavivirus E proteins. The folding of the protein leads to the neighboring locations of two fragments in EDIII. Using the crystal structure of the soluble monomer of DENV-2 and JEV E proteins, the relative locations of the EDI-EDIII linker region and the FG loop are shown in **Figure 5.14**.

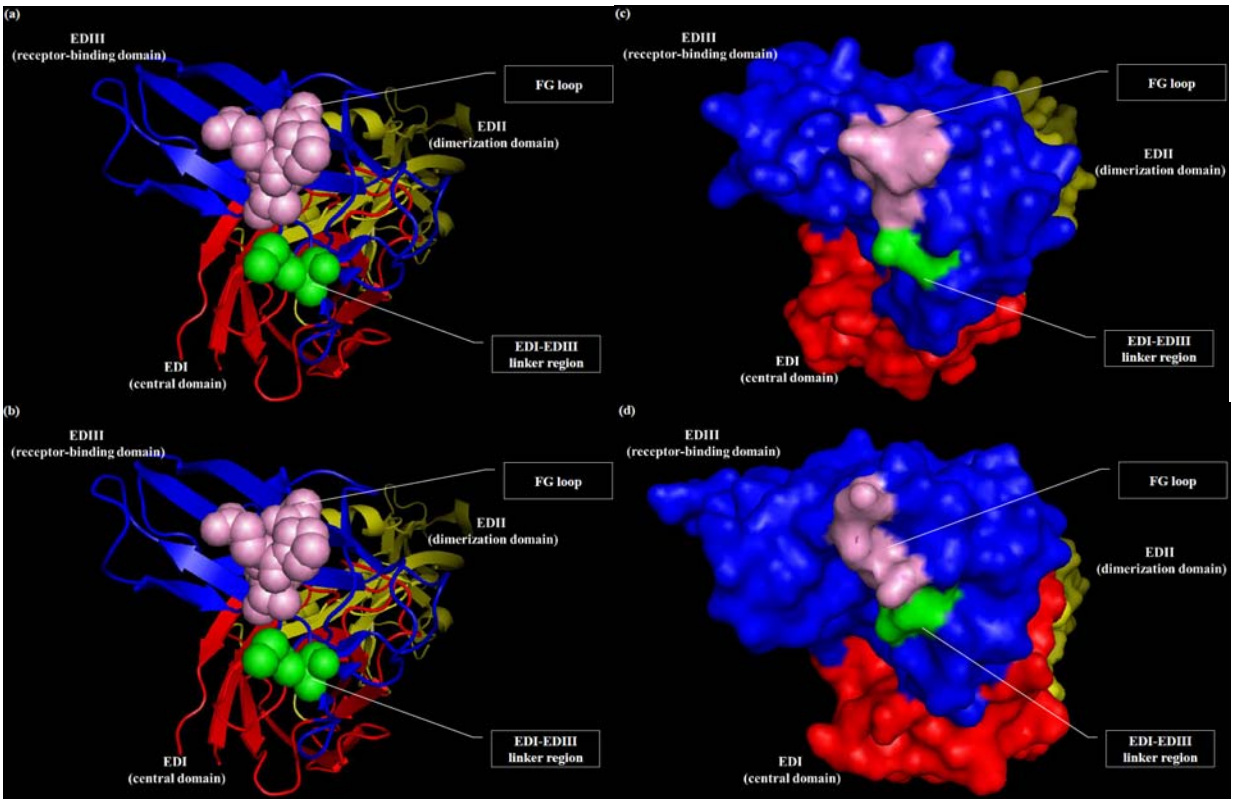

Figure 5.14 The relative locations of the EDI-EDIII linker region and the FG loop in the crystal structures of DENV-2 and JEV E protein pre-fusion monomers (PDB ID: 1TG8;3P54)

(a) DENV-2 E protein structure is displayed in cartoon representation with EDI, EDII, and EDIII labeled in red, yellow, and blue, respectively. The EDI-EDIII linker region is shown in green spheres and the FG loop is shown in pink spheres. (b) JEV E protein structure is displayed in cartoon representation with EDI, EDII, and EDIII labeled in red, yellow, and blue, respectively. The EDI-EDIII linker region is shown in green spheres and the FG loop is shown in pink spheres. (c) DENV-2 E protein structure is displayed in surface representation with EDI, EDII, and EDIII labeled in red, yellow and blue, respectively. The EDI-EDIII linker region and the FG loop is colored in green and pink, respectively. (d) JEV E protein structure is displayed in surface representation with EDI, EDII, and EDIII labeled in red, yellow and blue, respectively. The EDI-EDIII linker region and the FG loop is colored in green and pink, respectively.

The close proximity between the EDI-EDIII linker region and the FG loop suggests the M299I mutation and the T380R mutation are located in the neighboring region of YFV E

protein. Although the crystal structure of the YFV E protein has not yet been available, the available NMR structure of the recombinant YFV EDIII shown in **Figure 5.1** demonstrated the relatively locations of two independent segments of the E protein (Volk, May et al. 2009). Therefore, the further characterization of the mutations in the EDIII region should be expanded to the assessment of the phenotypic change associated the YFV E M299I-T380R double mutants.

C. Potential interactions with the mutations in the H1 helice of E protein

In the study described by de Wispelaere *et al*., the lethal T299F mutation, which is at the corresponding region of the Tyr297 in the YFV EDI-EDIII linker region, was compensated by the Q400H mutation which is located at the H1 helice of the transmembrane region in the DENV-2 E protein (de Wispelaere and Yang 2012). The viable mutant was recovered with the presence of both mutations and the further characterization of the single Q400H mutation suggested its potential role of enhancing the efficiency of viral particle assembly and virion secretion.

In the available sequences of YFV Asibi strain and 17D substrains, the A416T mutation located at the H1 helice of the transmembrane region in the E protein was found in all 17D-204 substrains and the 17DD Brazil substrain (Hahn, Dalrymple et al. 1987, dos Santos, Post et al. 1995, Stokes, Bauer et al. 2001). It is still unknown if the A416T mutation will provide the similar compensatory mechanism as the compensatory Q400H mutation in DENV-2 E protein.

We have successfully defined the M299I mutation in the YFV E protein is likely to be an attenuation determinant for the early stage of viral infection in *Ae. aegypti*. The mutation is likely to cause the delayed establishment of YFV infection in the mosquitoes. Its potential interaction with the additional neighboring T380R mutation, in other region of the E protein remains to be characterized. With the conserved sequences in the EDI-EDIII linker region, it is likely to provide the additional mechanisms for viral attenuation.

Chapter 6 - Major Findings, Conclusions, and Discussion

The research described in the dissertation has provided further knowledge contributing to an understanding of the phenotypic changes associated with the four amino acid substitutions in the E protein that occurred during the attenuation process to produce YFV 17D vaccine virus from its wild type Asibi parental virus. The chapter provides the summary of the major findings and the potential application of the knowledge generated in the study as well as the future directions in characterizing the potential attenuation mechanisms for YFV and other flaviviruses.

6.1 The T380R mutation in YFV EDIII

A. Major finding

The characterization of the Asibi T380R mutant and the 17D+Asibi M-E E T380R mutant demonstrated that the T380R mutation can slightly increase the viral infectivity in *Ae. aegypti*. The Asibi T380R mutant showed a insignificantly higher infection rate than the Asibi strain at 7, 10 and 14 d.p.i. The infection rate of the 17D+Asibi M-E E T380R mutant was significantly higher than the 17D+Asibi M-E chimera at 7 and 14 d.p.i. Although there was no demonstrable difference, the 17D+Asibi M-E E T380R mutant still resulted in the higher infection rate at 10 d.p.i. than the 17D+Asibi M-E chimera.

In contrast to the increase in the viral infectivity, the dissemination rate of the Asibi T380R mutant and the 17D+Asibi M-E E T380R mutant showed no significant difference from the infection rate of the wild type Asibi strain and the 17D+Asibi M-E chimera. Additionally, there was no significant increase in the average titers of homogenates derived from whole mosquitoes, bodies and secondary tissues infected by the Asibi E T380R mutant and the 17D+Asibi M-E E T380R mutant. The overall conclusion is therefore that the T380R mutation in the EDIII of YFV 17D strain does not on its own, contribute to the attenuated phenotype of this vaccine strain based on the higher infection rate, the comparable dissemination rate, and the similar average titers of homogenized tissues.

B. Comparison with the YFV structural-gene chimeras

The phenotypes of the YFV chimeras containing the structural genes of the Asibi and 17D strains provided the fundamental knowledge for the characterization of the individual

mutations in the three different domains of the E protein (McElroy, Tsetsarkin et al. 2006). The comparison of the infection and dissemination rate between the YFV chimeras and the E T380R mutants is summarized in **Figure 6.1** and **Figure 6.2**, respectively.

In the study described by McElroy *et al*., the chimerization of the EDIII from the 17D strain to the corresponding region of the Asibi strain significantly decreased the infection rate of Asibi strain from 72% to 38% (McElroy, Tsetsarkin et al. 2006). The T380R mutation is one of the five mutations present in EDIII of the 17D-204 strain. In contrast to the Asibi+17D+EDIII chimera which was shown to be significantly less infectious, the T380R mutation in the Asibi strain and the 17D+Asibi M-E chimera led to the increase of viral infectivity instead of the significant reduction in the infection rate. However, it must be remembered that in these experiments this T380R mutation was manipulated as part of a sequence substitution that included other mutations.

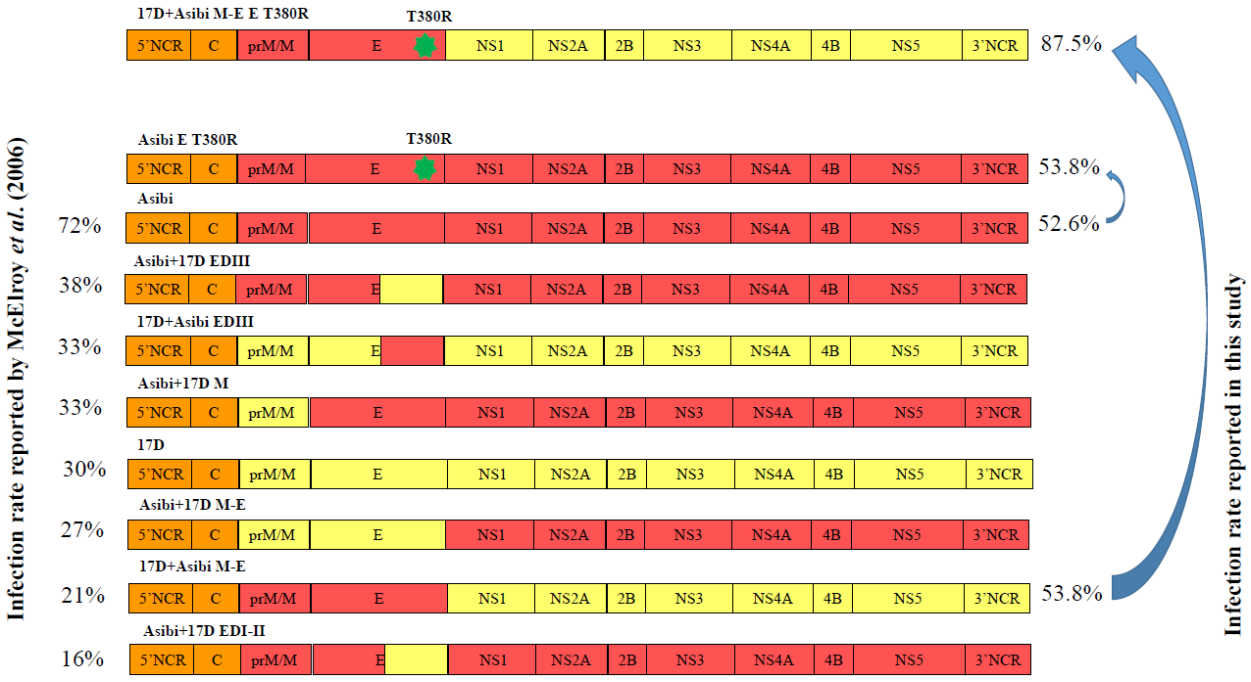

Figure 6.1 The infection rate of the YFV structural-gene chimeras reported by McElroy *et al.* (2006) and the YFV E T380R mutants

Similar to the significant reduction in the infection rate observed between the Asibi strain and the Asibi+17D EDIII chimera, the dissemination was significantly impaired by the chimerization of EDIII in the 17D strain to the corresponding region of the Asibi strain (83% vs.

32%). The Asibi E T380R mutant and the 17D+Asibi M-E E T380R mutant showed the comparable dissemination rate with the Asibi strain and the 17D+Asibi M-E chimera.

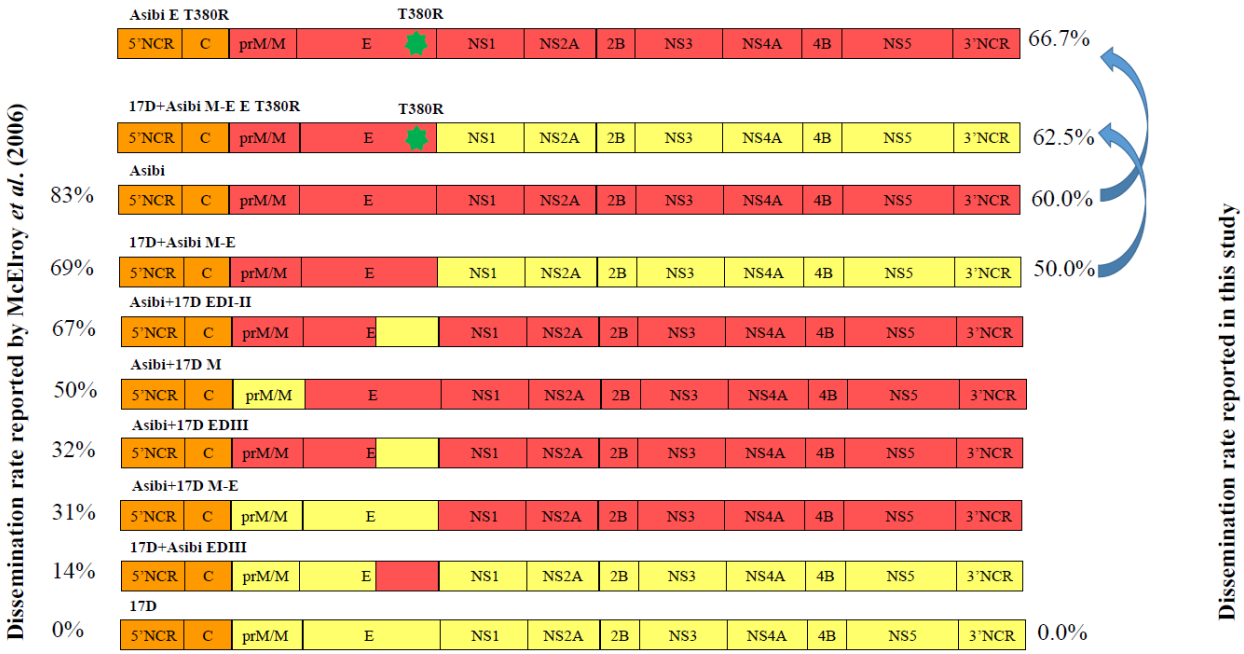

Figure 6.2 The dissemination rate of the YFV structural-gene chimeras reported by McElroy *et al.* (2006) and the YFV E T380R mutants

In conclusion, the Asibi E T380R mutant and the 17D+Asibi M-E E T380R mutant did not cause the significant viral attenuation in *Ae. aegypti* implicating that the attenuation observed in the Asibi+17D EDIII chimera is the consequence of attenuation caused by the other additional mutations in EDIII.

6.2 The G52R mutation in YFV EDI-EDII molecular hinge

A. Major finding

The most prominent phenotypic change associated with the G52R mutation at the interface of YFV EDI and EDII is the loss of viral infectivity. The infection rate of the Asibi E G52R mutant was significantly lower than that of the Asibi strain at 7 and 10 d.p.i.; whereas, the infection rate of the 17D+Asibi M-E E G52R mutant showed the significant lower infectivity than the 17D+Asibi M-E E G52R mutant at 7 d.p.i.

The single G52R mutation in the E protein was unable to completely prevent viral dissemination of the Asibi strain and the 17D+Asibi M-E chimera. The Asibi E G52R mutant and the 17D+Asibi M-E E G52R mutant were able to disseminate into the secondary tissues.

There was no significant reduction in the average titers of homogenized tissues from the mosquitoes infected by the YFV E G52R mutants in comparison to the wildtype controls. Therefore, based on the observation, the G52R mutation is likely to be a genetic determinant for viral infectivity.

B. Comparison with the YFV structural-gene chimeras

Experiments using the Asibi+17D EDI-EDII chimera demonstrated that the infection rate of *Ae. aegypti* was significantly lower than that of the Asibi strain at 14 d.p.i (McElroy, Tsetsarkin et al. 2006). The result suggests one or more of the five amino acid mutations in EDI and EDII of the 17D strain are likely to be the determinant of viral infectivity. The comparison of the infection rate and the dissemination rate in the experiment utilizing the YFV structural-gene chimeras and the YFV E G52R mutants is shown in **Figure 6.3** and **Figure 6.4**, respectively.

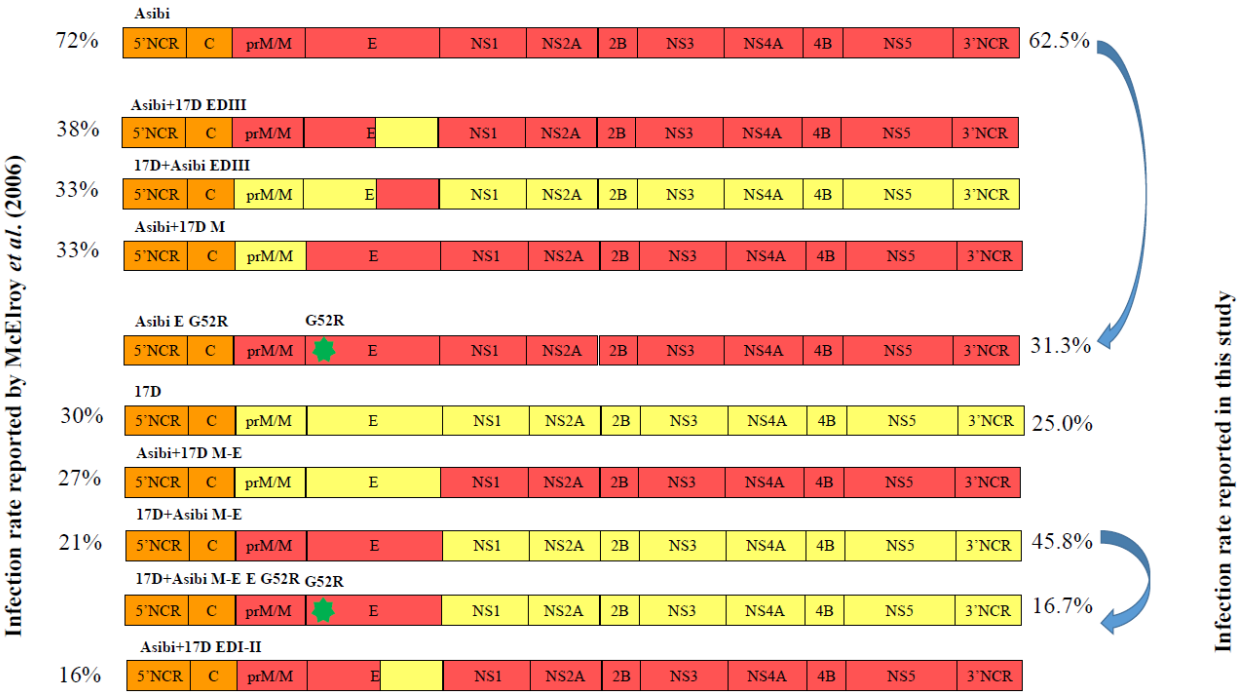

Figure 6.3 The infection rate of the YFV structural-gene chimeras reported by McElroy *et al.* (2006) and the YFV E G52R mutants

The introduction of the YFV 17D G52R mutation into the Asibi strain resulted in a lower infection rate (62.5% vs. 31.3%) similar to the decrease of viral infectivity observed by McElroy in *Ae. aegypti* orally challenged with the Asibi+17D EDI-II chimera. Although there was no demonstrable difference in the infection rate at 14 d.p.i. between the Asibi strain and the Asibi E

G52R mutant, the Asibi E G52R mutant had consistently and significantly lower infection rates when compared with the wild type Asibi strain at 10 and 14 d.p.i. The G52R mutation in the E protein also reduced the infectivity of the partially attenuated 17D+Asibi M-E chimera at 14 d.p.i. Similarly, in spite of the fact that there was no demonstrable difference in the infection rate observed at 10 and 14 d.p.i., the infection rate of the 17D+Asibi M-E E G52R mutant remained lower between 7 and 14 d.p.i. and there was a significant difference in the infection rate between the 17D+Asibi M-E chimera and the 17D+Asibi M-E E G52R mutant at 7 d.p.i. Therefore, the YFV E G52R mutants reproduced the phenotype with the lower viral infectivity similar to the Asibi+17D EDI-II chimera.

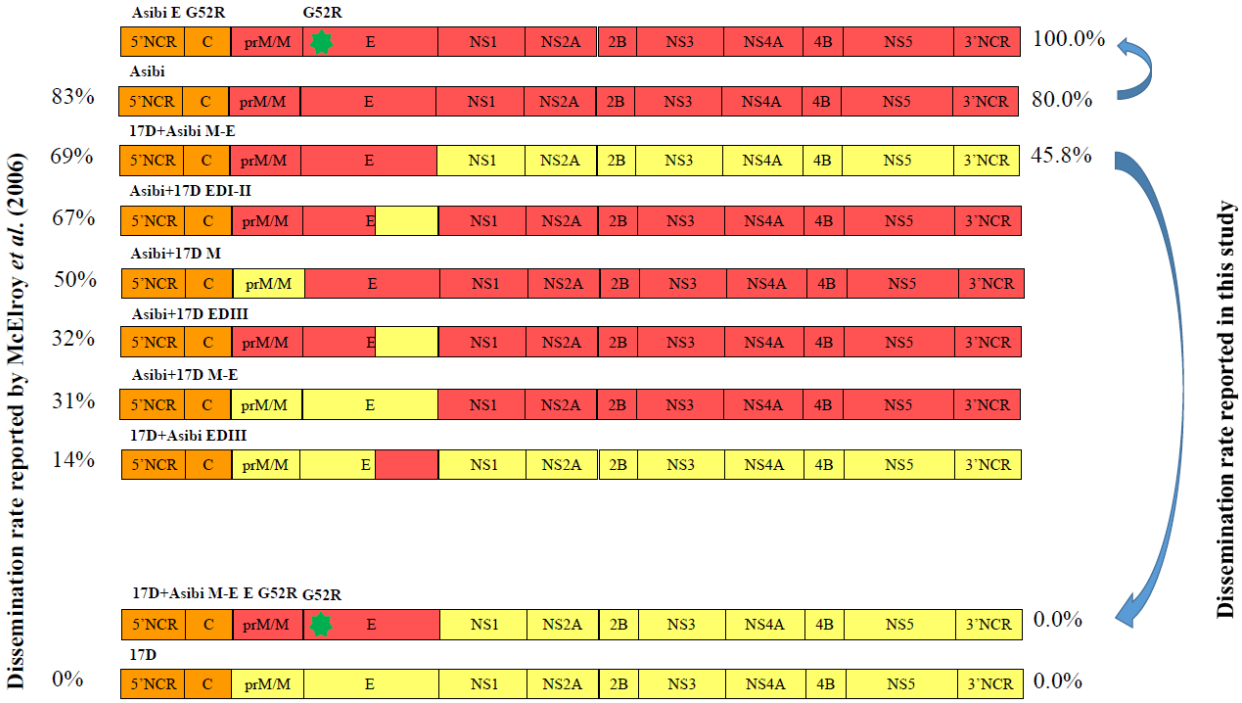

Figure 6.4 The dissemination rate of the YFV structural-gene chimeras reported by McElroy *et al.* (2006) and the YFV E G52R mutants

The comparable dissemination rate between the Asibi strain and the Asibi+17D EDI-II chimera at 14 d.p.i. suggested the five mutations in EDI and EDII of the 17D strain do not prevent the viral dissemination (McElroy, Tsetsarkin et al. 2006). The dissemination rate of the Asibi E G52R mutant was similar to that of the Asibi strain at 14 d.p.i. The disseminated form of infection was not observed in *Ae. aegypti* infected by the 17D+Asibi M-E E G52R mutant at 14 d.p.i. The low infection rate of the 17D+Asibi M-E G52R mutant may originate from not only

the attenuation caused by the G52R mutation in the E protein but also the presence of the additional attenuation determinants in the nonstructural proteins.

In summary, the comparison with the YFV wildtype controls and the results derived from the experiment of YFV structural-gene chimeras implicated that the G52R mutation in the E protein is responsible for the viral attenuation. The observation does not exclude the presence of additional attenuation determinants in the region of EDI and EDII.

6.3 The T173I mutation in YFV EDI G_0H_0 loop

A. Major finding

The T173I mutation in the E protein was shown to have the limited contribution to the attenuation of YFV. The infection rate of the Asibi E T173I mutant and the 17D+Asibi M-E E T173I mutant remained was similar to that of the Asibi strain and the 17D+Asibi M-E chimera between 7 and 14 d.p.i. The dissemination of the Asibi E T173I mutant and the 17D+Asibi M-E E T173I mutant was equally efficient to the Asibi strain and the 17D+Asibi M-E chimera. The average titers from the homogenized tissues suggested the YFV E T173I mutants did not show the difference in the capacity of viral replication from the wildtype controls.

B. Comparison with the YFV structural-gene chimeras

The infection rate and dissemination rate of YFV E T173I mutants are compared to the YFV structural-gene chimeras and shown in **Figure 6.5** and **Figure 6.6.**, respectively.

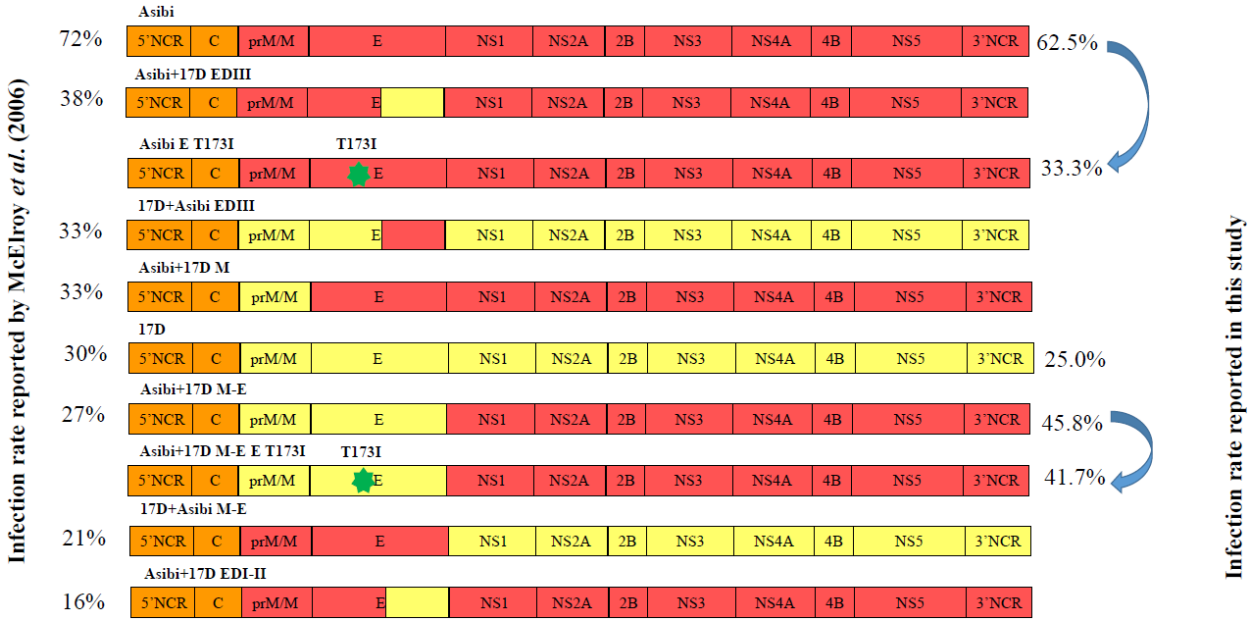

Figure 6.5 The infection rate of the YFV structural-gene chimeras reported by McElroy *et al.* (2006) and the YFV E T173I mutants

In contrast to the significantly lower infection rate of the Asibi+17D EDI-II chimera, the infection rate of the Asibi E T173I mutant (33.3%) was not significantly different to that of the Asibi strain (62.5%) at 14 d.p.i. Similarly, the infection rate of the 17D+Asibi M-E chimera (45.8%) did not show a significant difference from that of the 17D+Asibi M-E E T173I mutant (41.7%) at 14 d.p.i.

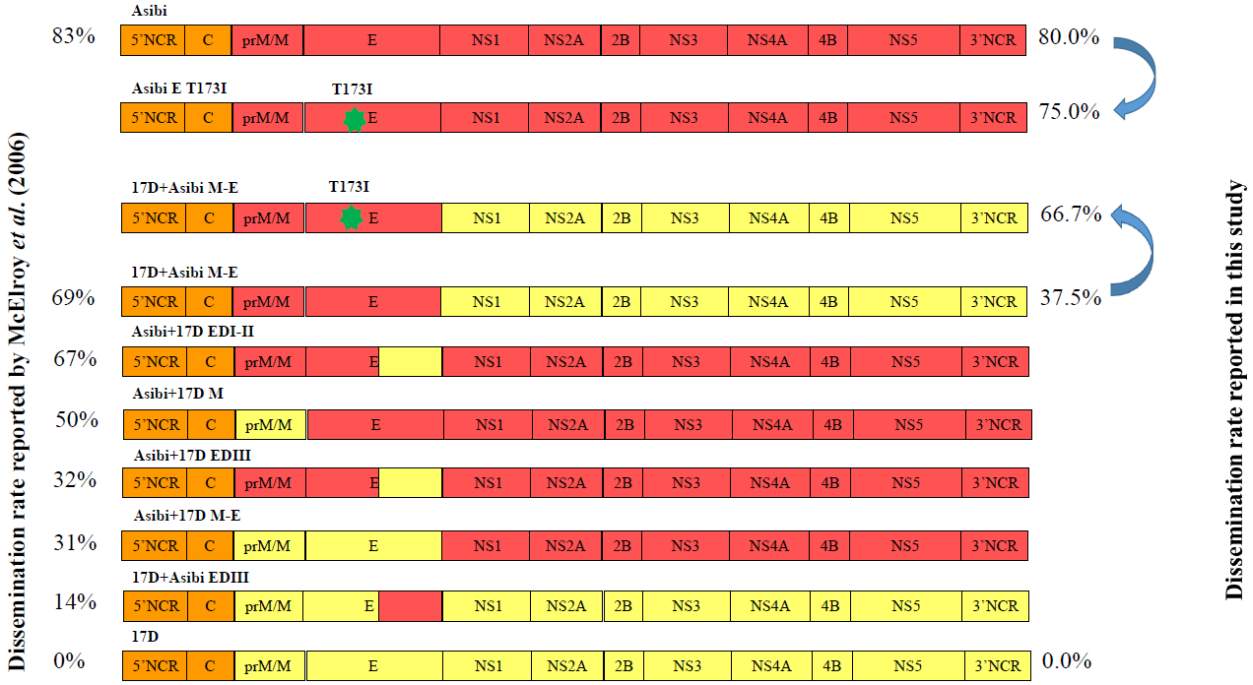

Figure 6.6 The dissemination rate of the YFV structural-gene chimeras reported by McElroy *et al.* (2006) and the YFV E T173I mutants

The dissemination rate of YFV E T173I mutants showed no significant difference from the wildtype controls. It is consistent with the comparable dissemination rate between the Asibi strain and the Asibi+17D-EDI-II chimera. The results are consistent with the observation that the Asibi+17D-EDI-II chimera disseminated in 69% of the infected *Ae. aegypti* at 14 d.p.i., which is comparable to the dissemination rate of the Asibi strain (83%). The Asibi E T173I mutant (75.0%) had the insignificantly lower dissemination rate than the Asibi strain (80.0%). The 17D+Asibi M-E E T173I mutant (66.7%) also had the similar transmission rate as the 17D+Asibi M-E chimera (37.5%) at 14 d.p.i.

In summary, the T173I mutation in the E protein of the Asibi strain did not lead to significant viral attenuation. The Asibi E T173I mutant did not resemble the phenotype of the Asibi+17D EDI-II chimera, which had the significantly lower infectivity than the Asibi strain. Therefore, we conclude that the T173I mutation is not an attenuation determinant of YFV in *Ae. aegypti.*

6.4 The combined G52R and T173I mutations in YFV EDI-EDII

A. Major finding

Both the Asibi E G52R-T173I double mutant and the 17D+Asibi M-E E G52R-T173I double mutant showed the significantly lower infectivity than the Asibi strain and the 17D+Asibi M-E chimera, respectively. The infection rate of the Asibi E G52R-T173I double mutant was significantly lower than the Asibi strain at 10 and 14 d.p.i. The infection rate of the 17D+Asibi M-E E G52R-T173I double mutant was significant lower than the 17D+Asibi M-E chimera at 7 and 14 d.p.i. The YFV E G52R-T173I double mutants maintained the attenuated phenotype of the lower infectivity observed in the YFV E G52R mutants.

The dissemination of the Asibi strain and the 17D+Asibi M-E chimera in infected *Ae. agypti* was not impaired by the G52R and T173I mutations. The infection of the Asibi E G52R-T173I double mutant and the 17D+Asibi M-E E G52R-T173I mutant resulted in the disseminated form of infection at a similar level of the Asibi strain and the 17D+Asibi M-E chimera. The average titers of whole mosquitoes, bodies and secondary bodies did not show a significant difference between the Asibi strain and the Asibi E G52R-T173I mutant or between the 17D+Asibi M-E chimera and the 17D+Asibi M-E E G52R-T173I double mutant.

B. Comparison with the YFV structural-gene chimeras

The infection and dissemination rate of the Asibi E G52R-T173I double mutant and the 17D+Asibi M-E E G52R-T173I double mutant is compared to the YFV structural-gene chimeras and shown in **Figure 6.7** and **Figure 6.8**, respectively.

The infection rate of the Asibi strain was significantly reduced by the 17D E G52R mutation in the EDI-EDII molecular hinge region and the 17D E T173I mutation in the H_0G_0 loop of EDI. The reduction in the infection by the Asibi E G52R-T173I double mutant resembled the reduction of the infection rate by the chimerization of the 17D EDI and EDII with the Asibi strain. The significant loss of viral infectivity was also found significant between the 17D+Asibi M-E chimera and the 17D+Asibi M-E E G52R-T173I double mutant.

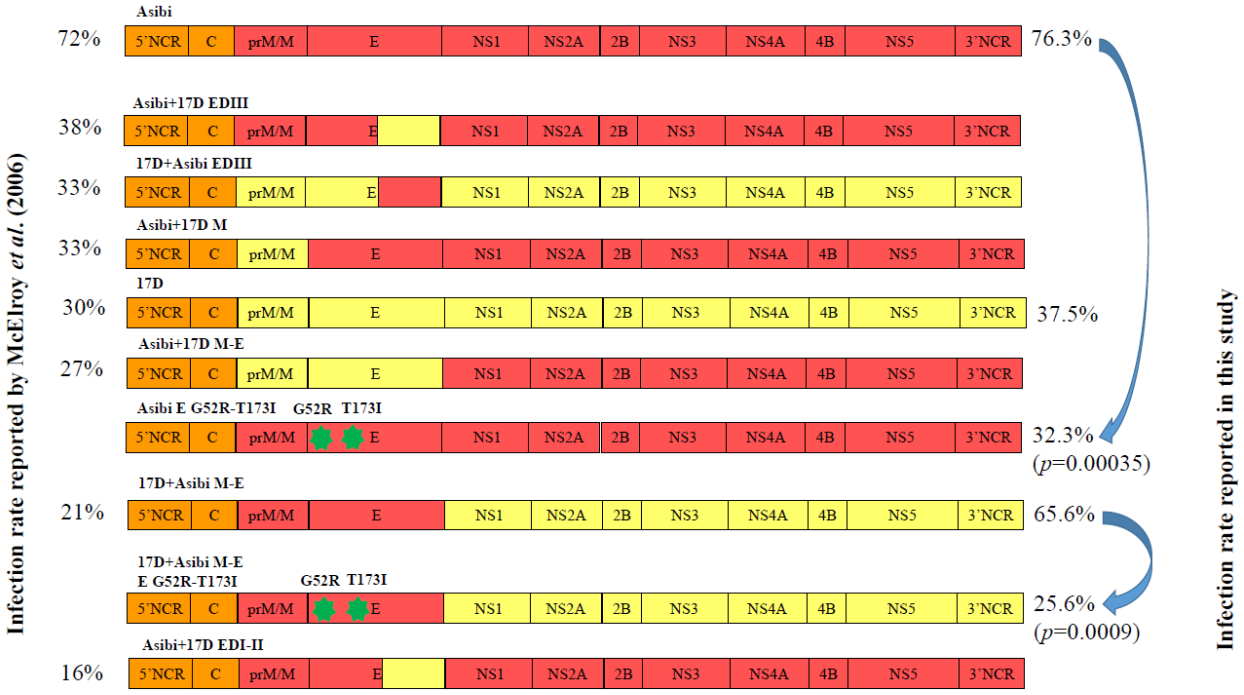

Figure 6.7 The infection rate of the YFV structural-gene chimeras reported by McElroy *et al.* (2006) and the YFV E G52R-T173I double mutants

Although both the Asibi E G52R-T173I double mutant and the 17D+Asibi M-E E G52R-T173I double mutant caused a decrease in the dissemination rate, there was no statistical significance identified in comparison to the Asibi strain and the 17D+Asibi M-E chimera, respectively. The results are consistent with the observation that the Asbi+17D EDI-II chimera, which contain all five mutations in EDI and EDII of 17D strain, did not show a significant reduction in the dissemination rate.

In conclusion, the Asibi E G52R-T173I double mutant and the 17D+Asibi M-E E G52R-T173I double mutant showed the significantly attenuated lower infectivity in comparison to the Asibi strain and the 17D+Asibi M-E chimera. The non-disseminating 17D phenotype was not achieved by inclusion of the G52R and T173I mutations in EDI and EDII of the Asibi strain or the 17D+Asibi M-E chimera. Therefore, neither the simultaneous presence of the G52R and T173I mutations nor the simultaneous presence of the G52R and T173I mutations with other attenuation determinants in the nonstructural genes resulted in the non-disseminating phenotype in the 17D strain.

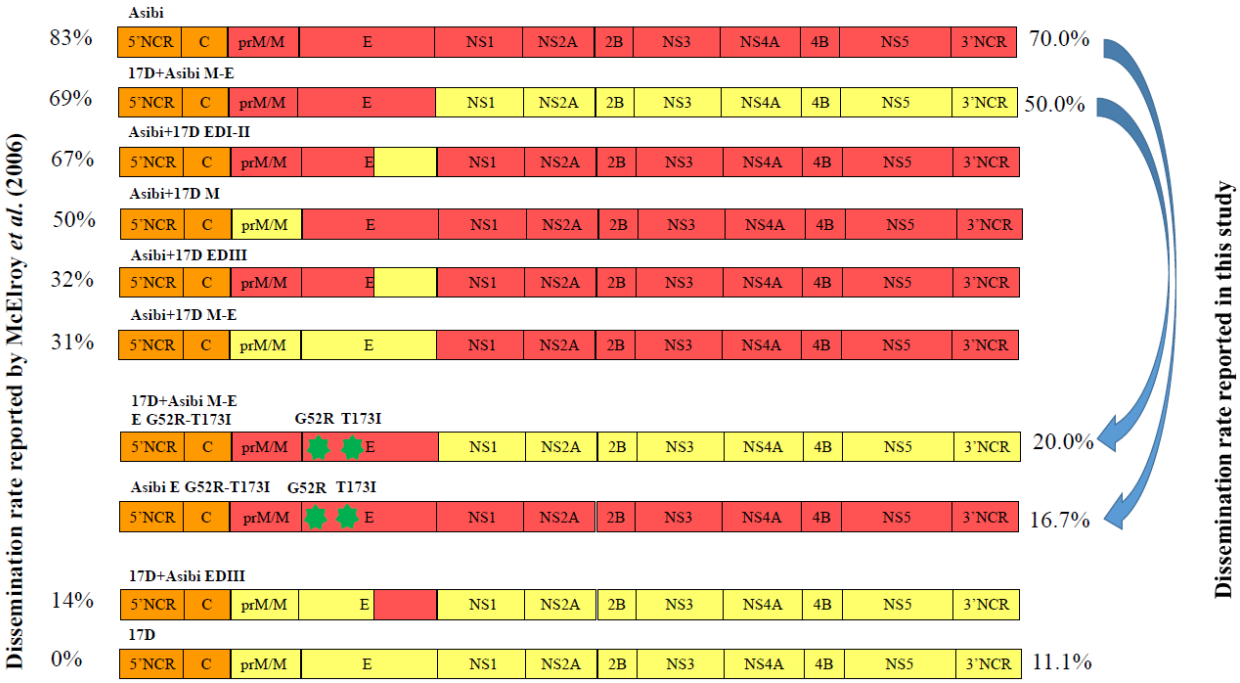

Figure 6.8 The dissemination rate of the YFV structural-gene chimeras reported by McElroy *et al.* (2006) and the YFV E G52R-T173I double mutants

6.5 The M299I mutation in YFV EDI-EDIII linker region

A. Major finding

The characterization of the M299I mutation in the Asibi strain suggested that the M299I mutation is likely to result in the attenuation at the early stage of viral infection in *Ae. aegypti*. The Asibi E M299I mutant showed a significantly lower infection rate than the Asibi strain at 7 d.p.i. However, the attenuation was not observed in the Asibi E M299I mutant at 10 and 14 d.p.i. In contrast to the attenuation observed between the Asibi strain and the Asibi E M299I mutant, the 17D+Asibi M-E E M299I mutant did not show any significant reduction of the infection rate between 7 and 14 d.p.i.

The dissemination of the Asibi E M299I mutant into the secondary tissues implicated that the single M299I mutation in the EDI-EDIII linker region is not sufficient to restrict the replication of the virus in the midgut of infected mosquitoes. There was no demonstrable difference in the dissemination rate between the Asibi strain and the Asibi E M299I mutant between 7 and 14 d.p.i. Although the dissemination rate of the 17D+Asibi M-E E M299I mutant

was lower than that of the 17D+Asibi M-E chimera at 7 and 10 d.p.i., there was no significant difference identified. At 14 d.p.i., the dissemination rate between the 17D+Asibi M-E chimera and the 17D+Asibi M-E E M299I mutant was indistinguishable. The average titers of homogenized whole mosquitoes, bodies and secondary tissues showed no significant difference between the Asibi strain and the Asibi E M299I mutant or between the 17D+Asibi M-E chimera and the 17D+Asibi M-E E M299I mutant.

The Asibi I299M reversion in the E protein of the 17D strain did not fully restore the virulent phenotype of the Asibi strain. The infection rate of the 17D strain and the 17D E I299M revertant showed no distinguishable difference between 7 and 14 d.p.i. Although the dissemination of the 17D E I299M revertant was observed at 7 and 14 d.p.i., The challenge of the 17D E I299M revertant resulted in a significantly lower infection rate than the 17D+Asibi M-E chimera at 10 and 14 d.p.i.

B. Comparison with the YFV structural-gene chimeras

The infection and dissemination rate of the Asibi E M299I mutant and the 17D+Asibi M-E E M299I mutant at 14 d.p.i. are compared with the YFV structural-gene chimeras as shown in **Figure 6.9** and **Figure 6.10**, respectively.

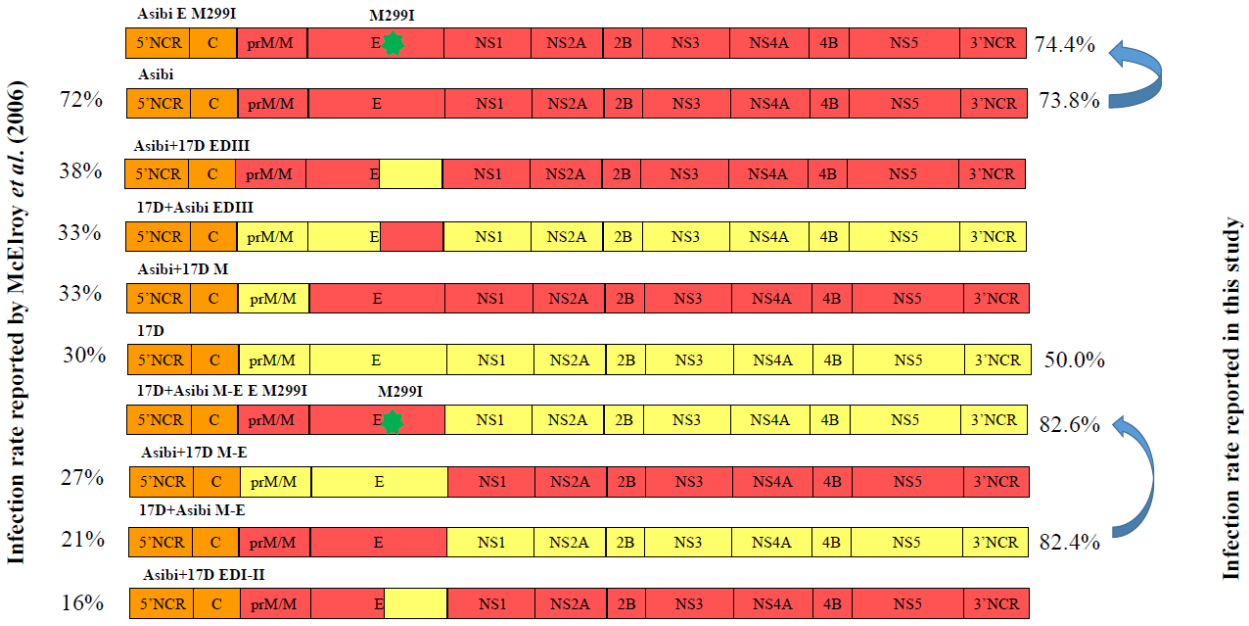

Figure 6.9 The infection rate of the YFV structural-gene chimeras reported by McElroy *et al.* (2006) and the YFV E M299I mutants

The infection rate of the Asibi+17D EDIII chimera at 14 d.p.i. was lower than the Asibi strain. The observation suggested that one or more of the five mutations in EDIII of the 17D strain are likely to be the genetic determinants for the restricted viral replication of the 17D strain in *Ae. aegypti*. Although the Asibi E M299I mutant showed a significantly lower infection rate at 7 d.p.i. than the Asibi strain, the evaluation of the potential viral attenuation caused by the M299I mutation, which is one of the five mutations, in the Asibi E M299I mutant and the 17D+Asibi M-E E M299I mutant demonstrated that the infection rate of both YFV E mutants had no significant difference in comparison to the wildtype controls at 14 d.p.i. Therefore, the observation suggested the continuous identification and characterization for other genetic determinants contributing to the low viral infectivity should further assess other mutations in YFV EDIII.

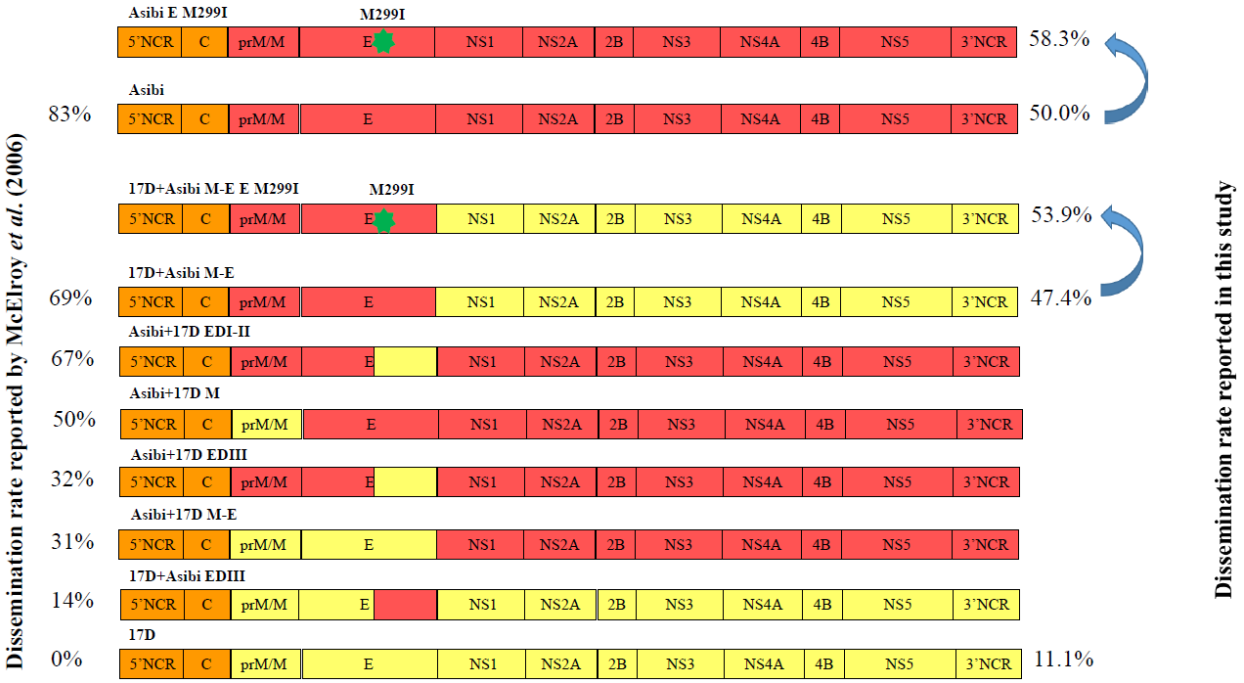

Figure 6.10 The dissemination rate of the YFV structural-gene chimeras reported by McElroy *et al.* (2006) and the YFV 17D E M299I mutants

In contrast to the significantly lower dissemination rate caused by the five mutations in the EDIII of the Asibi+17D EDIII at 14 d.p.i., the single 17D M299I mutation did prevent the viral dissemination from the midgut of the infected mosquitoes. The Asibi E M299I mutant showed only an insignificant change in the dissemination rate compared to the Asibi strain,

which was shown to have the most disseminating phenotype in the study of YFV structural-gene chimeras. Similarly, the dissemination of the 17D+Asibi M-E chimera was not impaired by the M299I mutation.

The assessment of the increase in viral infection and dissemination caused by the I299M genetic reversion is summarized in **Figure 6.11** and **Figure 6.12**, respectively.

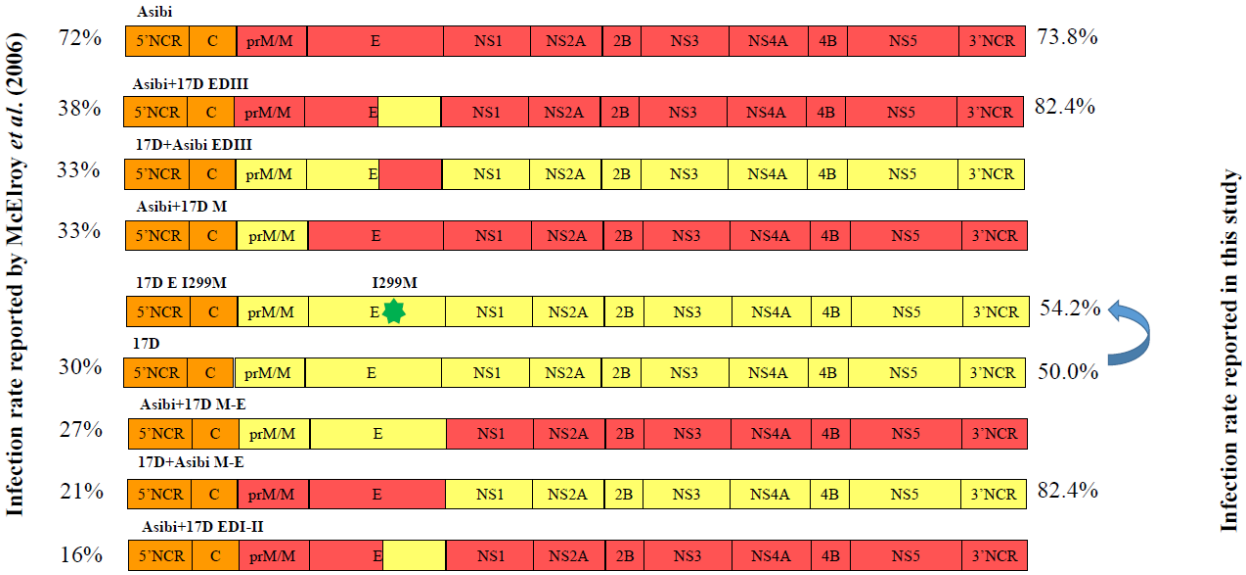

Figure 6.11 The infection rate of the YFV structural-gene chimeras reported by McElroy *et al.* (2006) and the YFV E I299M mutant

The I299M reversion caused a insignificant increase of the infectivity in the 17D strain at 14 d.p.i. The infectivity of the 17D+Asibi M-E chimera, which was comparable to the 17D strain in the study performed with the YFV structural-gene chimeras, remained significantly higher than the 17D E I299M revertant. The higher infection rate of the 17D+Asibi M-E chimera in this study than the 17D I299M revert is likely to arise from the higher viral titer in the viremic blood meals in this study (McElroy, Tsetsarkin et al. 2006). Although the viremic titer of the Asibi strain was relatively lower than that of the 17D E I299M mutant, the Asibi strain was still able to cause the insignificantly higher infection rate than the 17D E I299M mutant. The dissemination rate of the 17D E I299M mutant remained insignificantly lower than the Asibi strain and the 17D+Asibi M-E chimera at 14 d.p.i.

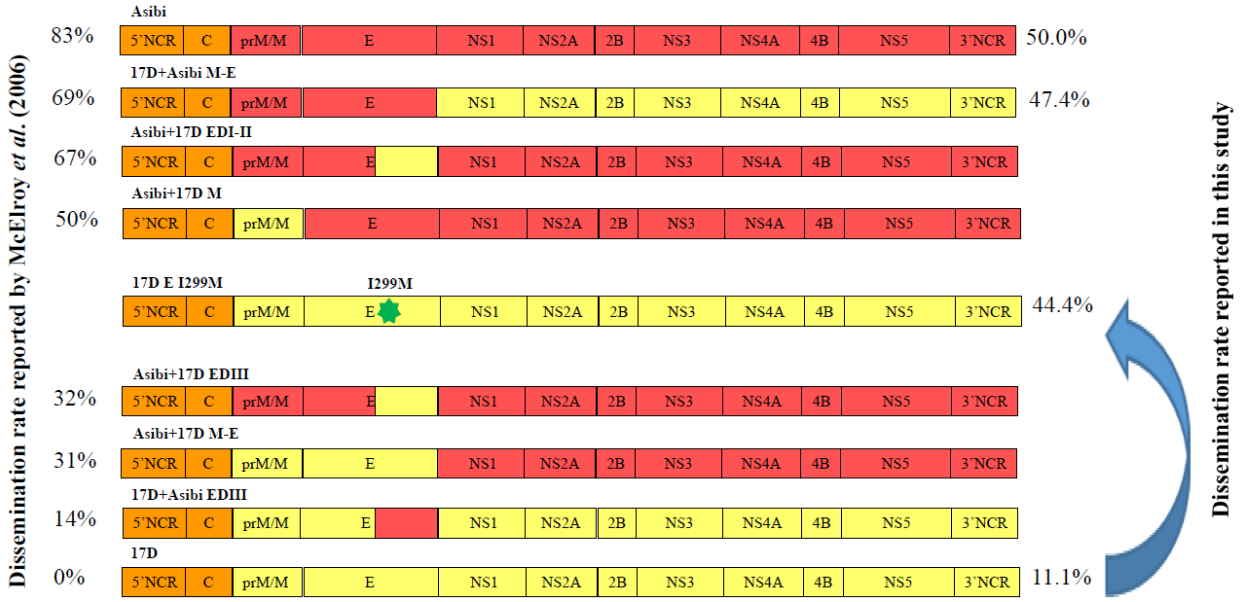

Figure 6.12 The dissemination rate of the YFV structural-gene chimeras reported by McElroy *et al.* (2006) and the YFV E I299M mutant

In summary, we have demonstrated that the 17D M299I mutation is likely to be a genetic determinant for viral attenuation in the mosquito, which occurs at the early stage of viral infection. However, the presence of additional attenuation determinants in YFV EDIII is required in order to significantly limit the viral infection and dissemination in *Ae. aegypti*. In the event of a I299M reversion in a 17D backbone, we would predict that it is unlikely to fully revert the phenotype to that of the infectious and disseminating form characteristic of wild type virulent strains of YFV. The 17D E I299M revertant was significantly less infectious than the 17D+Asibi M-E chimera, which was orally administered at a comparable titer, and insignificantly less infectious than the Asibi strain, which was challenged at a relatively lower titer. Therefore, the lower infection rate of the 17D E I299M revertant should significantly reduce the number of infected mosquitoes, which ultimately would still lead to a lower number of disseminated infections.

6.6 General conclusions and discussion

The study described in this dissertation provided the critical knowledge for the attenuation of YFV in *Ae. aegypti* by further defining the genetic determinants to single amino acid substitutions in the E protein. The mapping of the genetic determinants for the infection and

dissemination of YFV has become more specific to the level of single mutations in specific domains of YFV E protein.

The 17D E T380R mutation has been found to increase the viral infectivity of YFV in *Ae. aegypti*. The mutation has previously been demonstrated to be the genetic determinant for the higher binding affinity between the virions and GAG molecules on the cell surface (Lee and Lobigs 2008). The propagation of the YFV E T380R mutants in BHK-21 cells suggested that the T380R mutation is likely to enhance the propagation of YFV *in vitro*. It is still unknown if the increased propagation of the YFV E T380R mutants *in vitro* is the consequence of the increase in the viral entry resulted from the higher binding affinity of the putative receptors, GAG molecules. The higher infectivity of the YFV E T380R mutants in *Ae. aegypti* suggests the T380R mutation is a contributory genetic determinant for viral attenuation specifically in mammalian hosts. The increase of the viral infectivity by the T380R mutation in the E protein may be diminished whilst the multiple attenuation determinants in the structural and nonstructural proteins of the 17D strains collaboratively attenuate the virus (McElroy, Tsetsarkin et al. 2006, McElroy, Tsetsarkin et al. 2006).

The 17D E G52R mutation significantly attenuated the Asibi strain and the 17D+Asibi M-E chimera and resulted in the significantly lower infection rate in *Ae. aegypti* orally challenged by the Asibi E G52R mutant and the 17D+Asibi M-E E G52R mutant. The results suggested that the selective mutagenesis in the hydrophobic residues in the interface of EDI and EDII is potentially the effective approach to attenuation of YFV and other flaviviruses (Hurrelbrink and McMinn 2001, Butrapet, Childers et al. 2011). The dissemination of the YFV E G52R mutants was not impaired because the dissemination of the Asibi E G52R mutant and the 17D+Asibi M-E E G52R mutant was still observed and resulted in the comparable dissemination rate to the Asibi strain and the 17D+Asibi M-E chimera. It is likely that the attenuated phenotype of the 17D+Asibi M-E chimera further limited the incidence of the dissemination. Therefore, the dissemination of the 17D+Asibi M-E E G52R mutant only occurred at 7 d.p.i. in this study.

The 17D T173I mutation in the YFV E protein, which was previously demonstrated to be the attenuation determinant of mouse neurovirulence, did not result in the significant reduction of viral infection and dissemination in *Ae. aegypti*. The lack of the demonstrable difference in the infection and dissemination rate between the Asibi strain and the Asibi E G52R mutant and

between the 17D+Asibi M-E chimera and the 17D+Asibi M-E E G52R mutant suggests the T173I mutation is not a genetic determinant for the attenuation of YFV in *Ae. aegypti*.

The YFV 17D E G52R-T173I double mutants showed the similar phenotype observed in *Ae. aegypti* orally challenged by the single YFV E G52R mutants. The YFV E G52R-T173I double mutants were less infectious than the parental controls, the Asibi strain and the 17D+Asibi M-E chimera. The dissemination of the YFV E G52R-T173I mutants was also observed in infected *Ae. aegypti*. Therefore, the most plausible explanation for the attenuated phenotype which was associated with the G52R and T173I mutations and led to significantly lower infection rate and the comparable dissemination rate can be attributed to the attenuation caused by the G52R mutation, which also led to the significantly lower viral infectivity and the similar capacity of viral dissemination.

In contrast to the significantly lower infection and dissemination rate among *Ae. aegypti* orally infected by the Asibi+17D EDIII chimera, which contains five amino acid mutations in the EDIII of the 17D strains, at 14 d.p.i., the characterization of the single 17D M299I mutation in the YFV EDI-EDIII linker region suggested that the potential attenuation caused by the M299I mutation is limited at the early stage of viral infection. The infection rate of the Asibi E M299I mutant was significantly lower than that of the Asibi strain only at 7 d.p.i. The continuous propagation of the Asibi E M299I mutant in infected *Ae. aegypti* resulted in no demonstrable difference in the infection rate and the dissemination rate at 10 and 14 d.p.i. Additionally, the M299I mutation did not cause the significant difference in viral infection and dissemination by further attenuating the attenuated 17D+Asibi M-E chimera. The potential to increase the infection and dissemination by introducing the Asibi wild type I299M genetic reversion in the E protein of the 17D strain did not significantly increase the infection rate of the 17D strain but shows the capacity of viral dissemination was likely to be restored by the I299M mutation.

In conclusion, the study described in this dissertation has characterized four genetic mutations in the YFV E protein and identified two attenuation determinants, the G52R mutation in the EDI-EDII molecular hinge region and the M299I mutation in the EDI-EDIII linker region. The G52R mutation and the M299I mutation contributed to the viral attenuation predominantly by reducing the viral infectivity of YFV in *Ae. aegypti* and resembled the phenotype of the Asibi+17D EDI-II chimera and the Asibi+17D EDIII chimera, respectively. The identification of the G52R mutation as an attenuation determinant has provided the knowledge towards the more

definitive mapping of the attenuation caused by the mutations in EDI and EDII of the 17D strains without excluding the possibility of other mutations in EDI and EDII causing the attenuation. Although the M299I mutation was only able to cause the significantly lower infection rate at 7 d.p.i., the observation implicated that the lower infection rate among *Ae. aegypti* orally challenged by the Asibi+17D EDIII chimera at 14 d.p.i. may only be achieved in the presence of additional genetic mutations. Similarly, the reduced dissemination rate of the Asibi+17D EDIII chimera is likely to be the consequence of the attenuation caused by multiple genetic loci. With the two point mutations in the YFV E protein causing the significantly lower infection rate, we are able to conclude that the multiple genetic loci in the E protein are likely to contribute to the reduction of viral infectivity but the genetic loci in the E protein which govern the capacity of viral dissemination into the secondary tissues remain to be identified.

The results describe in this dissertation highlighted the possibility of the G52R mutation and the M299I mutation as candidates for the attenuation determinants of YFV. Furthermore, both mutations are located in the regions of the E protein, where the amino acid sequences are moderately- or highly-conserved in flaviviruses (Butrapet, Childers et al. 2011, de Wispelaere and Yang 2012). Currently, it is still unknown if the G52R mutation is able to cause the significant attenuation of YFV in the vertebrate host. The evidence from the 17D-variant Porterfield strain and the mutations in the homologous region in MVEV suggested its potential role of virulence determinant (Schlesinger, Chapman et al. 1996, Hurrelbrink and McMinn 2001). Therefore, the challenge of the YFV E G52R mutants performed in the available animal models will be helpful for determining the potential contribution of the G52R mutation to viral attenuation. Similarly, the challenge of the YFV E M299I mutants has not yet been performed to determine the phenotypic changes associated with the M299I mutation. The lack of naturally occurring mutants of YFV and other flaviviruses also limited the accessible tools to further characterize the M299I mutation in YFV EDI-EDIII linker region or other mutations in the corresponding region of other flaviviruses. With the significantly lower infection rate observed in the YFV E M299I mutants in this study and the impairment of viral particle assembly by the mutations in the DENV-2 EDI-EDIII linker region in mammalian cell lines, it is highly likely the M299I mutation will result in the viral attenuation of YFV in vertebrate hosts (de Wispelaere and Yang 2012).

Although the characterization of the T173I mutation in EDI did not identify it being responsible for the phenotypic change of YFV in *Ae. aegypti*, the importance of the T173I mutation for viral attenuation should not be underestimated because of its role as the neurovirulence marker of YFV in mice (Carey, Kemp et al. 1972, Ryman, Xie et al. 1997, Ryman, Ledger et al. 1998). With the available mouse model leading to the viscerotropic diseases, the characterization of the T173I mutation by testing its importance in contributing to the viscerotropism of YFV will lead to the more comprehensive understanding of the disease pathogenesis in the vertebrate host (Meier, Gardner et al. 2009).

Although the T380R mutation in YFV EDIII does not lead to the complete attenuation of YFV in *Ae. aegypti*, the importance of the T380R mutation should not be ignored since, it contributes to the attenuated phenotype of the 17D strain via its capacity to assist in the removal of virions from the blood stream (Lee and Lobigs 2008).. The phylogenetic analyses of YFV 17D vaccine strains suggested there are five conserved mutations, which are M299I, S305F, K331R, T380R and A416T in the EDIII between the 17D-204 substrain and the 17DD substrain. Our results have demonstrated the M299I mutation contributes to the attenuation during the early stage of YFV infection and the T380R mutation does not alter the phenotype of YFV in *Ae. aegypti*. The serial passage of YFV Asibi strain in the hamster model suggested the K331R mutation was unable to cause the significant phenotypic change (McArthur, Xiao et al. 2005). The future mapping of the genetic determinants in EDIII for the dissemination of YFV in *Ae. aegypti* should focus on the S305F mutation in the ectodomain of EDIII, where the physical interactions with the host cells and other domains of YFV E protein take place. Additionally, the mechanisms responsible for the increased viral infectivity of the YFV E T380R mutants remain unclear. The T380R mutation is located in the FG loop of YFV EDIII, where the mosquito-borne flaviviruses share the invariantly longer structure than the tick-borne flaviviruses (Rey, Heinz et al. 1995, Modis, Ogata et al. 2004). The presence of the T380R mutation in YFV EDIII resulted in not only the increase of the overall positive charge of the FG loop but also the formation of the RGD motif, which is also largely conserved in the mosquito-borne flaviviruses under the JEV serocomplex, which have been known to infect a wide variety of mosquito species.(Erb et al., 2010) Whether the increase of the positive charge by the substitutions with positively charged amino acids such as arginine in the FG loop or the presence of the RGD motif promotes the infection of the mosquito-borne flaviviruses in the vectors remains to be determined. Such

knowledge is critical for the understanding of the choice of vector species by arboviruses in nature and has the ultimately value in generating the biological non-transmissible live-attenuated vaccines by specifically knocking out or manipulating the genetic composition which promotes the infection in arthropod vectors or inserting the sequences that restricts the infectivity of specific mosquito-borne flaviviruses.

It is clear that the viral genetic sequences controlling the capacity of infection and dissemination of YFV in *Ae. aegypti* are likely to exist in multiple genetic loci of the E protein as the chimerization of the prM, E, NS2A, NS4B and 3' untranslated regions between the Asibi strain and the 17D strain led to the attenuation (Bredenbeek, Kooi et al. 2003, McElroy, Tsetsarkin et al. 2006, McElroy, Tsetsarkin et al. 2006). In this study focusing on the characterization of the mutations in the E protein, we have demonstrated the significant loss of viral infectivity can be achieved by at least two point mutations with the potential genetic determinants which limit the viral dissemination remained to be identified. It is likely that the completely attenuated phenotype resembling the 17D strain requires the assembly of multiple mutations reported in this study and the previously published studies (McElroy, Tsetsarkin et al. 2006, McElroy, Tsetsarkin et al. 2006).

In contrast to the significantly lower infection and dissemination rate at 14 d.p.i. observed in the Asibi+17D EDI-II and the Asibi+17D EDIII chimera, which contain multiple genetic mutations in specific domains of YFV E protein, reported by McElroy *et al*, the single point mutations in the E protein were found to cause the transiently but significantly lower infection rate at 7 and 10 d.p.i. according to the comparison between the wildtype controls and the mutants (McElroy, Tsetsarkin et al. 2006). Therefore, it is likely the presence of multiple genetic mutations is required to produce the attenuated phenotype at 14 d.p.i. after the continuous propagation of YFV in the permissive cells.

The histological examination reported by McElroy *et al*. has demonstrated the infection of the attenuated 17D+Asibi M-E chimera resulted in the distinct patterns in the distribution of antigens from the virulent Asibi strain in the epithelium of infected midguts. The infection of the 17D+Asibi M-E chimera and the 17D strain in the midgut of orally infected *Ae. aegypti* was described to be initially focal at 7 d.p.i. followed by the widespread of antigens at 10 and 14 d.p.i. in comparison with the homogeneous, widespread and dense distribution of viral antigens in the midgut of *Ae. aegypti* infected by the Asibi strain as early as 3 d.p.i. Additionally, the

dissemination of the attenuated 17D+Asibi M-E chimera into the secondary tissues was delayed compared to the Asibi strain although the 17D+Asibi M-E chimera maintained the capacity to disseminate into the same tissues as the Asibi strain (McElroy, Girard et al. 2008). Therefore, the attenuated phenotype of YFV might cause the lower number of the infected cells characterized by the focal distribution of viral antigens in the midgut or the prolonged period for viral replication prior to the dissemination into the other tissues. The similar histological examination will be helpful to determine the phenotypic changes caused by the G52R and M299I mutations in the infection and dissemination of YFV in *Ae. aegypti*. The quantity and distribution of the antigens among the epithelium in the midgut of infected mosquitoes will provide the critical knowledge for determining the change in the viral infectivity of the mutants. As the mutants with single point mutations only resulted in the significantly lower infection rate up to 10 d.p.i., the quantification in the number of antigen-positive epithelial cells especially prior to 7 d.p.i., when the infection rate of both mutants was significantly lower than the wildtype controls, will answer the critical question whether the mutations in the E protein of YFV 17D strains cause the significant loss of the viral infectivity via the less efficient viral entry and subsequently result in the focal distribution of viral antigens. The period required for the transition of the focal distribution of antigens into the widespread distribution of antigens in the infected midguts will provide the information to assess the potential impairment in the capacity of viral dissemination from the primary target cells of YFV. Such observations will be particularly important for the YFV E M299I mutants because the previously published mutagenesis studies in the corresponding region of DENV-2 E protein have suggested the mutants were associated with the lower efficiency of viral particle assembly (de Wispelaere and Yang 2012). Finally, the comparison on the length of the time required for the wildtype controls and the mutants to disseminate into salivary glands will be helpful in determining the differences in the length of the potential extrinsic incubation periods and the likelihood of being transmitted by the arthropod vectors. The characterization of viral dissemination into the secondary tissues described in this dissertation provided the fundamental understanding in whether the mutants are able to disseminate into any of the secondary tissues from the infected midguts. Further examination of the antigens of the mutants in the salivary glands will provide the direct assessment in the likelihood of transmission because the location viral replication in the salivary glands is required prior to the release of infectious virions into the saliva.

Similarly, the further histological examination comparing *Ae. aegypti* between the wildtype controls and the E T380R mutants will be helpful to determine the mechanism for the higher infection rate due to the T380R mutation in the E protein. Although it has been demonstrated as a determinant for the binding affinity with the cellular GAG molecules, the actual phenotype of the YFV E T380R mutants and the other GAG-binding variants of flaviviruses have not yet been characterized in orally infected arthropod vectors except for the oral infection experiments described in this dissertation (Lee and Lobigs 2002, Lee, Hall et al. 2004, Lee and Lobigs 2008). The characterization of the YFV T380R mutants in chapter 3 demonstrated that the T380R mutation in the FG loop of EDIII enhances the infectivity of YFV which carry the sequence of the E protein derived from the Asibi strain. The gap of knowledge prior to the full understanding of how the T380R mutation assists the establishment of infection still exists as the actual mechanisms of the increased infectivity remains unknown. The analyses on the differences in the primarily infected cells and the density of viral antigens in the mosquito midguts will provide the critical knowledge in how the accumulation of the positively-charged mutations in the serially passaged flaviviruses can alter the viral infectivity in the arthropod vectors (Lee and Lobigs 2000).

With the histological evidence, one can anticipate the knowledge can also provide the information regarding to the attenuation of other mosquito-borne flaviviruses because the mutations in the EDI-EDII molecular hinge region in DENV-2, DENV-3, JEV and MVEV and the mutations in the EDI-EDIII linker region of DENV-2 all led to the phenotypic changes that reduce the viral infectivity or virulence (Lee, Weir et al. 1997, Hurrelbrink and McMinn 2001, Monath, Arroyo et al. 2002, Butrapet, Childers et al. 2011, de Wispelaere and Yang 2012). The knowledge is not only critical for the mapping and characterization of attenuation determinants for YFV and other flaviviruses but also potentially applicable to the development of the approach to attenuate other RNA viruses, which share the structure of class II fusion proteins.

6.7 Future directions

A. Characterization of the mutations in the E protein of YFV 17D strains

The results in this dissertation have provided the mechanistic knowledge for viral attenuation caused by four of the eight conserved amino acid substitutions in the ectodomain of the E protein among YFV 17D vaccine strains (Hahn, Dalrymple et al. 1987, dos Santos, Post et

al. 1995). The remaining uncharacterized mutations in the ectodomain of the YFV E protein include the A170V in EDI, the K200T in EDII, and the S305F and the K331R in EDIII. The A170V in the EDI G_0 β-strand and the K331R mutation in the C_x β-strand are the conservative mutations that are expected to maintain the local structures and biochemical properties of the E protein. The minimal influence of the K331R mutation was reported by McArthur *et al*. and has been discussed in section 3.1 (McArthur, Xiao et al. 2005).

As described in **section 4.4,** the K200T mutation in EDII is the other non-conservative mutation remain uncharacterized in EDI and EDII of the YFV 17D strains and shared by the 17D-204 and 17DD substrains (Hahn, Dalrymple et al. 1987, dos Santos, Post et al. 1995). To achieve the more comprehensive understanding in the mechanisms that lead to the significantly lower infection rate of the Asibi+17D EDI-II in *Ae. aegypti*, the evaluation of the K200T mutation should be performed individually by introducing the single K200T mutation and collectively with the G52R mutation, which has been identified as an attenuation determinant in this study, in the Asibi strain and 17D+Asibi M-E chimera.

The other additional mutation that is biochemically non-conservative and remains uncharacterized is the S305F mutation in EDIII. The S305F mutation is conserved in the 17-204 and 17DD substrains. The structural change by substituting the Ser^{305} residue with phenylalanine is shown in **Figure 6.13** The sidechain of the phenylalanine substitution is exposed on the surface of the first β-sheet of YFV EDIII in the upper portion of the structure.

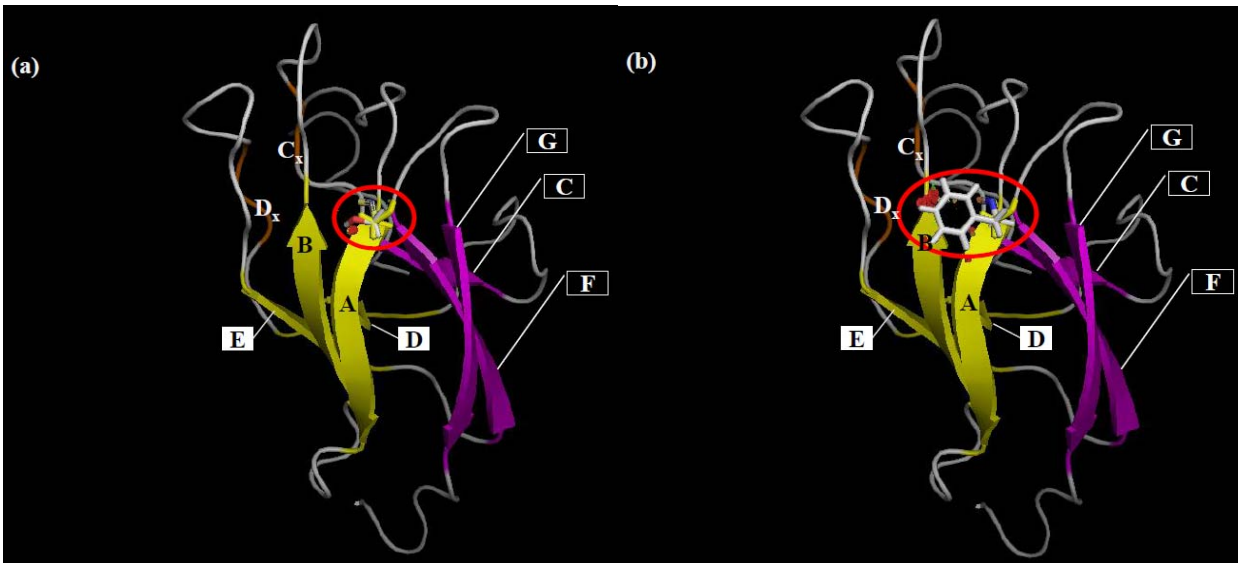

Figure 6.13 The S305F substitution in the A β-strand of YFV EDIII (PDB ID: 2JQM)

(a) The Ser305 residue is displayed with the sidechain containing the hydroxyl group highlighted in red. (b) The S305F substitution is displayed with the aromatic ring structure.

Clearly, the phenylalanine substitution in the amino-terminus of the A β-strand creates a structure that is unique among all the known structures of flavivirus EDIIIs. In all the known NMR structures of flavivirus EDIIIs, the EDIII of the members under the DENV-, YFV- and TBEV-serocomplexes only contain one amino acid with the aromatic-ring sidechain, which is usually packed in the space between the first and third β-sheets, at the first residue of the A β-strand. The EDIII of the members under the JEV-serocomplex contains two amino acid residues with the aromatic-ring sidechain packed in the space between the first and third β-sheets, at the first and third residues of the A β-strand. The amino acid residues containing the sidechain with the aromatic ring in the A β-strand of EDIII are shown in **Figure 6.14**.

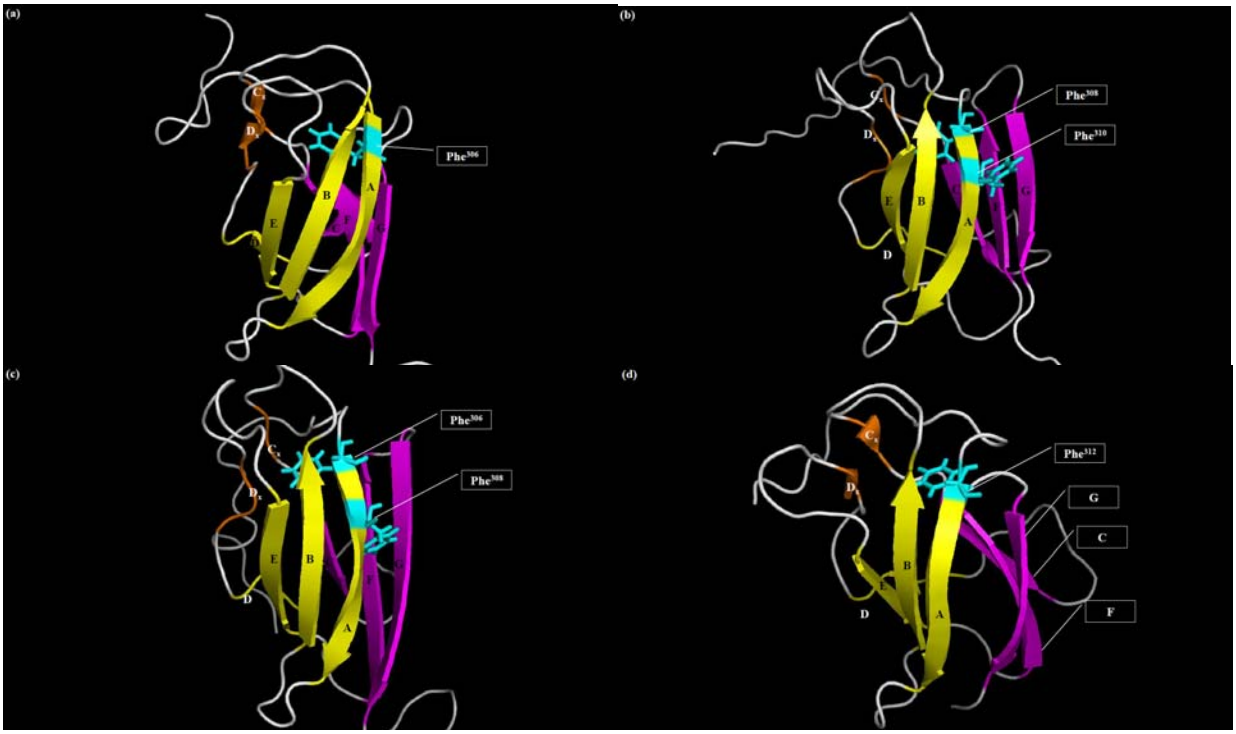

Figure 6.14 Locations and configurations of amino acid residues containing the aromatic-ring sidechain in the A β-strand of flavivirus EDIII (PDB ID: 2JSF;1PJW;1S6N;1Z3R) The NMR structures of flavivirus EDIIIs are listed in the following order, (a) DENV-2 EDIII, (b) JEV EDIII, (c) WNV EDIII and (d) OHFV EDIII. The first, second and third β-sheets are colored in yellow, orange and magenta, respectively. The amino acid residues containing the aromatic ring sidechain are colored in cyan and the structure of the sidechain is displayed in sticks structure.

Based on the available structure of flavivirus E proteins, it is clearly demonstrated that the A β-strand structure is part of the upper portion of EDIII, which is exposed on the surface of virion and likely to interact with the cellular receptors. Due to the lack of the crystal structure of YFV E protein, the S305F residue is shown in the corresponding region of the crystal structure of DENV-2 E dimer in **Figure 6.15**.Whether the unique structure caused by the phenylalanine substitution will result in the changes in the phenotype remains to be characterized.

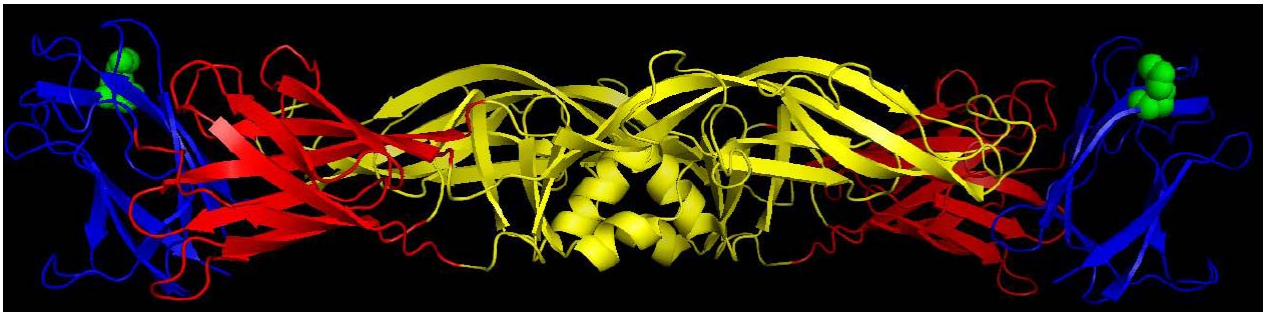

Figure 6.15 Diagrammatic representation of the location of the YFV S305F mutation in the corresponding region of DENV-2 E protein dimer (PDB ID:10AN)
The three domains are colored in red as EDI, yellow as EDII and blue as EDIII. The S305F mutation is shown in green spheres.

B. Characterization of the attenuation mechanism of YFV FNV

Although the parental Asibi strain and the FVV strain were isolated in the same outbreak in the West African coast, the different strategies of attenuating the virulent viruses led to the difference in genetic loci which contribute to the attenuated phenotypes of the 17D strains and the FNV strain (Wang, Ryman et al. 1995). Although the FNV strain has been found to be not only more immunogenic in humans and but also non-disseminating in *Ae. aegypti*, the understanding of the attenuation mechanisms for FNV remains limited (Strode and Rockefeller Foundation. International Health Division. 1951, Deubel 1981). After the manufacture and use of FNV in disease control were discontinued, the characterization on the genetic mutations in the FNV strain is limited to the conserved genetic mutations between the 17D strains and the FNV strain. Both the L36F mutation in the prM protein and the I95M mutation conserved in both vaccine strains in the NS4B protein resulted in the significantly lower infection and dissemination rate in *Ae. aegypti* (McElroy, Tsetsarkin et al. 2006, McElroy, Tsetsarkin et al. 2006).

Currently, the mutations in the E protein of the FNV strain have not yet been characterized for viral attenuation. Interestingly, the genetic heterogeneity exists extensively among the FNV stocks derived from difference sources potentially due to the heterogeneous nature of the FNV strain and the variation in passage history (Wang, Ryman et al. 1995). As reported by Vignuzzi *et al*., the greater genetic diversity of RNA virus may be associated with the higher virulence (Vignuzzi, Wendt et al. 2008). Therefore, the greater genetic diversity of FNV may also contribute to the high incidence of neurological symptoms reported in vaccinated individuals. However, it is clear the continuous propagation of the FVV strain resulted in the accumulation of mutations, which ultimately lead to the change of phenotypes. In the study reported by Wang *et al*., the phenotypes of the variants of the FNV strains in four different laboratories, FNV-FC, FNV-IP, FNV-NT and FNV-CT, showed the different phenotypes in mouse neurovirulence, mouse neuroinvasiveness and primate neurovirulence. The amino acid sequences of the E protein from the four FNV variants suggested there are only three consensus mutations which distinguish the four FNV variants from the FVV strain (Wang, Ryman et al. 1995). Among the four variants, the FNV-IP strain was reported to resemble the phenotype of FNV, which was used in the vaccination in French-speaking regions, with the loss of viscerotropic diseases and the increase of neurovirulence in non-human primates and mice (Strode and Rockefeller Foundation. International Health Division. 1951). Therefore, the FNV-IP strain will be used as a model to discuss the potential attenuation caused by the mutations located in the E protein of FNV.

There is a total of five amino acid mutations in the ectodomain of the E protein including the A54V mutation in the EDI-EDII molecular hinge region, the Q142R mutation and the N153K mutation in EDI and the G227E mutation and the N249D mutation in EDII between the FVV strain and the FNV-IP strain. Interestingly, there was no amino acid substitutions located in YFV EDIII (Wang, Ryman et al. 1995). The comparison of the locations of the mutations in the 17D strains and the FNV strain in the corresponding regions three-dimensional structure of DENV-2 E protein dimer is shown in **Figure 6.16**.

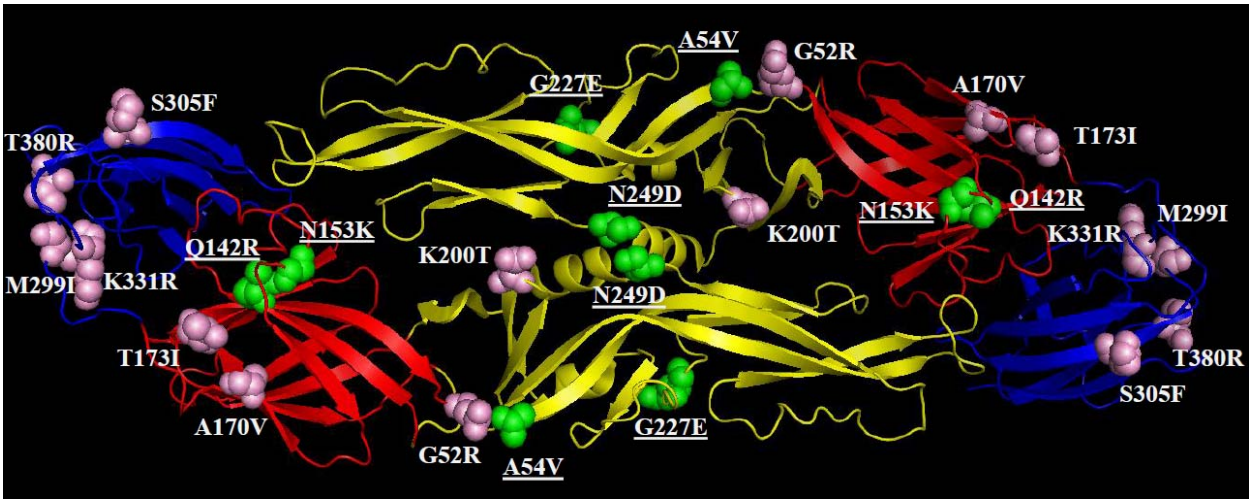

Figure 6.16 The locations of the mutations in the E protein of the 17D strains and the FNV strain in the crystal structure of DENV-2 E protein dimer are highlighted in spheres. (PDB ID: 1OAN)

The structurally central EDI is labeled in red. The dimerization EDII is labeled in yellow. The receptor-binding EDIII is labeled in blue. The mutations in the E protein of the 17D strains are shown in pink and labeled in bold-phased letters and numbers. The mutations in the E protein of the FNV strain are shown in green and labeled in bold-phase and underlined letters and numbers.

The most notable similarity in the locations of the mutations in the 17D strains and the FNV strain exist in the EDI-EDII molecular hinge region, which contains the G52R mutation in the 17D strains and the A54V mutation in the FNV strain. In contrast to the A170V and T173I mutations in the EDI G_0H_0 loop structure on the surface of the viral membrane facing $G_0H_0I_0B_0$ β-sheet, the Q142 mutation and the K153R mutation in EDI of the FNV strain are located in the E_0F_0 loop on the external surface of the $A_0C_0D_0E_0F_0$ β-sheet. The G227E mutation is located in the disordered linear structure between the h and i β-strands of EDII. The region is at the interface of the gfeah β-sheet in the center of EDII and the ij β-sheet forming the elongated structure containing the fusion loop (Rey, Heinz et al. 1995). The likelihood of the G227E serves as a attenuation determinant for viral attenuation is limited because the residue 227 of the E protein in the Asibi strain utilizes the glutamate residue, which is the same as the Glu^{227} residue in the FNV-IP strain (Wang, Jennings et al. 1997). Finally, the corresponding residue of the N249D mutation in DENV-2 E protein is located in the pocket 1 structure of the three pockets providing the interactions between the M protein and the E protein in order to form the E-M-M-E

heterotetramer on the surface of the virion. The structure of three pockets is stabilized largely by the hydrophobic interactions between the M protein and the E protein (Zhang, Ge et al. 2013). The aspartate substitution in the asparagine residue in the N249D mutation reduced the hydrophobicity of the residue but it is unclear whether the attenuation is caused by the destabilization due to the decrease of the hydrophobicity.

In summary, the difference in the locations where the mutations belonging to the 17D strains and the FNV strain are located suggests the potential attenuation caused by the mutations in the E protein of the FNV strain may depend on different mechanisms except for the A54V mutation in the EDI-EDII molecular hinge region. The identification of the attenuation determinants in FNV is likely to provide a different subset of mutagenesis targets for the rationale-based design of live-attenuated flavivirus vaccine candidates. The reverse genetics system of the Asibi strain can be considered as an appropriate tool for the characterization of the mutations in the FNV E protein because the sequences of the E protein between the Asibi strain and the FVV strain only differ at two residues at residue 227 and 331. The characterization of the A54V mutation will lead to the better understanding in the importance of the EDI-EDII molecular hinge region for viral attenuation because the A54V mutation is not only a biochemically conserved mutation and situated in the highly conserved hydrophobic region in the H1 peptide described in **Section 4.1**. The characterization of the N249D mutation in the M protein-binding pocket structure is expected to evaluate the potential of the selective destabilization of the hydrophobic interactions between the heterodimer of the M protein and the E protein as an approach to attenuate flaviviruses. In contrast to the 17D strains, which contain four amino acid substitutions in the ectodomain of EDIII, the sequence of the E proteins among the FNV variants suggested the lack of the mutation in the same region. The T380R mutation distinguishing the Asibi strain and the 17D strains has been characterized as the genetic determinant to increase the viral clearance and limit the viremia, which is required for the viral dissemination into the brains of intravenously challenged AG129 mice (Lee and Lobigs 2008). It will be particularly interesting to test if the introduction of the T380R mutation will further decrease the neurotropism of FNV. The mechanism will be potentially applicable to ensure the safety of the live-attenuated vaccine candidates that may require the further attenuation of the neurotropism.

C. Characterization of the attenuation mechanism of YFV Asibi HeLa-p6 variant

Although the mechanisms remain unknown, the attenuation of various mosquito-borne flaviviruses can be facilitated by the serial passage in HeLa cells (Dunster, Gibson et al. 1990). The serial passage of YFV in HeLa cells led to the Asibi HeLa-p6 variant that shows the different antigenic structures, which can potentially be attributed to the amino acid substitutions in the ectodomain of the E protein, and the significantly lower virulence in mice and monkeys (Converse, Kovatch et al. 1971, Dunster, Wang et al. 1999). The comparison with the porcine kidney (PK) cells-passaged YFV suggested the intrinsic factors in the HeLa cells are critical for the attenuation because the PK-cell-passaged YFV remained virulent to the vertebrate hosts (Converse, Kovatch et al. 1971). The nucleotide sequences of the E gene of the Asibi HeLa-p6 variant identified five mutations in the ectodomain (Dunster, Wang et al. 1999). In order to compare with the mutations determined in the 17D stains and the FNV-IP variant, the five mutations, Q27H, D155A, M228K, K331R and H390P, are mapped in the available crystal structure of DENV-2 E protein dimer and shown in **Figure 6.17**. The comparison of the mutations in the Asibi HeLa-p6 variant with the 17D strains and the FNV-IP variant is summarized in **Figure 6.19** and **Figure 6.20**, respectively.

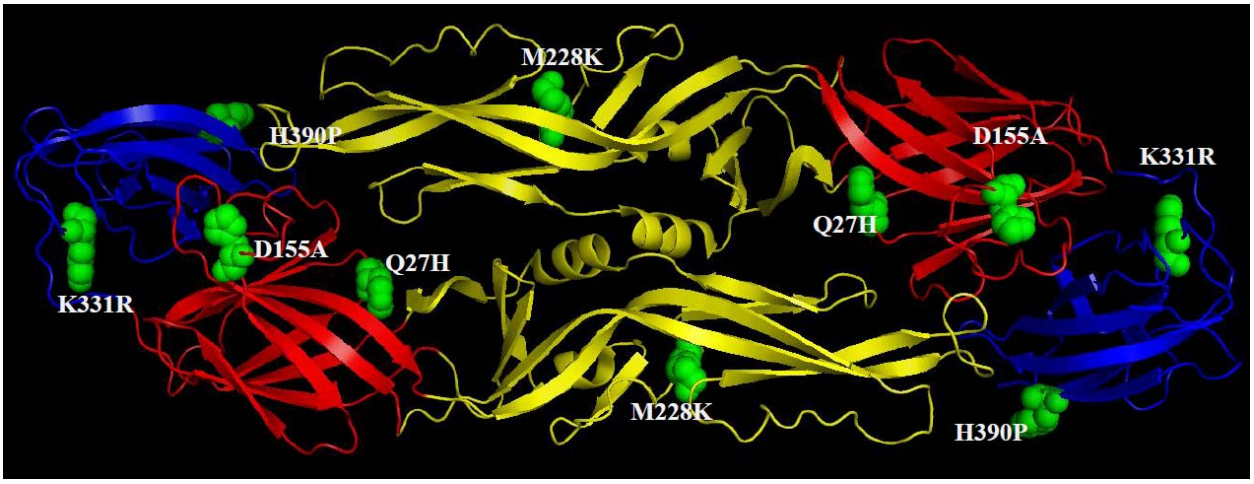

Figure 6.17 The locations of the mutations in the E protein of the Asibi HeLa-p6 variant in the crystal structure of DENV-2 E protein dimer are highlighted in spheres (PDB ID: 1OAN)

The structurally central EDI is labeled in red. The dimerization EDII is labeled in yellow. The receptor-binding EDIII is labeled in blue. The mutations in the E protein of the Asibi HeLa-p6 variant are shown in green and labeled in bold-phase letters and numbers.

In the structurally central EDI, the Q27H mutation and the D155A mutation are located in the B_0C_0 loop and the E_0F_0 loop structure on the external $A_0C_0D_0E_0F_0$ β-sheet. The $A_0C_0D_0E_0F_0$ β-sheet of EDI harbors the Q27H mutation and the D155A mutation above the inner $G_0H_0I_0B_0$ β-sheet. The M228K mutation is identified as part of the disordered structure between the h and i β-strands of EDII. The two regions have not been reported to contain any mutations in the E protein of the 17D strains. In EDIII, the K331R mutation in the small C_x β-strand is the conserved substitution between the 17D strains and the Asibi HeLa-p6 variant (Volk, May et al. 2009). The H390P mutation in EDIII is located at the carboxy-terminus of the ectodomain in the "stem" region prior to the H1 perimembrane helix structure (Zhang, Ge et al. 2013). The stem region was recently found to be packed against the disordered structure between the h and i β-strand, where the M228K mutation is located (Klein, Choi et al. 2013).

Among all the mutations identified in the E protein of the Asibi HeLa-p6 variant, the Q27H mutation in the B_0C_0 loop is located in the unique region between the His^{244} residue in EDII and the His^{282} residue in EDI (Stiasny, Fritz et al. 2011). The relative locations of the mutations and the histidine residues are shown in **Figure 6.18**. Both of the histidine residues are the conserved histidine residues that are subjected to protonation required for the destabilization of the dimer structure prior to the conformation change in the acidic endosome. Interestingly, the Q27H mutation between the His244 residue and the His282 residue results in the additional histidine residue between the two recipient residues of protons. It is unknown whether the substitution with histidine may influence the structural or biochemical properties.

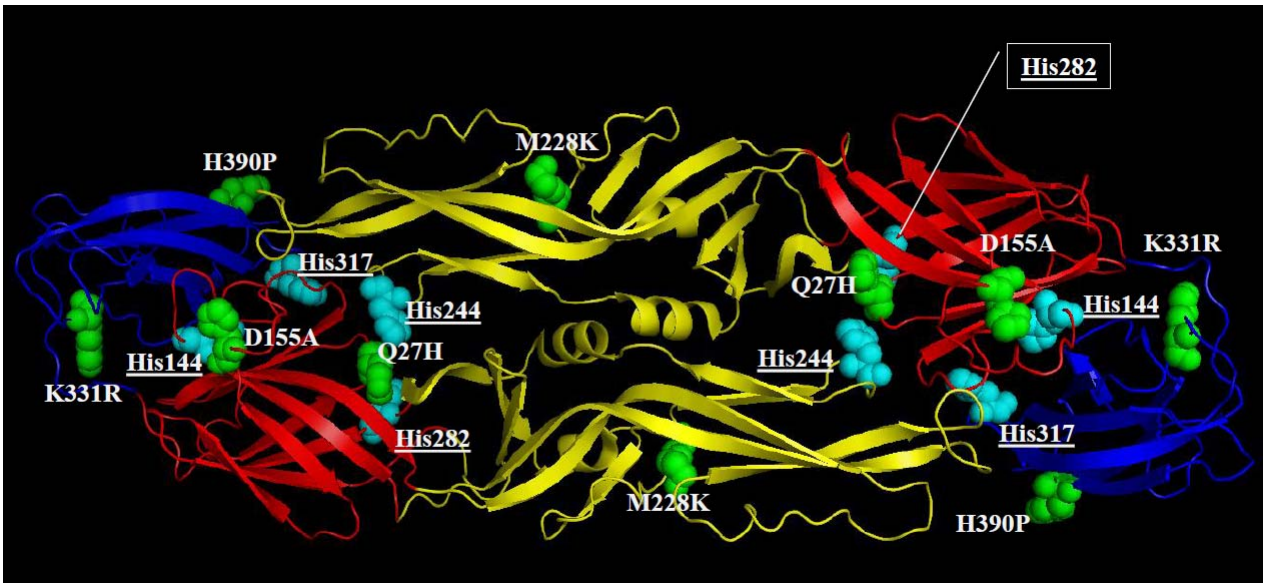

Figure 6.18 The locations of the mutations in the E protein of the Asibi HeLa-p6 variant and the conserved histidine residues as the protonation targets in the crystal structure of DENV-2 E protein dimer are highlighted in spheres (PDB ID: 1OAN)

The structurally central EDI is labeled in red. The dimerization EDII is labeled in yellow. The receptor-binding EDIII is labeled in blue. The mutations in the E protein of the Asibi HeLa-p6 variant are shown in green and labeled in bold-phased letters and numbers. The conserved histidine residues in the E protein are shown in cyan and labeled in bold-phase and underlined letters and numbers.

The mapping of the mutations in the E protein of the 17D strains and the Asibi HeLa-p6 variant suggested the potentially distinct attenuation determinants may exist. The location of the D155A mutation is distinct from the A170V and T173I mutations in EDI of the 17D strain, which are located at the G_0H_0 loop structure on the inner $G_0H_0I_0B_0$ β-sheet facing the viral membrane (Rey, Heinz et al. 1995). The presence of the K331R mutation is likely to be the conservative mutation, which has the limited contribution to viral attenuation similar to the phenotype from the variant of the Asibi strain derived from the passage in Syrian hamster (McArthur, Xiao et al. 2005).

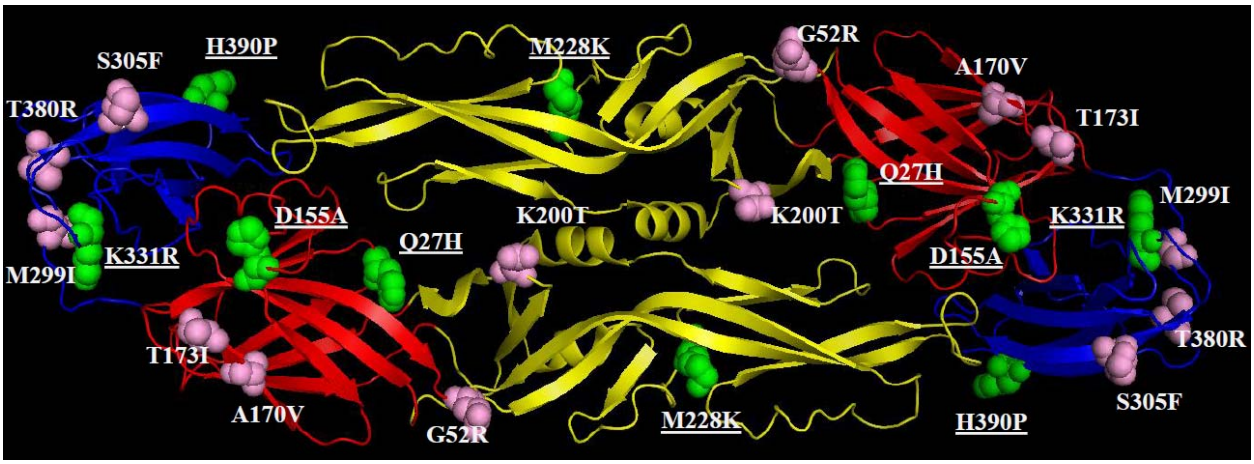

Figure 6.19 The locations of the mutations in the E protein of the 17D strains and the Asibi HeLa-p6 variant in the crystal structure of DENV-2 E protein dimer are highlighted in spheres (PDB ID: 1OAN)

The structurally central EDI is labeled in red. The dimerization EDII is labeled in yellow. The receptor-binding EDIII is labeled in blue. The mutations in the E protein of the 17D strains are shown in pink and labeled in bold-phased letters and numbers. The mutations

in the E protein of the Asibi HeLa-p6 variant are shown in green and labeled in bold-phase and underlined letters and numbers.

The locations of the mutations show the similarity between the FNV-IP variant and the Asibi HeLa-p6 variant. The D155A mutation in the Asibi HeLa-p6 variant and the Q142R mutation and the N153K mutation in the FNV-IP variant are all located in the E_0F_0 loop on the external $A_0C_0D_0E_0F_0$ β-sheet. However, the significant difference in the biochemical properties exists because the D155A mutation in the Asibi HeLa-p6 variant removes the negative charge on the side chain of the glutamate with the substitution of hydrophobic methyl group on the sidechain of alanine but the FNV-IP variant contains two mutations which both lead to the increase of the positive charges with the Q142R mutation and the N153K mutation. The M228K mutation in EDII is located at the junction of the gfeah β-sheet and the ij β-sheet. The local structure consists of the disordered linear structure, which also harbors the G227E mutation conserved in FNV and the FNV variants (Rey, Heinz et al. 1995, Wang, Ryman et al. 1995). It is unclear whether the two mutations in the same region result in the similar phenotypic changes.

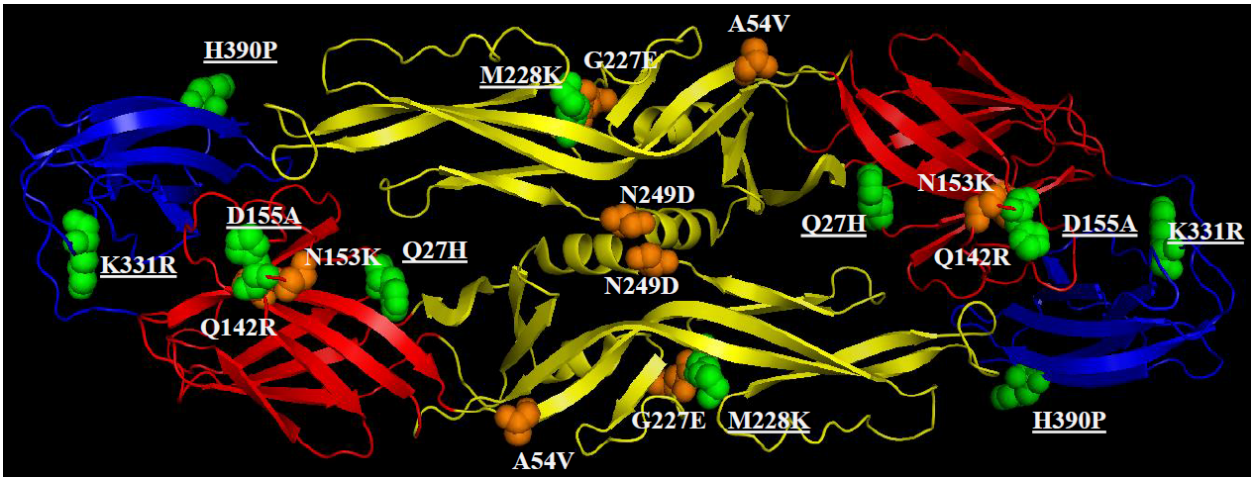

Figure 6.20 The locations of the mutations in the E protein of the FNV-IP variant and the Asibi HeLa-p6 variant in the crystal structure of DENV-2 E protein dimer are highlighted in spheres. (PDB ID: 1OAN)
The structurally central EDI is labeled in red. The dimerization EDII is labeled in yellow. The receptor-binding EDIII is labeled in blue. The mutations in the E protein of the FNV-IP variant are shown in orange and labeled in bold-phased letters and numbers. The mutations in the E protein of the Asibi HeLa-p6 variant are shown in green and labeled in bold-phase and underlined letters and numbers.

The analysis and comparison of the mutations in the E protein among three attenuated strains of YFV based on the structural biological information suggest dissimilar mechanism for viral attenuation may exist. The mutations in the FNV-IP strain and the Asibi HeLa-p6 variant share the similarity in the locations in the E protein. The further characterization on the similarity and the distinctions among the attenuation mechanisms will provide the knowledge required for a significant advancement in the capacity of generating the candidates of live-attenuated flavivirus vaccines by rationale design strategies. Additionally, the mechanistic characterization of the attenuation mechanisms requires not only the platform for mutagenesis based on the molecular virology tools but also the available crystal structures. In contrast to the available crystal structures for the E protein of flaviviruses under DENV-, JEV- and TBEV-serocomplexes, the crystal structure of YFV E protein has not yet been available. The importance of the available crystal structure of YFV E protein has become critical for the determination of viral attenuation and the virulence since the first attempt of characterizing the genetic determinants for neuroinvasiveness of the neuroadapted 17D variants published by Nickells *et al*. (Nickells, Cannella et al. 2008). The study correctly identified the genetic mutations at the Phe^{305}, Lys^{326} and Arg^{380} residues for the phenotypic change *in vitro* and further characterized the E326K mutation as the critical mutation for the neuroinvasiveness in mice. Although the study correctly predicted the locations of the three mutations based on the crystal structure of WNV E protein, the E326K mutation was later found in the BC loop of YFV EDIII, where the high diversity in the sequences and structures exist among flaviviruses (Volk, May et al. 2009, Zhang, Bovshik et al. 2010). The critical role of the crystal structure also can be exemplified by the clustering of mutations in specific regions of the E protein. Using the structurally homologous DENV-2 E protein in this dissertation, one can notice the A170V mutation and the T173I mutation in EDI and the M299I mutation and the T380R mutation in EDIII are located in the neighboring region. The precise determination of the structural change due to multiple mutations can only be achieved by the crystal structure of YFV E protein

D. Genetic heterogeneity of YFV in Ae. aegypti

Recently, the available deep sequencing tool further demonstrated the genetic heterogeneity of YFV is significantly lower in the 17D strains than the Asibi strain (Beck, Tesh et al. 2014). Such observation and the experiments of Polio virus suggest the diversity of the

viral population is critical for the disease pathogenesis and the attenuation (Vignuzzi, Wendt et al. 2008, Beck, Tesh et al. 2014, Tangy and Despres 2014).

In contrast to the discovery that the DENV-2 rapidly accumulated in the vertebrate hosts, the replication in arthropod vectors was reported to result in a less frequent occurrence of attenuation (Chen, Wu et al. 2003, Vasilakis, Deardorff et al. 2009). The current gap of knowledge in the process for the accumulation of mutations in the genomes of arboviruses is that the characterization has been performed with the highly-passaged neurovirulent DENV-2 New Guinea C strain *in vitro*. The experimental conditions may not necessarily reflect the selective barriers in the arthropod vectors (Hardy, Houk et al. 1983). Additionally, the highly-passaged neurovirulent virus may have resulted in the pre-selected viral populations based on the specific phenotype and the lack of the comparison with distinct phenotypes in mosquitoes further limits the likelihood of identifying critical mutations which result in the phenotypic changes in arthropods (Bray, Men et al. 1998).

The techniques used in this study to characterize the YFV mutants in mosquitoes can also be applied to the characterization of YFV derived from tissue culture, which not only exhibits the distinct phenotypes but also contains the genetic heterogeneity among different viral populations. The competition assay can be performed between the infectious-clone-recovered virus and the tissue-culture-derived virus by the insertion of specific genetic marker in the infectious-cloned-recovered virus, the simultaneously challenge of *Ae. aegypti* and the detection of the viral genomes in various mosquito tissues for the characterization of infection and dissemination. Such characterization will be helpful in providing answers to two critical questions regarding to the lifecycle and evolution of arboviruses, if the genetic heterogeneity is required for the infection and dissemination of YFV and if the replication of arboviruses in arthropod vectors results in the slower accumulation of mutations.

In conclusion, the study described in this dissertation has provided the evidence that the genetic determinants which limit the infection of YFV in *Ae. aegypti*. The understanding in the attenuation of YFV has been further improved from the characterization of the individual antigenic domains of the E protein to the identification of single attenuation determinants.

References

Acosta, E. G., V. Castilla and E. B. Damonte (2008). "Functional entry of dengue virus into Aedes albopictus mosquito cells is dependent on clathrin-mediated endocytosis." J Gen Virol **89**(Pt 2): 474-484.

Acosta, E. G., V. Castilla and E. B. Damonte (2011). "Infectious dengue-1 virus entry into mosquito C6/36 cells." Virus Res **160**(1-2): 173-179.

Acosta, E. G., V. Castilla and E. B. Damonte (2012). "Differential requirements in endocytic trafficking for penetration of dengue virus." PLoS One **7**(9): e44835.

Aitken, T. H., W. G. Downs and R. E. Shope (1977). "Aedes aegypti strain fitness for yellow fever virus transmission." Am J Trop Med Hyg **26**(5 Pt 1): 985-989.

Akondy, R. S., N. D. Monson, J. D. Miller, S. Edupuganti, D. Teuwen, H. Wu, F. Quyyumi, S. Garg, J. D. Altman, C. Del Rio, H. L. Keyserling, A. Ploss, C. M. Rice, W. A. Orenstein, M. J. Mulligan and R. Ahmed (2009). "The yellow fever virus vaccine induces a broad and polyfunctional human memory CD8+ T cell response." J Immunol **183**(12): 7919-7930.

Albecka, A., R. Montserret, T. Krey, A. W. Tarr, E. Diesis, J. K. Ball, V. Descamps, G. Duverlie, F. Rey, F. Penin and J. Dubuisson (2011). "Identification of new functional regions in hepatitis C virus envelope glycoprotein E2." J Virol **85**(4): 1777-1792.

Albuquerque, I. G., R. Marandino, A. P. Mendonca, R. M. Nogueira, P. F. Vasconcelos, L. R. Guerra, B. C. Brandao, A. P. Mendonca, G. R. Aguiar and P. A. Bacco (2012). "Chikungunya virus infection: report of the first case diagnosed in Rio de Janeiro, Brazil." Rev Soc Bras Med Trop **45**(1): 128-129.

Alhoot, M. A., S. M. Wang and S. D. Sekaran (2011). "Inhibition of dengue virus entry and multiplication into monocytes using RNA interference." PLoS Negl Trop Dis **5**(11): e1410.

Alhoot, M. A., S. M. Wang and S. D. Sekaran (2012). "RNA interference mediated inhibition of dengue virus multiplication and entry in HepG2 cells." PLoS One **7**(3): e34060.

Allison, S. L., J. Schalich, K. Stiasny, C. W. Mandl and F. X. Heinz (2001). "Mutational evidence for an internal fusion peptide in flavivirus envelope protein E." J Virol **75**(9): 4268-4275.

Altschul, S. F., T. L. Madden, A. A. Schaffer, J. Zhang, Z. Zhang, W. Miller and D. J. Lipman (1997). "Gapped BLAST and PSI-BLAST: a new generation of protein database search programs." Nucleic Acids Res **25**(17): 3389-3402.

Amaku, M., F. A. Coutinho and E. Massad (2011). "Why dengue and yellow fever coexist in some areas of the world and not in others?" Biosystems **106**(2-3): 111-120.

Anderson, C. R. and E. Osorno-Mesa (1946). "The laboratory transmission of yellow fever virus by Haemagogus splendens." Am J Trop Med Hyg **26**(5): 613-618.

Anez, G., R. Men, K. H. Eckels and C. J. Lai (2009). "Passage of dengue virus type 4 vaccine candidates in fetal rhesus lung cells selects heparin-sensitive variants that result in loss of infectivity and immunogenicity in rhesus macaques." J Virol **83**(20): 10384-10394.

Ang, F., A. P. Wong, M. M. Ng and J. J. Chu (2010). "Small interference RNA profiling reveals the essential role of human membrane trafficking genes in mediating the infectious entry of dengue virus." Virol J **7**: 24.

Arensburger, P., K. Megy, R. M. Waterhouse, J. Abrudan, P. Amedeo, B. Antelo, L. Bartholomay, S. Bidwell, E. Caler, F. Camara, C. L. Campbell, K. S. Campbell, C. Casola, M. T. Castro, I.

Chandramouliswaran, S. B. Chapman, S. Christley, J. Costas, E. Eisenstadt, C. Feschotte, C. Fraser-Liggett, R. Guigo, B. Haas, M. Hammond, B. S. Hansson, J. Hemingway, S. R. Hill, C. Howarth, R. Ignell, R. C. Kennedy, C. D. Kodira, N. F. Lobo, C. Mao, G. Mayhew, K. Michel, A. Mori, N. Liu, H. Naveira, V. Nene, N. Nguyen, M. D. Pearson, E. J. Pritham, D. Puiu, Y. Qi, H. Ranson, J. M. Ribeiro, H. M. Roberston, D. W. Severson, M. Shumway, M. Stanke, R. L. Strausberg, C. Sun, G. Sutton, Z. J. Tu, J. M. Tubio, M. F. Unger, D. L. Vanlandingham, A. J. Vilella, O. White, J. R. White, C. S. Wondji, J. Wortman, E. M. Zdobnov, B. Birren, B. M. Christensen, F. H. Collins, A. Cornel, G. Dimopoulos, L. I. Hannick, S. Higgs, G. C. Lanzaro, D. Lawson, N. H. Lee, M. A. Muskavitch, A. S. Raikhel and P. W. Atkinson (2010). "Sequencing of Culex quinquefasciatus establishes a platform for mosquito comparative genomics." Science **330**(6000): 86-88.

Arias, C. F., F. Preugschat and J. H. Strauss (1993). "Dengue 2 virus NS2B and NS3 form a stable complex that can cleave NS3 within the helicase domain." Virology **193**(2): 888-899.

Ashour, J., M. Laurent-Rolle, P. Y. Shi and A. Garcia-Sastre (2009). "NS5 of dengue virus mediates STAT2 binding and degradation." J Virol **83**(11): 5408-5418.

Baillie, G. J., S. O. Kolokotronis, E. Waltari, J. G. Maffei, L. D. Kramer and S. L. Perkins (2008). "Phylogenetic and evolutionary analyses of St. Louis encephalitis virus genomes." Mol Phylogenet Evol **47**(2): 717-728.

Barnett, E. D. (2007). "Yellow fever: epidemiology and prevention." Clin Infect Dis **44**(6): 850-856.

Barnett, H. C. (1956). "The transmission of Western equine encephalitis virus by the mosquito Culex tarsalis Coq." Am J Trop Med Hyg **5**(1): 86-98.

Barrett, A. D. (1997). "Yellow fever vaccines." Biologicals **25**(1): 17-25.

Barrett, A. D. and E. A. Gould (1986). "Antibody-mediated early death in vivo after infection with yellow fever virus." J Gen Virol **67 (Pt 11)**: 2539-2542.

Barrett, A. D. and S. Higgs (2007). "Yellow fever: a disease that has yet to be conquered." Annu Rev Entomol **52**: 209-229.

Barrett, A. D. and T. P. Monath (2003). "Epidemiology and ecology of yellow fever virus." Adv Virus Res **61**: 291-315.

Barrett, A. D., T. P. Monath, C. B. Cropp, J. A. Adkins, T. N. Ledger, E. A. Gould, J. J. Schlesinger, R. M. Kinney and D. W. Trent (1990). "Attenuation of wild-type yellow fever virus by passage in HeLa cells." J Gen Virol **71 (Pt 10)**: 2301-2306.

Barrett, A. D. and D. E. Teuwen (2009). "Yellow fever vaccine - how does it work and why do rare cases of serious adverse events take place?" Curr Opin Immunol **21**(3): 308-313.

Bartosch, B., J. Dubuisson and F. L. Cosset (2003). "Infectious hepatitis C virus pseudo-particles containing functional E1-E2 envelope protein complexes." J Exp Med **197**(5): 633-642.

Bauer, J. H. and N. P. Hudson (1928). "The Incubation Period of Yellow Fever in the Mosquito." J Exp Med **48**(1): 147-153.

Bauer, P., W. Rudin and H. Hecker (1977). "Ultrastructural changes in midgut cells of female Aedes aegypti L. (Insecta, Diptera) after starvation or sugar diet." Cell Tissue Res **177**(2): 215-219.

Beasley, D. W. (2011). "Vaccines and immunotherapeutics for the prevention and treatment of infections with West Nile virus." Immunotherapy **3**(2): 269-285.

Beasley, D. W. and A. D. Barrett (2002). "Identification of neutralizing epitopes within structural domain III of the West Nile virus envelope protein." J Virol **76**(24): 13097-13100.

Beck, A., R. B. Tesh, T. G. Wood, S. G. Widen, K. D. Ryman and A. D. Barrett (2014). "Comparison of the live attenuated yellow fever vaccine 17D-204 strain to its virulent parental strain Asibi by deep sequencing." J Infect Dis **209**(3): 334-344.

Benmerah, A., C. Lamaze, B. Begue, S. L. Schmid, A. Dautry-Varsat and N. Cerf-Bensussan (1998). "AP-2/Eps15 interaction is required for receptor-mediated endocytosis." J Cell Biol **140**(5): 1055-1062.

Bentley, M. D. and J. F. Day (1989). "Chemical ecology and behavioral aspects of mosquito oviposition." Annu Rev Entomol **34**: 401-421.

Berge, T. O., C. A. Gleiser, W. S. Gochenour, Jr., M. L. Miesse and W. D. Tigertt (1961). "Studies on the virus of Venezuelan equine encephalomyelitis. II. Modification by specific immune serum of response of central nervous system of mice." J Immunol **87**: 509-517.

Bertram, D. S. and R. G. Bird (1961). "Studies on mosquito-borne viruses in their vectors. I. The normal fine structure of the midgut epithelium of the adult female Aedes aegypti (L.) and the functional significance of its modification following a blood meal." Trans R Soc Trop Med Hyg **55**: 404-423.

Bielefeldt-Ohmann, H., M. Meyer, D. R. Fitzpatrick and J. S. Mackenzie (2001). "Dengue virus binding to human leukocyte cell lines: receptor usage differs between cell types and virus strains." Virus Res **73**(1): 81-89.

Billingsley, P. F. (1990). "Blood digestion in the mosquito, Anopheles stephensi Liston (Diptera: Culicidae): partial characterization and post-feeding activity of midgut aminopeptidases." Arch Insect Biochem Physiol **15**(3): 149-163.

Boffelli, D., M. A. Nobrega and E. M. Rubin (2004). "Comparative genomics at the vertebrate extremes." Nat Rev Genet **5**(6): 456-465.

Bogachek, M. V., E. V. Protopopova, V. B. Loktev, B. N. Zaitsev, M. Favre, S. K. Sekatskii and G. Dietler (2008). "Immunochemical and single molecule force spectroscopy studies of specific interaction between the laminin binding protein and the West Nile virus surface glycoprotein E domain II." J Mol Recognit **21**(1): 55-62.

Boonsanay, V. and D. R. Smith (2007). "Entry into and production of the Japanese encephalitis virus from C6/36 cells." Intervirology **50**(2): 85-92.

Borucki, M. K., B. J. Kempf, B. J. Blitvich, C. D. Blair and B. J. Beaty (2002). "La Crosse virus: replication in vertebrate and invertebrate hosts." Microbes Infect **4**(3): 341-350.

Bosio, C. F., B. J. Beaty and W. C. t. Black (1998). "Quantitative genetics of vector competence for dengue-2 virus in Aedes aegypti." Am J Trop Med Hyg **59**(6): 965-970.

Bosio, C. F., R. E. Fulton, M. L. Salasek, B. J. Beaty and W. C. t. Black (2000). "Quantitative trait loci that control vector competence for dengue-2 virus in the mosquito Aedes aegypti." Genetics **156**(2): 687-698.

Bowen, M. F. and E. E. Davis (1989). "The effects of allatectomy and juvenile hormone replacement on the development of host-seeking behaviour and lactic acid receptor sensitivity in the mosquito Aedes aegypti." Med Vet Entomol **3**(1): 53-60.

Brandriss, M. W. and J. J. Schlesinger (1984). "Antibody-mediated infection of P388D1 cells with 17D yellow fever virus: effects of chloroquine and cytochalasin B." J Gen Virol **65 (Pt 4)**: 791-794.

Brault, A. C., A. M. Powers, E. C. Holmes, C. H. Woelk and S. C. Weaver (2002). "Positively charged amino acid substitutions in the e2 envelope glycoprotein are associated with the emergence of venezuelan equine encephalitis virus." J Virol **76**(4): 1718-1730.

Brault, A. C., A. M. Powers, D. Ortiz, J. G. Estrada-Franco, R. Navarro-Lopez and S. C. Weaver (2004). "Venezuelan equine encephalitis emergence: enhanced vector infection from a single amino acid substitution in the envelope glycoprotein." Proc Natl Acad Sci U S A **101**(31): 11344-11349.

Bray, M., R. Men, I. Tokimatsu and C. J. Lai (1998). "Genetic determinants responsible for acquisition of dengue type 2 virus mouse neurovirulence." J Virol **72**(2): 1647-1651.

Bredenbeek, P. J., E. A. Kooi, B. Lindenbach, N. Huijkman, C. M. Rice and W. J. Spaan (2003). "A stable full-length yellow fever virus cDNA clone and the role of conserved RNA elements in flavivirus replication." J Gen Virol **84**(Pt 5): 1261-1268.

Breugelmans, J. G., R. F. Lewis, E. Agbenu, O. Veit, D. Jackson, C. Domingo, M. Bothe, W. Perea, M. Niedrig, B. D. Gessner, S. Yactayo and Y. A. group (2013). "Adverse events following yellow fever preventive vaccination campaigns in eight African countries from 2007 to 2010." Vaccine **31**(14): 1819-1829.

Brown, M. R., J. W. Crim and A. O. Lea (1986). "FMRFamide- and pancreatic polypeptide-like immunoreactivity of endocrine cells in the midgut of a mosquito." Tissue Cell **18**(3): 419-428.

Brown, M. R., A. S. Raikhel and A. O. Lea (1985). "Ultrastructure of midgut endocrine cells in the adult mosquito, Aedes aegypti." Tissue Cell **17**(5): 709-721.

Buckley, A. and E. A. Gould (1985). "Neutralization of yellow fever virus studied using monoclonal and polyclonal antibodies." J Gen Virol **66 (Pt 12)**: 2523-2531.

Butrapet, S., T. Childers, K. J. Moss, S. M. Erb, B. E. Luy, A. E. Calvert, C. D. Blair, J. T. Roehrig and C. Y. Huang (2011). "Amino acid changes within the E protein hinge region that affect dengue virus type 2 infectivity and fusion." Virology **413**(1): 118-127.

Calisher, C. H. (2013). Lifting the impenetrable veil : from yellow fever to Ebola hemorrhagic fever and SARS. Red Feather Lakes, Colo., Rockpile Press.

Calvert, A. E., K. L. Dixon, M. J. Delorey, C. D. Blair and J. T. Roehrig (2014). "Development of a small animal peripheral challenge model of Japanese encephalitis virus using interferon deficient AG129 mice and the SA14-14-2 vaccine virus strain." Vaccine **32**(2): 258-264.

Cammisa-Parks, H., L. A. Cisar, A. Kane and V. Stollar (1992). "The complete nucleotide sequence of cell fusing agent (CFA): homology between the nonstructural proteins encoded by CFA and the nonstructural proteins encoded by arthropod-borne flaviviruses." Virology **189**(2): 511-524.

Capelli, G., A. Drago, S. Martini, F. Montarsi, M. Soppelsa, N. Delai, S. Ravagnan, L. Mazzon, F. Schaffner, A. Mathis, M. Di Luca, R. Romi and F. Russo (2011). "First report in Italy of the exotic mosquito species Aedes (Finlaya) koreicus, a potential vector of arboviruses and filariae." Parasit Vectors **4**: 188.

Caplen, H., C. J. Peters and D. H. Bishop (1985). "Mutagen-directed attenuation of Rift Valley fever virus as a method for vaccine development." J Gen Virol **66 (Pt 10)**: 2271-2277.

Cardosa, J., M. H. Ooi, P. H. Tio, D. Perera, E. C. Holmes, K. Bibi and Z. Abdul Manap (2009). "Dengue virus serotype 2 from a sylvatic lineage isolated from a patient with dengue hemorrhagic fever." PLoS Negl Trop Dis **3**(4): e423.

Carey, D. E., G. E. Kemp, J. M. Troup, H. A. White, E. A. Smith, R. F. Addy, A. L. Fom, J. Pifer, E. M. Jones, P. Bres and R. E. Shope (1972). "Epidemiological aspects of the 1969 yellow fever epidemic in Nigeria." Bull World Health Organ **46**(5): 645-651.

CDC (1975). International catalogue of arboviruses; including certain other viruses of vertebrates, Centers for Disease Control and Prevention (U.S.).

CDC. (2014). "Yellow fever vaccine shortage." from http://wwwnc.cdc.gov/travel/news-announcements/yellow-fever-vaccine-shortage-2014.

Centers for Disease, C. and Prevention (2002). "Adverse events associated with 17D-derived yellow fever vaccination--United States, 2001-2002." MMWR Morb Mortal Wkly Rep **51**(44): 989-993.

Centers for Disease, C. and Prevention (2002). "Fatal yellow fever in a traveler returning from Amazonas, Brazil, 2002." MMWR Morb Mortal Wkly Rep **51**(15): 324-325.

Chamberlain, R. W. (1982). "Arbovirology--then and now." Am J Trop Med Hyg **31**(3 Pt 1): 430-437.

Chambers, T. J., A. Grakoui and C. M. Rice (1991). "Processing of the yellow fever virus nonstructural polyprotein: a catalytically active NS3 proteinase domain and NS2B are required for cleavages at dibasic sites." J Virol **65**(11): 6042-6050.

Chambers, T. J., C. S. Hahn, R. Galler and C. M. Rice (1990). "Flavivirus genome organization, expression, and replication." Annu Rev Microbiol **44**: 649-688.

Chambers, T. J., R. C. Weir, A. Grakoui, D. W. McCourt, J. F. Bazan, R. J. Fletterick and C. M. Rice (1990). "Evidence that the N-terminal domain of nonstructural protein NS3 from yellow fever virus is a serine protease responsible for site-specific cleavages in the viral polyprotein." Proc Natl Acad Sci U S A **87**(22): 8898-8902.

Chen, B. Q. and B. J. Beaty (1982). "Japanese encephalitis vaccine (2-8 strain) and parent (SA 14 strain) viruses in Culex tritaeniorhynchus mosquitoes." Am J Trop Med Hyg **31**(2): 403-407.

Chen, H. L., S. Y. Her, K. C. Huang, H. T. Cheng, C. W. Wu, S. C. Wu and J. W. Cheng (2010). "Identification of a heparin binding peptide from the Japanese encephalitis virus envelope protein." Biopolymers **94**(3): 331-338.

Chen, W., N. Gao, J. L. Wang, Y. P. Tian, Z. T. Chen and J. An (2008). "Vimentin is required for dengue virus serotype 2 infection but microtubules are not necessary for this process." Arch Virol **153**(9): 1777-1781.

Chen, W. J., H. R. Wu and S. S. Chiou (2003). "E/NS1 modifications of dengue 2 virus after serial passages in mammalian and/or mosquito cells." Intervirology **46**(5): 289-295.

Chen, Y., T. Maguire, R. E. Hileman, J. R. Fromm, J. D. Esko, R. J. Linhardt and R. M. Marks (1997). "Dengue virus infectivity depends on envelope protein binding to target cell heparan sulfate." Nat Med **3**(8): 866-871.

Cheng, G., J. Cox, P. Wang, M. N. Krishnan, J. Dai, F. Qian, J. F. Anderson and E. Fikrig (2010). "A C-type lectin collaborates with a CD45 phosphatase homolog to facilitate West Nile virus infection of mosquitoes." Cell **142**(5): 714-725.

Chernomordik, L. V. and M. M. Kozlov (2003). "Protein-lipid interplay in fusion and fission of biological membranes." Annu Rev Biochem **72**: 175-207.

Chiou, S. S. and W. J. Chen (2007). "Phenotypic changes in the Japanese encephalitis virus after one passage in Neuro-2a cells: generation of attenuated strains of the virus." Vaccine **26**(1): 15-23.

Chiou, S. S., H. Liu, C. K. Chuang, C. C. Lin and W. J. Chen (2005). "Fitness of Japanese encephalitis virus to Neuro-2a cells is determined by interactions of the viral envelope protein with highly sulfated glycosaminoglycans on the cell surface." J Med Virol **76**(4): 583-592.

Chosewood, L. C., D. E. Wilson, Centers for Disease Control and Prevention (U.S.) and National Institutes of Health (U.S.) (2009). Biosafety in microbiological and biomedical laboratories. Washington, D.C., U.S. Dept. of Health and Human Services, Public Health Service, Centers for Disease Control and Prevention, National Institutes of Health.

Chu, J. J., P. W. Leong and M. L. Ng (2006). "Analysis of the endocytic pathway mediating the infectious entry of mosquito-borne flavivirus West Nile into Aedes albopictus mosquito (C6/36) cells." Virology **349**(2): 463-475.

Chu, J. J. and M. L. Ng (2004). "Interaction of West Nile virus with alpha v beta 3 integrin mediates virus entry into cells." J Biol Chem **279**(52): 54533-54541.

Clements, D. E., B. A. Coller, M. M. Lieberman, S. Ogata, G. Wang, K. E. Harada, J. R. Putnak, J. M. Ivy, M. McDonell, G. S. Bignami, I. D. Peters, J. Leung, C. Weeks-Levy, E. T. Nakano and T. Humphreys (2010). "Development of a recombinant tetravalent dengue virus vaccine: immunogenicity and efficacy studies in mice and monkeys." Vaccine **28**(15): 2705-2715.

Coia, G., M. D. Parker, G. Speight, M. E. Byrne and E. G. Westaway (1988). "Nucleotide and complete amino acid sequences of Kunjin virus: definitive gene order and characteristics of the virus-specified proteins." J Gen Virol **69 (Pt 1)**: 1-21.

Converse, J. L., R. M. Kovatch, J. D. Pulliam, S. C. Nagle, Jr. and E. M. Snyder (1971). "Virulence and pathogenesis of yellow fever virus serially passaged in cell culture." Appl Microbiol **21**(6): 1053-1057.

Cook, S., G. Moureau, R. E. Harbach, L. Mukwaya, K. Goodger, F. Ssenfuka, E. Gould, E. C. Holmes and X. de Lamballerie (2009). "Isolation of a novel species of flavivirus and a new strain of Culex flavivirus (Flaviviridae) from a natural mosquito population in Uganda." J Gen Virol **90**(Pt 11): 2669-2678.

Crabtree, M. B., P. T. Nga and B. R. Miller (2009). "Isolation and characterization of a new mosquito flavivirus, Quang Binh virus, from Vietnam." Arch Virol **154**(5): 857-860.

Crabtree, M. B., R. C. Sang, V. Stollar, L. M. Dunster and B. R. Miller (2003). "Genetic and phenotypic characterization of the newly described insect flavivirus, Kamiti River virus." Arch Virol **148**(6): 1095-1118.

Crampton, J. M., C. B. Beard and C. Louis (1997). The molecular biology of insect disease vectors : a methods manual. London ; New York, Chapman and Hall.

Cupp, M. S., J. M. Ribeiro, D. E. Champagne and E. W. Cupp (1998). "Analyses of cDNA and recombinant protein for a potent vasoactive protein in saliva of a blood-feeding black fly, Simulium vittatum." J Exp Biol **201**(Pt 10): 1553-1561.

Daffis, S., R. E. Kontermann, J. Korimbocus, H. Zeller, H. D. Klenk and J. Ter Meulen (2005). "Antibody responses against wild-type yellow fever virus and the 17D vaccine strain: characterization with human monoclonal antibody fragments and neutralization escape variants." Virology **337**(2): 262-272.

Daffis, S., K. J. Szretter, J. Schriewer, J. Li, S. Youn, J. Errett, T. Y. Lin, S. Schneller, R. Zust, H. Dong, V. Thiel, G. C. Sen, V. Fensterl, W. B. Klimstra, T. C. Pierson, R. M. Buller, M. Gale, Jr., P. Y. Shi and M. S. Diamond (2010). "2'-O methylation of the viral mRNA cap evades host restriction by IFIT family members." Nature **468**(7322): 452-456.

Dalrymple, N. and E. R. Mackow (2011). "Productive dengue virus infection of human endothelial cells is directed by heparan sulfate-containing proteoglycan receptors." J Virol **85**(18): 9478-9485.

Darwish, M. A. and W. M. Hammon (1966). "Studies on Japanese B encephalitis virus vaccines from tissue culture. VI. Development of

a hamster kidney tissue culture inactivated vaccine for man. (1). Obtaining maximum titers of virus using an attenuated strain of OCT-541." J Immunol **96**(4): 691-698.

Das, S., S. Chakraborty and A. Basu (2010). "Critical role of lipid rafts in virus entry and activation of phosphoinositide 3' kinase/Akt signaling during early stages of Japanese encephalitis virus infection in neural stem/progenitor cells." J Neurochem **115**(2): 537-549.

Das, S., S. V. Laxminarayana, N. Chandra, V. Ravi and A. Desai (2009). "Heat shock protein 70 on Neuro2a cells is a putative receptor for Japanese encephalitis virus." Virology **385**(1): 47-57.

Davidson, M. M., H. Williams and J. A. Macleod (1991). "Louping ill in man: a forgotten disease." J Infect **23**(3): 241-249.

Davis, C. W., H. Y. Nguyen, S. L. Hanna, M. D. Sanchez, R. W. Doms and T. C. Pierson (2006). "West Nile virus discriminates between DC-SIGN and DC-SIGNR for cellular attachment and infection." J Virol **80**(3): 1290-1301.

Day, M. F. (1954). "The mechanism of food distribution to midgut or diverticula in the mosquito." Aust J Biol Sci **7**(4): 515-524.

De Cock, K. M., T. P. Monath, A. Nasidi, P. M. Tukei, J. Enriquez, P. Lichfield, R. B. Craven, A. Fabiyi, B. C. Okafor, C. Ravaonjanahary and et al. (1988). "Epidemic yellow fever in eastern Nigeria, 1986." Lancet **1**(8586): 630-633.

de Figueiredo, M. L., C. G. A. de, A. A. Amarilla, S. L. A. de, S. O. A. de, R. F. de Araujo, S. M. C. J. do, E. L. Durigon, V. H. Aquino and L. T. Figueiredo (2010). "Mosquitoes infected with dengue viruses in Brazil." Virol J **7**: 152.

De Rodaniche, E., P. Galindo and C. M. Johnson (1957). "Isolation of yellow fever virus from Haemagogus lucifer, H. equinus, H. spegazzinii falco, Sabethes chloropterus and Anopheles neivai

captured in Panama in the fall of 1956." Am J Trop Med Hyg **6**(4): 681-685.

de Wispelaere, M. and P. L. Yang (2012). "Mutagenesis of the DI/DIII linker in dengue virus envelope protein impairs viral particle assembly." J Virol **86**(13): 7072-7083.

Deardorff, E. R., R. A. Nofchissey, J. A. Cook, A. G. Hope, A. Tsvetkova, S. L. Talbot and G. D. Ebel (2013). "Powassan virus in mammals, Alaska and New Mexico, U.S.A., and Russia, 2004-2007." Emerg Infect Dis **19**(12): 2012-2016.

Deitsch, K. W., J. S. Chen and A. S. Raikhel (1995). "Indirect control of yolk protein genes by 20-hydroxyecdysone in the fat body of the mosquito, Aedes aegypti." Insect Biochem Mol Biol **25**(4): 449-454.

Dejnirattisai, W., A. Jumnainsong, N. Onsirisakul, P. Fitton, S. Vasanawathana, W. Limpitikul, C. Puttikhunt, C. Edwards, T. Duangchinda, S. Supasa, K. Chawansuntati, P. Malasit, J. Mongkolsapaya and G. Screaton (2010). "Cross-reacting antibodies enhance dengue virus infection in humans." Science **328**(5979): 745-748.

Dekker, T. and W. Takken (1998). "Differential responses of mosquito sibling species Anopheles arabiensis and An. quadriannulatus to carbon dioxide, a man or a calf." Med Vet Entomol **12**(2): 136-140.

Despres, P., A. Ruiz-Linares, A. Cahour, M. Girard, C. Wychowski and M. Bouloy (1990). "The 15 amino acid residues preceding the amino terminus of the envelope protein in the yellow fever virus polyprotein precursor act as a signal peptide." Virus Res **16**(1): 59-75.

Deubel, V., Camicas, J. L., Pandare, D., Robert, V., Digoutte, J. P., & Germain, M. (1981). "Développement de souches sauvages et vaccinales du virus de la fièvre jaune dans les cellules de aedes

aegypti et transmission au souriceau." Annales de l'Institut Pasteur/Virologie **132**(1): 41-50.

Diallo, M., Y. Ba, A. A. Sall, O. M. Diop, J. A. Ndione, M. Mondo, L. Girault and C. Mathiot (2003). "Amplification of the sylvatic cycle of dengue virus type 2, Senegal, 1999-2000: entomologic findings and epidemiologic considerations." Emerg Infect Dis **9**(3): 362-367.

Dinglasan, R. R., A. Alaganan, A. K. Ghosh, A. Saito, T. H. van Kuppevelt and M. Jacobs-Lorena (2007). "Plasmodium falciparum ookinetes require mosquito midgut chondroitin sulfate proteoglycans for cell invasion." Proc Natl Acad Sci U S A **104**(40): 15882-15887.

dos Santos, C. N., P. R. Post, R. Carvalho, Ferreira, II, C. M. Rice and R. Galler (1995). "Complete nucleotide sequence of yellow fever virus vaccine strains 17DD and 17D-213." Virus Res **35**(1): 35-41.

Downs, W. G., C. R. Anderson and L. Spence (1955). "Isolation of yellow fever virus from a human patient on the twelfth day of illness." Trans R Soc Trop Med Hyg **49**(6): 577-579.

Dungu, B., I. Louw, A. Lubisi, P. Hunter, B. F. von Teichman and M. Bouloy (2010). "Evaluation of the efficacy and safety of the Rift Valley Fever Clone 13 vaccine in sheep." Vaccine **28**(29): 4581-4587.

Dunster, L. M., C. A. Gibson, J. R. Stephenson, P. D. Minor and A. D. Barrett (1990). "Attenuation of virulence of flaviviruses following passage in HeLa cells." J Gen Virol **71 (Pt 3)**: 601-607.

Dunster, L. M., H. Wang, K. D. Ryman, B. R. Miller, S. J. Watowich, P. D. Minor and A. D. Barrett (1999). "Molecular and biological changes associated with HeLa cell attenuation of wild-type yellow fever virus." Virology **261**(2): 309-318.

Durbin, A. P., B. D. Kirkpatrick, K. K. Pierce, D. Elwood, C. J. Larsson, J. C. Lindow, C. Tibery, B. P. Sabundayo, D. Shaffer, K. R. Talaat,

N. A. Hynes, K. Wanionek, M. P. Carmolli, C. J. Luke, B. R. Murphy, K. Subbarao and S. S. Whitehead (2013). "A single dose of any of four different live attenuated tetravalent dengue vaccines is safe and immunogenic in flavivirus-naive adults: a randomized, double-blind clinical trial." J Infect Dis **207**(6): 957-965.

Edelman, R., C. O. Tacket, S. S. Wasserman, S. A. Bodison, J. G. Perry and J. A. Mangiafico (2000). "Phase II safety and immunogenicity study of live chikungunya virus vaccine TSI-GSD-218." Am J Trop Med Hyg **62**(6): 681-685.

Eldridge, B. F. and J. D. Edman (2003). Medical entomology : a textbook on public health and veterinary problems caused by arthropods. Dordrecht ; Boston, Kluwer Academic Publishers.

Ellis, B. R. and A. D. Barrett (2008). "The enigma of yellow fever in East Africa." Rev Med Virol **18**(5): 331-346.

Elton, N. W. (1955). "Anticipated progress of yellow fever in Guatemala and Mexico, 1955-59." Am J Public Health Nations Health **45**(7): 923-927.

Enayati, A. and J. Hemingway (2010). "Malaria management: past, present, and future." Annu Rev Entomol **55**: 569-591.

Erb, S. M., S. Butrapet, K. J. Moss, B. E. Luy, T. Childers, A. E. Calvert, S. J. Silengo, J. T. Roehrig, C. Y. Huang and C. D. Blair (2010). "Domain-III FG loop of the dengue virus type 2 envelope protein is important for infection of mammalian cells and Aedes aegypti mosquitoes." Virology **406**(2): 328-335.

Evans, A. M., K. G. Aimanova and S. S. Gill (2009). "Characterization of a blood-meal-responsive proton-dependent amino acid transporter in the disease vector, Aedes aegypti." J Exp Biol **212**(Pt 20): 3263-3271.

Farfan-Ale, J. A., M. A. Lorono-Pino, J. E. Garcia-Rejon, E. Hovav, A. M. Powers, M. Lin, K. S. Dorman, K. B. Platt, L. C. Bartholomay,

V. Soto, B. J. Beaty, R. S. Lanciotti and B. J. Blitvich (2009). "Detection of RNA from a novel West Nile-like virus and high prevalence of an insect-specific flavivirus in mosquitoes in the Yucatan Peninsula of Mexico." Am J Trop Med Hyg **80**(1): 85-95.

Fibriansah, G., J. L. Tan, S. A. Smith, A. R. de Alwis, T. S. Ng, V. A. Kostyuchenko, K. D. Ibarra, J. Wang, E. Harris, A. de Silva, J. E. Crowe, Jr. and S. M. Lok (2014). "A potent anti-dengue human antibody preferentially recognizes the conformation of E protein monomers assembled on the virus surface." EMBO Mol Med **6**(3): 358-371.

Foster, K. R., M. F. Jenkins and A. C. Toogood (1998). "The Philadelphia yellow fever epidemic of 1793." Sci Am **279**(2): 88-93.

Francis, T. I., D. L. Moore, G. M. Edington and J. A. Smith (1972). "A clinicopathological study of human yellow fever." Bull World Health Organ **46**(5): 659-667.

Franz, A. W., I. Sanchez-Vargas, Z. N. Adelman, C. D. Blair, B. J. Beaty, A. A. James and K. E. Olson (2006). "Engineering RNA interference-based resistance to dengue virus type 2 in genetically modified Aedes aegypti." Proc Natl Acad Sci U S A **103**(11): 4198-4203.

Franz, A. W., I. Sanchez-Vargas, J. Piper, M. R. Smith, C. C. Khoo, A. A. James and K. E. Olson (2009). "Stability and loss of a virus resistance phenotype over time in transgenic mosquitoes harbouring an antiviral effector gene." Insect Mol Biol **18**(5): 661-672.

Friend, W. G. and J. J. Smith (1977). "Factors affecting feeding by bloodsucking insects." Annu Rev Entomol **22**: 309-331.

Frierson, J. G. (2010). "The yellow fever vaccine: a history." Yale J Biol Med **83**(2): 77-85.

Fuller, S. D., J. A. Berriman, S. J. Butcher and B. E. Gowen (1995). "Low pH induces swiveling of the glycoprotein heterodimers in the Semliki Forest virus spike complex." Cell **81**(5): 715-725.

Galun, R., H. Vardimon-Friedman and S. Frankenburg (1993). "Gorging response of culicine mosquitoes (Diptera: Culicidae) to blood fractions." J Med Entomol **30**(3): 513-517.

Gardner, C. L., G. D. Ebel, K. D. Ryman and W. B. Klimstra (2011). "Heparan sulfate binding by natural eastern equine encephalitis viruses promotes neurovirulence." Proc Natl Acad Sci U S A **108**(38): 16026-16031.

Gardner, C. L. and K. D. Ryman (2010). "Yellow fever: a reemerging threat." Clin Lab Med **30**(1): 237-260.

Gavrilovskaya, I. N., M. Shepley, R. Shaw, M. H. Ginsberg and E. R. Mackow (1998). "beta3 Integrins mediate the cellular entry of hantaviruses that cause respiratory failure." Proc Natl Acad Sci U S A **95**(12): 7074-7079.

Geering, K. and T. A. Freyvogel (1975). "Lipase activity and stimulation mechanism of esterases in the midgut of female Aedes aegypti." J Insect Physiol **21**(6): 1251-1256.

Germain, M., D. B. Francy, T. P. Monath, L. Ferrara, J. Bryan, J. J. Salaun, G. Heme, J. Renaudet, C. Adam and J. P. Digoutte (1980). "Yellow fever in the Gambia, 1978--1979: entomological aspects and epidemiological correlations." Am J Trop Med Hyg **29**(5): 929-940.

Germi, R., J. M. Crance, D. Garin, J. Guimet, H. Lortat-Jacob, R. W. Ruigrok, J. P. Zarski and E. Drouet (2002). "Heparan sulfate-mediated binding of infectious dengue virus type 2 and yellow fever virus." Virology **292**(1): 162-168.

Gibbons, D. L., M. C. Vaney, A. Roussel, A. Vigouroux, B. Reilly, J. Lepault, M. Kielian and F. A. Rey (2004). "Conformational change

and protein-protein interactions of the fusion protein of Semliki Forest virus." Nature **427**(6972): 320-325.

Glattli, E., W. Rudin and H. Hecker (1987). "Immunoelectron microscopic demonstration of pancreatic polypeptide in midgut epithelium of hematophagous dipterans." J Histochem Cytochem **35**(8): 891-896.

Goddard, L. B., A. E. Roth, W. K. Reisen and T. W. Scott (2002). "Vector competence of California mosquitoes for West Nile virus." Emerg Infect Dis **8**(12): 1385-1391.

Gonzalez, L., H. W. Reid, I. Pow and J. S. Gilmour (1987). "A disease resembling louping-ill in sheep in the Basque region of Spain." Vet Rec **121**(1): 12-13.

Gooding, R. H. (1972). "Digestive processes of haematophagous insects--II. Trypsin from the sheep ked Melophagus ovinus (L.) (hippoboscidae, diptera) and its inhibition by mammalian sera." Comp Biochem Physiol B **43**(4): 815-824.

Gould, E. A. and A. Buckley (1989). "Antibody-dependent enhancement of yellow fever and Japanese encephalitis virus neurovirulence." J Gen Virol **70 (Pt 6)**: 1605-1608.

Gould, E. A., A. Buckley, N. Cammack, A. D. Barrett, J. C. Clegg, R. Ishak and M. G. Varma (1985). "Examination of the immunological relationships between flaviviruses using yellow fever virus monoclonal antibodies." J Gen Virol **66 (Pt 7)**: 1369-1382.

Gould, E. A., A. Buckley, P. A. Cane, S. Higgs and N. Cammack (1989). "Use of a monoclonal antibody specific for wild-type yellow fever virus to identify a wild-type antigenic variant in 17D vaccine pools." J Gen Virol **70 (Pt 7)**: 1889-1894.

Gould, E. A., X. de Lamballerie, P. M. Zanotto and E. C. Holmes (2003). "Origins, evolution, and vector/host coadaptations within the genus Flavivirus." Adv Virus Res **59**: 277-314.

Gould, E. A. and T. Solomon (2008). "Pathogenic flaviviruses." Lancet **371**(9611): 500-509.

Grimaldi, D. A. and M. S. Engel (2005). Evolution of the insects. Cambridge U.K. ; New York, Cambridge University Press.

Gritsun, T. S., E. C. Holmes and E. A. Gould (1995). "Analysis of flavivirus envelope proteins reveals variable domains that reflect their antigenicity and may determine their pathogenesis." Virus Res **35**(3): 307-321.

Gross, L. (2007). "Are "ultraconserved" genetic elements really indispensable?" PLoS Biol **5**(9): e253.

Grun, J. B. and M. A. Brinton (1986). "Characterization of West Nile virus RNA-dependent RNA polymerase and cellular terminal adenylyl and uridylyl transferases in cell-free extracts." J Virol **60**(3): 1113-1124.

Grun, J. B. and M. A. Brinton (1987). "Dissociation of NS5 from cell fractions containing West Nile virus-specific polymerase activity." J Virol **61**(11): 3641-3644.

Gubler, D. J. (2002). "The global emergence/resurgence of arboviral diseases as public health problems." Arch Med Res **33**(4): 330-342.

Gubler, D. J. and L. Rosen (1976). "Variation among geographic strains of Aedes albopictus in susceptibility to infection with dengue viruses." Am J Trop Med Hyg **25**(2): 318-325.

Guirakhoo, F., F. X. Heinz, C. W. Mandl, H. Holzmann and C. Kunz (1991). "Fusion activity of flaviviruses: comparison of mature and immature (prM-containing) tick-borne encephalitis virions." J Gen Virol **72 (Pt 6)**: 1323-1329.

Guy, B., B. Barrere, C. Malinowski, M. Saville, R. Teyssou and J. Lang (2011). "From research to phase III: preclinical, industrial and

clinical development of the Sanofi Pasteur tetravalent dengue vaccine." Vaccine **29**(42): 7229-7241.

Guzman, M. G., S. B. Halstead, H. Artsob, P. Buchy, J. Farrar, D. J. Gubler, E. Hunsperger, A. Kroeger, H. S. Margolis, E. Martinez, M. B. Nathan, J. L. Pelegrino, C. Simmons, S. Yoksan and R. W. Peeling (2010). "Dengue: a continuing global threat." Nat Rev Microbiol **8**(12 Suppl): S7-16.

Gwadz, R. W. (1969). "Regulation of blood meal size in the mosquito." J Insect Physiol **15**(11): 2039-2044.

Haddow, A. D., H. Guzman, V. L. Popov, T. G. Wood, S. G. Widen, A. D. Haddow, R. B. Tesh and S. C. Weaver (2013). "First isolation of Aedes flavivirus in the Western Hemisphere and evidence of vertical transmission in the mosquito Aedes (Stegomyia) albopictus (Diptera: Culicidae)." Virology **440**(2): 134-139.

Hahn, C. S., J. M. Dalrymple, J. H. Strauss and C. M. Rice (1987). "Comparison of the virulent Asibi strain of yellow fever virus with the 17D vaccine strain derived from it." Proc Natl Acad Sci U S A **84**(7): 2019-2023.

Hall, R. A., J. H. Scherret and J. S. Mackenzie (2001). "Kunjin virus: an Australian variant of West Nile?" Ann N Y Acad Sci **951**: 153-160.

Halstead, S. B. and S. J. Thomas (2010). "New vaccines for Japanese encephalitis." Curr Infect Dis Rep **12**(3): 174-180.

Hardy, J. L., G. Apperson, S. M. Asman and W. C. Reeves (1978). "Selection of a strain of Culex tarsalis highly resistant to infection following ingestion of western equine encephalomyelitis virus." Am J Trop Med Hyg **27**(2 Pt 1): 313-321.

Hardy, J. L., E. J. Houk, L. D. Kramer and W. C. Reeves (1983). "Intrinsic factors affecting vector competence of mosquitoes for arboviruses." Annu Rev Entomol **28**: 229-262.

Harrison, S. C. (2008). "Viral membrane fusion." Nat Struct Mol Biol **15**(7): 690-698.

Hearn, H. J., Jr., W. T. Soper and W. S. Miller (1965). "Loss in Virulence of Yellow Fever Virus Serially Passed in Hela Cells." Proc Soc Exp Biol Med **119**: 319-322.

Hecker, H. and W. Rudin (1981). "Morphometric parameters of the midgut cells of Aedes aegypti L. (Insecta, Diptera) under various conditions." Cell Tissue Res **219**(3): 619-627.

Hegedus, D., M. Erlandson, C. Gillott and U. Toprak (2009). "New insights into peritrophic matrix synthesis, architecture, and function." Annu Rev Entomol **54**: 285-302.

Heinz, F. X., R. Berger, W. Tuma and C. Kunz (1983). "A topological and functional model of epitopes on the structural glycoprotein of tick-borne encephalitis virus defined by monoclonal antibodies." Virology **126**(2): 525-537.

Heinz, F. X., K. Stiasny, G. Puschner-Auer, H. Holzmann, S. L. Allison, C. W. Mandl and C. Kunz (1994). "Structural changes and functional control of the tick-borne encephalitis virus glycoprotein E by the heterodimeric association with protein prM." Virology **198**(1): 109-117.

Helenius, A., J. Kartenbeck, K. Simons and E. Fries (1980). "On the entry of Semliki forest virus into BHK-21 cells." J Cell Biol **84**(2): 404-420.

Henderson, B. E., D. Metselaar, G. B. Kirya and G. L. Timms (1970). "Investigations into yellow fever virus and other arboviruses in the northern regions of Kenya." Bull World Health Organ **42**(5): 787-795.

Higgs, S. and E. A. Gould (1991). "Differences in fusogenicity and mouse neurovirulence of Japanese encephalitis viruses." Arch Virol **119**(1-2): 119-133.

Higgs, S., A. M. Powers and K. E. Olson (1993). "Alphavirus expression systems: applications to mosquito vector studies." Parasitol Today **9**(12): 444-452.

Hijikata, M., N. Kato, Y. Ootsuyama, M. Nakagawa, S. Ohkoshi and K. Shimotohno (1991). "Hypervariable regions in the putative glycoprotein of hepatitis C virus." Biochem Biophys Res Commun **175**(1): 220-228.

Hilgard, P. and R. Stockert (2000). "Heparan sulfate proteoglycans initiate dengue virus infection of hepatocytes." Hepatology **32**(5): 1069-1077.

Hillyer, J. F. and B. M. Christensen (2002). "Characterization of hemocytes from the yellow fever mosquito, Aedes aegypti." Histochem Cell Biol **117**(5): 431-440.

Hinten, S. R., G. A. Beckett, K. F. Gensheimer, E. Pritchard, T. M. Courtney, S. D. Sears, J. M. Woytowicz, D. G. Preston, R. P. Smith, Jr., P. W. Rand, E. H. Lacombe, M. S. Holman, C. B. Lubelczyk, P. T. Kelso, A. P. Beelen, M. G. Stobierski, M. J. Sotir, S. Wong, G. Ebel, O. Kosoy, J. Piesman, G. L. Campbell and A. A. Marfin (2008). "Increased recognition of Powassan encephalitis in the United States, 1999-2005." Vector Borne Zoonotic Dis **8**(6): 733-740.

Holbrook, M. R. (2012). "Kyasanur forest disease." Antiviral Res **96**(3): 353-362.

Holt, R. A., G. M. Subramanian, A. Halpern, G. G. Sutton, R. Charlab, D. R. Nusskern, P. Wincker, A. G. Clark, J. M. Ribeiro, R. Wides, S. L. Salzberg, B. Loftus, M. Yandell, W. H. Majoros, D. B. Rusch, Z. Lai, C. L. Kraft, J. F. Abril, V. Anthouard, P. Arensburger, P. W. Atkinson, H. Baden, V. de Berardinis, D. Baldwin, V. Benes, J. Biedler, C. Blass, R. Bolanos, D. Boscus, M. Barnstead, S. Cai, A. Center, K. Chaturverdi, G. K. Christophides, M. A. Chrystal, M. Clamp, A. Cravchik, V. Curwen, A. Dana, A. Delcher, I. Dew, C. A.

Evans, M. Flanigan, A. Grundschober-Freimoser, L. Friedli, Z. Gu, P. Guan, R. Guigo, M. E. Hillenmeyer, S. L. Hladun, J. R. Hogan, Y. S. Hong, J. Hoover, O. Jaillon, Z. Ke, C. Kodira, E. Kokoza, A. Koutsos, I. Letunic, A. Levitsky, Y. Liang, J. J. Lin, N. F. Lobo, J. R. Lopez, J. A. Malek, T. C. McIntosh, S. Meister, J. Miller, C. Mobarry, E. Mongin, S. D. Murphy, D. A. O'Brochta, C. Pfannkoch, R. Qi, M. A. Regier, K. Remington, H. Shao, M. V. Sharakhova, C. D. Sitter, J. Shetty, T. J. Smith, R. Strong, J. Sun, D. Thomasova, L. Q. Ton, P. Topalis, Z. Tu, M. F. Unger, B. Walenz, A. Wang, J. Wang, M. Wang, X. Wang, K. J. Woodford, J. R. Wortman, M. Wu, A. Yao, E. M. Zdobnov, H. Zhang, Q. Zhao, S. Zhao, S. C. Zhu, I. Zhimulev, M. Coluzzi, A. della Torre, C. W. Roth, C. Louis, F. Kalush, R. J. Mural, E. W. Myers, M. D. Adams, H. O. Smith, S. Broder, M. J. Gardner, C. M. Fraser, E. Birney, P. Bork, P. T. Brey, J. C. Venter, J. Weissenbach, F. C. Kafatos, F. H. Collins and S. L. Hoffman (2002). "The genome sequence of the malaria mosquito Anopheles gambiae." Science **298**(5591): 129-149.

Hosoi, T. (1958). "Adenosine-5'-phosphates as the stimulating agent in blood for inducing gorging of the mosquito." Nature **181**(4624): 1664-1665.

Huang, K. C., M. C. Lee, C. W. Wu, K. J. Huang, H. Y. Lei and J. W. Cheng (2008). "Solution structure and neutralizing antibody binding studies of domain III of the dengue-2 virus envelope protein." Proteins **70**(3): 1116-1119.

Huang, Y. J., J. T. Nuckols, K. M. Horne, D. Vanlandingham, M. Lobigs and S. Higgs (2014). "Mutagenesis analysis of T380R mutation in the envelope protein of yellow fever virus." Virol J **11**: 60.

Hudson, A., L. Bowman and C. W. Orr (1960). "Effects of absence of saliva on blood feeding by mosquitoes." Science **131**(3415): 1730-1731.

Hudson, P. J., R. Norman, M. K. Laurenson, D. Newborn, M. Gaunt, L. Jones, H. Reid, E. Gould, R. Bowers and A. Dobson (1995). "Persistence and transmission of tick-borne viruses: Ixodes ricinus and louping-ill virus in red grouse populations." Parasitology **111 Suppl**: S49-58.

Hung, J. J., M. T. Hsieh, M. J. Young, C. L. Kao, C. C. King and W. Chang (2004). "An external loop region of domain III of dengue virus type 2 envelope protein is involved in serotype-specific binding to mosquito but not mammalian cells." J Virol **78**(1): 378-388.

Hurlbut, H. S. (1956). "West Nile virus infection in arthropods." Am J Trop Med Hyg **5**(1): 76-85.

Hurrelbrink, R. J. and P. C. McMinn (2001). "Attenuation of Murray Valley encephalitis virus by site-directed mutagenesis of the hinge and putative receptor-binding regions of the envelope protein." J Virol **75**(16): 7692-7702.

Hurrelbrink, R. J., A. Nestorowicz and P. C. McMinn (1999). "Characterization of infectious Murray Valley encephalitis virus derived from a stably cloned genome-length cDNA." J Gen Virol **80 (Pt 12)**: 3115-3125.

Jia, X. Y., T. Briese, I. Jordan, A. Rambaut, H. C. Chi, J. S. Mackenzie, R. A. Hall, J. Scherret and W. I. Lipkin (1999). "Genetic analysis of West Nile New York 1999 encephalitis virus." Lancet **354**(9194): 1971-1972.

Jiang, Q., M. Hall, F. G. Noriega and M. Wells (1997). "cDNA cloning and pattern of expression of an adult, female-specific chymotrypsin from Aedes aegypti midgut." Insect Biochem Mol Biol **27**(4): 283-289.

Jindadamrongwech, S., C. Thepparit and D. R. Smith (2004). "Identification of GRP 78 (BiP) as a liver cell expressed receptor element for dengue virus serotype 2." Arch Virol **149**(5): 915-927.

Kalhok, S. E., L. M. Tabak, D. E. Prosser, W. Brook, A. E. Downe and B. N. White (1993). "Isolation, sequencing and characterization of two cDNA clones coding for trypsin-like enzymes from the midgut of Aedes aegypti." Insect Mol Biol **2**(2): 71-79.

Kapoor, M., L. Zhang, P. M. Mohan and R. Padmanabhan (1995). "Synthesis and characterization of an infectious dengue virus type-2 RNA genome (New Guinea C strain)." Gene **162**(2): 175-180.

Kark, J. D., Y. Aynor and C. J. Peters (1982). "A rift Valley fever vaccine trial. I. Side effects and serologic response over a six-month follow-up." Am J Epidemiol **116**(5): 808-820.

Kark, J. D., Y. Aynor and C. J. Peters (1985). "A Rift Valley fever vaccine trial: 2. Serological response to booster doses with a comparison of intradermal versus subcutaneous injection." Vaccine **3**(2): 117-122.

Kato, D., S. Era, I. Watanabe, M. Arihara, N. Sugiura, K. Kimata, Y. Suzuki, K. Morita, K. I. Hidari and T. Suzuki (2010). "Antiviral activity of chondroitin sulphate E targeting dengue virus envelope protein." Antiviral Res **88**(2): 236-243.

Kato, N., R. Dasgupta, C. T. Smartt and B. M. Christensen (2002). "Glucosamine:fructose-6-phosphate aminotransferase: gene characterization, chitin biosynthesis and peritrophic matrix formation in Aedes aegypti." Insect Mol Biol **11**(3): 207-216.

Kato, N., C. R. Mueller, J. F. Fuchs, K. McElroy, V. Wessely, S. Higgs and B. M. Christensen (2008). "Evaluation of the function of a type I peritrophic matrix as a physical barrier for midgut epithelium invasion by mosquito-borne pathogens in Aedes aegypti." Vector Borne Zoonotic Dis **8**(5): 701-712.

Kato, N., C. R. Mueller, V. Wessely, Q. Lan and B. M. Christensen (2005). "Mosquito glucosamine-6-phosphate N-acetyltransferase: cDNA, gene structure and enzyme kinetics." Insect Biochem Mol Biol **35**(6): 637-646.

Kay, B. H., J. D. Edman, I. D. Fanning and P. Mottram (1989). "Larval diet and the vector competence of Culex annulirostris (Diptera: Culicidae) for Murray Valley encephalitis virus." J Med Entomol **26**(5): 487-488.

Keelapang, P., R. Sriburi, S. Supasa, N. Panyadee, A. Songjaeng, A. Jairungsri, C. Puttikhunt, W. Kasinrerk, P. Malasit and N. Sittisombut (2004). "Alterations of pr-M cleavage and virus export in pr-M junction chimeric dengue viruses." J Virol **78**(5): 2367-2381.

Kielian, M. (2006). "Class II virus membrane fusion proteins." Virology **344**(1): 38-47.

Kim, E., M. Okumura, H. Sawa, T. Miyazaki, D. Fujikura, S. Yamada, K. Sugahara, M. Sasaki and T. Kimura (2011). "Paradoxical effects of chondroitin sulfate-E on Japanese encephalitis viral infection." Biochem Biophys Res Commun **409**(4): 717-722.

Kimura, T., M. Sasaki, M. Okumura, E. Kim and H. Sawa (2010). "Flavivirus encephalitis: pathological aspects of mouse and other animal models." Vet Pathol **47**(5): 806-818.

Kinney, R. M., S. Butrapet, G. J. Chang, K. R. Tsuchiya, J. T. Roehrig, N. Bhamarapravati and D. J. Gubler (1997). "Construction of infectious cDNA clones for dengue 2 virus: strain 16681 and its attenuated vaccine derivative, strain PDK-53." Virology **230**(2): 300-308.

Kitchener, S. (2004). "Viscerotropic and neurotropic disease following vaccination with the 17D yellow fever vaccine, ARILVAX." Vaccine **22**(17-18): 2103-2105.

Klein, D. E., J. L. Choi and S. C. Harrison (2013). "Structure of a dengue virus envelope protein late-stage fusion intermediate." J Virol **87**(4): 2287-2293.

Klimstra, W. B., K. D. Ryman and R. E. Johnston (1998). "Adaptation of Sindbis virus to BHK cells selects for use of heparan sulfate as an attachment receptor." J Virol **72**(9): 7357-7366.

Knipe, D. M. and P. M. Howley (2013). Fields virology. Philadelphia, PA, Wolters Kluwer/Lippincott Williams & Wilkins Health.

Knox, J., R. U. Cowan, J. S. Doyle, M. K. Ligtermoet, J. S. Archer, J. N. Burrow, S. Y. Tong, B. J. Currie, J. S. Mackenzie, D. W. Smith, M. Catton, R. J. Moran, C. A. Aboltins and J. S. Richards (2012). "Murray Valley encephalitis: a review of clinical features, diagnosis and treatment." Med J Aust **196**(5): 322-326.

Kolykhalov, A. A., E. V. Agapov, K. J. Blight, K. Mihalik, S. M. Feinstone and C. M. Rice (1997). "Transmission of hepatitis C by intrahepatic inoculation with transcribed RNA." Science **277**(5325): 570-574.

Kostyuchenko, V. A., P. L. Chew, T. S. Ng and S. M. Lok (2014). "Near-atomic resolution cryo-electron microscopic structure of dengue serotype 4 virus." J Virol **88**(1): 477-482.

Kramer, L. D., J. L. Hardy and S. B. Presser (1983). "Effect of temperature of extrinsic incubation on the vector competence of Culex tarsalis for western equine encephalomyelitis virus." Am J Trop Med Hyg **32**(5): 1130-1139.

Krey, T., J. d'Alayer, C. M. Kikuti, A. Saulnier, L. Damier-Piolle, I. Petitpas, D. X. Johansson, R. G. Tawar, B. Baron, B. Robert, P. England, M. A. Persson, A. Martin and F. A. Rey (2010). "The disulfide bonds in glycoprotein E2 of hepatitis C virus reveal the tertiary organization of the molecule." PLoS Pathog **6**(2): e1000762.

Krishnan, M. N., B. Sukumaran, U. Pal, H. Agaisse, J. L. Murray, T. W. Hodge and E. Fikrig (2007). "Rab 5 is required for the cellular entry of dengue and West Nile viruses." J Virol **81**(9): 4881-4885.

Kroschewski, H., S. L. Allison, F. X. Heinz and C. W. Mandl (2003). "Role of heparan sulfate for attachment and entry of tick-borne encephalitis virus." Virology **308**(1): 92-100.

Kuhn, R. J., W. Zhang, M. G. Rossmann, S. V. Pletnev, J. Corver, E. Lenches, C. T. Jones, S. Mukhopadhyay, P. R. Chipman, E. G. Strauss, T. S. Baker and J. H. Strauss (2002). "Structure of dengue virus: implications for flavivirus organization, maturation, and fusion." Cell **108**(5): 717-725.

Kuno, G. and G. J. Chang (2006). "Characterization of Sepik and Entebbe bat viruses closely related to yellow fever virus." Am J Trop Med Hyg **75**(6): 1165-1170.

La Linn, M., J. A. Eble, C. Lubken, R. W. Slade, J. Heino, J. Davies and A. Suhrbier (2005). "An arthritogenic alphavirus uses the alpha1beta1 integrin collagen receptor." Virology **336**(2): 229-239.

Labuda, M., V. Danielova, L. D. Jones and P. A. Nuttall (1993). "Amplification of tick-borne encephalitis virus infection during co-feeding of ticks." Med Vet Entomol **7**(4): 339-342.

Laemmert, H. W., Jr. and H. W. Kumm (1950). "The susceptibility of howler monkeys to yellow fever virus." Am J Trop Med Hyg **30**(5): 723-731.

Lai, C. J., A. P. Goncalvez, R. Men, C. Wernly, O. Donau, R. E. Engle and R. H. Purcell (2007). "Epitope determinants of a chimpanzee dengue virus type 4 (DENV-4)-neutralizing antibody and protection against DENV-4 challenge in mice and rhesus monkeys by passively transferred humanized antibody." J Virol **81**(23): 12766-12774.

Lai, C. J., B. T. Zhao, H. Hori and M. Bray (1991). "Infectious RNA transcribed from stably cloned full-length cDNA of dengue type 4 virus." Proc Natl Acad Sci U S A **88**(12): 5139-5143.

Lee, E., R. A. Hall and M. Lobigs (2004). "Common E protein determinants for attenuation of glycosaminoglycan-binding variants of Japanese encephalitis and West Nile viruses." J Virol **78**(15): 8271-8280.

Lee, E. and M. Lobigs (2000). "Substitutions at the putative receptor-binding site of an encephalitic flavivirus alter virulence and host cell tropism and reveal a role for glycosaminoglycans in entry." J Virol **74**(19): 8867-8875.

Lee, E. and M. Lobigs (2002). "Mechanism of virulence attenuation of glycosaminoglycan-binding variants of Japanese encephalitis virus and Murray Valley encephalitis virus." J Virol **76**(10): 4901-4911.

Lee, E. and M. Lobigs (2008). "E protein domain III determinants of yellow fever virus 17D vaccine strain enhance binding to glycosaminoglycans, impede virus spread, and attenuate virulence." J Virol **82**(12): 6024-6033.

Lee, E., R. C. Weir and L. Dalgarno (1997). "Changes in the dengue virus major envelope protein on passaging and their localization on the three-dimensional structure of the protein." Virology **232**(2): 281-290.

Lee, E., P. J. Wright, A. Davidson and M. Lobigs (2006). "Virulence attenuation of Dengue virus due to augmented glycosaminoglycan-binding affinity and restriction in extraneural dissemination." J Gen Virol **87**(Pt 10): 2791-2801.

Lee, J. W., J. J. Chu and M. L. Ng (2006). "Quantifying the specific binding between West Nile virus envelope domain III protein and the cellular receptor alphaVbeta3 integrin." J Biol Chem **281**(3): 1352-1360.

Lee, V. H. and D. L. Moore (1972). "Vectors of the 1969 yellow fever epidemic on the Jos Plateau, Nigeria." Bull World Health Organ **46**(5): 669-673.

Lefeuvre, A., P. Marianneau and V. Deubel (2004). "Current Assessment of Yellow Fever and Yellow Fever Vaccine." Curr Infect Dis Rep **6**(2): 96-104.

Lerch, T. F. and M. S. Chapman (2012). "Identification of the heparin binding site on adeno-associated virus serotype 3B (AAV-3B)." Virology **423**(1): 6-13.

Lescar, J., A. Roussel, M. W. Wien, J. Navaza, S. D. Fuller, G. Wengler, G. Wengler and F. A. Rey (2001). "The Fusion glycoprotein shell of Semliki Forest virus: an icosahedral assembly primed for fusogenic activation at endosomal pH." Cell **105**(1): 137-148.

Levitt, N. H., H. H. Ramsburg, S. E. Hasty, P. M. Repik, F. E. Cole, Jr. and H. W. Lupton (1986). "Development of an attenuated strain of chikungunya virus for use in vaccine production." Vaccine **4**(3): 157-162.

Levkovich, E. N. (1945). "[Etiology of the new type of encephalitis]." Nevropatol Psikhiatriia **14**(2): 20-25.

Lin, Y. L., H. Y. Lei, Y. S. Lin, T. M. Yeh, S. H. Chen and H. S. Liu (2002). "Heparin inhibits dengue-2 virus infection of five human liver cell lines." Antiviral Res **56**(1): 93-96.

Lindquist, L. and O. Vapalahti (2008). "Tick-borne encephalitis." Lancet **371**(9627): 1861-1871.

Littig, K. S., Pratt, H.D., Tinker, M.E. (1966). Entomological handbook for Aedes aegypti eradication

Liu, H., S. S. Chiou and W. J. Chen (2004). "Differential binding efficiency between the envelope protein of Japanese encephalitis

virus variants and heparan sulfate on the cell surface." J Med Virol **72**(4): 618-624.

Lodish, H. F. (2013). Molecular cell biology. New York, W.H. Freeman and Co.

Lorenz, L., B. J. Beaty, T. H. Aitken, G. P. Wallis and W. J. Tabachnick (1984). "The effect of colonization upon aedes aegypti susceptibility to oral infection with yellow fever virus." Am J Trop Med Hyg **33**(4): 690-694.

Luca, V. C., C. A. Nelson and D. H. Fremont (2013). "Structure of the St. Louis encephalitis virus postfusion envelope trimer." J Virol **87**(2): 818-828.

Mackenzie, J. S. B., A.D.T.; Deubel, V. (2002). Japanese encephalitis and West Nile Viruses, Springer.

Macnamara, F. N. (1953). "Reactions following neurotropic yellow fever vaccine given by scarification in Nigeria." Trans R Soc Trop Med Hyg **47**(3): 199-208.

Mancini, E. J., M. Clarke, B. E. Gowen, T. Rutten and S. D. Fuller (2000). "Cryo-electron microscopy reveals the functional organization of an enveloped virus, Semliki Forest virus." Mol Cell **5**(2): 255-266.

Mandl, C. W., F. Guirakhoo, H. Holzmann, F. X. Heinz and C. Kunz (1989). "Antigenic structure of the flavivirus envelope protein E at the molecular level, using tick-borne encephalitis virus as a model." J Virol **63**(2): 564-571.

Mandl, C. W., H. Kroschewski, S. L. Allison, R. Kofler, H. Holzmann, T. Meixner and F. X. Heinz (2001). "Adaptation of tick-borne encephalitis virus to BHK-21 cells results in the formation of multiple heparan sulfate binding sites in the envelope protein and attenuation in vivo." J Virol **75**(12): 5627-5637.

Maramorosch, K. and A. H. McIntosh (1994). Arthropod cell culture systems. Boca Raton, CRC Press.

Marquardt, W. C. and B. C. Kondratieff (2005). Biology of disease vectors. Burlington, MA, Elsevier Academic Press.

Mattar, S., N. Komar, G. Young, J. Alvarez and M. Gonzalez (2011). "Seroconversion for West Nile and St. Louis encephalitis viruses among sentinel horses in Colombia." Mem Inst Oswaldo Cruz **106**(8): 976-979.

McArthur, M. A., S. Y. Xiao and A. D. Barrett (2005). "Phenotypic and molecular characterization of a non-lethal, hamster-viscerotropic strain of yellow fever virus." Virus Res **110**(1-2): 65-71.

McClain, D. J., P. R. Pittman, H. H. Ramsburg, G. O. Nelson, C. A. Rossi, J. A. Mangiafico, A. L. Schmaljohn and F. J. Malinoski (1998). "Immunologic interference from sequential administration of live attenuated alphavirus vaccines." J Infect Dis **177**(3): 634-641.

McElroy, K. L., Y. A. Girard, C. E. McGee, K. A. Tsetsarkin, D. L. Vanlandingham and S. Higgs (2008). "Characterization of the antigen distribution and tissue tropisms of three phenotypically distinct yellow fever virus variants in orally infected Aedes aegypti mosquitoes." Vector Borne Zoonotic Dis **8**(5): 675-687.

McElroy, K. L., K. A. Tsetsarkin, D. L. Vanlandingham and S. Higgs (2005). "Characterization of an infectious clone of the wild-type yellow fever virus Asibi strain that is able to infect and disseminate in mosquitoes." J Gen Virol **86**(Pt 6): 1747-1751.

McElroy, K. L., K. A. Tsetsarkin, D. L. Vanlandingham and S. Higgs (2006). "Manipulation of the yellow fever virus non-structural genes 2A and 4B and the 3'non-coding region to evaluate genetic determinants of viral dissemination from the Aedes aegypti midgut." Am J Trop Med Hyg **75**(6): 1158-1164.

McElroy, K. L., K. A. Tsetsarkin, D. L. Vanlandingham and S. Higgs (2006). "Role of the yellow fever virus structural protein genes in viral dissemination from the Aedes aegypti mosquito midgut." J Gen Virol **87**(Pt 10): 2993-3001.

McGee, C. E., M. G. Lewis, M. S. Claire, W. Wagner, J. Lang, B. Guy, K. Tsetsarkin, S. Higgs and T. Decelle (2008). "Recombinant chimeric virus with wild-type dengue 4 virus premembrane and envelope and virulent yellow fever virus Asibi backbone sequences is dramatically attenuated in nonhuman primates." J Infect Dis **197**(5): 693-697.

McMahon, A. W., R. B. Eidex, A. A. Marfin, M. Russell, J. J. Sejvar, L. Markoff, E. B. Hayes, R. T. Chen, R. Ball, M. M. Braun, M. Cetron and G. Yellow Fever Working (2007). "Neurologic disease associated with 17D-204 yellow fever vaccination: a report of 15 cases." Vaccine **25**(10): 1727-1734.

McMinn, P. C., E. Lee, S. Hartley, J. T. Roehrig, L. Dalgarno and R. C. Weir (1995). "Murray valley encephalitis virus envelope protein antigenic variants with altered hemagglutination properties and reduced neuroinvasiveness in mice." Virology **211**(1): 10-20.

Medigeshi, G. R., A. J. Hirsch, D. N. Streblow, J. Nikolich-Zugich and J. A. Nelson (2008). "West Nile virus entry requires cholesterol-rich membrane microdomains and is independent of alphavbeta3 integrin." J Virol **82**(11): 5212-5219.

Meertens, L., X. Carnec, M. P. Lecoin, R. Ramdasi, F. Guivel-Benhassine, E. Lew, G. Lemke, O. Schwartz and A. Amara (2012). "The TIM and TAM families of phosphatidylserine receptors mediate dengue virus entry." Cell Host Microbe **12**(4): 544-557.

Meier, K. C., C. L. Gardner, M. V. Khoretonenko, W. B. Klimstra and K. D. Ryman (2009). "A mouse model for studying viscerotropic disease caused by yellow fever virus infection." PLoS Pathog **5**(10): e1000614.

Mendez, J. A., E. Parra, M. Neira and G. J. Rey (2007). "[Detection of yellow fever virus by reverse transcriptase polymerase chain reaction in wild monkeys: a sensitive tool for epidemiologic surveillance]." Biomedica **27**(3): 461-467.

Mercer, J., M. Schelhaas and A. Helenius (2010). "Virus entry by endocytosis." Annu Rev Biochem **79**: 803-833.

Messer, W. B., B. Yount, K. E. Hacker, E. F. Donaldson, J. P. Huynh, A. M. de Silva and R. S. Baric (2012). "Development and characterization of a reverse genetic system for studying dengue virus serotype 3 strain variation and neutralization." PLoS Negl Trop Dis **6**(2): e1486.

Miller, B. R. and D. Adkins (1988). "Biological characterization of plaque-size variants of yellow fever virus in mosquitoes and mice." Acta Virol **32**(3): 227-234.

Miller, B. R. and C. J. Mitchell (1991). "Genetic selection of a flavivirus-refractory strain of the yellow fever mosquito Aedes aegypti." Am J Trop Med Hyg **45**(4): 399-407.

Miller, J. D., R. G. van der Most, R. S. Akondy, J. T. Glidewell, S. Albott, D. Masopust, K. Murali-Krishna, P. L. Mahar, S. Edupuganti, S. Lalor, S. Germon, C. Del Rio, M. J. Mulligan, S. I. Staprans, J. D. Altman, M. B. Feinberg and R. Ahmed (2008). "Human effector and memory CD8+ T cell responses to smallpox and yellow fever vaccines." Immunity **28**(5): 710-722.

Miller, J. L., B. J. de Wet, L. Martinez-Pomares, C. M. Radcliffe, R. A. Dwek, P. M. Rudd and S. Gordon (2008). "The mannose receptor mediates dengue virus infection of macrophages." PLoS Pathog **4**(2): e17.

Modis, Y., S. Ogata, D. Clements and S. C. Harrison (2003). "A ligand-binding pocket in the dengue virus envelope glycoprotein." Proc Natl Acad Sci U S A **100**(12): 6986-6991.

Modis, Y., S. Ogata, D. Clements and S. C. Harrison (2004). "Structure of the dengue virus envelope protein after membrane fusion." Nature **427**(6972): 313-319.

Monath, T. P. (1999). "Facing up to re-emergence of urban yellow fever." Lancet **353**(9164): 1541.

Monath, T. P. (2001). "Yellow fever: an update." Lancet Infect Dis **1**(1): 11-20.

Monath, T. P. (2010). "Suspected yellow fever vaccine-associated viscerotropic adverse events (1973 and 1978), United States." Am J Trop Med Hyg **82**(5): 919-921.

Monath, T. P., J. Arroyo, I. Levenbook, Z. X. Zhang, J. Catalan, K. Draper and F. Guirakhoo (2002). "Single mutation in the flavivirus envelope protein hinge region increases neurovirulence for mice and monkeys but decreases viscerotropism for monkeys: relevance to development and safety testing of live, attenuated vaccines." J Virol **76**(4): 1932-1943.

Monath, T. P., K. Soike, I. Levenbook, Z. X. Zhang, J. Arroyo, S. Delagrave, G. Myers, A. D. Barrett, R. E. Shope, M. Ratterree, T. J. Chambers and F. Guirakhoo (1999). "Recombinant, chimaeric live, attenuated vaccine (ChimeriVax) incorporating the envelope genes of Japanese encephalitis (SA14-14-2) virus and the capsid and nonstructural genes of yellow fever (17D) virus is safe, immunogenic and protective in non-human primates." Vaccine **17**(15-16): 1869-1882.

Morrill, J. C., L. Carpenter, D. Taylor, H. H. Ramsburg, J. Quance and C. J. Peters (1991). "Further evaluation of a mutagen-attenuated Rift Valley fever vaccine in sheep." Vaccine **9**(1): 35-41.

Mosso, C., I. J. Galvan-Mendoza, J. E. Ludert and R. M. del Angel (2008). "Endocytic pathway followed by dengue virus to infect the mosquito cell line C6/36 HT." Virology **378**(1): 193-199.

Moudy, R. M., A. F. Payne, B. L. Dodson and L. D. Kramer (2011). "Requirement of glycosylation of West Nile virus envelope protein for infection of, but not spread within, Culex quinquefasciatus mosquito vectors." Am J Trop Med Hyg **85**(2): 374-378.

Muller, D. A. and P. R. Young (2013). "The flavivirus NS1 protein: molecular and structural biology, immunology, role in pathogenesis and application as a diagnostic biomarker." Antiviral Res **98**(2): 192-208.

Munoz-Jordan, J. L., G. G. Sanchez-Burgos, M. Laurent-Rolle and A. Garcia-Sastre (2003). "Inhibition of interferon signaling by dengue virus." Proc Natl Acad Sci U S A **100**(24): 14333-14338.

Murray, J., L. Wilson and S. Kellie (2000). "Phosphatidylinositol-3' kinase-dependent vesicle formation in macrophages in response to macrophage colony stimulating factor." J Cell Sci **113 Pt 2**: 337-348.

Mutebi, J. P. and A. D. Barrett (2002). "The epidemiology of yellow fever in Africa." Microbes Infect **4**(14): 1459-1468.

Nasidi, A., T. P. Monath, K. DeCock, O. Tomori, R. Cordellier, O. D. Olaleye, T. O. Harry, J. A. Adeniyi, A. O. Sorungbe, A. O. Ajose-Coker and et al. (1989). "Urban yellow fever epidemic in western Nigeria, 1987." Trans R Soc Trop Med Hyg **83**(3): 401-406.

Nassar Eda, S., E. L. Chamelet, T. L. Coimbra, L. T. de Souza, A. Suzuki, I. B. Ferreira, M. V. da Silva, I. M. Rocco and A. P. Travassos da Rosa (1995). "Jungle yellow fever: clinical and laboratorial studies emphasizing viremia on a human case." Rev Inst Med Trop Sao Paulo **37**(4): 337-341.

Nawa, M. (1997). "Japanese encephalitis virus infection in Vero cells: the involvement of intracellular acidic vesicles in the early phase of viral infection was observed with the treatment of a specific

vacuolar type H+-ATPase inhibitor, bafilomycin A1." Microbiol Immunol **41**(7): 537-543.

Nawa, M., T. Takasaki, K. Yamada, I. Kurane and T. Akatsuka (2003). "Interference in Japanese encephalitis virus infection of Vero cells by a cationic amphiphilic drug, chlorpromazine." J Gen Virol **84**(Pt 7): 1737-1741.

Nelson, J., N. V. McFerran, G. Pivato, E. Chambers, C. Doherty, D. Steele and D. J. Timson (2008). "The 67 kDa laminin receptor: structure, function and role in disease." Biosci Rep **28**(1): 33-48.

Nene, V., J. R. Wortman, D. Lawson, B. Haas, C. Kodira, Z. J. Tu, B. Loftus, Z. Xi, K. Megy, M. Grabherr, Q. Ren, E. M. Zdobnov, N. F. Lobo, K. S. Campbell, S. E. Brown, M. F. Bonaldo, J. Zhu, S. P. Sinkins, D. G. Hogenkamp, P. Amedeo, P. Arensburger, P. W. Atkinson, S. Bidwell, J. Biedler, E. Birney, R. V. Bruggner, J. Costas, M. R. Coy, J. Crabtree, M. Crawford, B. Debruyn, D. Decaprio, K. Eiglmeier, E. Eisenstadt, H. El-Dorry, W. M. Gelbart, S. L. Gomes, M. Hammond, L. I. Hannick, J. R. Hogan, M. H. Holmes, D. Jaffe, J. S. Johnston, R. C. Kennedy, H. Koo, S. Kravitz, E. V. Kriventseva, D. Kulp, K. Labutti, E. Lee, S. Li, D. D. Lovin, C. Mao, E. Mauceli, C. F. Menck, J. R. Miller, P. Montgomery, A. Mori, A. L. Nascimento, H. F. Naveira, C. Nusbaum, S. O'Leary, J. Orvis, M. Pertea, H. Quesneville, K. R. Reidenbach, Y. H. Rogers, C. W. Roth, J. R. Schneider, M. Schatz, M. Shumway, M. Stanke, E. O. Stinson, J. M. Tubio, J. P. Vanzee, S. Verjovski-Almeida, D. Werner, O. White, S. Wyder, Q. Zeng, Q. Zhao, Y. Zhao, C. A. Hill, A. S. Raikhel, M. B. Soares, D. L. Knudson, N. H. Lee, J. Galagan, S. L. Salzberg, I. T. Paulsen, G. Dimopoulos, F. H. Collins, B. Birren, C. M. Fraser-Liggett and D. W. Severson (2007). "Genome sequence of Aedes aegypti, a major arbovirus vector." Science **316**(5832): 1718-1723.

Ng, M. L. and L. C. Lau (1988). "Possible involvement of receptors in the entry of Kunjin virus into Vero cells." Arch Virol **100**(3-4): 199-211.

Ni, H., N. J. Burns, G. J. Chang, M. J. Zhang, M. R. Wills, D. W. Trent, P. G. Sanders and A. D. Barrett (1994). "Comparison of nucleotide and deduced amino acid sequence of the 5' non-coding region and structural protein genes of the wild-type Japanese encephalitis virus strain SA14 and its attenuated vaccine derivatives." J Gen Virol **75 (Pt 6)**: 1505-1510.

Nickells, J., M. Cannella, D. A. Droll, Y. Liang, W. S. Wold and T. J. Chambers (2008). "Neuroadapted yellow fever virus strain 17D: a charged locus in domain III of the E protein governs heparin binding activity and neuroinvasiveness in the SCID mouse model." J Virol **82**(24): 12510-12519.

Nickells, M. and T. J. Chambers (2003). "Neuroadapted yellow fever virus 17D: determinants in the envelope protein govern neuroinvasiveness for SCID mice." J Virol **77**(22): 12232-12242.

Noisakran, S., N. Onlamoon, K. Pattanapanyasat, H. M. Hsiao, P. Songprakhon, N. Angkasekwinai, K. Chokephaibulkit, F. Villinger, A. A. Ansari and G. C. Perng (2012). "Role of CD61+ cells in thrombocytopenia of dengue patients." Int J Hematol **96**(5): 600-610.

Noriega, F. G., K. A. Edgar, W. G. Goodman, D. K. Shah and M. A. Wells (2001). "Neuroendocrine factors affecting the steady-state levels of early trypsin mRNA in Aedes aegypti." J Insect Physiol **47**(4-5): 515-522.

Oliphant, T., M. Engle, G. E. Nybakken, C. Doane, S. Johnson, L. Huang, S. Gorlatov, E. Mehlhop, A. Marri, K. M. Chung, G. D. Ebel, L. D. Kramer, D. H. Fremont and M. S. Diamond (2005). "Development of a humanized monoclonal antibody with

therapeutic potential against West Nile virus." Nat Med **11**(5): 522-530.

Osorio, J. E., C. Y. Huang, R. M. Kinney and D. T. Stinchcomb (2011). "Development of DENVax: a chimeric dengue-2 PDK-53-based tetravalent vaccine for protection against dengue fever." Vaccine **29**(42): 7251-7260.

Oviedo, M. V., W. S. Romoser, C. B. James, F. Mahmood and W. K. Reisen (2011). "Infection dynamics of western equine encephalomyelitis virus (Togaviridae: Alphavirus) in four strains of Culex tarsalis (Diptera: Culicidae): an immunocytochemical study." Res Rep Trop Med **2011**(2): 65-77.

Papa, A., V. Pavlidou and A. Antoniadis (2008). "Greek goat encephalitis virus strain isolated from Ixodes ricinus, Greece." Emerg Infect Dis **14**(2): 330-332.

Parikh, G. R., J. D. Oliver and L. C. Bartholomay (2009). "A haemocyte tropism for an arbovirus." J Gen Virol **90**(Pt 2): 292-296.

Patterson, K. D. (1992). "Yellow fever epidemics and mortality in the United States, 1693-1905." Soc Sci Med **34**(8): 855-865.

Pedersen, C. E., Jr., D. M. Robinson and F. E. Cole, Jr. (1972). "Isolation of the vaccine strain of Venezuelan equine encephalomyelitis virus from mosquitoes in Louisiana." Am J Epidemiol **95**(5): 490-496.

Peltier, M. (1947). "Yellow fever vaccination, simple or associated with vaccination against smallpox, of the populations of French West Africa by the method of the Pasteur Institute of Dakar." Am J Public Health Nations Health **37**(8): 1026-1032.

Perera-Lecoin, M., L. Meertens, X. Carnec and A. Amara (2014). "Flavivirus entry receptors: an update." Viruses **6**(1): 69-88.

Phuc, H. K., M. H. Andreasen, R. S. Burton, C. Vass, M. J. Epton, G. Pape, G. Fu, K. C. Condon, S. Scaife, C. A. Donnelly, P. G. Coleman, H. White-Cooper and L. Alphey (2007). "Late-acting dominant lethal genetic systems and mosquito control." BMC Biol **5**: 11.

Pierro, D. J., E. L. Powers and K. E. Olson (2008). "Genetic determinants of Sindbis virus mosquito infection are associated with a highly conserved alphavirus and flavivirus envelope sequence." J Virol **82**(6): 2966-2974.

Pinto, M. R. and A. R. Filipe (1971). "The yellow fever epidemic in Luanda in 1971." Bull Soc Pathol Exot Filiales **64**(5): 708-710.

Pittman, P. R., C. T. Liu, T. L. Cannon, R. S. Makuch, J. A. Mangiafico, P. H. Gibbs and C. J. Peters (1999). "Immunogenicity of an inactivated Rift Valley fever vaccine in humans: a 12-year experience." Vaccine **18**(1-2): 181-189.

Plevka, P., A. J. Battisti, J. Junjhon, D. C. Winkler, H. A. Holdaway, P. Keelapang, N. Sittisombut, R. J. Kuhn, A. C. Steven and M. G. Rossmann (2011). "Maturation of flaviviruses starts from one or more icosahedrally independent nucleation centres." EMBO Rep **12**(6): 602-606.

Pokidysheva, E., Y. Zhang, A. J. Battisti, C. M. Bator-Kelly, P. R. Chipman, C. Xiao, G. G. Gregorio, W. A. Hendrickson, R. J. Kuhn and M. G. Rossmann (2006). "Cryo-EM reconstruction of dengue virus in complex with the carbohydrate recognition domain of DC-SIGN." Cell **124**(3): 485-493.

Poland, J. D., C. H. Calisher, T. P. Monath, W. G. Downs and K. Murphy (1981). "Persistence of neutralizing antibody 30-35 years after immunization with 17D yellow fever vaccine." Bull World Health Organ **59**(6): 895-900.

Pugachev, K. V., F. Guirakhoo and T. P. Monath (2005). "New developments in flavivirus vaccines with special attention to yellow fever." Curr Opin Infect Dis **18**(5): 387-394.

Querec, T., S. Bennouna, S. Alkan, Y. Laouar, K. Gorden, R. Flavell, S. Akira, R. Ahmed and B. Pulendran (2006). "Yellow fever vaccine YF-17D activates multiple dendritic cell subsets via TLR2, 7, 8, and 9 to stimulate polyvalent immunity." J Exp Med **203**(2): 413-424.

Racaniello, V. R. and D. Baltimore (1981). "Molecular cloning of poliovirus cDNA and determination of the complete nucleotide sequence of the viral genome." Proc Natl Acad Sci U S A **78**(8): 4887-4891.

Rao, T. R. (1964). "Vectors of Dengue and Chikungunya Viruses: A Brief Review." Indian J Med Res **52**: 719-726.

Reed, K. E. and C. M. Rice (2000). "Overview of hepatitis C virus genome structure, polyprotein processing, and protein properties." Curr Top Microbiol Immunol **242**: 55-84.

Reinhardt, C. and H. Hecker (1973). "Structure and function of the basal lamina and of the cell junctions in the midgut epithelium (stomach) of female Aedes aegypti L.(Insecta, Diptera)." Acta Trop **30**(4): 213-236.

Rey, F. A., F. X. Heinz, C. Mandl, C. Kunz and S. C. Harrison (1995). "The envelope glycoprotein from tick-borne encephalitis virus at 2 A resolution." Nature **375**(6529): 291-298.

Reyes-Del Valle, J., S. Chavez-Salinas, F. Medina and R. M. Del Angel (2005). "Heat shock protein 90 and heat shock protein 70 are components of dengue virus receptor complex in human cells." J Virol **79**(8): 4557-4567.

Ribeiro, J. M., R. Charlab and J. G. Valenzuela (2001). "The salivary adenosine deaminase activity of the mosquitoes Culex

quinquefasciatus and Aedes aegypti." J Exp Biol **204**(Pt 11): 2001-2010.

Ribeiro, J. M. and J. G. Valenzuela (1999). "Purification and cloning of the salivary peroxidase/catechol oxidase of the mosquito Anopheles albimanus." J Exp Biol **202**(Pt 7): 809-816.

Ribeiro, J. M. C. and B. Arca (2009). "From Sialomes to the Sialoverse: An Insight into Salivary Potion of Blood-Feeding Insects." Advances in Insect Physiology, Vol 37 **37**: 59-+.

Rice, C. M., A. Grakoui, R. Galler and T. J. Chambers (1989). "Transcription of infectious yellow fever RNA from full-length cDNA templates produced by in vitro ligation." New Biol **1**(3): 285-296.

Richardson, J., A. Molina-Cruz, M. I. Salazar and W. t. Black (2006). "Quantitative analysis of dengue-2 virus RNA during the extrinsic incubation period in individual Aedes aegypti." Am J Trop Med Hyg **74**(1): 132-141.

Robert, V., M. Lhuillier, D. Meunier, J. L. Sarthou, N. Monteny, J. P. Digoutte, M. Cornet, M. Germain and R. Cordellier (1993). "[Yellow fever virus, dengue 2 and other arboviruses isolated from mosquitos, in Burkina Faso, from 1983 to 1986. Entomological and epidemiological considerations]." Bull Soc Pathol Exot **86**(2): 90-100.

Roehrig, J. T., S. Butrapet, N. M. Liss, S. L. Bennett, B. E. Luy, T. Childers, K. L. Boroughs, J. L. Stovall, A. E. Calvert, C. D. Blair and C. Y. Huang (2013). "Mutation of the dengue virus type 2 envelope protein heparan sulfate binding sites or the domain III lateral ridge blocks replication in Vero cells prior to membrane fusion." Virology **441**(2): 114-125.

Roussel, A., J. Lescar, M. C. Vaney, G. Wengler, G. Wengler and F. A. Rey (2006). "Structure and interactions at the viral surface of the

envelope protein E1 of Semliki Forest virus." Structure **14**(1): 75-86.

Ruoslahti, E. (1996). "RGD and other recognition sequences for integrins." Annu Rev Cell Dev Biol **12**: 697-715.

Ruzek, D., V. V. Yakimenko, L. S. Karan and S. E. Tkachev (2010). "Omsk haemorrhagic fever." Lancet **376**(9758): 2104-2113.

Ryman, K. D., C. L. Gardner, C. W. Burke, K. C. Meier, J. M. Thompson and W. B. Klimstra (2007). "Heparan sulfate binding can contribute to the neurovirulence of neuroadapted and nonneuroadapted Sindbis viruses." J Virol **81**(7): 3563-3573.

Ryman, K. D., T. N. Ledger, G. A. Campbell, S. J. Watowich and A. D. Barrett (1998). "Mutation in a 17D-204 vaccine substrain-specific envelope protein epitope alters the pathogenesis of yellow fever virus in mice." Virology **244**(1): 59-65.

Ryman, K. D., H. Xie, T. N. Ledger, G. A. Campbell and A. D. Barrett (1997). "Antigenic variants of yellow fever virus with an altered neurovirulence phenotype in mice." Virology **230**(2): 376-380.

Sabchareon, A., D. Wallace, C. Sirivichayakul, K. Limkittikul, P. Chanthavanich, S. Suvannadabba, V. Jiwariyavej, W. Dulyachai, K. Pengsaa, T. A. Wartel, A. Moureau, M. Saville, A. Bouckenooghe, S. Viviani, N. G. Tornieporth and J. Lang (2012). "Protective efficacy of the recombinant, live-attenuated, CYD tetravalent dengue vaccine in Thai schoolchildren: a randomised, controlled phase 2b trial." Lancet **380**(9853): 1559-1567.

Sakoonwatanyoo, P., V. Boonsanay and D. R. Smith (2006). "Growth and production of the dengue virus in C6/36 cells and identification of a laminin-binding protein as a candidate serotype 3 and 4 receptor protein." Intervirology **49**(3): 161-172.

Salas-Benito, J., J. Reyes-Del Valle, M. Salas-Benito, I. Ceballos-Olvera, C. Mosso and R. M. del Angel (2007). "Evidence that the

45-kD glycoprotein, part of a putative dengue virus receptor complex in the mosquito cell line C6/36, is a heat-shock related protein." Am J Trop Med Hyg **77**(2): 283-290.

Salas-Benito, J. S. and R. M. del Angel (1997). "Identification of two surface proteins from C6/36 cells that bind dengue type 4 virus." J Virol **71**(10): 7246-7252.

Salazar, M. I., J. H. Richardson, I. Sanchez-Vargas, K. E. Olson and B. J. Beaty (2007). "Dengue virus type 2: replication and tropisms in orally infected Aedes aegypti mosquitoes." BMC Microbiol **7**: 9.

Samreen, B., S. Khaliq, U. A. Ashfaq, M. Khan, N. Afzal, M. A. Shahzad, S. Riaz and S. Jahan (2012). "Hepatitis C virus entry: role of host and viral factors." Infect Genet Evol **12**(8): 1699-1709.

Sappington, T. W., V. A. Kokoza, W. L. Cho and A. S. Raikhel (1996). "Molecular characterization of the mosquito vitellogenin receptor reveals unexpected high homology to the Drosophila yolk protein receptor." Proc Natl Acad Sci U S A **93**(17): 8934-8939.

Sawyer, W. A., S. F. Kitchen and W. Lloyd (1932). "Vaccination against Yellow Fever with Immune Serum and Virus Fixed for Mice." J Exp Med **55**(6): 945-969.

Schlesinger, J. J. and M. W. Brandriss (1981). "Antibody-mediated infection of macrophages and macrophage-like cell lines with 17D-yellow fever virus." J Med Virol **8**(2): 103-117.

Schlesinger, J. J., M. W. Brandriss and T. P. Monath (1983). "Monoclonal antibodies distinguish between wild and vaccine strains of yellow fever virus by neutralization, hemagglutination inhibition, and immune precipitation of the virus envelope protein." Virology **125**(1): 8-17.

Schlesinger, J. J., S. Chapman, A. Nestorowicz, C. M. Rice, T. E. Ginocchio and T. J. Chambers (1996). "Replication of yellow fever virus in the mouse central nervous system: comparison of

neuroadapted and non-neuroadapted virus and partial sequence analysis of the neuroadapted strain." J Gen Virol **77 (Pt 6)**: 1277-1285.

Schliessmann, D. J. (1967). "Aedes aegypti eradication program of the United States--progress report 1965." Am J Public Health Nations Health **57**(3): 460-465.

Schmidt, K., M. Keller, B. L. Bader, T. Korytar, S. Finke, U. Ziegler and M. H. Groschup (2013). "Integrins modulate the infection efficiency of West Nile virus into cells." J Gen Virol **94**(Pt 8): 1723-1733.

Schneider, B. S. and S. Higgs (2008). "The enhancement of arbovirus transmission and disease by mosquito saliva is associated with modulation of the host immune response." Trans R Soc Trop Med Hyg **102**(5): 400-408.

Scott, T. W. and W. Takken (2012). "Feeding strategies of anthropophilic mosquitoes result in increased risk of pathogen transmission." Trends Parasitol **28**(3): 114-121.

Shannon, R. C., L. Whitman and M. Franca (1938). "Yellow Fever Virus in Jungle Mosquitoes." Science **88**(2274): 110-111.

Shi, P. Y., M. Tilgner, M. K. Lo, K. A. Kent and K. A. Bernard (2002). "Infectious cDNA clone of the epidemic west nile virus from New York City." J Virol **76**(12): 5847-5856.

Shrestha, B., S. K. Austin, K. A. Dowd, A. N. Prasad, S. Youn, T. C. Pierson, D. H. Fremont, G. D. Ebel and M. S. Diamond (2012). "Complex phenotypes in mosquitoes and mice associated with neutralization escape of a Dengue virus type 1 monoclonal antibody." Virology **427**(2): 127-134.

Shrestha, B., J. D. Brien, S. Sukupolvi-Petty, S. K. Austin, M. A. Edeling, T. Kim, K. M. O'Brien, C. A. Nelson, S. Johnson, D. H. Fremont and M. S. Diamond (2010). "The development of

therapeutic antibodies that neutralize homologous and heterologous genotypes of dengue virus type 1." PLoS Pathog **6**(4): e1000823.

Shriver, Z., I. Capila, G. Venkataraman and R. Sasisekharan (2012). "Heparin and heparan sulfate: analyzing structure and microheterogeneity." Handb Exp Pharmacol(207): 159-176.

Sil, B. K., L. M. Dunster, T. N. Ledger, M. R. Wills, P. D. Minor and A. D. Barrett (1992). "Identification of envelope protein epitopes that are important in the attenuation process of wild-type yellow fever virus." J Virol **66**(7): 4265-4270.

Simizu, B. T., T. (1988). Vero Cells: Origin, Properties and Biomedical Applications, Department of Microbiology, School of Medicine, Chiba University.

Simonsen, P. E. and M. E. Mwakitalu (2013). "Urban lymphatic filariasis." Parasitol Res **112**(1): 35-44.

Sinnis, P., A. Coppi, T. Toida, H. Toyoda, A. Kinoshita-Toyoda, J. Xie, M. M. Kemp and R. J. Linhardt (2007). "Mosquito heparan sulfate and its potential role in malaria infection and transmission." J Biol Chem **282**(35): 25376-25384.

Smith, D. R. (2012). "An update on mosquito cell expressed dengue virus receptor proteins." Insect Mol Biol **21**(1): 1-7.

Smith, D. R., A. P. Adams, J. L. Kenney, E. Wang and S. C. Weaver (2008). "Venezuelan equine encephalitis virus in the mosquito vector Aedes taeniorhynchus: infection initiated by a small number of susceptible epithelial cells and a population bottleneck." Virology **372**(1): 176-186.

Smith, H. H. and M. Theiler (1937). "The Adaptation of Unmodified Strains of Yellow Fever Virus to Cultivation in Vitro." J Exp Med **65**(6): 801-808.

Smith, T. J., R. H. Cheng, N. H. Olson, P. Peterson, E. Chase, R. J. Kuhn and T. S. Baker (1995). "Putative receptor binding sites on alphaviruses as visualized by cryoelectron microscopy." Proc Natl Acad Sci U S A **92**(23): 10648-10652.

Smithburn, K. C. and A. J. Haddow (1946). "Isolation of yellow fever virus from African mosquitoes." Am J Trop Med Hyg **26**: 261-271.

Smithburn, K. C., A. J. Haddow and W. H. Lumsden (1949). "An outbreak of sylvan yellow fever in Uganda with Aedes (Stegomyia) africanus Theobald as principal vector and insect host of the virus." Ann Trop Med Parasitol **43**(1): 74-89.

Song, B. H., G. N. Yun, J. K. Kim, S. I. Yun and Y. M. Lee (2012). "Biological and genetic properties of SA(1)(4)-14-2, a live-attenuated Japanese encephalitis vaccine that is currently available for humans." J Microbiol **50**(4): 698-706.

Soper, F. L. (1963). "The elimination of urban yellow fever in the Americas through the eradication of Aedes aegypti." Am J Public Health Nations Health **53**: 7-16.

Soper, F. L. (1967). "Aedes aegypti and yellow fever." Bull World Health Organ **36**(4): 521-527.

Spielman, A. (1971). "Bionomics of autogenous mosquitoes." Annu Rev Entomol **16**: 231-248.

Spielman, A. (1974). "Effect of synthetic juvenile hormone on ovarian diapause of Culex pipiens mosquitoes." J Med Entomol **11**(2): 223-225.

Sriurairatna, S. and N. Bhamarapravati (1977). "Replication of dengue-2 virus in Aedes albopictus mosquitoes. An electron microscopic study." Am J Trop Med Hyg **26**(6 Pt 1): 1199-1205.

Stadler, K., S. L. Allison, J. Schalich and F. X. Heinz (1997). "Proteolytic activation of tick-borne encephalitis virus by furin." J Virol **71**(11): 8475-8481.

Stiasny, K., R. Fritz, K. Pangerl and F. X. Heinz (2011). "Molecular mechanisms of flavivirus membrane fusion." Amino Acids **41**(5): 1159-1163.

Stock, N. K., N. Boschetti, C. Herzog, M. S. Appelhans and M. Niedrig (2012). "The phylogeny of yellow fever virus 17D vaccines." Vaccine **30**(6): 989-994.

Stokes, A., J. H. Bauer and N. P. Hudson (2001). "The transmission of yellow fever to Macacus rhesus. 1928." Rev Med Virol **11**(3): 141-148.

Strode, G. K. and Rockefeller Foundation. International Health Division. (1951). Yellow fever. New York,, McGraw-Hill.

Stuiver, I., Z. Ruggeri and J. W. Smith (1996). "Divalent cations regulate the organization of integrins alpha v beta 3 and alpha v beta 5 on the cell surface." J Cell Physiol **168**(3): 521-531.

Su, C. M., C. L. Liao, Y. L. Lee and Y. L. Lin (2001). "Highly sulfated forms of heparin sulfate are involved in japanese encephalitis virus infection." Virology **286**(1): 206-215.

Suksanpaisan, L., T. Susantad and D. R. Smith (2009). "Characterization of dengue virus entry into HepG2 cells." J Biomed Sci **16**: 17.

Sukupolvi-Petty, S., S. K. Austin, M. Engle, J. D. Brien, K. A. Dowd, K. L. Williams, S. Johnson, R. Rico-Hesse, E. Harris, T. C. Pierson, D. H. Fremont and M. S. Diamond (2010). "Structure and function analysis of therapeutic monoclonal antibodies against dengue virus type 2." J Virol **84**(18): 9227-9239.

Sumiyoshi, H., C. H. Hoke and D. W. Trent (1992). "Infectious Japanese encephalitis virus RNA can be synthesized from in vitro-ligated cDNA templates." J Virol **66**(9): 5425-5431.

Surtees, G. (1967). "Factors affecting the oviposition of Aedes aegypti." Bull World Health Organ **36**(4): 594-596.

Tabachnick, W. J. (1994). "Genetics of Insect Vector Competence for Arboviruses." Advances in Disease Vector Research **10**: 93-108.

Tabachnick, W. J., G. P. Wallis, T. H. Aitken, B. R. Miller, G. D. Amato, L. Lorenz, J. R. Powell and B. J. Beaty (1985). "Oral infection of Aedes aegypti with yellow fever virus: geographic variation and genetic considerations." Am J Trop Med Hyg **34**(6): 1219-1224.

Tajima, S., T. Takasaki, S. Matsuno, M. Nakayama and I. Kurane (2005). "Genetic characterization of Yokose virus, a flavivirus isolated from the bat in Japan." Virology **332**(1): 38-44.

Tangy, F. and P. Despres (2014). "Yellow fever vaccine attenuation revealed: loss of diversity." J Infect Dis **209**(3): 318-320.

Taylor, P. R., S. Gordon and L. Martinez-Pomares (2005). "The mannose receptor: linking homeostasis and immunity through sugar recognition." Trends Immunol **26**(2): 104-110.

Taylor, R. M., M. A. Haseeb and T. H. Work (1955). "A regional reconnaissance on yellow fever in the Sudan; with special reference to primate hosts." Bull World Health Organ **12**(5): 711-725.

Tesh, R. B., D. J. Gubler and L. Rosen (1976). "Variation among goegraphic strains of Aedes albopictus in susceptibility to infection with chikungunya virus." Am J Trop Med Hyg **25**(2): 326-335.

Theiler, M. and H. H. Smith (1937). "The Effect of Prolonged Cultivation in Vitro Upon the Pathogenicity of Yellow Fever Virus." J Exp Med **65**(6): 767-786.

Theiler, M. and H. H. Smith (1937). "The Use of Yellow Fever Virus Modified by in Vitro Cultivation for Human Immunization." J Exp Med **65**(6): 787-800.

Thepparit, C. and D. R. Smith (2004). "Serotype-specific entry of dengue virus into liver cells: identification of the 37-kilodalton/67-kilodalton high-affinity laminin receptor as a dengue virus serotype 1 receptor." J Virol **78**(22): 12647-12656.

Tignor, G. H., J. Casals and R. E. Shope (1993). "The yellow fever epidemic in Ethiopia, 1961-1962: retrospective serological evidence for concomitant Ebola or Ebola-like virus infection." Trans R Soc Trop Med Hyg **87**(2): 162.

Tio, P. H., W. W. Jong and M. J. Cardosa (2005). "Two dimensional VOPBA reveals laminin receptor (LAMR1) interaction with dengue virus serotypes 1, 2 and 3." Virol J **2**: 25.

Tiwari, V., E. Maus, I. M. Sigar, K. H. Ramsey and D. Shukla (2012). "Role of heparan sulfate in sexually transmitted infections." Glycobiology **22**(11): 1402-1412.

Tsetsarkin, K. A., D. L. Vanlandingham, C. E. McGee and S. Higgs (2007). "A single mutation in chikungunya virus affects vector specificity and epidemic potential." PLoS Pathog **3**(12): e201.

Valinotto, L. E., P. R. Barrero, M. Viegas, M. C. Alvarez Lopez and A. S. Mistchenko (2012). "Molecular evidence of St. Louis encephalitis virus infection in patients in Buenos Aires, Argentina." J Clin Virol **54**(4): 349-351.

Valle, R. P. and B. Falgout (1998). "Mutagenesis of the NS3 protease of dengue virus type 2." J Virol **72**(1): 624-632.

van den Hurk, A. F., S. A. Ritchie and J. S. Mackenzie (2009). "Ecology and geographical expansion of Japanese encephalitis virus." Annu Rev Entomol **54**: 17-35.

van der Most, R. G., J. Corver and J. H. Strauss (1999). "Mutagenesis of the RGD motif in the yellow fever virus 17D envelope protein." Virology **265**(1): 83-95.

Van Epps, H. L. (2005). "Broadening the horizons for yellow fever: new uses for an old vaccine." J Exp Med **201**(2): 165-168.

Vanlandingham, D. L., K. Tsetsarkin, K. A. Klingler, C. Hong, K. L. McElroy, M. J. Lehane and S. Higgs (2006). "Determinants of vector specificity of o'nyong nyong and chikungunya viruses in Anopheles and Aedes mosquitoes." Am J Trop Med Hyg **74**(4): 663-669.

Vasilakis, N., E. R. Deardorff, J. L. Kenney, S. L. Rossi, K. A. Hanley and S. C. Weaver (2009). "Mosquitoes put the brake on arbovirus evolution: experimental evolution reveals slower mutation accumulation in mosquito than vertebrate cells." PLoS Pathog **5**(6): e1000467.

Vervaeke, P., M. Alen, S. Noppen, D. Schols, P. Oreste and S. Liekens (2013). "Sulfated Escherichia coli K5 polysaccharide derivatives inhibit dengue virus infection of human microvascular endothelial cells by interacting with the viral envelope protein E domain III." PLoS One **8**(8): e74035.

Vignuzzi, M., E. Wendt and R. Andino (2008). "Engineering attenuated virus vaccines by controlling replication fidelity." Nat Med **14**(2): 154-161.

Vlaycheva, L., M. Nickells, D. A. Droll and T. J. Chambers (2004). "Yellow fever 17D virus: pseudo-revertant suppression of defective virus penetration and spread by mutations in domains II and III of the E protein." Virology **327**(1): 41-49.

Volk, D. E., L. Chavez, D. W. Beasley, A. D. Barrett, M. R. Holbrook and D. G. Gorenstein (2006). "Structure of the envelope protein

domain III of Omsk hemorrhagic fever virus." Virology **351**(1): 188-195.

Volk, D. E., S. H. Gandham, F. J. May, A. Anderson, A. D. Barrett and D. G. Gorenstein (2007). "NMR assignments of the yellow fever virus envelope protein domain III." Biomol NMR Assign **1**(1): 49-50.

Volk, D. E., F. J. May, S. H. Gandham, A. Anderson, J. J. Von Lindern, D. W. Beasley, A. D. Barrett and D. G. Gorenstein (2009). "Structure of yellow fever virus envelope protein domain III." Virology **394**(1): 12-18.

Voss, J. E., M. C. Vaney, S. Duquerroy, C. Vonrhein, C. Girard-Blanc, E. Crublet, A. Thompson, G. Bricogne and F. A. Rey (2010). "Glycoprotein organization of Chikungunya virus particles revealed by X-ray crystallography." Nature **468**(7324): 709-712.

Walker, T., P. H. Johnson, L. A. Moreira, I. Iturbe-Ormaetxe, F. D. Frentiu, C. J. McMeniman, Y. S. Leong, Y. Dong, J. Axford, P. Kriesner, A. L. Lloyd, S. A. Ritchie, S. L. O'Neill and A. A. Hoffmann (2011). "The wMel Wolbachia strain blocks dengue and invades caged Aedes aegypti populations." Nature **476**(7361): 450-453.

Wallis, G. P., T. H. Aitken, B. J. Beaty, L. Lorenz, G. D. Amato and W. J. Tabachnick (1985). "Selection for susceptibility and refractoriness of Aedes aegypti to oral infection with yellow fever virus." Am J Trop Med Hyg **34**(6): 1225-1231.

Wang, E., A. C. Brault, A. M. Powers, W. Kang and S. C. Weaver (2003). "Glycosaminoglycan binding properties of natural venezuelan equine encephalitis virus isolates." J Virol **77**(2): 1204-1210.

Wang, E., K. D. Ryman, A. D. Jennings, D. J. Wood, F. Taffs, P. D. Minor, P. G. Sanders and A. D. Barrett (1995). "Comparison of the

genomes of the wild-type French viscerotropic strain of yellow fever virus with its vaccine derivative French neurotropic vaccine." J Gen Virol **76 (Pt 11)**: 2749-2755.

Wang, G. P. and F. D. Bushman (2006). "A statistical method for comparing viral growth curves." J Virol Methods **135**(1): 118-123.

Wang, H., A. D. Jennings, K. D. Ryman, C. M. Late, E. Wang, H. Ni, P. D. Minor and A. D. Barrett (1997). "Genetic variation among strains of wild-type yellow fever virus from Senegal." J Gen Virol **78 (Pt 6)**: 1349-1352.

Warrener, P., J. K. Tamura and M. S. Collett (1993). "RNA-stimulated NTPase activity associated with yellow fever virus NS3 protein expressed in bacteria." J Virol **67**(2): 989-996.

Watterson, D., B. Kobe and P. R. Young (2012). "Residues in domain III of the dengue virus envelope glycoprotein involved in cell-surface glycosaminoglycan binding." J Gen Virol **93**(Pt 1): 72-82.

Watts, D. M., S. Pantuwatana, G. R. DeFoliart, T. M. Yuill and W. H. Thompson (1973). "Transovarial transmission of LaCrosse virus (California encephalitis group) in the mosquito, Aedes triseriatus." Science **182**(4117): 1140-1141.

Weaver, S. C. and A. D. Barrett (2004). "Transmission cycles, host range, evolution and emergence of arboviral disease." Nat Rev Microbiol **2**(10): 789-801.

Weaver, S. C. and W. K. Reisen (2010). "Present and future arboviral threats." Antiviral Res **85**(2): 328-345.

Welsch, S., S. Miller, I. Romero-Brey, A. Merz, C. K. Bleck, P. Walther, S. D. Fuller, C. Antony, J. Krijnse-Locker and R. Bartenschlager (2009). "Composition and three-dimensional architecture of the dengue virus replication and assembly sites." Cell Host Microbe **5**(4): 365-375.

Weng, M. H., J. C. Lien, Y. M. Wang, H. L. Wu and C. Chin (1997). "Susceptibility of three laboratory strains of Aedes albopictus (Diptera: Culicidae) to Japanese encephalitis virus from Taiwan." J Med Entomol **34**(6): 745-747.

Whitman, L. (1937). "The Multiplication of the Virus of Yellow Fever in Aedes Aegypti." J Exp Med **66**(2): 133-143.

WHO (1967). Arboviruses and human disease. Report of a WHO Scientific Group. World Health Organ Tech Rep Ser. **369:** 1-84.

WHO (1985). Arthropod-borne and rodent-borne viral diseases. Report of a WHO Scientific Group. World Health Organ Tech Rep Ser. **719:** 1-116.

WHO (1985). "Yellow fever in the Americas." Bull Pan Am Health Organ **19**(2): 209-212.

WHO (2009). Dengue: Guidelines for Diagnosis, Treatment, Prevention and Control: New Edition. Geneva.

WHO. (2014). "Chikungunya." from http://www.who.int/mediacentre/factsheets/fs327/en/.

WHO. (2014). "Global Yellow Fever Data Base." from http://apps.who.int/globalatlas/default.asp.

WHO. (2014). "Yellow fever."

Williams, M. C., J. P. Woodall, P. S. Corbet and J. D. Gillett (1965). "O'nyong-Nyong Fever: An Epidemic Virus Disease in East Africa. 8. Virus Isolations from Anopheles Mosquitoes." Trans R Soc Trop Med Hyg **59**: 300-306.

Woodall, J. P., J. R. Dykes and M. C. Williams (1968). "The reaction of a species of colobus monkey to inoculation with yellow fever virus." Ann Trop Med Parasitol **62**(4): 528-535.

Woodward, T. M., B. R. Miller, B. J. Beaty, D. W. Trent and J. T. Roehrig (1991). "A single amino acid change in the E2 glycoprotein of Venezuelan equine encephalitis virus affects replication and dissemination in Aedes aegypti mosquitoes." J Gen Virol **72 (Pt 10)**: 2431-2435.

Wright, F. M. (2001). "The 1878 yellow fever epidemic in Memphis." J Miss State Med Assoc **42**(1): 9-13.

Wu, K. P., C. W. Wu, Y. P. Tsao, T. W. Kuo, Y. C. Lou, C. W. Lin, S. C. Wu and J. W. Cheng (2003). "Structural basis of a flavivirus recognized by its neutralizing antibody: solution structure of the domain III of the Japanese encephalitis virus envelope protein." J Biol Chem **278**(46): 46007-46013.

Wu, S. J., G. Grouard-Vogel, W. Sun, J. R. Mascola, E. Brachtel, R. Putvatana, M. K. Louder, L. Filgueira, M. A. Marovich, H. K. Wong, A. Blauvelt, G. S. Murphy, M. L. Robb, B. L. Innes, D. L. Birx, C. G. Hayes and S. S. Frankel (2000). "Human skin Langerhans cells are targets of dengue virus infection." Nat Med **6**(7): 816-820.

Xiao, S. Y., H. Guzman, A. P. da Rosa, H. B. Zhu and R. B. Tesh (2003). "Alteration of clinical outcome and histopathology of yellow fever virus infection in a hamster model by previous infection with heterologous flaviviruses." Am J Trop Med Hyg **68**(6): 695-703.

Xie, X., S. Gayen, C. Kang, Z. Yuan and P. Y. Shi (2013). "Membrane topology and function of dengue virus NS2A protein." J Virol **87**(8): 4609-4622.

Yamamoto, N., T. Kimura and A. Ohyama (1987). "Multiplication and distribution of type 2 dengue and Japanese encephalitis viruses in Toxorhynchites splendens after intrathoracic inoculation." Arch Virol **97**(1-2): 37-47.

Yamshchikov, V., V. Mishin and F. Cominelli (2001). "A new strategy in design of +RNA virus infectious clones enabling their stable propagation in E. coli." Virology **281**(2): 272-280.

Yamshchikov, V. F., G. Wengler, A. A. Perelygin, M. A. Brinton and R. W. Compans (2001). "An infectious clone of the West Nile flavivirus." Virology **281**(2): 294-304.

Yang, S., M. He, X. Liu, X. Li, B. Fan and S. Zhao (2013). "Japanese encephalitis virus infects porcine kidney epithelial PK15 cells via clathrin- and cholesterol-dependent endocytosis." Virol J **10**: 258.

Yazi Mendoza, M., J. S. Salas-Benito, H. Lanz-Mendoza, S. Hernandez-Martinez and R. M. del Angel (2002). "A putative receptor for dengue virus in mosquito tissues: localization of a 45-kDa glycoprotein." Am J Trop Med Hyg **67**(1): 76-84.

Yu, I. M., W. Zhang, H. A. Holdaway, L. Li, V. A. Kostyuchenko, P. R. Chipman, R. J. Kuhn, M. G. Rossmann and J. Chen (2008). "Structure of the immature dengue virus at low pH primes proteolytic maturation." Science **319**(5871): 1834-1837.

Zacks, M. A. and S. Paessler (2010). "Encephalitic alphaviruses." Vet Microbiol **140**(3-4): 281-286.

Zhang, R., C. F. Hryc, Y. Cong, X. Liu, J. Jakana, R. Gorchakov, M. L. Baker, S. C. Weaver and W. Chiu (2011). "4.4 A cryo-EM structure of an enveloped alphavirus Venezuelan equine encephalitis virus." EMBO J **30**(18): 3854-3863.

Zhang, S., E. I. Bovshik, R. Maillard, G. D. Gromowski, D. E. Volk, C. H. Schein, C. Y. Huang, D. G. Gorenstein, J. C. Lee, A. D. Barrett and D. W. Beasley (2010). "Role of BC loop residues in structure, function and antigenicity of the West Nile virus envelope protein receptor-binding domain III." Virology **403**(1): 85-91.

Zhang, W., P. R. Chipman, J. Corver, P. R. Johnson, Y. Zhang, S. Mukhopadhyay, T. S. Baker, J. H. Strauss, M. G. Rossmann and R.

J. Kuhn (2003). "Visualization of membrane protein domains by cryo-electron microscopy of dengue virus." Nat Struct Biol **10**(11): 907-912.

Zhang, W., B. Kaufmann, P. R. Chipman, R. J. Kuhn and M. G. Rossmann (2013). "Membrane curvature in flaviviruses." J Struct Biol **183**(1): 86-94.

Zhang, X., P. Ge, X. Yu, J. M. Brannan, G. Bi, Q. Zhang, S. Schein and Z. H. Zhou (2013). "Cryo-EM structure of the mature dengue virus at 3.5-A resolution." Nat Struct Mol Biol **20**(1): 105-110.

Zhang, Y., J. Corver, P. R. Chipman, W. Zhang, S. V. Pletnev, D. Sedlak, T. S. Baker, J. H. Strauss, R. J. Kuhn and M. G. Rossmann (2003). "Structures of immature flavivirus particles." EMBO J **22**(11): 2604-2613.

Zhang, Y., W. Zhang, S. Ogata, D. Clements, J. H. Strauss, T. S. Baker, R. J. Kuhn and M. G. Rossmann (2004). "Conformational changes of the flavivirus E glycoprotein." Structure **12**(9): 1607-1618.

Zhao, Z., T. Date, Y. Li, T. Kato, M. Miyamoto, K. Yasui and T. Wakita (2005). "Characterization of the E-138 (Glu/Lys) mutation in Japanese encephalitis virus by using a stable, full-length, infectious cDNA clone." J Gen Virol **86**(Pt 8): 2209-2220.

Zheng, Y., C. Sanchez-San Martin, Z. L. Qin and M. Kielian (2011). "The domain I-domain III linker plays an important role in the fusogenic conformational change of the alphavirus membrane fusion protein." J Virol **85**(13): 6334-6342.

Zhou, G., J. Isoe, W. A. Day and R. L. Miesfeld (2011). "Alpha-COPI coatomer protein is required for rough endoplasmic reticulum whorl formation in mosquito midgut epithelial cells." PLoS One **6**(3): e18150.

Zhu, Y. Z., M. M. Cao, W. B. Wang, W. Wang, H. Ren, P. Zhao and Z. T. Qi (2012). "Association of heat-shock protein 70 with lipid rafts

is required for Japanese encephalitis virus infection in Huh7 cells." J Gen Virol **93**(Pt 1): 61-71.

Zieler, H., C. F. Garon, E. R. Fischer and M. Shahabuddin (2000). "A tubular network associated with the brush-border surface of the Aedes aegypti midgut: implications for pathogen transmission by mosquitoes." J Exp Biol **203**(Pt 10): 1599-1611.

Zou, G., Y. L. Chen, H. Dong, C. C. Lim, L. J. Yap, Y. H. Yau, S. G. Shochat, J. Lescar and P. Y. Shi (2011). "Functional analysis of two cavities in flavivirus NS5 polymerase." J Biol Chem **286**(16): 14362-14372.

Zwiebel, L. J. and W. Takken (2004). "Olfactory regulation of mosquito-host interactions." Insect Biochem Mol Biol **34**(7): 645-652.

Appendix A - Screening of viable YFV mutants

The cDNA infectious clones of the YFV mutants were generated with the materials and methods described in **Section 2.2**. To confirm the viability of YFV mutants, the growth curves in the electroporated BHK-21 cells were monitored for at least two independent electroporations. The average titers of the wildtype Asibi strain and the 17D+Asibi M-E chimera were obtained from four independent electroporations. Viable YFV mutants were selected for the *per os* infection of *Ae. aegypti*.

Due to the adaptation which arises from the process of serial passage in tissue culture conditions, the propagation 17D+Asibi M-E chimera reached insignificantly higher titers in electroporated BHK-21 cells than the Asibi strain. However, the Asibi strain has been reported to be significantly more infectious and disseminating than the 17D+Asibi M-E chimera in spite of the lower average titers of the recovered viruses.

1. T380R mutation in EDIII

The recovery of the YFV E T380R mutants is summarized in **Figure. 2.4**. The T380R mutation increased the propagation of the Asibi strain and the 17D+Asibi M-E chimera in BHK-21 cells. The Asibi E T380R mutant and the 17D+Asibi M-E E T380R mutant were recovered in two independent electroporations.

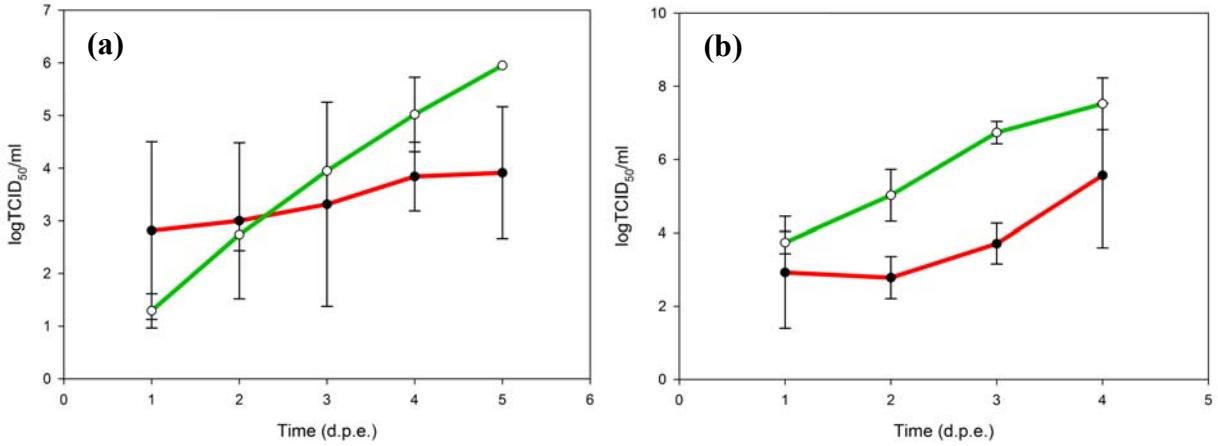

Figure A.1 Replication of YFV E T380R mutants in electroporated BHK-21 cells
(a) The titers of the Asibi strain and the Asibi E T380R mutant are shown in red and green lines, respectively. (b) The titers of the 17D+Asibi M-E chimera and the 17D+Asibi M-E E T380R mutant are shown in red and green lines, respectively.

The Asibi E T380R mutant showed the insignificantly lower titer at 1 (2.81 $logTCID_{50}$/ml vs. 1.29 $logTCID_{50}$/ml, $p>0.05$) and 2 (3.00 $logTCID_{50}$/ml vs. 2.73 $logTCID_{50}$/ml, $p>0.05$) d.p.e. than the Asibi strain. And, the viral titers of the Asibi E T380R mutant were higher than the Asiib strain at 3 (3.31 $logTCID_{50}$/ml vs. 3.95 $logTCID_{50}$/ml, $p>0.05$), 4 (3.84 $logTCID_{50}$/ml vs. 5.02 $logTCID_{50}$/ml, $p>0.05$) and 5 (3.91 $logTCID_{50}$/ml vs. 5.95 $logTCID_{50}$/ml, $p>0.05$) d.p.e. with no statistically significant difference.

Although there was no demonstrable difference, the 17D+Asibi M-E E T380R mutant propagated to the higher titers than the 17D+Asibi M-E chimera at 1 (2.92 $logTCID_{50}$/ml vs. 3.74 $logTCID_{50}$/ml, $p>0.05$), 2 (2.78 $logTCID_{50}$/ml vs. 5.02 $logTCID_{50}$/ml, $p>0.05$), 3 (3.71 $logTCID_{50}$/ml vs. 6.74 $logTCID_{50}$/ml, $p>0.05$), and 4 (5.57 $logTCID_{50}$/ml vs, 7.02 $logTCID_{50}$/ml, $p>0.05$) d.p.e.

In summary, both the Asibi E T380R mutant and the 17D+Asibi M-E E T380R mutant were able to propagate to the relatively higher titers in electroporated BHK-21 cells.

2. G52R mutation in EDI-EDII molecular higne region and T173I in EDI

The average titers of the YFV E G52R-T173I mutants are shown in **Figure 2.5**. The Asibi E G52R-T173I mutant and the 17D+Asibi M-E E G52R-T173I mutant were recovered from six independent electroporations.

The Asibi E G52R-T173I double mutant showed the insignificantly lower titers than the Asibi strain at 1 (2.82 $logTCID_{50}$/ml vs. 1.81 $logTCID_{50}$/ml, $p>0.05$), 2 (3.00 $logTCID_{50}$/ml vs, 1.95 $logTCID_{50}$/ml, $p>0.05$), 3 (3.32 $logTCID_{50}$/ml vs. 2.79 $logTCID_{50}$/ml, $p>0.05$), 4 (3.84 $logTCID_{50}$/ml vs. 3.02 $logTCID_{50}$/ml, $p>0.05$) and 5 (3.91 $logTCID_{50}$/ml vs. 3.43 $logTCID_{50}$/ml, $p>0.05$) d.p.e.

Similarly, the insignificantly lower titers were observed in the BHK-21 cells electroporated with the viral RNA of the 17D+Asibi M-E E G52R-T173I double mutant than the 17D+Asibi M-E chimera at 1 (2.92 $logTCID_{50}$/ml vs. 2.73 $logTCID_{50}$/ml, $p>0.05$), 2 (2.78 $logTCID_{50}$/ml vs. 2.19 $logTCID_{50}$/ml, $p>0.05$), 3 (3.71 $logTCID_{50}$/ml vs. 3.43 $logTCID_{50}$/ml, $p>0.05$) and 4 (5.57 $logTCID_{50}$/ml vs. 4.01 $logTCID_{50}$/ml, $p>0.05$) d.p.e.

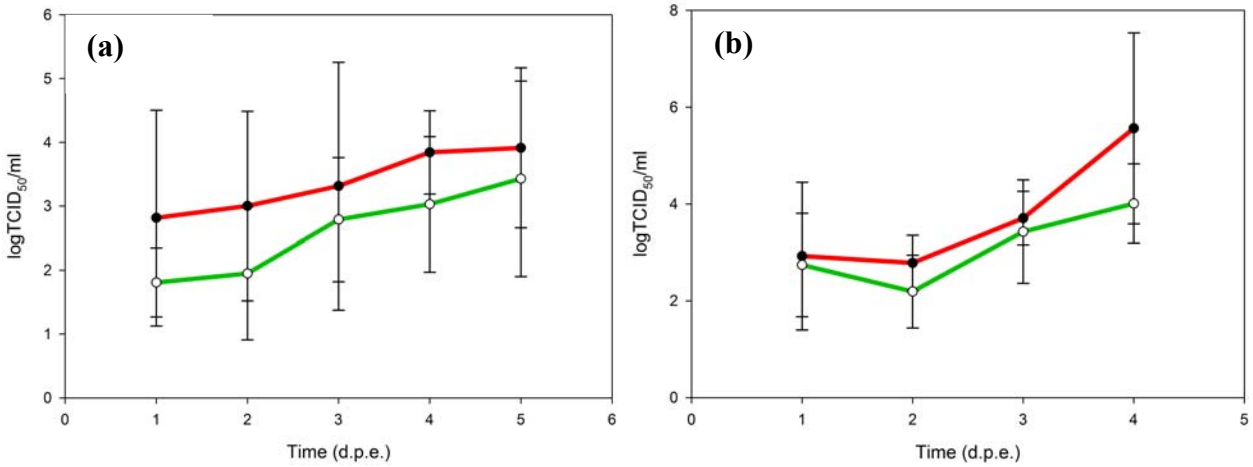

Figure A.2 Replication of YFV E G52R-T173I double mutants in electroporated BHK-21 cells

(a) The titers of the Asibi strain and the Asibi E G52R-T173I double mutant are shown in red and green lines, respectively. (b) The titers of the 17D+Asibi M-E chimera and the 17D+Asibi M-E E G52R-T173I double mutant are shown in red and green lines, respectively.

The titers of the YFV E G52R-T173I double mutants suggest the G52R mutation and the T173I mutation in the E protein result in the insignificantly lower titers for both the Asibi strain and the 17D+Asibi M-E chimera.

3. S305F, P325S and T380R mutations in EDIII

The replication of the YFV E S305F-P325S-T380R mutants in electroporated BHK-21 cells is summarized in **Figure 2.6**. The Asibi E S305F-P325S-T380R mutant and the 17D+Asibi M-E E S305F-P325S-T380R mutant were covered from two independent electroporations.

Although there was no significant difference, the Asibi E S305F-P325S-T380R mutant propagated to the insignificantly lower titers than the Asibi strain in 1 (2.82 $logTCID_{50}$/ml vs. 1.06 $logTCID_{50}$/ml, $p>0.05$), 2 (3.00 $logTCID_{50}$/ml vs. 2.52 $logTCID_{50}$/ml, $p>0.05$), 3 (3.31 $logTCID_{50}$/ml vs. 2.24 $logTCID_{50}$/ml, $p>0.05$), 4 (3.84 $logTCID_{50}$/ml vs. 2.74 $logTCID_{50}$/ml, $p>0.05$), and 5 (3.91 $logTCID_{50}$/ml vs. 1.52 $logTCID_{50}$/ml, $p>0.05$) d.p.e.

The replication of the 17D+Asibi M-E E S305F-P325S-T380R mutant in electroporated BHK-21 cells led to the comparable titers to the 17D+Asibi M-E chimera at 1 (2.92 $logTCID_{50}$/ml vs. 3.40 $logTCID_{50}$/ml, $p>0.05$), 2 (2.78 $logTCID_{50}$/ml vs. 3.74 $logTCID_{50}$/ml,

p>0.05), 3 (3.71 logTCID$_{50}$/ml vs. 6.02 logTCID$_{50}$/ml, p>0.05) and 4 (5.57 logTCID$_{50}$/ml vs. 5.40 logTCID$_{50}$/ml, p>0.05) d.p.e.

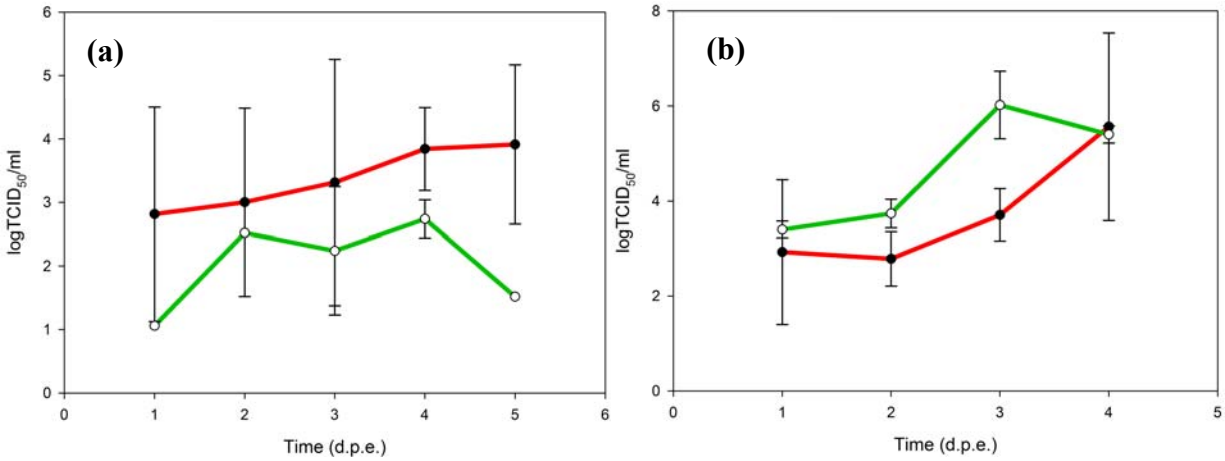

Figure A.3 Replication of YFV E S305F-P325S-T380R double mutants in electroporated BHK-21 cells

(a) The titers of the Asibi strain and the Asibi E S305F-P325S-T380R mutant are shown in red and green lines, respectively. (b) The titers of the 17D+Asibi M-E chimera and the 17D+Asibi M-E E S305F-P325S-T380R mutant are shown in red and green lines, respectively.

The S305F, P325S and T380R mutations in the YFV E protein resulted in the insignificantly lower titer of the Asibi E S305F-P325S-T380R mutant than the Asibi strain. In contrast to the lower viral titers observed in the Asibi E S305F-P325S-T380R mutant, the replication of the 17D+Asibi M-E E S305F-P325S-T380R mutant in electroporated BHK-21 cells showed the insignificantly higher titers at 1,2 and 3 d.p.e. than the 17D+Asibi M-E chimera.

4. G52R mutation in EDI-EDII molecular hinge region, T173I mutation in EDI and S305F and P325S mutations in EDIII

The propagation of the YFV E G52R-T173I-S305F-P325S mutants is shown in **Figure 2.7**. The Asibi E G52R-T173I-S305F-P325S mutant and the 17D+Asibi M-E E G52R-T173I-S305F-P325S mutant were covered from three and six independent electroporations, respectively.

The comparable yield in electroporated BHK-21 cells between the Asibi strain and the Asibi E G52R-T173I-S305F-P325S mutant was observed at 1 (2.82 logTCID$_{50}$/ml vs. 2.91 logTCID$_{50}$/ml, p>0.05), 2 (3.00 logTCID$_{50}$/ml vs. 3.07 logTCID$_{50}$/ml, p>0.05), 3 (3.32

logTCID$_{50}$/ml vs. 2.07 logTCID$_{50}$/ml, p>0.05), and 5 (3.91 logTCID$_{50}$/ml vs. 3.72 logTCID$_{50}$/ml, p>0.05) d.p.e. except for 4 d.p.e. (3.84 logTCID$_{50}$/ml vs. 2.76 logTCID$_{50}$/ml, p=0.038)

There was no significant difference in the viral titers between the 17D+Asibi M-E chimera and the 17D+Asibi M-E E G52R-T173I-S305F-P325S mutant at 1 (2.92 logTCID$_{50}$/ml vs. 2.99 logTCID$_{50}$/ml, p>0.05), 2 (2.78 logTCID$_{50}$/ml vs. 2.45 logTCID$_{50}$/ml, p>0.05), 3 (3.71 logTCID$_{50}$/ml vs. 3.19 logTCID$_{50}$/ml, p>0.05) and 4 (5.57 logTCID$_{50}$/ml vs. 4.33 logTCID$_{50}$/ml, p>0.05) d.p.e.

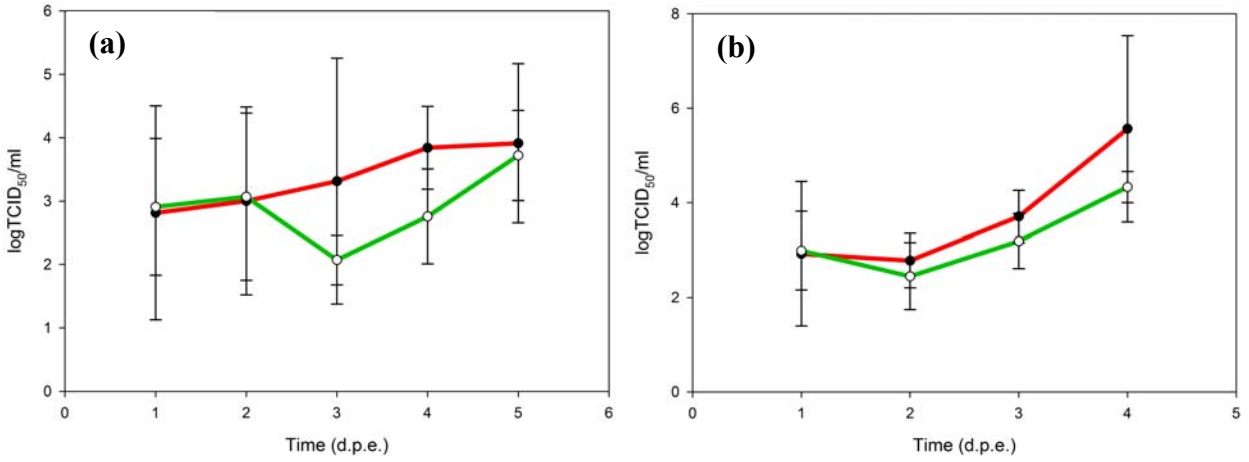

Figure A.4 Replication of YFV E G52R-T173I-S305F-P325S mutants in electroporated BHK-21 cells

(a) The titers of the Asibi strain and the Asibi E G52R-T173I-S305F-P325S mutant are shown in red and green lines, respectively. (b) The titers of the 17D+Asibi M-E chimera and the 17D+Asibi M-E E G52R-T173I-S305F-P325S mutant are shown in red and green lines, respectively.

In summary, the replication of the YFV E G52R-T173I-S305F-P325S mutants in BHK-21 cells resulted in the lower average viral titers without demonstrable difference from the average viral titers of wildtype controls.

5. G52R mutation in EDI-EDII molecular hinge region, T173I mutation in EDI and S305F, P325S and T380R mutations in EDIII

The five mutations, G52R, T173I, S305F, P325S and T380R, are introduced in the E protein of the Asibi strain and the 17D+Asibi M-E chimera. The replication of the G52R-T173I-S305F-P325S-T380R mutants and the wildtype controls is summarized in **Figure 2.8**. The Asibi

E G52R-T173I-S305F-P325S-T380R mutant and the 17D+Asibi M-E E G52R-T173I-S305F-P325S-T380R mutant were recovered from two independent electroporations.

The average titers of the Asibi E G52R-T173I-S305F-P325S-T380R mutant in the electroporated BHK-21 cells were insignificantly lower than the Asibi strain at 1 (2.82 $logTCID_{50}$/ml vs. 1.29 $logTCID_{50}$/ml, $p>0.05$), 2 (3.00 $logTCID_{50}$/ml vs. 1.29 $logTCID_{50}$/ml, $p>0.05$), 3 (3.32 $logTCID_{50}$/ml vs. 2.40 $logTCID_{50}$/ml, $p>0.05$), and 4 (3.84 $logTCID_{50}$/ml vs. 1.74 $logTCID_{50}$/ml , $p>0.05$) d.p.e.

Similarly, the 17D+Asibi M-E E G52R-T173I-S305F-P325S-T380R mutant propagated to the insignificantly lower average titers than the 17D+Asibi M-E chimera at 1 (2.92 $logTCID_{50}$/ml vs, 3.02 $logTCID_{50}$/ml, $p>0.05$), 2 (2.78 $logTCID_{50}$/ml vs, 2,95 $logTCID_{50}$/ml, $p>0.05$), 3 (3.71 $logTCID_{50}$/ml vs. 3.74 $logTCID_{50}$/ml, $p>0.05$), and 4 (5.57 $logTCID_{50}$/ml vs. 3.52 $logTCID_{50}$/ml, $p>0.05$) d.p.e.

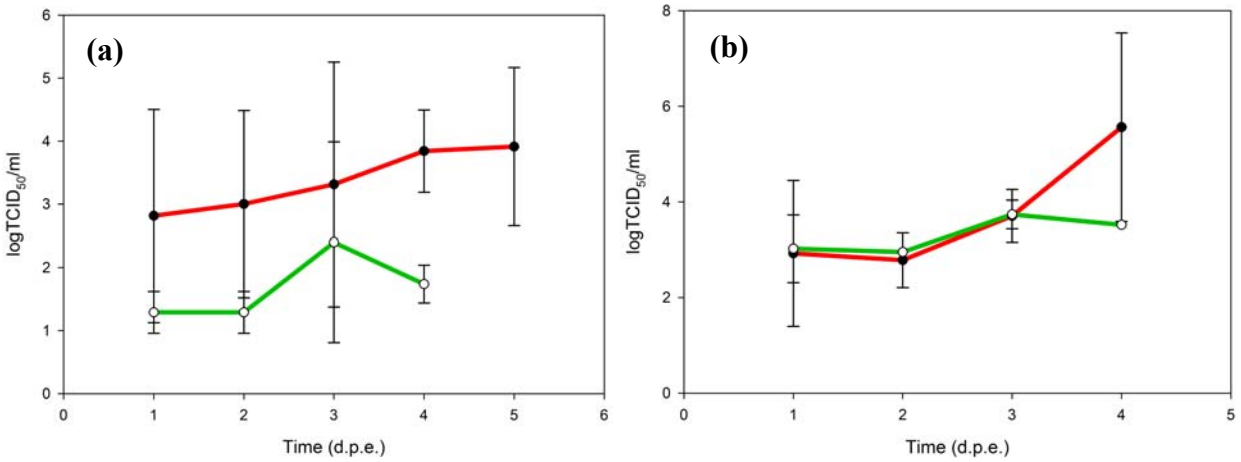

Figure A.5 Replication of YFV E G52R-T173I-S305F-P325S-T380R mutants in electroporated BHK-21 cells

(a) The titers of the Asibi strain and the Asibi E G52R-T173I-S305F-P325S-T380R mutant are shown in red and green lines, respectively. (b) The titers of the 17D+Asibi M-E chimera and the 17D+Asibi M-E E G52R-T173I-S305F-P325S-T380R mutant are shown in red and green lines, respectively.

Although there was no significant difference between the wildtype controls and the mutants, the five point mutations, G52R, T173I, S305F, P325S and T380R, led to the lower viral titers in both the Asibi strain and the 17D+Asibi M-E chimera.

6. Mutations in the E protein of the Asibi HeLa-p6 variant

The chimeras were generated by chimerizing the E gene derived from the Asibi HeLa-p6 variant with the corresponding region in the Asibi strain and the 17D+Asibi M-E chimera. The recovery and propagation of YFV E HeLa-p6 mutants in BHK-21 cells are shown in **Figure 2.9**. The Asibi E HeLa-p6 mutant and the 17D+Asibi M-E E HeLa-p6 mutant were recovered from three independent electroporations.

The propagation of the Asibi E HeLa-p6 mutant resulted in the similar titers to the Asibi strain at 1 (2.82 $logTCID_{50}$/ml vs. 2.14 $logTCID_{50}$/ml, $p>0.05$), 2 (3.00 $logTCID_{50}$/ml vs. 3.14 $logTCID_{50}$/ml, $p>0.05$) and 3 (3.32 $logTCID_{50}$/ml vs. 3.28 $logTCID_{50}$/ml, $p>0.05$) d.p.e. The average titers of the Asibi E HeLa-p6 mutant were insignificantly lower than the Asibi strain at 4 (3.84 $logTCID_{50}$/ml vs. 2.47 $logTCID_{50}$/ml, $p>0.05$) and 5 (3.91 $logTCID_{50}$/ml vs. 2.47 $logTCID_{50}$/ml, $p>0.05$) d.p.e.

The replication of the 17D+Asibi M-E E HeLa-p6 mutant and the 17D+Asibi M-E chimera led to the similar viral titers at 1 (2.92 $logTCID_{50}$/ml vs. 2.58 $logTCID_{50}$/ml, $p>0.05$), 2 (2.78 $logTCID_{50}$/ml vs. 3.00 $logTCID_{50}$/ml, $p>0.05$), 3 (3.71 $logTCID_{50}$/ml vs. 3.52 $logTCID_{50}$/ml, $p>0.05$), and 4 (5.57 $logTCID_{50}$/ml vs. 4.52 $logTCID_{50}$/ml , $p>0.05$) d.p.e.

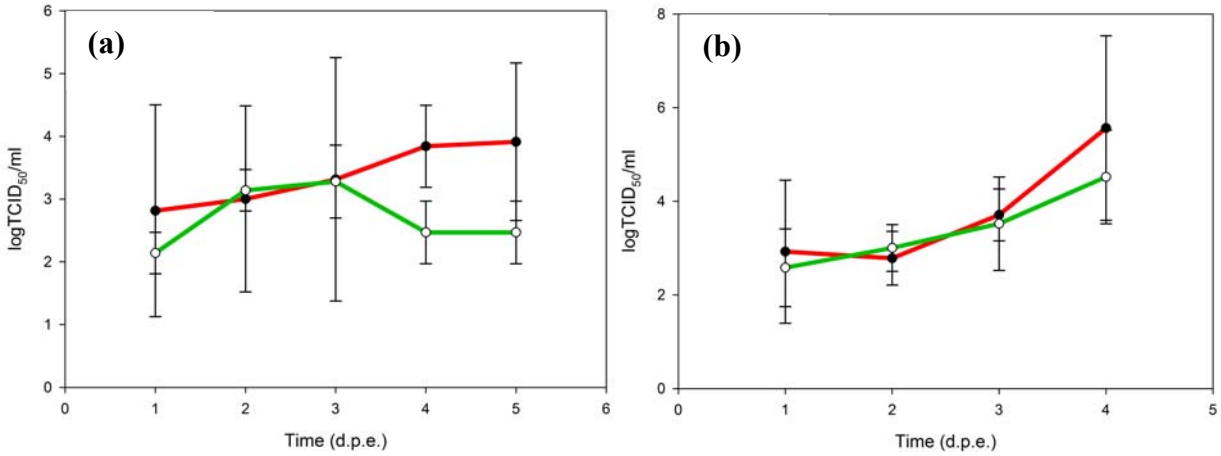

Figure A.6 Replication of YFV E HeLa-p6 mutants in electroporated BHK-21 cells

(a) The titers of the Asibi strain and the Asibi E HeLa-p6 mutant are shown in red and green lines, respectively. (b) The titers of the 17D+Asibi M-E chimera and the 17D+Asibi M-E E HeLa-p6 mutant are shown in red and green lines, respectively.

The chimerization of the E gene between the Asibi strain and the Asibi HeLa-p6 variant resulted in the lower average peaked titer than the Asibi strain. Similarly, the 17D+Asibi M-E E HeLa-p6 mutant showed the lower average peaked titer than the 17D+Asibi M-E chimera.

In conclusion, the screening of the viable YFV mutant suggested the feasibility of utilizing the YFV E T380R mutant as the starting material to characterize the mutations in YFV EDIII because of the relatively higher average titers in BHK-21 cells electroporated by the RNA of the Asibi E T380R mutant and the 17D+Asibi M-E E T380R mutant. Additionally, the propagation of the YFV G52R-T173I double mutants demonstrated the feasibility of using the mutants to characterize the two non-conservative mutations in EDI and EDII of YFV.